Surface Complexation Reaction for White Light Emission from Quantum Dots

A thesis submitted by

Sabyasachi Pramanik

Roll No. 136122001

to

Indian Institute of Technology Guwahati

for the award of the degree of

Doctor of Philosophy

Department of Chemistry

Indian Institute of Technology Guwahati
Guwahati – 781039
India

July 2018

Abstract

The prime aim of the present thesis is to pursue complexation reaction on the surface of a quantum dot (Qdot). This is deemed to be useful in fabricating a single component biocompatible white light emitting (WLE) nanocomposite, having properties close to day bright light, with an aim to detect human disease responsive molecules at single particle level. In response to the recent demand of reducing the global energy consumption, the fabrication of the single component WLE materials, with high brightness, longer photostability, in comparison to multicomponent based WLE generation, is necessary. The conventional WLE materials, fabricated based on either the mixing of different color emitting material or coating of phosphor on a blue emitting lamp suffer from the drawbacks like color aging, self-absorption, nonradiative energy transfer, undesirable changes in chromaticity color coordinates and complicated processing technique, and consequently their application potential is limited. That is the motivation of this thesis to fabricate a single component WLE nanocomposites using the simple, unique, greener and cost-effective idea of decorating the surface of a Qdot with different luminescent inorganic complex. While there is vast literature available on the uses of a WLE nanocomposites in light emitting applications; however, their use as sensing platforms for the detection human diseases is not yet explored. The concept of using single WLE nanocomposite as a sensing platform for the detection of human disease responsive molecule is entirely based on the selective chemical interaction of the analyte with any of the emitting species present in the WLE nanocomposite – which would lead to change in their visual color chromaticity and blinking profiles. The current thesis addresses the following two main challenges.

(i) The fabrication of single component biocompatible photostable WLE nanocomposite, with properties close to day bright light, based on the concept of complexation on the surface of presynthesized nanoscale emitters, especially Qdots.

(ii) The use of the single WLE nanocomposite towards sensing of human disease responsive molecules at single particle level by observing the changes in their color, chromaticity and blinking pattern.

The present thesis is divided into six chapters. Brief discussion of each chapter is given below.

Chapter 1 consists of the introduction of the thesis and literature review of quantum dot, WLE materials, single particle probe and sensors.

Chapter 2 describes the formation of a single component photostable WLE nanocomposite based on the simultaneous formation of two different inorganic complex (blue emitting metal acetylsalicylate ($M(ASA)_2$ where $M:Mn^{2+}/Zn^{2+}$ and ASA= acetyl salicylic acid) and green emitting zinc quinolate (ZnQ_2) on the surface of a presynthesized orange emitting Mn^{2+} doped ZnS Qdot. The complexed Qdot is called herein as quantum dot complex (QDC).

Chapter 3 discusses the fabrication of a bio-friendly white light emitting nanocomposite by incorporating green emitting QDC (composed of ZnQ_2 complex and ZnS Qdot) in a blue protein matrix – consisted of red emitting gold nanoclusters.

Chapter 4 demonstrates the fabrication of a high temperature sustainable single component WLE nanocomposite, with properties close to day bright light in terms of the chromaticity, color rendering index (CRI) and correlated color temperature (CCT), by forming a greenish blue ZnQ_2 complex on the shell surface of a red emitting $CuInS_2$/ZnS core/shell Qdot.

Chapter 5 describes the utilization of a nontoxic WLE nanocomposite, fabricated based on the formation of blue emitting $Zn(MSA)_2$ complex on the surface of a yellow emitting ZnO Qdot, toward detection of the neurotransmitter dopamine at possibly single particle level. This was achieved followed by monitoring the changes in the visual color, chromaticity and on/off blinking characteristics of the single WLE QDC.

Chapter 6 contains conclusion of the thesis and future prospects.

Statement

This thesis entitled **"*Surface Complexation Reaction for White Light Emission from Quantum Dots*"** is a work of research and investigation carried out by me under the supervision of Dr. Arun Chattopadhyay, Professor, Department of Chemistry, Indian Institute of Technology Guwahati. This thesis has been submitted by me to the Department of Chemistry, Indian Institute of Technology Guwahati for the award of the degree of Doctor of Philosophy. I further declare that this work has not been submitted anywhere else for any degree, diploma, associateship or membership etc. of any Institute or University to the best of my knowledge.

_____

Sabyasachi Pramanik
Department of Chemistry
IIT Guwahati,
Guwahati-781039, Assam
India
Date:
Place: Guwahati, Assam

Certificate

It is certified that the thesis entitled **"*Surface Complexation Reaction for White Light Emission from Quantum Dots*"** being submitted to the Indian Institute of Technology Guwahati by Sabyasachi Pramanik (Roll. No. 136122001) for the award of the degree of Doctor of Philosophy in Chemistry, is a bonafide record of research work carried out by him. The information and data reported by him are solely the results of his original findings. He has meticulously carried out the investigations and followed the guidelines of the laboratory. This work has not been submitted elsewhere for any degree or diploma.

_____

Arun Chattopadhyay
Thesis Supervisor
Professor,
Department of Chemistry,
IIT Guwahati,
Guwahati-781039, Assam,
India.
Date:
Place: Guwahati, Assam

Dedicated to my

Parents and Grandfather

Acknowledgements

I would like to express my sincere gratitude to my supervisor Prof. Arun Chattopadhyay, who has taught me the first step of research. It is undoubted that without his aspiring and valuable guidance, I wouldn't be going in the direction that I am today and I shall remain indebted for his mentorship. I feel extremely lucky to have such an enthusiastic and inspiring advisor in my life. Thank you very much Sir.

I am extremely thankful to my doctoral committee members for their valuable suggestions and advice regarding research works.

I would like to express my deepest appreciation to my collaborators for their kind help and valuable suggestions. I would also like to thank my past and present lab members for their help and providing a friendly surroundings in the lab.

I would like to acknowledge all the faculty and staff members of Department of Chemistry and Centre for Nanotechnology for their endless support. I am also thankful to the Central Instrument Facility and Department of Physics of IIT Guwahati for allowing me to use the sophisticated instruments.

I am highly grateful to all of my friends for their encouragement and well wishes.

Last but not least, a heartfelt acknowledgment goes to my parents and family members for their endless support and timeless love.

Blessed to have all of you.

Sabyasachi

Table of Contents

Chapter 1

Introduction

The advantages of quantum dot (Qdot – composed of zero dimensional semiconductor nanocrystal) have emerged recently in the field of nanoscience and nanotechnology. Over the last three decades, despite of designing other various nanostructures, Qdots have helped develop nanoscience and nanotechnology with their remarkable optical features (such as large absorption cross section, broad excitation range, tunable and sharp emission, high brightness, and low photobleaching).[1-6] The unique optical features of Qdots have led to their wide range of applications ranging from solar cells, lasers, catalysis and to sensing and biodiagnostics.[1-6] This has helped keep the field of Qdots active over the last 30 years.[1] They have also found their way into a number of commercial uses. Hence, the Qdots will bring new and challenging platforms for researchers and scientists from different disciplines to pursue their dreams.

1.1 Quantum Dots

Quantum dots (Qdots), are small sized zero dimensional semiconductor nanocrystals with a size range of 1-10 nm, which is large enough to form a crystal lattice unit with hundreds of atoms and small enough to confine the motion of their charge carriers.[2-6] These have conferred Qdots with the remarkable optical properties in between the bulk material and a molecule. [2-6]

1.1.1 Discovery

The scientific journey of Qdots began in 1981 with discovery of semiconductor nanocrystal in doped glass matrix by Alexey I. Ekimov at Vasilov State Optical Institute of Russia.[7] Later in 1985, Louis E. Brus first synthesized colloidal semiconductor nanocrystal (cadmium sulphide) during working at AT&T Bell Labs.[8] But the term "Quantum Dot" was first coined by Mark Reed.[9] However, the real breakthrough came after one decade of research, when Murray et al. first introduced a hot injection technique to obtain nearly monodispersed CdX (X=S/Se/Te) Qdots.[10] After this revolutionary work, till date the Qdots have been extensively investigated for commercial applications.

1.1.2 Applications

Since their discovery, Qdots have become one of the building blocks of modern nanoscience and technology. The fascinating optical features (such as high photoluminescence quantum yield, resistance to photo bleaching, and broad excitation range) of Qdots, make them potential candidates for replacement of the conventional organic dyes and pave new roads in the field of fluorescence imaging, sensing, photocatalysis and photovoltaics.[2,3,5,11-15] In addition to these, Qdots have gained most of their attention for advanced technological applications in the field of electronic, optoelectronic, thermoelectronic devices, flexible electronic circuitry, photodetectors, and electrode with higher charge capacitor. [2,3,5,11-15]

1.1.3 The Unique Optical Properties of Qdots and Controlling Parameters

1.1.3.1 Quantum Confinement Effect

The attractiveness of Qdots arises due to their tunable distinctive optical properties. The uniqueness of the Qdots is the result of the three dimensional confinement of their electron-hole pair in the electronic excited state, which is otherwise known as quantum confinement effect.[16-19] This effect arises when the physical dimension of the Qdot is reduced and to be comparable with that of the wavelength of the electron, related to Bohr exciton-radius of their bulk form. Upon photo irradiation of the Qdot, one electron is excite from valence band to conduction band and in turn leaving a hole in the valence band. This electron and hole pair electrostatically attracts each other to form the exciton, which behaves like a particle in one dimensional box.[16-19] Therefore, when the size of the Qdot is less than that of the size of the exciton Bohr-radius of the bulk material then a strong confinement effect is observed. With decreasing size of the Qdot, the confinement of exciton increases and as a result optical bandgap of the Qdot increases. Therefore, the bandgap engineering offers to tune the electronic and optical properties of Qdots for various desired applications.[6,18]

1.1.3.2 Absorption and Photoluminescence

The photons having energy equal to or greater than the bandgap energy are able to excite the electrons from valence band to conduction band of Qdots (Figure 1.1).[6,18] The corresponding absorption spectrum reflects the physical nature of the Qdots. The position of the spectrum depends on the size of the Qdots, whereas their size distribution determines the width and shape of that spectrum. An interesting feature is that Qdots exhibits high molar extinction coefficients and absorption in the UV-vis region. As a consequence, low intensity light is sufficient to excite them in a broad spectral range. Following photoexcitation, the excited electron is able to relax back to the valence band through radiative or non-radiative pathways (Figure 1.1). The radiative recombination of the electron–hole pair within the bandgap leads to the emission of photon, which is largely dependent on the defect states of the nanocrystal. In Qdots, mainly two types of defects control the emission properties, one is internal defects and another is surface defects. The internal defects in Qdots arise due to the translocation of atoms or incorporation of impurity, while incompletely bonded surface atom of a terminated lattice of Qdots is responsible for surface defect states. [6,18]

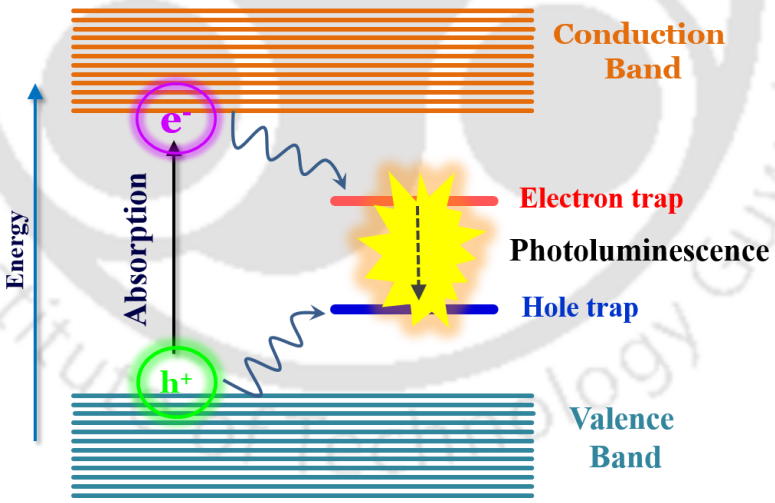

Figure 1.1. Schematic representation of absorption and trap state emission processes in semiconductor nanocrystal.

The abovementioned optical features of Qdots mainly depend on the three parameters – size, impurity doping and surface. The study of these three factors gives rise to understanding of the optical properties of Qdots and their influence on the

technological applications. The effect of these three parameters on controlling the optical features of Qdots are described in the following section.

(i) Size

The physical dimension of Qdot is key to controlling their emission color. Qdots exhibit size dependent absorption and emission features due to their quantum confinement effect. The radiative recombination of the electron-hole pair from band edge or from surface trap states is responsible for the emission features of Qdots. The correlation between size and band gap energy of Qdot is obtained from Brus equation.[18]

$$E_g(Qdot) = E_g(bulk) + \left(\frac{h^2}{8R^2}\right)\left(\frac{1}{m_e} + \frac{1}{m_h}\right) - \frac{1.8e^2}{4\pi\varepsilon\varepsilon_0 R}$$

Where, E_g corresponds to band gap, h is Planck constant, R is radius of Qdot, m_e and m_h correspond to effective mass of electron and hole respectively, and ε is the dielectric constant of the material. This equation reveals that the size of a Qdot and its bandgap energy is inversely proportional to each other. Therefore, as the size of the Qdot is reduced, the absorption and emission maxima are shifted to shorter wavelengths, while the opposite effect is observed for larger size Qdots. For example, the emission color of CdSe/ZnS Qdots could be tuned across the whole visible region (400-700 nm) by changing their diameters (Figure 1.2.).[19-20]

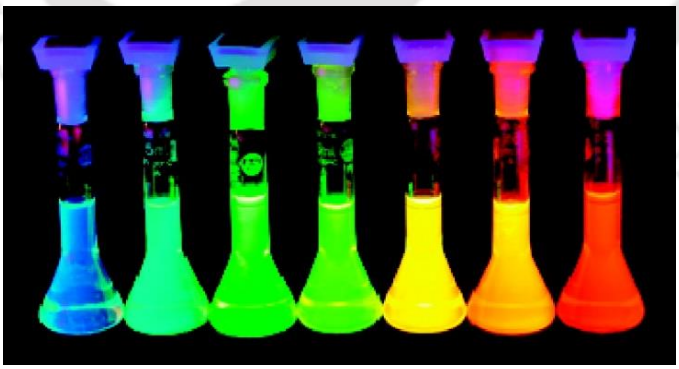

Figure 1.2. Fluorescence image of 1.7 to 5 nm sized CdSe/ZnS core-shell Qdots. (Reprinted with permission from reference 19. Copyright 2002 John Wiley and Sons)

(ii) Impurity Doping

Incorporating atomic impurities into the lattice of Qdots, results in change in their optical and electronic properties without changing their size.[21-26] The doping of impurity generates an intraband energy state that allows the radiative recombination to emit light at higher wavelength. The doped Qdots exhibit exciting properties – such as longer excited state lifetime, paramagnetic properties, large Stokes shift – which could improve the applicability of Qdots in biolabelling and light emitting devices. Recent studies have focused on the doping of lanthanides and transition elements into Qdots to improve their optical and electronic properties. In this regard, In, Ga, Cu and Mn doped semiconductor nanocrystals have gained much attention as bright emitters covering the whole visible region. As for example, the Mn^{2+} doping into the host lattice of ME (M=Zn/Cd and E =S/Se) showed bright luminescence in the yellow to orange region of the visible spectrum, whereas the Cu doped ZnS and ZnSe generate cyan and green color emissions, respectively (Figure 1.3).[23,27-30] Interestingly, the Mn doping in ZnSe/CdSe/ZnSe core/shell/shell Qdots extended the limited yellow-orange dopant emission window to a visible window – covering from blue to red (Figure 1.3).[27]

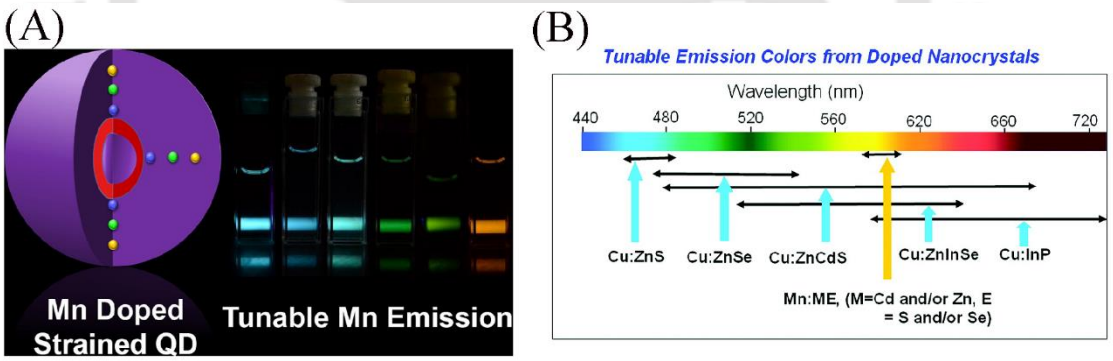

Figure 1.3. (A) Luminescence images of Mn doped ZnSe/CdSe/ZnSe core/shell Qdots. The emission tunability was achieved by controlling the epitaxial shell growth on ZnSe Core. (Reprinted with permission from reference 27. Copyright 2014 American Chemical Society) **(B)** Schematic representation of emission color tunability of Cu doped semiconductor nanocrystals. (Reprinted with permission from reference 28. Copyright 2011 American Chemical Society)

(iii) Surface

The surface of Qdots is an important aspect – in addition to their size and shape – in order to dictate their physical and chemical properties and thus to their potential applications.[6,29-32] The atoms on the surface of a Qdot are coordinativly unsaturated due to termination of crystal array on the surface and that leads to their different chemical

nature in comparison to the core atoms. This unsaturated bonds or unbonded orbitals point outwards from the crystal face of Qdots and for this reason these bonds are referred as "dangling bonds".[6,29-32] These dangling bonds are highly reactive with external chemical species. Due to their high surface area, Qdots possess a large number of dangling bonds or unpassivated orbitals on the surface, which lead to the formation of their band structure within the bandgap and could effectively trap the charge carrier, resulting in increase in non-radiative decay rate and lowering of quantum yield of the Qdots. Thus, the chemical reactivity and emission properties, especially quantum yield, depend on the presence and nature of the surface dangling bonds or unpassivated orbitals in Qdot.

1.1.4. Surface Modification

The modification of the surface of the presynthesized Qdots is an important factor in order to alter and/or improve their solubility and emission characteristics for their desired applications in the field ranging from biodiagnostics to optoelectronics. [29-32] The dangling bonds present on the surface of the presynthesized Qdots could be passivated through modification of their surface with chemical and/or biological moieties. In this regard, several strategies such as core/shell formation, conjugation of molecules, coating of polymers and ligand exchange have already demonstrated their use for changing the properties of the Qdots (in addition, to reserving their structural integrity) and make them suitable for their anticipated applications.[29-32] The details of the some of the surface modification strategies are discussed below.

1.1.4.1. Shell Passivation

For applications of Qdots in light emitting devices as well as in biology, it is beneficial to coat the surface of Qdots with an inorganic shell to make it more stable and brighter.[33-35] The formation of inorganic layer passivates the surface dangling bonds of Qdots as well as it creates a potential energy barrier, concentrating the electron-hole pair in core and thus preventing their leakage from the surface defects. Removal of surface defects through shell formation dramatically improves the hidden photoluminescence quantum yield of Qdots. As for example, CdSe/ZnS core/shell Qdots showed 10-20 times brighter luminescence than only CdSe core material.[34-35] The other advantage of coating is that the shell material having the element of smaller atomic radii (compared to atomic radii

of the core's element) is important for ligand binding, which can accommodate large number of organic ligand as capping agent to improve the colloidal stability. [33-35]

1.1.4.2. Ligand Exchange

To augment the stability of Qdots, the native ligand (serve as capping agent) on the surface of Qdots can be replaced with strong anchoring group containing ligand, which is able to form metal-ligand coordination with the surface free metal ions of Qdot. The incoming ligand provides new optical properties and functionalities to the surface modified Qdots. For example, the ligand exchange between dodecylamine and 3-mercaptopropionic acid on the surface of a CdSe Qdots led to a broad range of emission across the visible region (Figure 1.4 A).[36] Till date the ligand exchange strategy is extensively used to modulate the surface for desired practical applications especially for biological application. For example, the hydrophobic $CuInS_2$/ZnS Qdots is transferred to aqueous phase, using the glutathione and 3-mercaptopropionic acid as ligands, for bioimaging applications (Figure 1.4 B).[37]

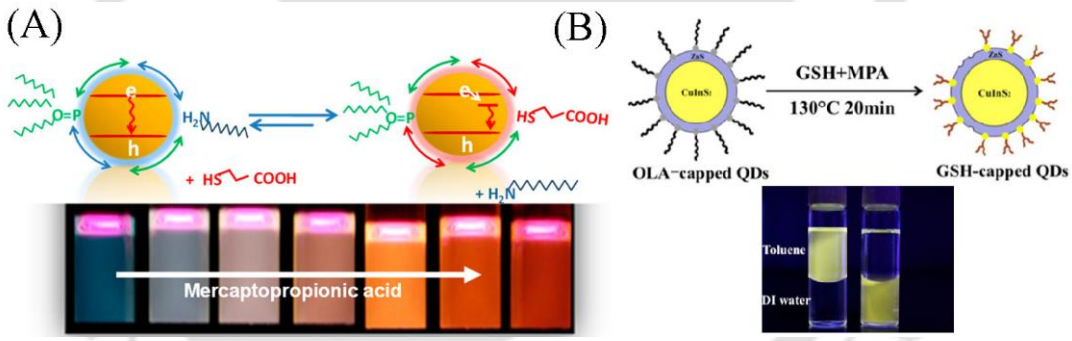

Figure 1.4. (A) Ligand exchange with 3-mercaptopropionic acid on the surface of dodecylamine capped CdSe Qdots. The broad tunable emission color depends on the concentration of 3-mercaptopropionic acid on the surface. (Reprinted with permission from reference 36. Copyright 2010 American Chemical Society) **(B)** Glutathione and 3-mercaptopropionic acid assisted ligand exchange of $CuInS_2$/ZnS Qdots. (Reprinted with permission from reference 37. Copyright 2015 American Chemical Society)

Since the surface attached molecule dictates the chemical and optical properties of Qdots, so the precise ligand attachments on the surface of Qdots are necessary for sensing contaminants, making biomarkers, measuring intracellular pH and targeted drug delivery. However, lowering of the photoluminescence quantum yield caused by the exchange of ligands is one of the drawbacks of the ligand exchange strategy. Apart from that, the surface modified Qdots have some other issues like aggregation of Qdots,

unstable molecular coating, and lower solubility. Hence, there is a need to develop newer methodology for surface modification of presynthesized Qdots in order to overcome the aforesaid shortcomings.

1.1.4.3 Surface Complexation Reaction

Complexation reaction on the surface of Qdots, using external organic ligand, is a newly developed interesting surface modification strategy to achieve the surface modified Qdots with superior optical and thermal properties in comparison to the parent components.[38-42] The surface complexation reaction is completely different and unique surface modification strategy with respect to the traditional ligand exchange. So far, non-fluorescent metal chalcogenide complexes (MCC) have been used as capping agent of the Qdots for their surface functionalization.[43-44] However, the formation of inorganic complex on the surface of a Qdot using a complexation reaction between the chemically active surface cation (of Qdots) and an external organic ligand can be considered important. This leads to the formation of a newly luminescent single component nanocomposite, termed here in as quantum dot complex (QDC). The QDC exhibits superior optical (such as high quantum yield and longer emission life time) and thermal (especially, stability at higher temperatures) properties compared to the constituents (Qdot and inorganic complex). The enhancement in the characteristic properties of inorganic complexes are noticed when they formed on the surface Qdots.[38-32]

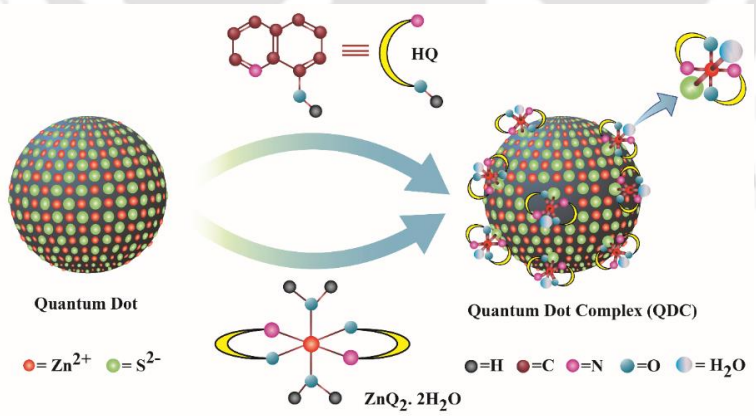

Figure 1.5. (A) Schematic representation of formation of quantum dot complex following reaction between ZnS Qdots and 8-Hydroxyquinoline ligand. (Reprinted with permission from reference 38. Copyright 2014 The Royal Society of Chemistry)

For example, complexation reaction of 8-hydroxyquinoline ligand with surface Zn^{2+} ions of ZnS Qdots led to the formation of green emitting zincquinolate (ZnQ_2) complex on the surface of Qdots (Figure 1.5).[38] The ZnQ_2 attached ZnS Qdot (i.e., QDC) exhibited high photoluminescence quantum yield, longer emissive lifetime, and higher thermal stability compared to the only ZnS and ZnQ_2. It is to be mentioned here that the extent of complex formation and attachment of the complex on the surface of Qdots depend on the binding nature of the chelating ligand. Thus, the formed surface complex defines the properties, especially emission characteristics, of QDC. Therefore, the formation of different colored luminescent complexes on the surface of Qdots may have use in fabricating different light emitting device (LED) materials and sensing of important molecules.

1.1.5. Applications of Surface Complexation Reaction

1.1.5.1. Phase Transfer

The solubility and stability of Qdots, in aqueous phase, is an important aspect for biological applications, especially for hydrophobic Qdots. That created the importance of phase transfer reaction of those hydrophobic Qdot, using different surface modification strategies (such as ligand exchange, encapsulating Qdot in polymer/protein/ silica matrix or conjugating Qdots with nucleotide) in order to make them biologically amenable. However, the major drawbacks related to increase in particle size and lowering of quantum yield of the Qdots limited their use. This created a scope for the use complexation reaction in transferring the hydrophobic Qdots from non-polar phase to aqueous phase. As for example, complexation reaction between hydrophobic Zn^{2+} doped CdS Qdots with 8-hydroxyquinoline resulted their transfer from nonpolar (hexane) to polar (water) phase (Figure 1.6).[39] That the formation of dual complexes (ZnQ_2 and CdQ_2) on the surface of Zn^{2+} doped CdS Qdots is responsible for highly efficient phase transfer process and may be helpful for biological applications and synthesis of aqueous based nanocomposites.

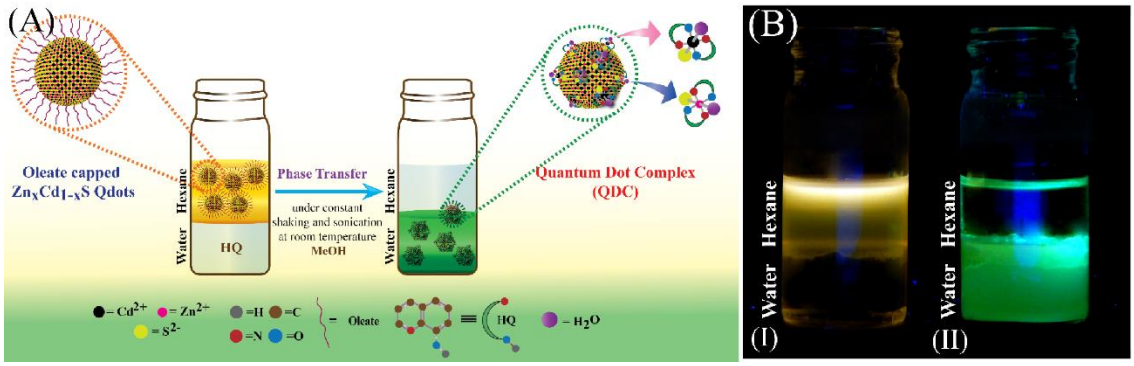

Figure 1.6. (A) Schematic representation and **(B)** digital photographs in presence of UV light of Zn doped CdS Qdots before and after phase transfer by using the surface complexation reaction with 8-Hydroxyquinoline ligand (Reprinted with permission from reference 39. Copyright 2014 American Chemical Society)

1.1.5.2. Targeted Cellular Imaging

Multifunctional nanomaterial is an emergent class of materials for biodiagnostics and therapeutic applications. Surface functionalization of Qdots, specifically complexation reaction, provides a new dimension in synthesizing multifunctional nanocomposite. For instance, a magnetofluorescent biocompatible nanocomposite has been synthesized by performing the complexation reaction (using 8-hydroxyquinoline ligand) on the surface of a superparamagnetic iron oxide nanoparticle (SPION) conjugated ZnS Qdot (Fe_3O_4–ZnS).[41] The combinatorial effect of superior optical properties (such as high photoluminescence quantum yield, longer emissive life time, and low photobleaching rate) of QDC and superparamagnetic nature of SPION offers a new nanocomposite, which could be able to spatially image cervical cancerous cells and thus indicated their use as a targeted cellular imaging agent.

1.1.5.3. Chromaticity Tuning

The fabrication of a single component nanocomposite, with multicolor emissions, has a great demand for solid state lighting and ratiometric sensing. Using surface complexation strategy one can easily make multicolor emitting nanocomposite. For example, chelation of the surface metal ion of Mn^{2+} doped ZnS Qdots with 8-hydroxyquinoline ligand led to the formation of double channel emitting QDC (Figure 1.7).[40] The dual emissions from QDC is because of two different independent emitters – one is from surface attached zincquinolate complexes (with green emission) and the other one is from Mn^{2+} dopant (orange emission). Interestingly, the dual emitting QDC exhibited excitation dependent

tunability in emission color and chromaticity, which is an important factor for solid state lighting of demand and choice.

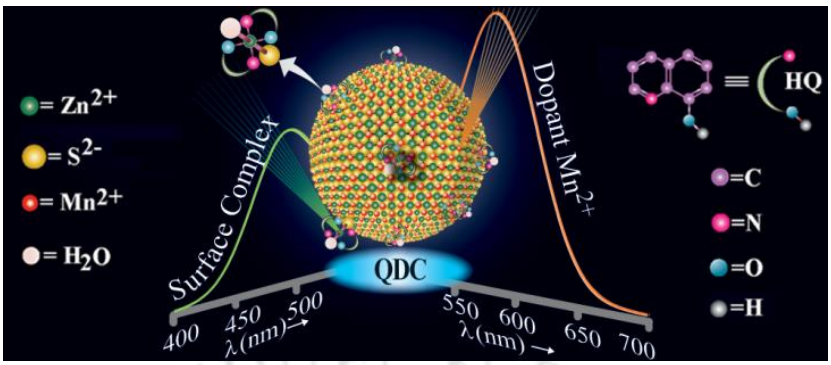

Figure 1.7. Schematic representation of dual color emitting surface complexed Mn^{2+} doped ZnS Qdots (Reprinted with permission from reference 35. Copyright 2015 American Chemical Society)

However, the generation of white light, with chromaticity (and other optical parameters) close to bright day light, is limited due to absence of emission throughout the whole range of visible emission window (400-700 nm) for a single wavelength of excitation. That motivates me to pursue my doctoral thesis towards the fabrication of a single component environment-friendly white light emitting nanocomposite, using the basic concept of the complexation chemistry on the surface of a Qdot, with an aim to use them as a sensing platform for the detection of human diseases.

1.2. Light Emitting Diodes and White Light Emission

The discovery of incandescent bulb in 1880 by Thomas Alva Edison is an epochal breakthrough in artificial lighting.[45] However, the high energy consumption of Edison's bulb is calling for another revolution in lighting applications to fabricate highly efficient light emitting devices. In recent times, the next generation illumination system, light emitting diode (LED) is a breakthrough solution for growing global energy consumption. The high brightness, longer lifetime, lower energy consumption and higher efficiencies of LEDs have the potential to replace the traditional light sources and subsequently revolutionize the artificial lighting industry market.[46-55] Until the last two decades, LEDs were able to generate only yellow, red and green color emissions, which limited their applications in fabricating signals and indicators. Next, the discovery of high efficiency GaN based blue LEDs led to an era of fabricating white light emitting diode based on the

coating of yellow phosphors on blue GaN. This is apt for the dream to replace the conventional lighting devices from our day to day life. The white light emitting device has a variety of applications in household lamp, street light, headlight of automobile, camera flash and in smartphone. However, the fabrication of white light emitting materials has several downsides, which need to be addressed properly in a simple, cost effective and eco-friendly way.[47,54-55] The nanomaterials, especially the Qdots (due to high brightness, longer stability, and easy processability) is one of the potential candidate for fabrication of high efficient white LEDs. There are mainly two approaches to achieve white light emission – one is multicomponent based and another one is single component based.[55] The details are discussed in the subsequent section.

1.2.1. Multicomponent System

Multicomponent based method, a conventional technique to generate white light emission from Qdots, could be achieved in two ways, the details is described in the following section.

(i) Color mixing – In this approach, discrete color emitting Qdots are blended together to get white light emission. In this case, the white light emitting material could be fabricated either based on the combinations of the three primary colors such as, red, green, and blue emitting Qdots or two complementary colors (blue and yellow).[46-57] As for example, a blue emitting carbon dot is mixed with green and red emitting ZnCuInS core/shell Qdot in order to achieve white light emission (Figure 1.8).[56]

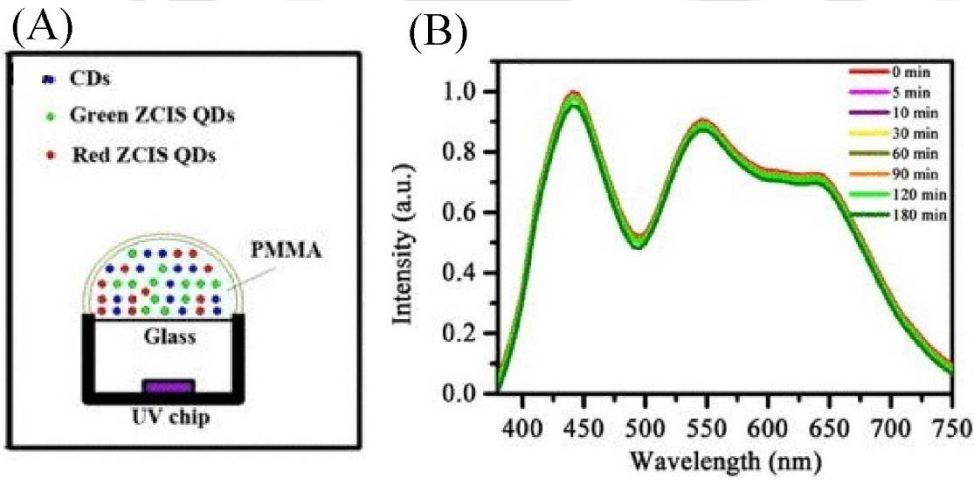

Figure 1.8. (A) Schematic representation of white light emitting diode (WLED) – contained the mixture of blue carbon dots (CDs), red and green emitting ZnCuInS (ZCIS) Qdots over a UV chip. **(B)** Electroluminescence spectra of a WLED at different time intervals. (Reprinted with permission from reference 56. Copyright 2014 American Institute of Physics)

(ii) Phosphor coating – In this method, yellow emitting cerium doped yttrium aluminum garnet (Ce:YAG) phosphor is coated on a blue LED chip. Here, blue LED is used as a excitation source, which excites the Ce:YAG phosphor to emit the yellow light and the balanced combination of yellow and blue light as a whole produces white light.[46-55] For example, yellow emitting $CuInS_2$/ZnS Qdots is coated on a blue LED to get the desired white light emission.[58]

1.2.1.1. Disadvantages of Multicomponent System

However, both the aforementioned approaches have several drawbacks, which reduce the efficiencies and color rendering indexes of the white light emitting devices.[59-66] For color mixing approaches, there is a complexity of homogeneous blending of the discrete color emitting Qdots and need of sophisticated optics. Apart from that, the color aging, self-absorption, nonradiative energy transfer, undesirable changes in chromaticity color coordinates and complicated processing technique of these methods lead to a low efficiency white light emitting devices.[59] In this regard, a single-component Qdot based white light emitting nanocomposite would be a superior alternative for white light emitting devices.

1.2.2. Single-component System

Single component white light emitting systems are much more advantageous than multicomponent systems and have the potential to surmount the aforesaid shortcomings.[59-66] This could simplify the fabrication processes of white lighting devices. There are few reports on single component based white light emitting systems. Some literature reports suggest that by controlling the extent of doping in the crystals lattice of Qdots or functionalizing the organic molecule on the surface of a Qdot white light emission could be generated. As for example, a white light emission has been achieved through co-doping of Mn and Cu in ZnSe Qdots. The Mn and Cu are incorporated in the host matrix of ZnSe in such a way that the emission characteristics of both the dopants remain intact in the host matrix. The combination of two dopant emissions of doubly doped Qdots, one at 490 nm (due to Cu ion) and another at 585 nm (due to Mn ion), led to the generation of white light emission (Figure 1.9.).[59-60] In another work, surface functionalization of Qdot was used as a tool to get white light emission. For instance, a single white light emitting nanostructures has been synthesized through binding of a blue fluorescent oligofluorene on the silica surface, which was coated on an orange emitting core/shell (CdSe/ZnS) Qdots (Figure 1.10).[61]

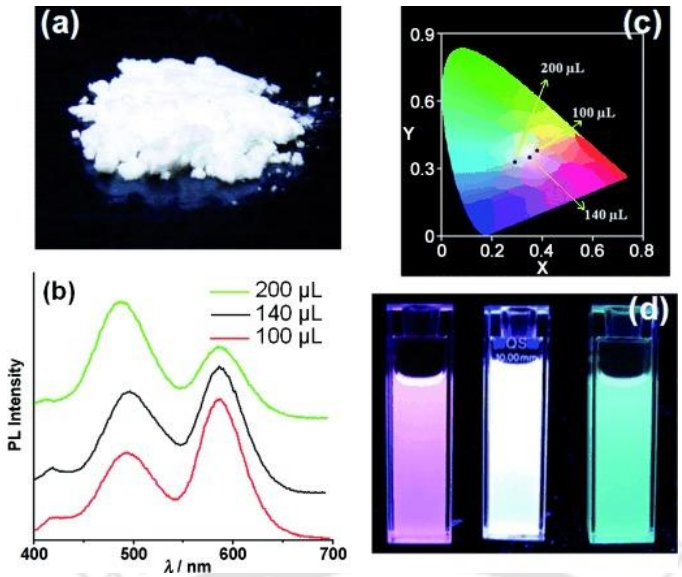

Figure 1.9. (a) Digital photograph of white light emitting Cu and Mn co-doped ZnSe Qdots in solid state. **(b)** Emission spectra, **(c)** CIE chromaticity diagram and **(d)** solution phase digital photograph of Cu and Mn co-doped ZnSe Qdots with varying amount of Cu precursor. (Reprinted with permission from reference 59. Copyright 2011 John Wiley and Sons)

Apart from that, it is also possible to generate a Qdot based single component white light emitting nanocomposite without functionalizing the organic dye on the surface or atomic doping in the host matrix of Qdots. Literature reports suggest that by controlling the broad trap state emission of Qdots (during synthesis) white light emission could be acheived.[58-61] As for example, a white light emission has been achieved from a pyrolytically synthesized magic sized CdSe Qdots. The narrow size distribution and large Stokes shift of this ultra-small sized Qdots resulted in broad emission covering the whole visible region and thus to the generation of white light emission (Figure 1.11). [61]

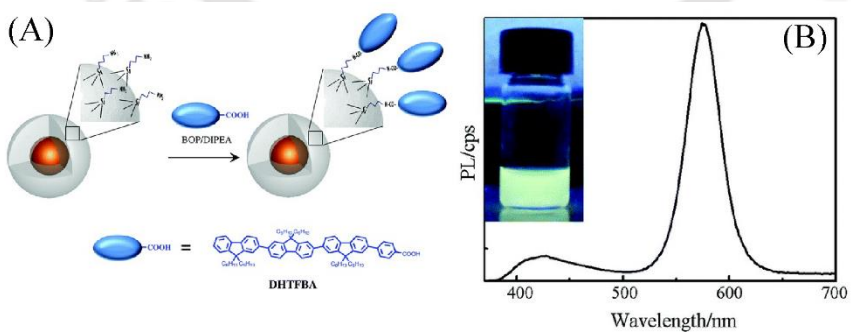

Figure 1.10. (A) Schematic representation of fabrication of white light emitting nanostructures. Silica coated CdSe/ZnS Qdots was functionalized with blue emitting oligofluorene to get white light emission. **(B)** Emission spectrum and digital photograph of white light emitting nanostructures. (Reprinted with permission from reference 61. Copyright 2014 The Royal Society of Chemistry)

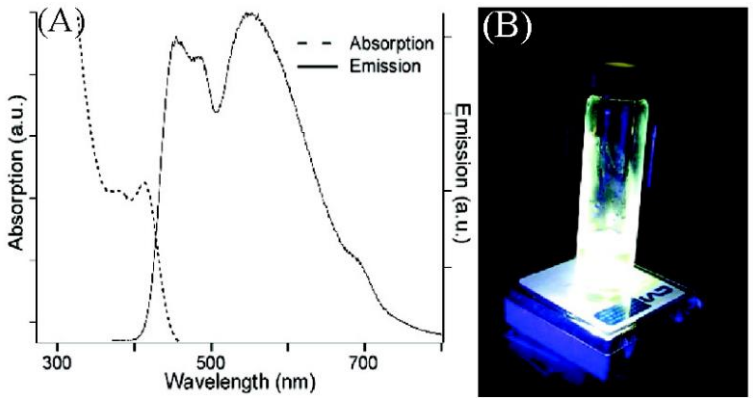

Figure 1.11. (A) Absorption and emission spectrum, and (B) digital photograph of magic sized white light emitting CdSe Qdots. (Reprinted with permission from reference 66. Copyright 2005 American Chemical Society)

However, the aforementioned white light generation strategies have some serious drawbacks. The photobleaching and difficulties in controlling the covalent binding restricted the applications of the white light emitting systems fabricated based on the functionalization of Qdots with organic dyes. On the other hand, the delicate balance of the emission maximum from the dopant and/or size of Qdots is an essential requirement to achieve white light emission through doping and/or size based strategies. However, it is difficult to achieve the white light emission by either controlling ratio of the dopant or size distribution during synthesis. Additionally, the use of toxic Qdots for white light generation limited their practical applications. In these circumstances, a non-toxic and easy to process single component Qdot-based nanocomposite, having the broad emission throughout the visible window, is strongly desirable. This motivates me to come up with the idea of the formation of different luminescent inorganic complexes on the surface of a non-toxic Qdots to achieve a single component biofriendly white light emitting nanocomposite. In this regard, the room temperature post synthetic surface functionalization of the Qdots with highly luminescent and very stable inorganic complexes makes the fabrication process easier and user friendly for fabricating white light emitting materials. The choice of suitable complexing agent and the extent of complexation reaction on the surface are the crucial factors to attain white light emission from the surface complexed Qdots. The present thesis will address the four possibilities of the generation of a white light emission from a Qdot using surface complexation reaction and consequently use one of them as an optical sensor for detecting the human diseases, based on the changes in the visual color, chromaticity and blinking patterns.

1.3 Quantum Dot based Optical Sensors

Understanding the biological environment is a key criterion for early diagnosis of diseases. To exploit this, detection and quantification of toxic elements and molecules causing human diseases become important for developing sensors and biodiagnostics devices. Recently, a lot of attention has been devoted to the nanoparticles, especially Qdots, for development of optical nanoprobes.[67-74] The unique optical properties and ease of the surface functionalization of Qdots, provide them with handy platforms for designing versatile and sensitive optical sensors. There are two conventional methods for luminescence based sensing: one is emission intensity dependent signal acquisition and another is ratiometric optical approach. However, in the quenching based sensing of analytes, using a nanoprobe with single wavelength emission, the emission intensity may fluctuate due to presence of several analyte-independent factors such as instrumental factors or changes in local environments, which lead to the inaccurate determination of analyte specificity. Additionally, visual detection using this kind of nanoprobe is not possible since after interaction with the analyte the nanoprobe may become colorless. On the other hand, ratiometric sensors could surmount the issues related to absolute intensity dependent nanoprobe and be able to provide more accurate and sensitive detection of analyte.[67,73] Ratiometric nanoprobes provide self-calibration of signal reading, where one emission peak acts as a reference signal to the other emission peak.[67] This can be achieved by attaching one or two dye molecule on the surface of Qdots. However, the combination of two or more independent emissive systems for making ratiometric nanoprobe may be limited due to their complicated fabrication procedure.

In response to these challenges, an approach to implement a visual detection of analyte with the help of a chemically combined Qdots with inorganic complex. There are a huge number of literature reports on luminescent sensors using the Qdots but none of them reported the white light emitting nanomaterial based visual detection. The reaction or interaction of analyte with one of the specific components of white light emitting material led to generation of different color and chromaticity. Thus, white light emitting inorganic complex coupled Qdots could be used for fabrication of sensitive and target specific optical sensors. In this thesis, a highly sensitive and selective method for visual detection of a neurotransmitter (here dopamine is used), following interaction with white light emitting quantum dot complex, is described.

Dopamine, a redox active neurotransmitter, plays a vital role in the human brain activity and behaviours such as sleep, attention, cognition, motivation, and learning. Importantly, the abnormal content, especially at lower level, of dopamine in biological fluids (such as extracellular fluid of the central nervous system, urine and blood plasma), may indicate neurological disorders and several nervous system diseases, such as Parkinson's disease and schizophrenia. Thus, the detection of dopamine is significant for practical clinical diagnosis.[74-75]

However, the ultrasensitive detection and accurate quantification of the target molecules are not possible through ensemble studies. Thus, the high sensitivity and accurate quantification is highly desirable and that could be achieved only when the sensing of analyte at single particle level is possible.

1.3.1 Sensing at Single Particle Level

The exciting properties of a Qdots at single molecular resolution remain largely to be explored. Sensing or detection of molecule at single particle level provides a platform to accurately quantify the target molecule and understand the mechanistic pathway. In contrast to the conventional ensemble studies, the single particle based measurements offers several advantages such as ultra-sensitivity, low sample requirement, fast analysis, and high signal to noise ratio. This may have significant impact for quantitative sensing of analytes and thus on the development of ultrasensitive biosensors. [76-82]

1.3.1.1 Blinking in Single Qdots

The fluorescence intermittency or blinking is a unique signature of a single Qdot.[83-88] The blinking has been considered as a blessing in disguise for single molecule studies because it can be used as a tool to detect the single Qdots. However, for various technological applications blinking is an obstacle where high photoluminescence quantum yield is desirable. Fluorescence intermittency or blinking is a distinctive property of single particle or single molecule, where the emission intensity of the single entity switches between "on" (emitting state) and "off" (non-emitting state) state in presence of a continuous illumination of light.[83-88] The origin of blinking in Qdots is still subject of extensive research. However, a number of literature reports suggest various models to explain the reason behind the blinking of Qdots, among them the widely accepted model is trap state assisted Auger recombination.[83-88] The Qdots exhibit

fluctuation in emission intensity in between on and off state because of photoinduced charging (on→off) and following re-neutralization (off→on) of Qdots. Most probably the four process – radiative recombination, trapping, de-trapping, and nonradiative Auger recombination is responsible for the blinking phenomenon in Qdots (Figure 1.12).[85,86,89]

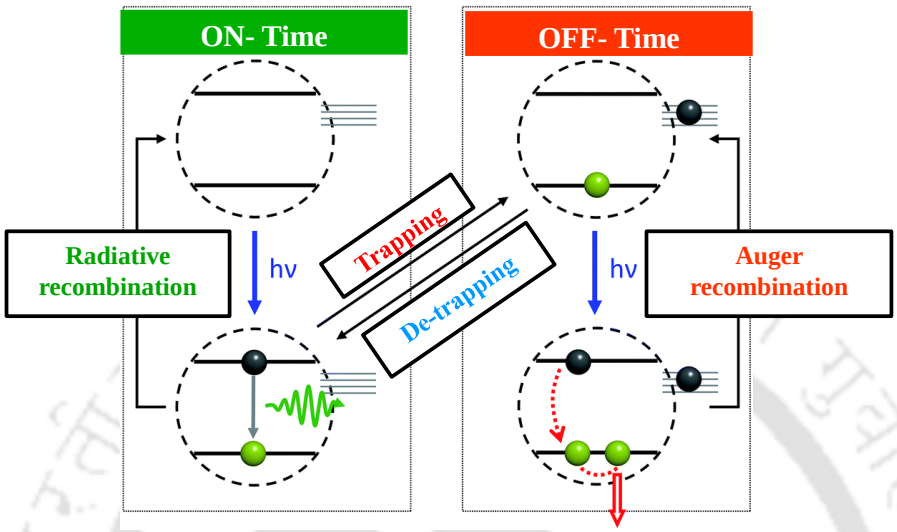

Figure 1.12. Schematic diagram of different phenomena that controls the photoluminescence blinking processes in Qdots (Reprinted with permission from reference 89. Copyright 2016 The Royal Society of Chemistry)

Under photoexcitation an uncharged Qdot generates an electron-hole pair (exciton), which recombine radiatively to emit a photon (on state). But in presence of excess charge carrier the exciton energy non-radiatively is transferred to another charge carrier instead of photon emission and in turn off state occurs. This process is known as Auger recombination.[85,86,89] Hence, the on and off times of a blinking trajectory rely on the lifetimes of charged and neutral state of Qdots, which directly correlate with the rate of de-trapping and trapping processes.[89]

1.3.1.2 Blinking Statistics of Single Qdots

Single molecule spectroscopic analysis reveals wealth information about the photophysical phenomena involving Qdots. Blinking statistics is an important tool to understand the photophysical behavior of Qdots. For quantitative analysis of the blinking traces a probability density function is calculated using the binning time and distribution of on and off time events.[90-93] The probability density is calculated using the following equation – $P_{(i)}(t) = \frac{N_i(t)}{N_{i,total}} \times \frac{1}{\Delta t_{i,av}}$; (i= on or off). Here P_i is the probability density of

on or off events at time t, N_i is the number of on or off events, $N_{i,total}$ is the total number of events and $\Delta t_{i,av}$ is average of the time intervals of the procedding and following events. This probability densities of the blinking traces in Qdots generally follow power law or truncated power law statistics. The truncated power law is $P_i(t) = At^{-\alpha}e^{-t\tau}$; (i=on or off) where A= amplitude, α= power law exponent, τ = saturation rate. The power law exponent is an important parameter to describe the changes in blinking dynamics. For Qdots, the values of power law exponent typically found within the range of 1 to 2.[93] This exponent value reflects the duration of the corresponding events in the blinking traces, the higher the value of the exponent lesser the time duration of that corresponding events (e.g. if the α_{on} value is higher than α_{off} value, then the particle will be at on state for smaller duration of time compared to their off state). The power law exponents largely depends on the emission characteristics of Qdots, which are related to the surface functionalization and surrounding environment. Therefore, the power exponents could be considered as significant parameters to describe the consequences of chemical reactions or physical alteration on the surface of Qdots.

1.3.1.3 Applications of Single Qdots

(i) Single Particle Tracking – The application of Qdots as a fluorescent biomarker is largely extended with the development of advanced techniques for single particle tracking.[79,94] The use of single Qdot as a nanoprobe can elucidate various biological processes in a living body. Using the single Qdot, imaging and tracking techniques of various protein targets such as nerve growth factor, glycine receptor, and serotonin transporter have been successfully tracked and well demonstrated.[94-99] The application window has been further extended to single Qdot as nanocarriers for in vivo drug delivery and as artificial cargo of synaptic vesicle for neurotransmitter secretion.

(ii) Single Qdot based Detection – Single Qdot based nanosensor has the potential to detect the analyte with ultrahigh sensitivity and accurate quantification of target molecules. Ultrasensitive detection of point mutation, multiplexed of HIV-1 and HIV-2 DNAs, miRNA have been demonstrated by using single Qdot based DNA and RNA assay.[100-103] Additionally,the single Qdot based enzyme activity assay of different enzymes (such as ATPase, telomerase, DNA glycosylase, alkaline phosphatase, and renin) have been developed.[104-108] Apart from that, important biological small molecules

such as glucose, galactose, and maltose have been detected by using the single Qdot based optical nanoprobe.[109-110]

However, the detection and accurate quantification of biomolecule (which are usually responsible for causing human diseases) at single particle level based on the variation of blinking statistics of a white light emitting single Qdot is yet to be explored. In this thesis, a highly sensitive and selective method for the visual detection of a neurotransmitter (dopamine) at single particle level using white light emitting single QDC has been demonstrated. Hence, the study of single WLE QDC will bring a newer paradigm towards the understanding of their photophysical behaviours at single particle resolution and developing powerful methodology for the development of ultrasensitive biosensors.

1.4 Overview of the Thesis

The main focus of the thesis is the formation of luminescent inorganic complexes on the surface of Qdots to synthesize single component white light emitting nanocomposites and then use this white light emitting Qdot complex for sensitive detection and quantification of important biomolecules at single Qdot level. The thesis contains four individual research work and the work highlights are listed below.

Chapter 2 describes the formation of single component photostable white light emitting nanocomposite based on the simultaneous formation of two different inorganic complex (blue emitting metal acetylsalicylates ($M(ASA)_2$ where $M:Mn^{2+}/Zn^{2+}$ and ASA=acetylsalicylic acid) and green emitting zinc quinolate (ZnQ_2)) on the surface of a presynthesized orange emitting Mn^{2+} doped ZnS Qdot. The complexed Qdot is called herein as quantum dot complex (QDC).

Chapter 3 discusses the fabrication of a bio-friendly white light emitting nanocomposite by incorporating green emitting QDC (being composed of ZnQ_2 complex and ZnS Qdot) in a blue protein matrix - consisted of red emitting gold nanocluster.

Chapter 4 demonstrates the fabrication of a high temperature sustainable single component WLE nanocomposite, with properties close to day bright light in terms of the

chromaticity, color rendering index (CRI) and correlated color temperature (CCT), by forming a greenish blue ZnQ_2 complex on the shell surface of a red emitting $CuInS_2$/ZnS core/shell Qdot.

Chapter 5 describes the utilization of a nontoxic white light emitting nanocomposite, fabricated based on the formation of blue emitting $Zn(MSA)_2$ (MSA=N-methylsalicylaldimine) complex on the surface of a yellow emitting ZnO Qdot, toward detection of the neurotransmitter dopamine at possibly single particle level. This was achieved by monitoring the changes in the visual color, chromaticity and on/off blinking characteristics of a single white light emitting QDC.

Chapter 6 contains conclusion of the thesis and future prospects.

References:

1. Rogach, A. L Quantum Dots Still Shining Strong 30 Years On *ACS Nano* **2014**, *8*, 6511–6512.

2. Kovalenko, M. V.; Manna, L.; Cabot, A.; Hens, Z.; Talapin, D. V.; Kagan, C. R.; Klimov, V. I.; Rogach, A. L.; Reiss, P.; Milliron, D. J.; Guyot-Sionnnest, P.; Konstantatos, G.; Parak, W. J.; Hyeon, T.; Korgel, B. A.; Murray, C. B.; Heiss, W. Prospects of Nanoscience with Nanocrystals *ACS Nano* **2015**, *9*, 1012−1057.

3. Owen, J.; Brus, L. Chemical Synthesis and Luminescence Applications of Colloidal Semiconductor Quantum Dots *J. Am. Chem. Soc.* **2017**, *139*, 10939−10943

4. Kim, J. Y.; Voznyy, O.; Zhitomirsky, D.; Sargent, E. H. 25th Anniversary Article: Colloidal Quantum Dot Materials and Devices: A Quarter- Century of Advances. *Adv. Mater*. **2013**, 25, 4986–5010

5. Pietryga, J. M.; Park, Y.-S.; Lim, J.; Fidler, A. F.; Bae, W. K.; Brovelli, S.; Klimov, V. I. Spectroscopic and Device Aspects of Nanocrystal Quantum Dots *Chem. Rev.* **2016**, 116, 10513– 10622.

6. Smith, A. M.; Nie, S. Semiconductor Nanocrystals: Structure, Properties, and Band Gap Engineering *Acc. Chem. Res.* **2010**, *43*, 190-200.

7. Ekimov A. I.; Onushchenko A. A. Quantum Size Effect in Three-dimensional Microscopic Semiconductor Crystals *JETP Lett.* **1981**, *6*, 345–349.

8. Rossetti, R.; Nakahara, S.; Brus, L. E. Quantum Size Effects in the Redox Potentials, Resonance Raman Spectra, and Electronic Spectra of CdS Crystallites in Aqueous Solutions *J. Chem. Phys*. **1983**, *79*, 1086-1088.

9. Reed, M. A.; Randall, J. N.; Aggarwal, R. J.; Matyi, R. J.; Moore, T. M.; Wetsel, A. E. Observation of Discrete Electronic States in a Zero-dimensional Semiconductor Nanostructure *Phys Rev Lett.* **1988**, *60*, 535–537.

10. Murray, C. B.; Norris, D. J.; Bawendi, M. G. Synthesis and Characterization of Nearly Monodisperse CdE (E = Sulfur, Selenium, Tellurium) Semiconductor Nanocrystallites. *J. Am. Chem. Soc.* **1993**, 115, 8706–8715.

11. Kamat, P. V. Semiconductor Surface Chemistry as Holy Grail in Photocatalysis and Photovoltaics. *Acc. Chem. Res.* **2017**, *50*, 527−531.

12. Weiss, E.A. Designing the Surfaces of Semiconductor Quantum Dots for Colloidal Photocatalysis. *ACS Energy Lett*. **2017**, *2*, 1005−1013

13. Hildebrandt, N.; Spillmann, C. M.; Algar, W. R.; Pons, T.; Stewart, M. H.; Oh, E.; Susumu, K.; Diaz, S. A.; Delehanty, J. B.; Medintz, I. L., Energy Transfer with Semiconductor Quantum Dot Bioconjugates: A Versatile Platform for Biosensing, Energy harvesting, and other Developing Applications. *Chem. Rev.* **2016,** *117*, 536-711.

14. Medintz, I. L.; Stewart, M. H.; Trammell, S. A.; Susumu, K.; Delehanty, J. B.; Mei, B. C.; Melinger, J. S.; Balnco-Canosa, J. B.; Dawson, P. E.; Mattoussi, H. Quantum-

Dot/Dopamine Bioconjugates Function as Redox Coupled Assemblies for In Vitro and Intracellular pH Sensing *Nat. Mater*. **2010**, *9*, 676– 684.

15. Sato, S.; Arai, T.; Morikawa, T.; Uemura, K.; Suzuki, T. M.; Tanaka, H.; Kajino, T. Selective CO2 Conversion to Formate Conjugated with H_2O Oxidation Utilizing Semiconductor/Complex Hybrid Photocatalysts. *J. Am. Chem. Soc*. **2011**, *133*, 15240–15243.

16. Brus, L. E. Electron-electron and electron-hole interactions in small semiconductor crystallites: The size dependence of the lowest excited electronic state *J. Chem. Phys.*, **1984**, *80*, 4403-4409.

17. Kippeny, T.; Swafford, L. A.; Rosenthal, S. J. Semiconductor nanocrystals: A Powerful Visual Aid for Introducing the Particle in a Box. *J. Chem. Ed.* **2002,** *79*, 1094-1100.

18. Murphy, C. J.; Coffer, J. L. Quantum Dots: A Primer *Applied Spectroscopy* **2002**, *56*, 16A-27A

19. Rogach, A. L.; Talapin, D. V.; Shevchenko, E. V.; Kornowski, A.; Haase, M.; Weller, H., Organization of matter on different size scales: monodisperse nanocrystals and their superstructures. *Adv. Funct. Mater.* **2002,** *12*, 653-664.

20. Talapin, D. V.; Rogach, A. L.; Kornowski, A.; Haase, M.; Weller, H. HighlyLuminescent Monodisperse CdSe and CdSe/ZnS Nanocrystals Synthesized in aHexadecylamine−Trioctylphosphine Oxide−Trioctylphospine Mixture. *Nano Lett.***2001,** *1*, 207-211.

21. Pradhan, N.; Adhikari, S. D.; Nag, A.; Sarma, D. D. Luminescence, Plasmonic and Magnetic Properties of Doped Semiconductor Nanocrystals: Current Developments and Future Prospects *Angew. Chem., Int. Ed.* **2017**, 56, 7038 – 7054.

22. Luther, J. M.; Pietryga, J. M. Stoichiometry Control in Quantum Dots: A Viable analog to Impurity Doping of Bulk Materials. *ACS Nano* **2013**, *7*, 1845–1849.

23. Pandey, A.; Sarma, D. D. Recent Advances in Manganese Doped II-VI Semiconductor Quantum Dots. *Z. Anorg. Allg. Chem.* **2016,** *642* , 1331-1339.

24. Tavasoli, E.; Guo, Y.; Kunal, P.; Grajeda, J.; Gerber, A.; Vela, J. Surface Doping Quantum Dots with Chemically Active Native Ligands: Controlling Valence without Ligand Exchange. *Chem. Mater.* **2012,** *24*, 4231-4241.

25. Kamat, P. V. Semiconductor Nanocrystals: To Dope or Not to Dope *J. Phys. Chem. Lett.*, **2011**, *2*, 2832–2833.

26. Begum, R.; Chattopadhyay, A. Redox-Tuned Three-Color Emission in Double (Mn and Cu) Doped Zinc Sulfide Quantum Dots *J. Phys. Chem. Lett.* **2014**, *5*, 126– 130.

27. Hazarika, A.; Pandey, A.; Sarma, D. D. Rainbow Emission from an Atomic Transition in Doped Quantum Dots *J. Phys. Chem. Lett.* **2014**, *5*, 2208– 2213.

28. Pradhan, N.; Sarma, D. D. Advances in Light-Emitting Doped Semiconductor Nanocrystals *J. Phys. Chem. Lett.* **2011**, *2*, 2818– 2826.

29. Boles, M. A.; Ling, D.; Hyeon, T.; Talapin, D. V., The surface science of nanocrystals. *Nat. Mater.***2016,** *15*, 141-153

30. Hines, D. A.; Kamat, P. V. Recent Advances in Quantum Dot Surface Chemistry *ACS Appl. Mater. Interfaces* **2014**, *6*, 3041– 3057.

31. Frederick, M. T.; Amin, V. A.; Weiss, E. A. Optical Properties of Strongly Coupled Quantum Dot−Ligand Systems. *J. Phys. Chem. Lett.* **2013**, 4, 634−640.

32. Owen, J. The Coordination Chemistry of Nanocrystal Surfaces. *Science* **2015***, 347,* 615-616.

33. McBride, J.; Treadway, J.; Feldman, L. C.; Pennycook, S. J.; Rosenthal, S. J. Structural basis for near unity quantum yield core/shell nanostructures. *Nano Lett.* **2006**, *6*, 1496–1501.

34. Dabbousi, B. O.; Rodriguez-Viejo, J.; Mikulec, F. V.; Heine, J. R.; Mattoussi, H.; Ober, R.; Jensen, K. F.; Bawendi, M. G. (CdSe)ZnS core-shell quantum dots: Synthesis and characterization of a size series of highly luminescent nanocrystallites. *J. Phys. Chem. B* **1997**, *101*, 9463–9475.

35. Hines, M. A.; Guyot-Sionnest, P. Synthesis and characterization of strongly luminescing ZnS-capped CdSe nanocrystals. *J. Phys. Chem.* **1996**, *100*, 468-471.

36. Baker, D. R.; Kamat, P. V. Tuning the Emission of CdSe Quantum Dots by Controlled Trap Enhancement *Langmuir* **2010**, *26*, 11272– 11276.

37. Zhao, C.; Bai, Z.; Liu, X.; Zhang, Y.; Zou, B.; Zhong, H. Small GSH-Capped $CuInS_2$ Quantum Dots: MPA-Assisted Aqueous Phase Transfer and Bioimaging Applications *ACS Appl. Mater. Interfaces* **2015**, 7, 17623– 17629.

38. Bhandari, S.; Roy, S.; Chattopadhyay, A. Enhanced Photoluminescence and Thermal Stability of Zinc Quinolate Following Complexation on the Surface of Quantum Dot. *RSC Adv.* **2014**, *4*, 24217-24221.

39. Bhandari, S.; Roy, S.; Pramanik, S.; Chattopadhyay, A. Surface Complexation Reaction for Phase Transfer of Hydrophobic Quantum Dot from Nonpolar to Polar Medium. *Langmuir* **2014**, *30*, 10760-10765.

40. Bhandari, S.; Roy, S.; Pramanik, S.; Chattopadhyay, A. Double Channel Emission from a Redox Active Single Component Quantum Dot Complex. *Langmuir* **2015,** *31*, 551-561.

41. Bhandari, S.; Khandelia, R.; Pan, U. N.; Chattopadhyay, A. Surface Complexation-Based Biocompatible Magnetofluorescent Nanoprobe for Targeted Cellular Imaging. *ACS Appl. Mater. Interfaces*, **2015**, *7*, 17552–17557.

42. Roy, S.; Bhandari, S.; Chattopadhyay, A. Quantum Dot Surface Mediated Unprecedented Reaction of Zn^{2+} and Copper Quinolate Complex. *J. Phys. Chem. C* **2015**, *119*, 21191– 21197.

43. Kovalenko, M. V.; Scheele, M.; Talapin, D. V. Colloidal Nanocrystals with Molecular Metal Chalcogenide Surface Ligands *Science* **2009**, *324*, 1417– 1420.

44. Kovalenko, M. V.; Bodnarchuk, M. I.; Zaumseil, J.; Lee, J. S.; Talapin, D. V. Expanding the Chemical Versatility of Colloidal Nanocrystals Capped with Molecular Metal Chalcogenide Ligands *J. Am. Chem. Soc.* **2010**, *132*, 10085– 10092.

45. Edison, T. A. Electric Lamp **1880**, *U.S. Patent No. US223898 (A)*.

46. Shang, Y.; Ning, Z., Colloidal quantum-dots surface and device structure engineering for high-performance light-emitting diodes. *Natl. Sci. Rev.* **2017,** *4*, 170-183

47. Su, L.; Zhang, X.; Zhang, Y.; Rogach, A. L., Recent progress in quantum dot based white light-emitting devices. *Top. Curr. Chem.* **2016,** *374*, 42.

48. Yang, Y.; Zheng, Y.; Cao, W.; Titov, A.; Hyvonen, J.; Manders, J. R.; Xue, J.; Holloway, P. H.; Qian, L., High-efficiency light-emitting devices based on quantum dots with tailored nanostructures. *Nat. Photonics* **2015,** *9*, 259-266.

49. Choi, M. K.; Yang, J.; Kang, K.; Kim, D. C.; Choi, C.; Park, C.; Kim, S. J.; Chae, S. I.; Kim, T.-H.; Kim, J. H., Wearable red–green–blue quantum dot light-emitting diode array using high-resolution intaglio transfer printing. *Nat. Commun.***2015,** *6*, 7149

50. Kim, T.-H.; Cho, K.-S.; Lee, E. K.; Lee, S. J.; Chae, J.; Kim, J. W.; Kim, D. H.; Kwon, J.-Y.; Amaratunga, G.; Lee, S. Y., Full-colour quantum dot displays fabricated by transfer printing. *Nat. Photonics* **2011,** *5*, 176-182

51. Wood, V.; Bulović, V., Colloidal quantum dot light-emitting devices. *Nano reviews* **2010,** *1*, 5202.

52. Talapin, D. V.; Lee, J.-S.; Kovalenko, M. V.; Shevchenko, E. V., Prospects of colloidal nanocrystals for electronic and optoelectronic applications. *Chem. Rev.* **2009,** *110*, 389-458.

53. Rogach, A. L.; Gaponik, N.; Lupton, J. M.; Bertoni, C.; Gallardo, D. E.; Dunn, S.; Li Pira, N.; Paderi, M.; Repetto, P.; Romanov, S. G., Light-emitting diodes with semiconductor nanocrystals. *Angew. Chem., Int. Ed.* **2008,** *47*, 6538-6549;

54. Nakamura, S.; Mukai, T.; Senoh, M., Candela-class high-brightness InGaN/AlGaN double-heterostructure blue-light-emitting diodes. *Appl. Phys. Lett.* **1994,** *64*, 1687-1689.

55. Zhao, X. Commercialization of Quantum Dot White Light Emitting Diode Technology. *Massachusetts Institute of Technology*, 2006.

56. Sun, C.; Zhang, Y.; Wang, Y.; Liu, W.; Kalytchuk, S.; Kershaw, S. V.; Zhang, T.; Zhang, X.; Zhao, J.; Yu, W. W.; Rogach, A. L., High color rendering index white light emitting diodes fabricated from a combination of carbon dots and zinc copper indium sulfide quantum dots. *Appl. Phys. Lett.* **2014,** *104*, 261106.

57. Maiti, D.K.; Roy, S.; Baral, A.; Banerjee, A. A Fluorescent Gold-Cluster Containing a New Three Component System for White Light Emission through a Cascade of Energy Transfer. *J. Mater. Chem. C* **2014**, *2*, 6574−6581.

58. Song, W.; Yang, H. Efficient White-Light-Emitting Diodes Fabricated from Highly Fluorescent Copper Indium Sulfide Core/Shell Quantum Do *Chem. Mater.* **2012**, *24*, 1961−1967

59. Panda, S. K.; Hickey, S. G.; Demir, H. V.; Eychmuller, A. Bright White-Light Emitting Manganese and Copper Co-Doped ZnSe Quantum Dots. *Angew. Chem., Int. Ed.* 2011, 50, 4432−4436.

60. Sharma, V. K.; Guzelturk, B.; Erdem, T.; Kelestemur, Y.; Demir, H. V. Tunable White-Light-Emitting Mn-Doped ZnSe Nanocrystals. *ACS Appl. Mater. Interfaces* **2014**, *6*, 3654−3660.

61. Fanizza, E.; Urso, C.; Pinto, V.; Cardone, A.; Ragni, R.; Depalo, N.; Curri, M. L.; Agostiano, A.; Farinola, G. M.; Striccoli, M. Single White Light Emitting Hybrid Nanoarchitectures Based on Functionalized Quantum Dots. *J. Mater. Chem. C* **2014**, *2*, 5286−5291.

62. Kima, N.; Leeb, J.; Ana, H.; Panga, C.; Choa, S. M.; Chaea, H. Color Temperature Control of Quantum Dot White Light Emitting Diodes by Grafting Organic Fluorescent Molecules. *J. Mater. Chem. C* **2014**, *2*, 9800−9804.

63. Sapra, S.; Mayilo, S.; Klar, T. A.; Rogach, A. L.; Feldmann, J. Bright White-Light Emission from Semiconductor Nanocrystals: by Chance and by Design. *Adv. Mater.* **2007**, *19*, 569−572.

64. Nag, A.; Sarma, D. D. White Light from Mn^{2+}-Doped CdS Nanocrystals: A New Approach. *J. Phys. Chem. C* **2007**, *111*, 13641− 13644.

65. Rosson, T. E.; Claiborne, S. M.; McBride, J. R.; Stratton, B. S.; Rosenthal, S. J. Bright White Light Emission from Ultrasmall Cadmium Selenide Nanocrystals. *J. Am. Chem. Soc.* **2012**, *134*, 8006−8009.

66. Bowers, M. J.; McBride, J. R.; Rosenthal, S. J. White-Light Emission from Magic-Sized Cadmium Selenide Nanocrystals *J. Am. Chem. Soc.* **2005** *127*, 44, 15378-15379.

67. Huang, X.; Song, J.; Yung, B. C.; Huang, X.; Xiong, Y.; Chen, X., Ratiometric optical nanoprobes enable accurate molecular detection and imaging. *Chem. Soc. Rev.* **2018,** *47*, 2873-2920

68. Hildebrandt, N.; Spillmann, C. M.; Algar, W. R.; Pons, T.; Stewart, M. H.; Oh, E.; Susumu, K.; Diaz, S. A.; Delehanty, J. B.; Medintz, I. L., Energy transfer with semiconductor quantum dot bioconjugates: A versatile platform for biosensing, energy harvesting, and other developing applications. *Chem. Rev.* **2016,** *117*, 536-711

69. Yao, J.; Yang, M.; Duan, Y., Chemistry, biology, and medicine of fluorescent nanomaterials and related systems: new insights into biosensing, bioimaging, genomics, diagnostics, and therapy. *Chem. Rev.* **2014,** *114*, 6130-6178.

70. Stanisavljevic, M.; Krizkova, S.; Vaculovicova, M.; Kizek, R.; Adam, V., Quantum dots-fluorescence resonance energy transfer-based nanosensors and their application. *Biosens. Bioelectron.* **2015,** *74*, 562-574

71. Wu, P.; Yan, X.-P., Doped quantum dots for chemo/biosensing and bioimaging. *Chem. Soc. Rev.* **2013,** *42*, 5489-5521.

72. Wang, Y.; Hu, R.; Lin, G.; Roy, I.; Yong, K.-T., Functionalized quantum dots for biosensing and bioimaging and concerns on toxicity. *ACS Appl. Mater. Interfaces* **2013,** *5*, 2786-2799;

73. Silvi, S.; Credi, A., Luminescent sensors based on quantum dot–molecule conjugates. *Chem. Soc. Rev.* **2015,** *44*, 4275-4289.

74. Jie, Y.; Wang, N.; Cao, X.; Xu, Y.; Li, T.; Zhang, X.; Wang, Z. L. Self-Powered Triboelectric Nanosensor with Poly(tetrafluoroethylene) Nanoparticle Arrays for Dopamine Detection. *ACS Nano* **2015**, *9*, 8376– 8383.

75. Van Dersarl, J. J.; Mercanzini, A.; Renaud, P. Integration of 2d and 3d Thin Film Glassy Carbon Electrode Arrays for Electrochemical Dopamine Sensing in Flexible Neuroelectronic Implants *Adv. Funct. Mater*. **2015**, *25*, 78– 84.

76. Hu, J.; Wang, Z.-y.; Li, C.-c.; Zhang, C.-y., Advances in single quantum dot-based nanosensors. *Chem. Commun.* **2017,** *53*, 13284-13295.

77. Opperwall, S. R.; Divakaran, A.; Porter, E. G.; Christians, J. A.; Den Hartigh, A. J.; Benson, D. E. Wide Dynamic Range Sensing with Single Quantum Dot Biosensors. *ACS Nano* **2012**, *6*, 8078-8086

78. Ma, F.; Li, Y.; Tang, B.; Zhang, C.-y., Fluorescent biosensors based on single-molecule counting. *Acc. Chem. Res.* **2016,** *49*, 1722-1730.

79. Chang, J. C.; Rosenthal, S. J., Single quantum dot imaging in living cells. *Cellular and Subcellular Nanotechnology*, Springer: 2013, 149-162;

80. Bruni, F.; Pedrini, J.; Bossio, C.; Santiago-Gonzalez, B.; Meinardi, F.; Bae, W. K.; Klimov, V. I.; Lanzani, G.; Brovelli, S., Two-Color Emitting Colloidal Nanocrystals as Single-Particle Ratiometric Probes of Intracellular pH. *Adv. Funct. Mater.* **2017,** *27* 1605533.

81. Scholl, B.; Liu, H. Y.; Long, B. R.; McCarty, O. J.; O'Hare, T.; Druker, B. J.; Vu, T. Q., Single particle quantum dot imaging achieves ultrasensitive detection capabilities for Western immunoblot analysis. *ACS nano* **2009,** *3*, 1318-1328;

82. Bhatia, D.; Arumugam, S.; Nasilowski, M.; Joshi, H.; Wunder, C.; Chambon, V.; Prakash, V.; Grazon, C.; Nadal, B.; Maiti, P. K., Quantum dot-loaded monofunctionalized DNA icosahedra for single-particle tracking of endocytic pathways. *Nat. Nanotechnol.* **2016,** *11*, 1112-1119.

83. Nirmal, M.; Dabboussi, B. O.; Bawendi, M.; Macklin, J. J.; Trautman, J. K.; Harris, T. D.; Brus, L. E. Fluorescence intermittency in single cadmium selenide nanocrystals. *Nature* **1996**, *383*, 802–804.

84. Empedocles, S. A.; Bawendi, M. Spectroscopy of single CdSe nanocrystallites. *Acc. Chem. Res.* **1999**, *32*, 389–396.

85. Efros, A. L.; Nesbitt, D. J. Origin and Control of Blinking in Quantum Dots. *Nat. Nanotechnol*. **2016**, *11*, 661– 671.

86. Galland, C.; Ghosh, Y.; Steinbruck, A.; Sykora, M.; Hollingsworth, J. A.; Klimov, V. I.; Htoon, H. Two Types of Luminescence Blinking Revealed by Spectroelectrochemistry of Single Quantum Dots. *Nature* **2011**, *479*, 203–207

87.Yuan, G.; Gómez, D. E.; Kirkwood, N.; Boldt, K.; Mulvaney, P., Two mechanisms determine quantum dot blinking. *ACS nano* **2018,** *12*, 3397-3405.

88. Krauss, T. D.; Peterson, J. J., Bright future for fluorescence blinking in semiconductor nanocrystals. *J. Phys. Chem. Lett.* **2010,** *1*, 1377-1382.

89. Chung, H.; Cho, K.-S.; Koh, W.-K.; Kim, D.; Kim, J., Composition-dependent trap distributions in CdSe and InP quantum dots probed using photoluminescence blinking dynamics. *Nanoscale* **2016,** *8*, 14109-14116.

90. Kuno, M.; Fromm, D. P.; Hamann, H. F.; Gallagher, A.; Nesbitt, D. J. Nonexponential 'blinking' kinetics of single CdSe quantum dots: a universal power law behavior. *J. Chem. Phys.* **2000** *, 112***,** 3117–3120.

91. Kuno, M., Fromm, D. P., Hamann, H. F., Gallagher, A. & Nesbitt, D. J. 'On/off' fluorescence intermittency of single semiconductor quantum dots. *J. Chem. Phys.* **2001**, *115***,** 1028–1040.

92. Shimizu, K. T.; Neuhauser, R. G.; Leatherdale, C. A.; Empedocles, S. A.; Woo, W.; Bawendi, M. G., Blinking statistics in single semiconductor nanocrystal quantum dots. *Phys. Rev. B* **2001,** *63*, 205316.

93. Suppressing the Fluorescence Blinking of Single Quantum Dots Encased in N-type Semiconductor Nanoparticles. Li, B.; Zhang, G. F.; Wang, Z.; Li, Z. J.; Chen, R. Y.; Qin, C. B.; Gao, Y.; Xiao, L. T.; Jia, S. T. *Sci. Rep*. **2016**, *6*, 32662.

94. Shen, H.; Tauzin, L. J.; Baiyasi, R.; Wang, W.; Moringo, N.; Shuang, B.; Landes, C. F. Single Particle Tracking: From Theory to Biophysical Applications *Chem. Rev.* **2017,** *117*, 7331– 7376.

95. Dahan, M.; Levi, S.; Luccardini, C.; Rostaing, P.; Riveau, B.; Triller, A. Diffusion dynamics of glycine receptors revealed by single-quantum dot tracking *Science* **2003**, *302*, 442–445

96. Cui, B.; Wu, C.; Chen, L.; Ramirez, A.; Bearer, E. L.; Li, W.-P.; Mobley, W. C.; Chu, S., One at a time, live tracking of NGF axonal transport using quantum dots. *Proc. Natl. Acad. Sci. U. S. A.* **2007,** *104*, 13666-13671.

97. Chang, J. C.; Tomlinson, I. D.; Warnement, M. R.; Ustione, A.; Carneiro, A. M.; Piston, D. W.; Blakely, R. D.; Rosenthal, S. J., Single molecule analysis of serotonin transporter regulation using antagonist-conjugated quantum dots reveals restricted, p38 MAPK-dependent mobilization underlying uptake activation. *J. Neurosci.* **2012,** *32*, 8919-8929.

98. Tada, H.; Higuchi, H.; Wanatabe, T. M.; Ohuchi, N., In vivo real-time tracking of single quantum dots conjugated with monoclonal anti-HER2 antibody in tumors of mice. *Cancer Res.* **2007,** *67*, 1138-1144.

99. Ehrensperger, M.-V.; Hanus, C.; Vannier, C.; Triller, A.; Dahan, M., Multiple association states between glycine receptors and gephyrin identified by SPT analysis. *Biophys. J.* **2007,** *92*, 3706-3718.

100. Zhang, C.-Y.; Yeh, H.-C.; Kuroki, M. T.; Wang, T.-H., Single-quantum-dot-based DNA nanosensor. *Nat. Mater.***2005,** *4*, 826-831.

101. Zhang, C.-y.; Hu, J., Single quantum dot-based nanosensor for multiple DNA detection. *Anal. Chem.* **2010,** *82*, 1921-1927.

102. Lin, S.; Gregory, R. I., MicroRNA biogenesis pathways in cancer. *Nat Rev Cancer.* **2015,** *15*, 321-333.

103. Pritchard, C. C.; Cheng, H. H.; Tewari, M., MicroRNA profiling: approaches and considerations. *Nat Rev Genet.***2012,** *13*, 358-359.

104. Hsin, T. M.; Yeung, E. S., Single-Molecule Reactions in Liposomes. *Angew. Chem., Int. Ed.* **2007,** *46*, 8032-8035.

105. Long, Y.; Zhang, L.-f.; Zhang, Y.; Zhang, C.-y., Single quantum dot based nanosensor for renin assay. *Anal. Chem.* **2012,** *84*, 8846-8852.

106. Sugawa, M.; Nishikawa, S.; Iwane, A. H.; Biju, V.; Yanagida, T., Single-Molecule FRET Imaging for Enzymatic Reactions at High Ligand Concentrations. *Small* **2010,** *6*, 346-350.

107. Wang, L.-j.; Ma, F.; Tang, B.; Zhang, C.-y., Base-excision-repair-induced construction of a single quantum-dot-based sensor for sensitive detection of DNA glycosylase activity. *Anal. Chem.* **2016,** *88*, 7523-7529.

108. Zhu, G.; Yang, K.; Zhang, C.-y., A single quantum dot-based biosensor for telomerase assay. *Chem. Commun.***2015,** *51*, 6808-6811

109. Medintz, I. L.; Clapp, A. R.; Mattoussi, H.; Goldman, E. R.; Fisher, B.; Mauro, J. M., Self-assembled nanoscale biosensors based on quantum dot FRET donors. *Nat. Mater.* **2003,** *2*, 630.

110. Freeman, R.; Bahshi, L.; Finder, T.; Gill, R.; Willner, I., Competitive analysis of saccharides or dopamine by boronic acid-functionalized CdSe–ZnS quantum dots. *Chem. Commun.* **2009,** 764-766.

Chapter 2

Synchronous Tricolor Emission-Based White Light from Quantum Dot Complex

The generation of synchronous tricolor emission for a single wavelength excitation from a quantum dot complex (QDC) is described here. The single-component QDC was formed out of a complexation reaction, at room temperature, between ligand free Mn^{2+}-doped ZnS quantum dots (Qdots) and a mixture of two organic ligands (acetylsalicylic acid and 8-hydroxyquinoline). Furthermore, the tunability in chromaticity color coordinates, which is important for solid-state lighting, was achieved following the synthesis of QDC. Moreover, the photostable QDC emitted white light (λ_{ex} - 320 nm) with (0.30, 0.33) and (0.32, 0.32) chromaticity color coordinates in the liquid and the solid phases, respectively. Hence, the white light-emitting QDC may be a superior material for light-emitting applications.

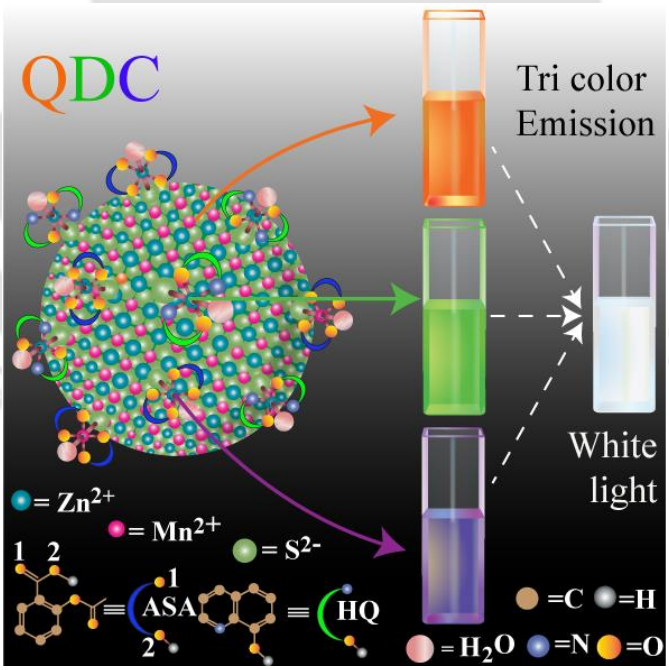

***[*J. Phys. Chem. Lett.* 2015, *6,* 1270−1274] - Reproduced by permission from the American Chemical Society.**

2.1. Experimental Section

2.1.1. Materials. Acetylsalicylic acid (ASA, Sigma-Aldrich), 8-hydroxyquinoline (HQ, Merck), zinc acetate dihydrate (99%, Merck), manganese acetate tetrahydrate (99%, Merck), sodium sulphide (58%, Merck), methanol (Merck), potassium bromide (Sigma-Aldrich), rhodamine 6G (98%, Sigma), quinine sulphate (Sigma-Aldrich) and sulphuric acid (Merck) were used as received without further purification. All the experiments were performed with the use of Mili-Q grade water.

2.1.2. Synthesis of Mn^{+2} doped ZnS quantum dots. Stabilizer-free Mn^{+2} doped ZnS quantum dots (Qdots) were synthesized by simple aqueous precipitation reaction following an earlier reported method.[1] To synthesize bare Mn^{+2} doped ZnS Qdots, 5.0 mM of zinc acetate dihydrate and 0.1 mM of manganese acetate tetrahydrate were dissolved in a 50 mL water under constant stirring at 70-80^{0}C. After 5 min of constant stirring, 5.0 mM of sodium sulphide was added to the reaction mixture and the resulting mixture was refluxed for 3h at 100^{0}C. The so obtained colloidal dispersion was centrifuged at a speed of 25000 rpm for 10 min and the resulting pellet was redispersed in a 50 mL of water under sonication and the same cycle was repeated. Finally, the pellet obtained, after washing and centrifugation cycles (twice), was redispersed into 200 mL Mili-Q water and the colloidal dispersion was used for further experiments.

2.1.3. Preparation of Ligand Solutions.

(i) ASA Solution: 1.0 mM of ASA solution was prepared by dissolving appropriate amount of acetylsalicylic acid in methanol under sonication.

(ii) HQ Solution: Similarly, 1.0 mM of HQ solution was prepared in methanol.

(iii) Ratiometric mixture of ASA and HQ Solution: 1.0 mM methanolic solution of HQ and ASA were mixed with different ratios [(a) 1:0, (b) 4:1, (c) 3:2, (d) 1:1 (e) 2:3, (f) 1:4 and (g) 0:1] to obtain the desired mixtures of the two ligands.

2.1.4. Synthesis of White light emitting (WLE) Quantum Dot Complex (QDC). The synthesis of QDC was carried out following reaction between ligand free Mn^{2+}-doped ZnS Qdots and the mixture of ASA and HQ ligands. Briefly, to 2.0 mL aqueous dispersion of as such Qdots (with absorption value of 0.09 at 320 nm), a solution with a mixture of 1.0 mM ASA and 1.0 mM HQ at different molar ratio was added sequentially. The mixtures were kept at room temperature for 10 min. The resulting mixtures were centrifuged at a speed of 25000 rpm for 20 min. The obtained pellets were

redispersed into the same amount of solvent (water) and was used for further experiments. To have tricolor emission with similar emission intensities at 410, 500 and 588 nm, respectively (when excited by 320 nm light), the QDC was synthesized by adding 1:1 molar ratio of the ASA and HQ to a 2.0 mL water dispersion of the Qdots (at 0.014 mM concentrations). The product QDC was characterized by using UV-vis analysis, photoluminescence, Fourier transform infrared spectroscopy, electron paramagnetic resonance analysis, zeta potential measurement, atomic absorption spectroscopic measurement, x-ray diffraction, transmission electron microscopy, and CIE analysis.

2.1.5. Synthesis and Characterization of $M(ASA)_2.2H_2O$ Complex (M=Zn and Mn):

(A) Synthesis of $Zn(ASA)_2.2H_2O$ Complex. $Zn(ASA)_2.2H_2O$ was synthesized by metathesis reaction, following previously reported methods.[2-3] 10.0 mM of acetylsalicylic acid (ASA) was dissolved in 20 mL hot ethanol with stoichiometric amount of potassium hydroxide pellets in a round bottom flask and the mixture was stirred continuously to obtain the clear solution. Then 5.0 mM of zinc acetate dihydrate was dissolved in minimum amount of water to prevent hydrolysis and added slowly to the reaction mixture. The resulting solution was refluxed at 70 ^{0}C for 1 h with continuous stirring. The so-obtained white precipitates were washed several times with cold water and ethanol solution to remove the unreacted precursor zinc salt and ASA ligand. The washed product was recrystallized in methanol solvent and the so-obtained white crystalline products were used for further experiments.

(B) $Mn(ASA)_2.2H_2O$ Complex Synthesis: Similar procedure (as above) was followed to synthesize $Mn(ASA)_2.2H_2O$ complex by using manganese acetate tetrahydrate as a precursor salt instead of zinc salt.

2.1.6. Control experiments:

(A) Effect of sulphide ions on the optical properties of $M(ASA)_2$ complex (M=Zn and Mn). To 2.0 mL 0.5 mM methanolic solution of the $M(ASA)_2$ complex a pinch of solid sodium sulphide was added and the spectroscopic changes were monitored spectroflurometrically.

(B) Effect of electron quencher (Cu^{2+} ions) on the QDC. 20.0 µL of 5.0 mM of Cu^{2+} solution was added to the 2.0 mL dispersion of Qdots, which led to the quenching of dopant emission. Then the resulting solution was centrifuged and the so-obtained pellet was redispersed into the same amount of solvent and further treated with 1.0 mM methanolic solution of ASA to form the complex on the dopant emission quenched Qdots. Separately, 20.0 µL of 5.0 mM of Cu^{2+} solution was added to the 2.0 mL dispersion of the ASA treated Qdots, then centrifuged and redispersed into same amount of solvent to check the effect of Cu^{2+} on the emission of ASA treated Qdots.

2.2. Results and Discussion

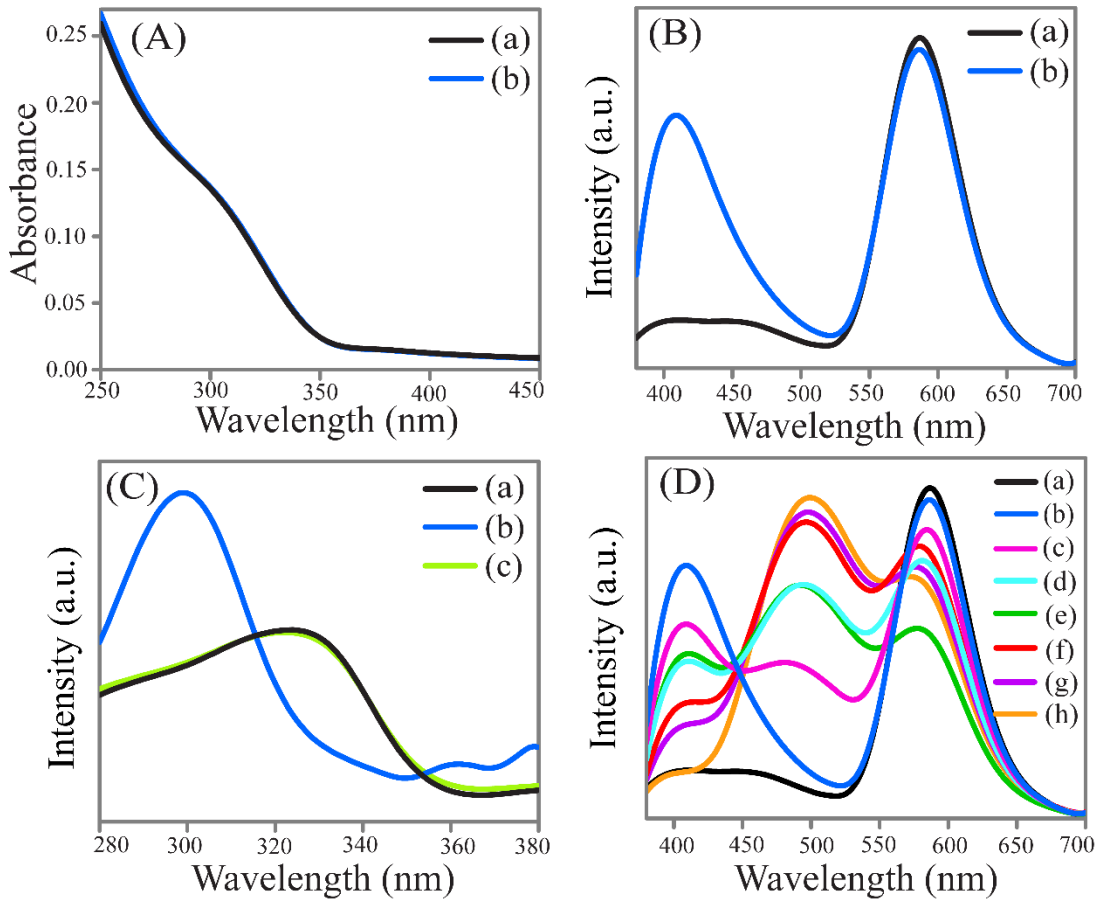

Figure 2.1 (A) UV−vis and **(B)** emission (λ_{ex} = 320 nm) spectra of (a) ligand-free Mn^{2+} doped ZnS Qdots and (b) ASA-added Mn^{2+}-doped ZnS Qdots. **(C)** Excitation spectra of (a) ligand-free Mn^{2+}-doped ZnS Qdots at λ_{em} = 588 nm and (b,c) ASA-added Mn^{2+} doped ZnS Qdots at λ_{em} = 410 and 588 nm, respectively. **(D)** Emission (λ_{ex} = 320 nm) spectra of Qdots following complexation with the mixture of 1.0 mM of ASA and HQ with ratio: (a) 0:0, (b) 1:0, (c) 4:1, (d) 3:2, (e) 1:1 (f) 2:3, (g) 1:4, and (h) 0:1.

The absorption spectrum of the Qdots showed an excitonic band of ZnS at 320 nm (Figure 2.1A) while the emission spectrum (at λ_{ex}-320 nm) of the Qdots consisted of two peaks: a sharp peak at 588 nm due to Mn^{2+} dopants and comparatively broad emission with weaker peaks at 440 nm and 460 nm due to the host ZnS (Figure 2.1B).[1,4-6] When the aqueous dispersion of the Qdots was treated with ASA, there was no significant change in the absorption spectrum (Figure 2.1A) of the Qdots. Even though ASA has an absorption peak at 295 nm (Figure A.2.1 A, Appendix), its concentration on the Qdot might be sufficiently low to not have contributed to the strong absorption due to the Qdots. In contrast, the emission spectrum (at λ_{ex}-320 nm) of ASA treated Qdots had a new emission peak at 410 nm, in addition to the original dopant emission at 588 nm. Additionally, while the intensity of the peak at 588 nm was reduced partially, the peak at 440 nm vanished completely (Figure 2.1B). Interestingly, the excitation spectrum exhibited distinct peaks at 295 and 320 nm, when emission maxima were probed at 410 nm and 588 nm, respectively (Figure 2.1C). Additionally, ASA emitted at 410 nm (with λ_{ex}-295 nm), the intensity of which increased upon addition of Mn^{2+} or Zn^{2+} ions (Figure. A.2.1 B-C, Appendix). Further, $M(ASA)_2.2H_2O$ complexes (M= Zn or Mn) treated Qdots showed similar enhancement in emission intensity at 410 nm (Figure A.2.2, Appendix). There was also remnant of emission at 460 nm (with λ_{ex}-320 nm). Since the luminescence spectra were recorded following centrifugation and redispersion of the Qdots, it is plausible that $M(ASA)_2$ complexes were attached to the Qdots. The identity of the emissions obtained following two processes (i.e. treatment of Qdots with ASA and $M(ASA)_2$) indicated formation of identical species. Separately, addition of Na_2S to solution of $M(ASA)_2.2H_2O$ complexes also resulted in the enhancement in emission intensity at 410 nm. The results indicated that attachment of sulphide to the complexes enhanced their emission intensities. Overall, the observations could be explained based on the formation of $M(ASA)_2$ complexes on the surface of the Qdots through the dangling sulphide bond (Figure A.2.3, Appendix). This is similar to previous observation of formation of MQ_2 ($M=Zn^{2+}/Mn^{2+}$) complexes on the surface of ZnS or Mn^{2+}-doped ZnS Qdots with coordination via dangling sulphide bonds, which replaced one of the water molecules of the original complex ($M(ASA)_2.2H_2O$).[6-8]

Interestingly, treatment of the QDC with Cu^{2+} ions led to quenching of luminescence due to Mn^{2+} ions (at 588 nm); however, the emission at 410 nm due to the ASA complex was not affected. This was carried out in order to demonstrate the different

emission behaviours of the dopant ion (i.e. Mn^{2+}) and surface complex of the Qdots. The results showed that doped Qdots emission was quenched in the presence of Cu^{2+}, while upon complexation Qdots exhibited emission peak at 410 nm (under the same conditions). This clearly indicated that the source of the emission of metal ASA complexes is completely different from dopant emission. Further, when ASA treated Qdots were further treated with Cu^{2+}, the emission due to metal ASA remained nearly unaffected, while the emission due to Mn^{2+} was completely quenched. The results demonstrated that the emissions from the QDC due to the dopant and the complex are independent of each other (Figure A.2.4, Appendix).[6]

As is clear from the above results, the currently synthesized QDC having Mn^{2+}-doped ZnS Qdot, with the presence of surface complex of $M(ASA)_2$, emitted in the blue (410 nm) and orange (588 nm). Now, in order to create white light emitting source, the presence of green emitting species was needed in the same entity. Previous observations in the laboratory indicated that the formation of ZnQ_2 on the surface of the ZnS Qdot gives rise to green emission. [6-8] This provided an ideal choice of synthesizing a single entity consisting of tricolor emitting species. Thus, when the aqueous dispersion of Mn^{2+}-doped ZnS Qdots was treated with the mixtures of ASA and HQ at different molar ratio, the emission spectra (λ_{ex}-320 nm) exhibited three emission peaks, with different emission intensities at 410, 500 and 588 nm, respectively. Given that the spectra were recorded following centrifugation of the product and then redispersion in water, it can be concluded that the product consisted of three emitting species in the same entity and consisting of the Qdot, and complexes of the type $M(ASA)_2$ and ZnQ_2. It is important to note here that the intensity of the emission of the component color could be tuned by varying the molar ratio of added ligands (Figure 2.1D). This means the emission color is tunable by the extent of component complexation. Thus, while addition of either of the ligands reduced the emission of the peak at 588 nm (due to Mn^{2+}), the intensities of the peaks at 410 nm and 500 nm were commensurate with the concentration of ASA and HQ ligands, respectively. We also observed that, with the Qdots having an absorbance value of 0.09 at 320 nm, the perfect white light emission (upon excitation at 320 nm) could be achieved from the product obtained following their reaction with a mixture of ASA and HQ at 1:1 molar ratio (at 0.014 mM concentrations).

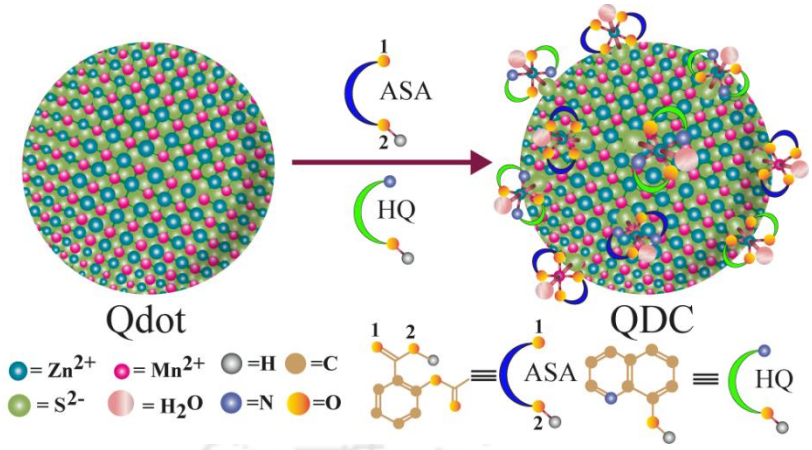

Scheme 2.1 Schematic representation of the room-temperature complexation reaction between Mn^{2+}-doped ZnS Qdots and a mixture of two organic ligands (ASA and HQ), leading to the formation of quantum dot complex (QDC).

Based on the above observations it can be concluded that two types of complexes i.e. $M(ASA)_2$ and MQ_2 ;(M=Zn or Mn) were formed on the surface of the Qdots. [1,2, 6-8] A schematic representation of the room temperature complexation reaction of the doped Qdots with the mixture of ASA and HQ is available in scheme. 2.1 The complexes – in conjunction with the Qdots – gave rise to emissions at three different colors. The three color emissions, by a single wavelength excitation (of 320 nm), in the QDC could be considered to originate from three independent sources: (a) from the highest occupied molecular orbital (HOMO) to the lowest unoccupied molecular orbital (LUMO) transition of surface $M(ASA)_2$ complexes (M= Zn^{2+} and Mn^{2+}; λ_{em}-410 nm); (b) from surface ZnQ_2 complex (λ_{em}-500 nm; since MnQ_2 has negligible luminescence) and (c) from the $^4T_1$-$^6A_1$ transition involving Mn^{2+} dopant ions of the Qdots (λ_{em}-588 nm).[12-15] It is to be mentioned here that both surface metal ions (Zn^{2+} and Mn^{2+}) of Qdots were possibly involved in complexation reaction with ASA and HQ. Even though HQ has stronger chelating affinity than ASA to metal ions, the concentration-dependent complexation reaction in a short time span might have led to the formation of both the metal complexes of HQ and ASA. Further, the complexation constants for the formation of QDC were calculated by monitoring the changes in emission intensities at 410 and 500 nm, at different concentrations of ASA and HQ (Figure A.2.5, Appendix) and based on a method reported earlier.[9] The details are described in the appendix section. The surface complexation constants of ASA and HQ to form QDC were found to be $(1.50 \pm 0.38)\times10^4$ M^{-1} and $(5.80 \pm 0.18)\times10^4$ M^{-1}, respectively. The results indicate the stronger

complexation affinity of HQ over ASA to Qdots, which is in support of other observations. Further, since the constant for HQ is about 4 times that of ASA, it is likely that both the ligands –when present as nearly equimolar mixture in a liquid medium - would react with the same Qdot (rather than separate Qdots), considering the fact that reactivity of either of the ligands with any of the Qdots would remain the same. Hence, the formation of complexes of ASA and HQ to the same Qdot may be more favorable over their individual complex formation to different set of Qdots. The presence of three emissive species in QDC was further confirmed from the excitation spectra probed at three different emission maxima (Figure 2.2). The peak at 295 nm corresponds to surface $M(ASA)_2$ complexes (akin to Na_2S added $M(ASA)_2$ complexes as in, Figure. A.2.3); that at 365 nm corresponds to surface ZnQ_2 species; while the peak at 320 nm is due to the transition in the Qdots. The overlapping excitation spectra supported the observation of the single wavelength excitation for three emissions. On the other hand, the UV-vis spectrum of the QDC showed the absorption behavior similar to the product of only HQ treated Qdots, which indicates that the absorption owing to ASA contributed very little to the absorption characteristics of QDC (Figure 2.2).

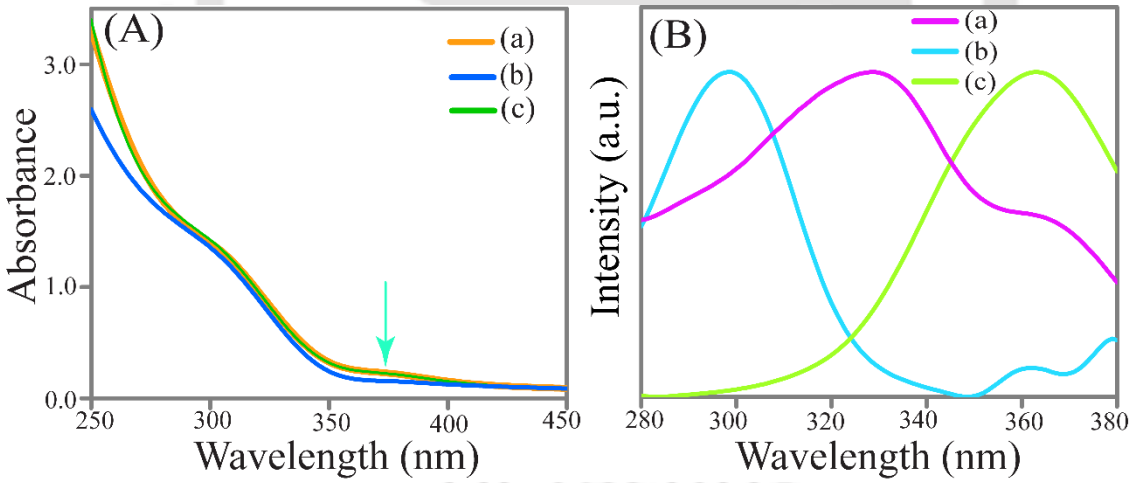

Figure 2.2. (A) UV-vis spectra of (a) HQ added Qdots, (b) ASA added Qdots and (c) QDC. **(B)** excitation spectra of QDC at emission wavelengths of (a) 588 nm, (b) 410 nm and (c) 500 nm respectively (Cyan arrow indicates the appearance of broad absorption peak due to formation of surface ZnQ_2 complex).

Further, the photoluminescence quantum yield (QY) of the QDC was found to be 2.2% while that of the Qdots was 0.6% QY, both measured at the excitonic wavelength (320 nm) of the Qdots (Table A.2.1, Appendix). On the other hand, addition of ASA or

HQ (only) to the Qdots exhibited 0.7 and 0.8 % QYs, respectively (Table A.2.1, Appendix). Further, the time-dependent photo-irradiation results showed that QDC (with regard to three different emitting species) was 4-5 times as much photostable as rhodamine 6G (Figure A.2.6 and Table A.2.2, Appendix). For example, rhodamine 6G showed decrease in photoluminescence with a rate of 0.015% per sec while that was 0.003, 0.003 and 0.004% for the QDC as measured by monitoring emission maxima at 588 (due to dopant of Qdot), 500 (due to surface ZnQ_2) and 410 nm (due to surface $M(ASA)_2$, where M: Zn or Mn), respectively. Additionally, zeta potential measurements of the QDC in the medium, being measured with a value of 30.4±1.0 mV, indicated their colloidal stability in water, which is essential for processing for further applications (Figure A.2.7 and Table A.2.3, Appendix).[6]

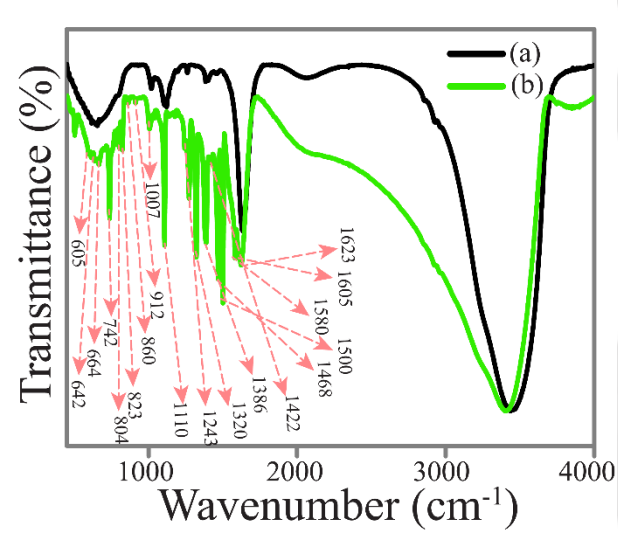

Figure 2.3. FTIR spectra of (a) Qdots and (b) QDC.

Fourier transform infrared spectroscopic measurements revealed the presence of both the characteristic peaks of metal ASA and HQ complexes – which are absent in as such Qdots (Figure 2.3 and Table A.2.4, Appendix).[2,3, 6-8,10] Importantly, the presence of peak at 1110 cm^{-1} due to metal coordinated HQ and ASA in QDC (–C –O–M), while the ratio of peak intensity at 3333 cm^{-1} and 1110 cm^{-1} being 0.8 indicates the formation of octahedral metal quinolate complexes of HQ.[6,7,10] Additionally, the absence of the stretching frequency due to carboxylic group of ASA at 1690 cm^{-1} and the appearance of a new peak at 1320 cm^{-1}, being attributed to the chelation through the two oxygen end of the carboxylic group of ASA, revealed the presence and metal coordination of ASA – in addition to HQ, on the surface of the Qdots.

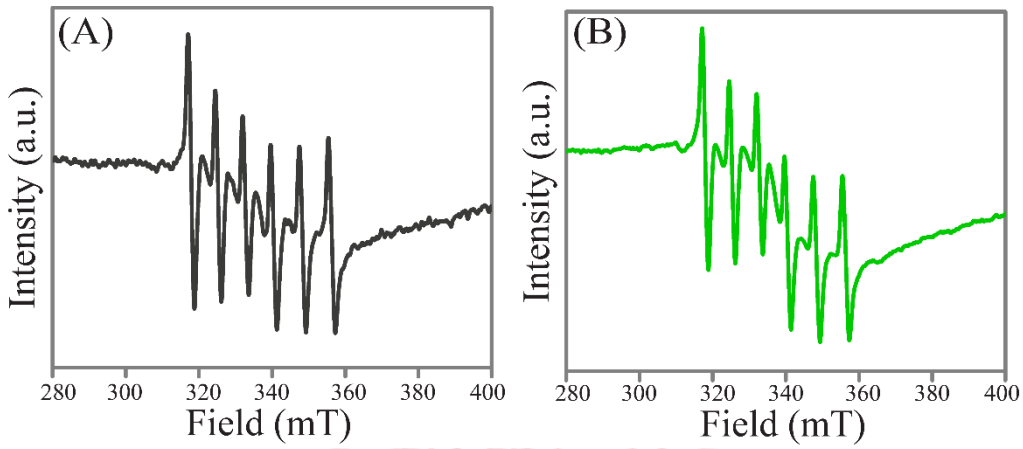

Figure 2.4. Electron paramagnetic resonance spectra of **(A)** Mn^{2+} doped ZnS Qdots and **(B)** QDC.

Electron paramagnetic resonance (EPR) experiments revealed the occurrence of prominent peaks due to the presence of Mn^{2+} ions in the crystals before and after complexation reaction. Moreover, the appearance of weak peaks at the edges of the spectrum indicated the formation of octahedral Mn^{2+} complexes of the Qdots with ASA and HQ, which led to the reduction in the dipolar Mn^{2+} – Mn^{2+}interaction, known to occur on the surface of Qdots due to clustering of ions (Figure. 2.4).[1,6,7] Therefore, the surface Mn^{2+} ions of the Qdots, in addition to Zn^{2+} ions, were also involved in the formation of complexes with the mixture of ASA and HQ. Further, the metal ion concentrations in the Qdots, as obtained from atomic absorption spectroscopic (AAS) measurements, remained nearly unaltered following complexation with the mixture of ASA and HQ. This means that there was no significant etching of metal ions during the formation of QDCs (Table A.2.5, Appendix). [1,4-6]

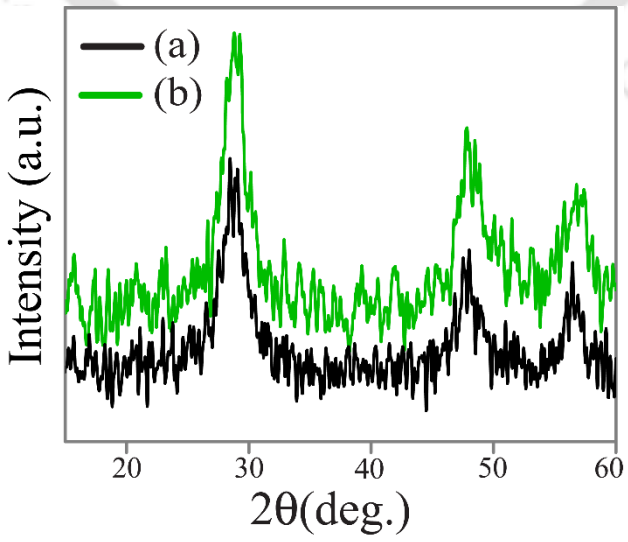

Figure 2.5. Powder X-ray diffraction pattern of (a) Mn^{2+} doped ZnS Qdots and (b) QDC.

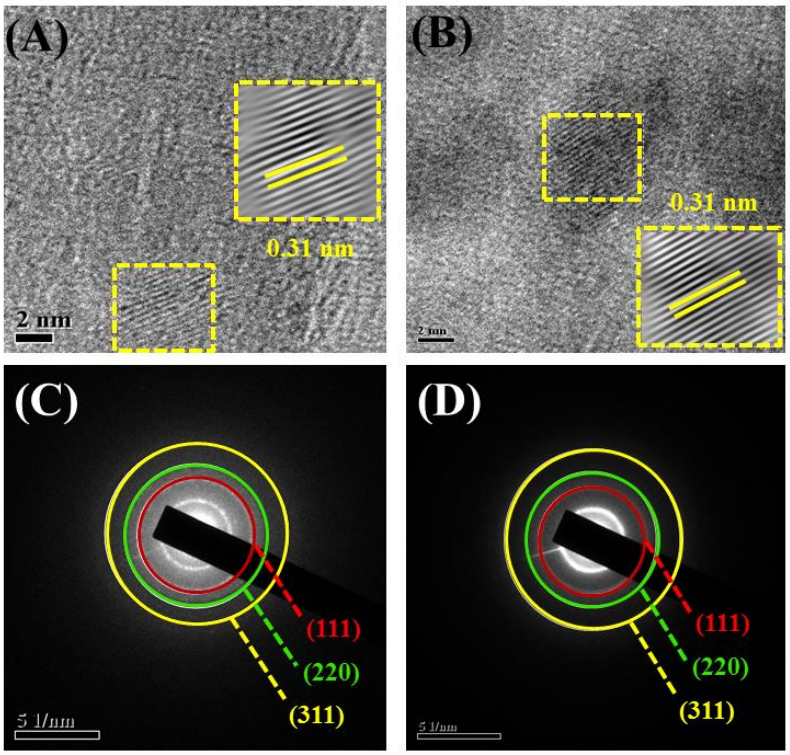

Figure 2.6. High resolution transmission electron microscopy (HRTEM) (scale bar- 2 nm) and corresponding inverse fast Fourier transform (IFFT) (inset square boxes) images of **(A)** Mn^{2+} doped ZnS Qdots and **(B)** QDC. Selected area electron diffraction (SAED) (scale bar: 5 nm^{-1}) images of **(C)** Mn^{2+} doped ZnS Qdots and **(D)** QDC

The preservation of the integrity of the nanocrystals upon formation of QDC was further supported by X-ray diffraction (XRD) and transmission electron microscopy (TEM) measurements.[1,4-6] Thus, the characteristics peaks of cubic ZnS due to (111), (220) and (311) planes in the powder XRD patterns and the lattice spacing (0.3 nm) of (111) plane in high resolution TEM of Qdots were preserved following complexation reactions with the mixture of ASA and HQ (Figure 2.5 and 2.6A-B).[1,4-6] Further, selected area electron diffraction (SAED) studies (Figure 2.6C-D) also supported the observations from XRD and HRTEM. Also, there was no significant change in the dimensions of the nanocrystals before and after complexation reaction (Figure 2.7).

The importance of the candidature of an emitting material is primarily decided by its conformity to chromaticity color coordinates In this regard, the as-synthesized Qdots had coordinates of (0.48, 0.41), far away from perfect white emission (Figure 2.8A and Table A.2.6, Appendix). On the other hand, the chromaticity coordinates for complexed Qdots i.e. QDC (Figure. 2.8A and Table A.2.6, Appendix) could be as best as (0.30,

0.33), thus qualifying for a model white light emitter. Also, as in Figure. 2.8B, the QDC had the best white light emission following excitation at 320 nm. Additionally, that the excitation dependent emission behaviour of the QDC (Figure. A.2.8, Appendix) exhibited tunability in CIE chromaticity color coordinates (Figure A.2.9 and Table A.2.7, Appendix), provides impetus for its use in the solid state lighting. On the other hand, addition of ASA or HQ (only) to the Qdots did not lead to products the chromaticity coordinates of such an emitter (Figure. A.2.10 and Table A.2.8, Appendix). This clearly indicates the importance of the presence of both the ligands (ASA and HQ) on the surface of the Qdots (in the form of the QDC), in order to have a perfect white light emitter.

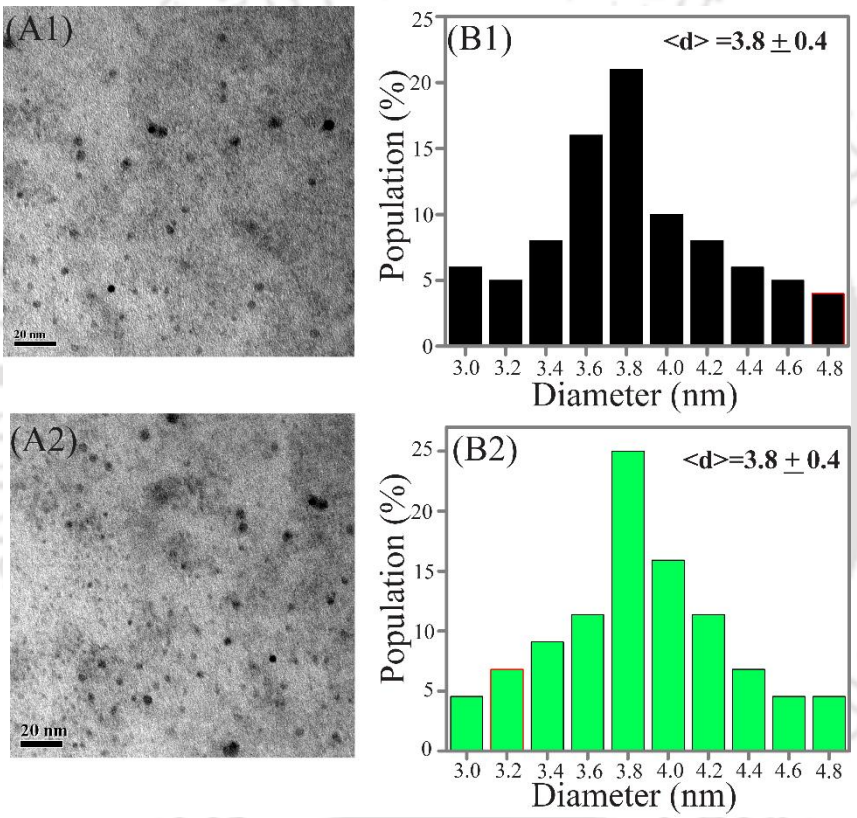

Figure 2.7. Representative **(A)** TEM images and **(B)** corresponding particle size distribution of (1) Mn^{2+} doped ZnS Qdots and (2) QDC: here <d> indicates the average diameter of the particles.

Further, there was no significant change observed in chromaticity coordinates of white light emitting QDC by varying the temperature in the range of 25-85 ^{0}C, while slight decrease in QY of the QDC was noticed when temperature was changed from 25 ^{0}C to 85 ^{0}C (Figure A.2.11, Tables A.2.9 and A.2.10, Appendix). The results clearly indicated the thermal stability of the white light emitting QDC in the liquid medium i.e. in terms of intactness of the chromaticity coordinates.

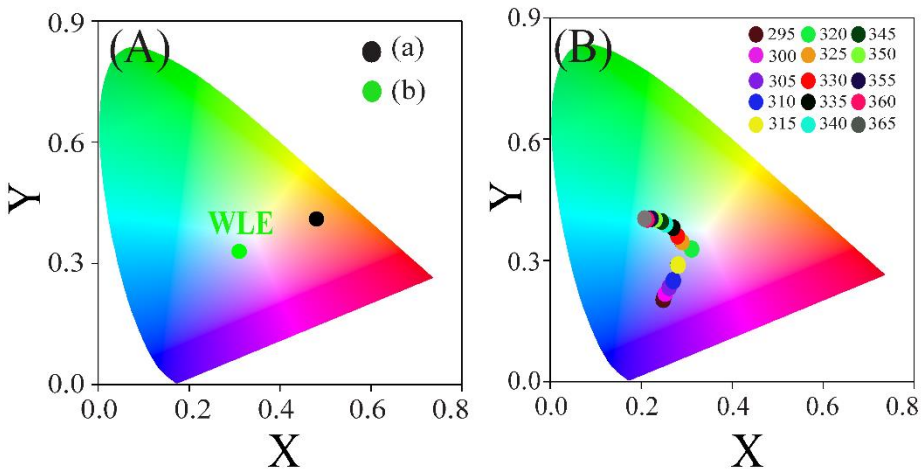

Figure 2.8. (A) CIE chromaticity diagram (at λ_{ex} - 320 nm) of (a) Mn^{2+} doped ZnS Qdots and (b) QDC. **(B)** CIE chromaticity diagram of QDC at different excitation wavelengths.

The white light emission from the QDC – being present in water as dispersion- could also be observed visually and thus photographed (Figure. 2.9). Importantly, when excited by 320 nm light, the dispersion of Qdots appeared orange (Figure. 2.9A), while QDC exhibited white (Figure. 2.9B). Interestingly, green and blue emission colors (Figure 2.9C and 2.9D) were observed when the same QDC was probed at excitation wavelengths of 365 nm (of ZnQ_2) and 295 {of $M(ASA)_2$}. It may be mentioned here that 365 nm is the excitation maximum of the emission at 500 nm due to ZnQ_2, while 295 nm is that due to $M(ASA)_2$, when probed at 410 nm. This was further supported by the appearance of green and blue colored emissions from the same Qdots when treated with only HQ and ASA, respectively (Figure. A.2.11, Appendix). Thus it can be concluded that formation of complexes of two species with component emissions at blue and green, in conjunction with orange emission due to the Qdot gave rise to white light emission.

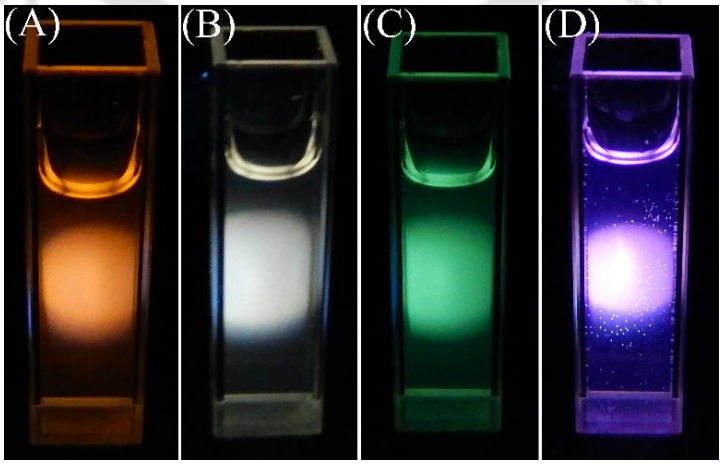

Figure 2.9. Digital photographs (in solution phase) of **(A)** Qdots at λ_{ex} - 320 nm **(B–D)** QDC at λ_{ex}- 320, 365, and 295 nm, respectively. A spectrofluorimeter was used as the excitation source.

Further, in order for the QDC to be of versatile use especially for solid-state lighting, its emission characteristics in the solid state ought to conform to the emitting characteristics of white light emitting (WLE) source. This was achieved by drop-casting a thin film of WLE QDC on a quartz substrate, which generated bright white light upon excitation by 320 nm light (using a spectrofluorimeter; Figure 2.10A). Additionally, the presence of three main emission peaks at 410, 500 and 588 nm, respectively, in the emission spectrum (λ_{ex}-320 nm) and (0.32, 0.32) chromaticity coordinates in the CIE diagram of the thin film made of WLE QDC indicated the suitability of its luminescence in the solid phase for WLE application. (Figure 2.10B-C). Further, the WLE QDC was found photostable as observed for all three different emitting species (Figure 2.10D). Hence, the white light emitting nature of QDC in the solid state may be useful for further practical utilization in fabricating the light emitting devices.

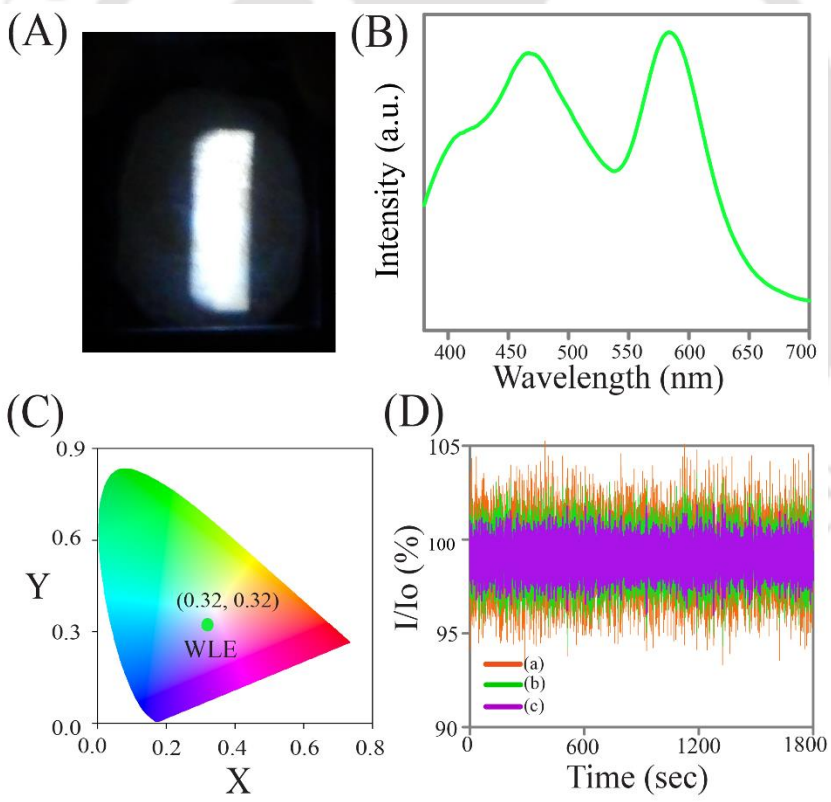

Figure 2.10. (A) Digital photograph, **(B)** emission spectrum, **(C)** corresponding CIE diagram and **(D)** photostability as monitored at (a) 588, (b) 500 and (c) 410 nm emission maxima, of a thin film made of WLE QDC on a quartz slide. The excitation source was the 320 nm light of a spectrofluorimeter.

2.3. Conclusion

In summary, complexation on the surface of ligand free Mn^{2+}-doped ZnS Qdots with the mixture of two organic ligands (ASA and HQ) led to the formation of single component system – called as quantum dot complex (QDC). The QDC exhibited tri-color emission based white light (with CIE coordinates 0.30, 0.33 in solution phase and 0.32, 0.32 in the solid phase) following a single wavelength excitation. Importantly, the precise control over chromaticity and colors of the QDC via changing the excitation wavelengths and molar ratio of the two organic ligands were achieved. The emission due to formation of two complexes on the surface of possibly the same Qdot is a new way of achieving high efficiency white light emitting materials based on three independently emitting components. That the synchronous tri-color emission could be obtained from the same species and which is dispersible in water auger well for future light emitting and other devices. Finally, the ability to control emission color based on chemistry of Qdots would provide a new and important entrant in the domain of light emitting devices.

References:

(1) Begum, R.; Bhandari, S.; Chattopadhyay, A. Surface Ion Engineering of Mn^{2+}-Doped ZnS Quantum Dots Using Ion-Exchange Resins. *Langmuir* **2012**, *28*, 9722−9728.

(2) Lemoine, P.; Viossat, B.; Dung, N.H.; Tomas, A.; Morgant, G.; Greenaway, F.T.; Sorenson, J.R.J. Synthesis, Crystal Structures, and Anti-Convulsant Activities of Ternary [Zn^{II}(3,5-diisopropylsalicylate)$_2$], [Zn^{II}(salicylate)$_2$] and [Zn^{II}(Aspirinate)$_2$] Complexes. *J. Inorg. Biochem*. **2004**, *98*, 1734–1749.

(3) Lambia, J.N.; Nsehyuka, A.T.; Egbewatt, N.; Cafferata, L.F.R.; Arvia, A.J. Synthesis, Spectral Properties and Thermal Behavior of Zinc(II) Acetylsalicylate. *Thermochimica Acta* **2003**, *398*, 145–151.

(4) Begum, R.; Chattopadhyay, A. Redox-Tuned Three-Color Emission in Double (Mn and Cu) Doped Zinc Sulfide Quantum Dots. *J. Phys. Chem. Lett*., **2014**, *5*, 126–130.

(5) Begum, R.; Chattopadhyay, A. In Situ Reversible Tuning of Photoluminescence of Mn^{2+} Doped ZnS Quantum Dots by Redox Chemistry. *Langmuir* **2011**, *27*, 6433−6439.

(6) Bhandari, S.; Roy, S.; Pramanik, S.; Chattopadhyay, A. Double Channel Emission from a Redox Active Single Component Quantum Dot Complex. *Langmuir* **2015,** *31*, 551-561.

(7) Bhandari, S.; Roy, S.; Chattopadhyay, A. Enhanced Photoluminescence and Thermal Stability of Zinc Quinolate Following Complexation on the Surface of Quantum Dot. *RSC Adv.* **2014**, *4*, 24217-24221.

(8) Bhandari, S.; Roy, S.; Pramanik, S.; Chattopadhyay, A. Surface Complexation Reaction for Phase Transfer of Hydrophobic Quantum Dot from Nonpolar to Polar Medium. *Langmuir* **2014**, *30*, 10760-10765.

(9) Baker, D. R.; Kamat, P. V. Tuning the Emission of CdSe Quantum Dots by Controlled Trap Enhancement. *Langmuir* **2010**, *26*, 11272–11276.

(10) Pan, H.; Liang, F.; Mao, C.; Zhu, J.; Chen, H. Highly Luminescent Zinc(II)-Bis(8-hydroxyquinoline) Complex Nanorods: Sonochemical Synthesis, Characterizations, and Protein Sensing. *J. Phys. Chem. B* **2007**, *111*, 5767−5772.

Chapter 3

Gold Nanocluster and Quantum Dot Complex in Protein for Biofriendly White-Light-Emitting Material

Synthesis of a biofriendly highly luminescent white-light-emitting nanocomposite is described here. The composite consisted of Au nanoclusters and ZnQ_2 complex (on the surface of ZnS quantum dots) embedded in protein. The combination of red, green, and blue luminescence from clusters, complex, and protein, respectively, led to white light generation.

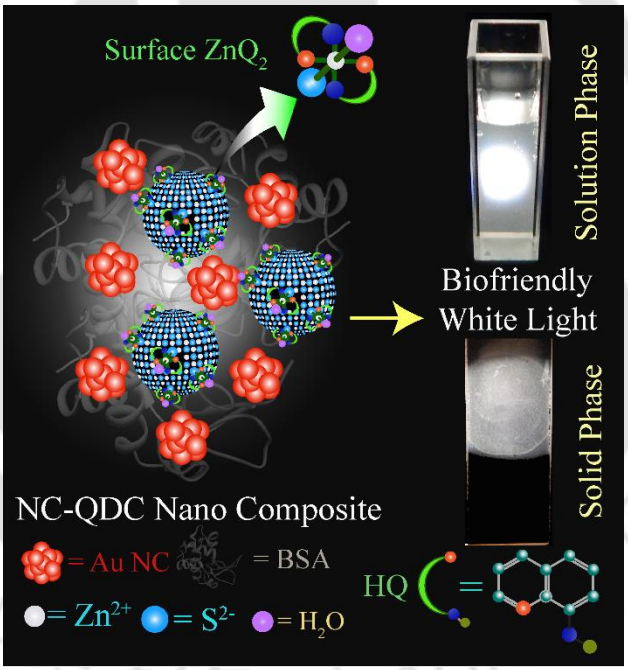

***[*ACS Appl. Mater. Interfaces* 2016, *8*, 1600−1605] - Reproduced by permission from American chemical society.**

3.1. Experimental Section

3.1.1. Materials. Gold(III) chloride solution ($HAuCl_4$, Sigma-Aldrich), bovine serum albumin (BSA, Sisco Research Laboratories Pvt. Ltd.), sodium hydroxide (NaOH, Merck), zinc acetate dihydrate (99%, Merck, India), sodium sulphide (58%, Merck), 8-hydroxyquinoline (HQ, Merck), quinine sulfate (Fluka), rhodamine 6G (Sigma-Aldrich), methanol (Merck), sulphuric acid (Merck) and ethanol (Merck) were purchased and used without any further purification. Milli-Q ultrapure water (>18 MΩ cm, Millipore) was used in all the experiments.

3.1.2. Synthesis of BSA stabilized gold nanoclusters (Au NCs). BSA stabilized Au NCs were synthesized based on an earlier reported method.[1,2] Briefly, 5.0 mL of 10.0 mM aqueous $HAuCl_4$ solution was mixed with 5.0 mL of 50.0 mg/mL BSA solution under vigorous stirring at 37 °C for 2 min. Then 1.0 M NaOH solution was added such that the pH of the reaction mixture was ~12.0. The resulting solution was allowed to stir for 12 h and this led to the formation of BSA stabilized Au NCs. The synthesized nanoclusters were characterized using transmission electron microscopy (TEM), UV-vis and photoluminescence (PL) spectroscopy.

3.1.3. Synthesis of BSA stabilized Au NC-ZnS Qdot (NC-Qdot) nanocomposite. 3.3 mL of the as-prepared BSA stabilized Au NCs was diluted with water to 10 mL and the pH was adjusted to ~6.8. From this, 5.0 mL of the Au NCs dispersion was taken and to it – under constant stirring at 50 °C – aqueous solutions of zinc acetate dihydrate (10.0 mL of 2.5 mM) and sodium sulphide (10.0 mL of 2.5 mM) were added at a time. The reaction was continued for 3 h and the resulting dispersion was centrifuged at 25000 rpm and 4 °C for 10 min. The pellet so obtained (after centrifugation and washing) was redispersed in 60.0 mL of water (using an ultrasonic bath) and that was used for further experiments. The synthesized composite was characterized using X-ray diffraction (XRD), TEM, HRTEM, UV-vis, and PL spectroscopy.

3.1.4. Preparation of Ligand (HQ) Solutions. 1.0 mM of 8-hydroxy quinoline (HQ) solution in methanol was prepared using sonication.

3.1.5. Synthesis of white light emitting (WLE) Au NCs–Quantum dot complex (NC-QDC) nanocomposite. NC-QDC nanocomposite was synthesized following the reaction between BSA stabilized Au NC-ZnS Qdot nanocomposite and 8-hydroxyquinoline (HQ). Four different volumes of 1.0 mM HQ (in methanol; the details

of which are described in appendix Table A.3.2) were added to 3.0 mL of as-prepared NC-Qdot nanocomposite (with absorbance of 0.198 at 365 nm) in different vials and the resulting dispersions were centrifuged at 25000 rpm and 4 °C for 10 min. The pellets obtained were redispersed separately in 3.0 mL of water and their emission spectra (at λ_{ex}-365 nm) and corresponding CIE (Commission internationale de l'éclairage) chromaticity coordinates were obtained. It is important to mention here that as the best chromaticity coordinates were obtained for the dispersion of NC-Qdot nanocomposite mixed with 4.98 μM of HQ, all the characterizations were carried out using this dispersion. The powder XRD, TEM, HRTEM, UV-vis spectroscopy, PL spectroscopy, circular dichroism spectroscopy, zeta potential measurement and time resolved photoluminescence analysis were carried out to characterize the NC-QDC nanocomposite.

3.1.6. Synthesis of BSA stabilized ZnS Qdots. To synthesize BSA stabilized ZnS Qdots, 37 mg of BSA was dissolved in 5.0 mL of water under constant stirring at 50 °C. Then the aqueous solution of Zinc acetate dihydrate (2.5 mM) and sodium sulphide (2.5 mM) were added at a time to the reaction mixture – allowed to stir continuously for 3 hrs at 50 °C. After that the resulting solution was centrifuged (25000 rpm) and so obtained pellet was redispersed at 60 mL of water. This dispersion was used for further experiments.

3.1.7. Control experiment.

(A) White light from the mixture of BSA stabilized Au NCs and BSA stabilized ZnS Qdots – following complexation with HQ. 200 μL of BSA stabilized Au NCs (pH-6.8) was mixed with 2.8 mL of as synthesized BSA stabilized ZnS Qdots in a cuvette. To this mixture 15 μL of 1.0 mM HQ was added and the mixture was stirred for 10 min. The emission spectrum (with chromaticity coordinates) of the resulting mixture was then recorded. Further, the resulting mixture was centrifuged at a speed of 25000 rpm. The so obtained supernatant was collected and the pellet was redispersed separately in the same amount of solvent and finally the emission spectra (with chromaticity coordinates) of both (pellet and supernatant) were recorded.

3.2. Results and Discussion

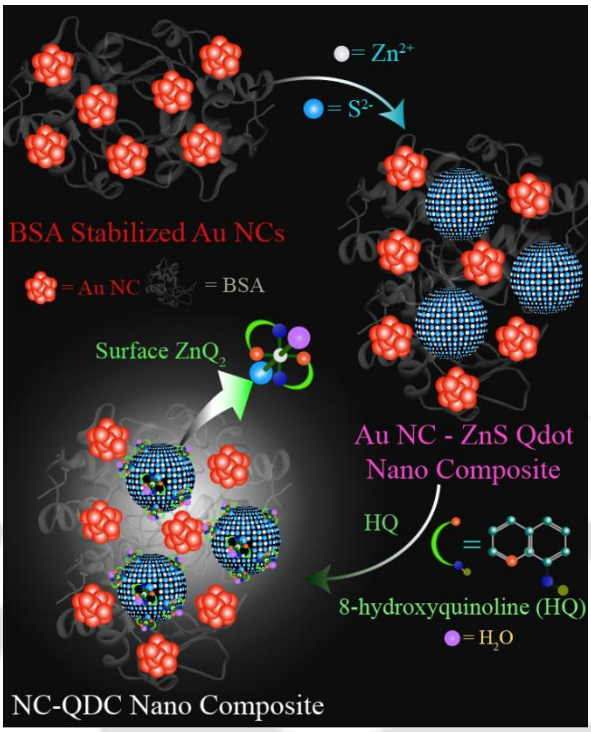

Scheme 3.1. Schematic representation of the formation of white-light-emitting Au nanocluster-quantum dot complex (NC-QDC) nanocomposite.

Scheme 3.1 illustrates the various steps involved in the formation of the WLE nanocomposite. First of all, Au NCs were synthesized using the BSA protein as the template. This was followed by the synthesis of ZnS Qdots in the presence of BSA stabilized NCs. Finally, HQ was added to the medium resulting in the formation of ZnQ_2 on the surface of the Qdot, thus generating the desired WLE NC-QDC composite.

The BSA stabilized Au NCs of size 1.8 ± 0.4 nm were synthesized (at pH 12.0) following earlier reports (Figure A.3.1, Appendix).[1,2] In the same host (following adjustment of the pH to 6.8), 4.5 ± 1.4 nm sized ZnS Qdots were grown next, to synthesize NC-Qdot nanocomposite (Figure 3.1A and Figure 3.1B). The presence of lattice fringes with 0.3 nm separation in the high-resolution transmission electron microscopic (HRTEM) image supported the formation of cubic ZnS in the NC-Qdot composite (Figure 3.1C).[3,5,6] Similar observation was made from the selected area electron diffraction (SAED) analysis of the NC-Qdot composite (Figure 3.1 D). Furthermore, the presence of the characteristic peaks of cubic ZnS (at 28.6°, 47.9° and

56.5°) in the powder X-ray diffraction (XRD) pattern also supported the formation of the NC-Qdot composite (Figure 3.2). [3,5,6]

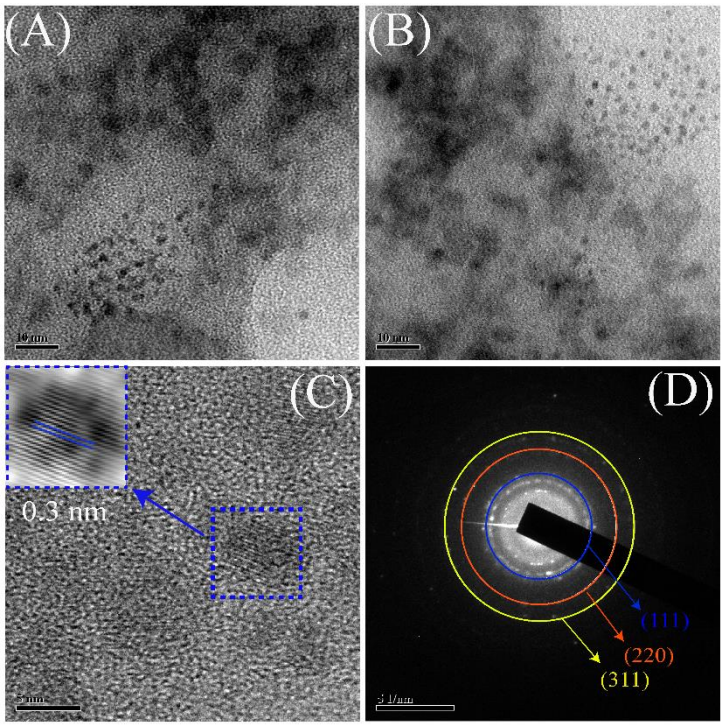

Figure 3.1. (A, B) Representative transmission electron microscopic (TEM, scale bar-10 nm) images; **(C)** high resolution transmission electron microscopic image (HRTEM, scale bar-5 nm) and corresponding inverse fast Fourier transform (IFFT, inset square box) image and **(D)** selected area electron diffraction (SAED, scale bar- 5 nm^{-1}) image of Au NC-ZnS Qdot composite.

The protein acts as a stabilizer (host) for the Qdots and the clusters. Earlier reports showed that the reducing ability of aromatic amino acid residues (such as tyrosine and tryptophan) and the cysteine residues of the BSA protein under basic pH (~12) helped in the formation of Au NCs (from $AuCl_4^-$) and stabilization of the Au NCs, respectively.[1,12,16] In a similar vein, the effective binding ability of the various amino acid functional groups such as amine, carboxyl, thiol and imidazole facilitated the formation and stabilization of ZnS Qdots in the BSA matrix.[20] Hence, during formation of the NC-Qdot composite, at first the cysteine residues (of BSA) might have been involved in stabilizing the Au NCs in the protein while the remaining functional groups (such as thiol, amine, imidazole and carboxyl) of the BSA which were free might have stabilized the ZnS Qdots. It is also plausible that during their formation, both the Qdots and Au nanoclusters were attached partially with the protein with portions exposed to the water not being bonded to the protein. On the other hand, if differently stabilized (with different ligands) were reacted with the protein there may be no association between the two

(either Qdot or nanocluster) as the stabilizer will prevent that. On the other hand, the water exposed part of the Qdot can easily react with HQ to form Qdot-ZnQ_2 complex. As is clear from our synthetic protocol an in situ synthesis has been used to fabricate the white light emitting material following sequential incorporation of Au NCs, ZnS Qdots and the inorganic complex. It would be rather difficult to predict the association constant and the exact ratio of Au NCs, ZnS Qdots and BSA protein, in the NC-Qdot and NC-QDC nanocomposite. The preservation of the nature of the NC-Qdot composite, following complexation with HQ, was confirmed by HRTEM, SAED and XRD analyses (Figure 3.3). This clearly demonstrated that the integrity of the NC-Qdot composite remained the same upon formation of the NC-QDC composite.

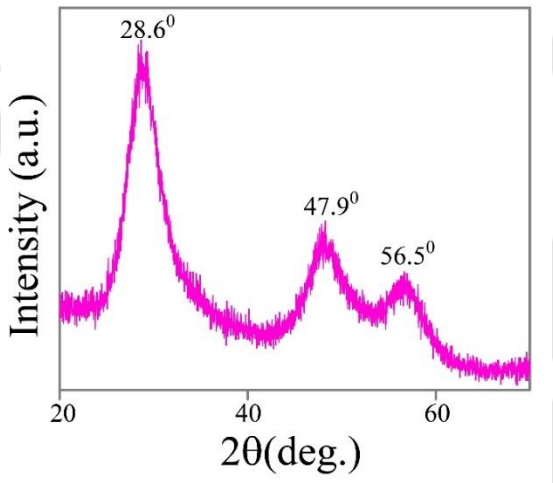

Figure 3.2. Powder X-ray diffraction (XRD) pattern of Au NC-ZnS Qdot (NC-Qdot) composite.

Further, circular dichroism (CD) spectroscopy was carried out to probe the conformational changes in the BSA protein following the synthesis of Au NCs and ZnS Qdots. [12,16,17] The native BSA showed two negative peaks – one at 210 nm and the other at 222 nm due to α-helical structure of the protein. On synthesizing Au NCs in BSA template at pH 12, the peak at 210 nm had a blue-shift to 208 nm and the peak at 222 nm became shallower. [12,16,17] Upon changing the pH of the BSA-stabilized Au NCs to 6.8, the peak at 222 nm became even shallower as compared to BSA-stabilized Au NCs at pH~12 (Figure A.3.2, Appendix). The observed changes in the conformation of BSA may be due to the change in pH of the medium. [12,16,17] Following this, the formation of ZnS Qdots in the BSA stabilizing Au NCs (without having any change in pH~6.8 of the medium) led to drastic changes in the secondary structure of BSA protein. This clearly indicated the effect of ZnS formation on the conformation of the BSA template at a fixed pH of the medium. [12,16,17] However, after addition of HQ (without having any change in

pH ~6.8 of the medium) to Au NC-ZnS Qdot, no significant (additional) change in the conformation of the BSA protein was observed. Thus, it can be concluded that there were changes in the secondary structure of the BSA protein due to formation of Au NCs and ZnS in the BSA template. This may be the resaon for the observed changes in the optical charateriscs of the Au NCs embedded in BSA proetin during the formation of WLE NC-QDC nanocomposite.

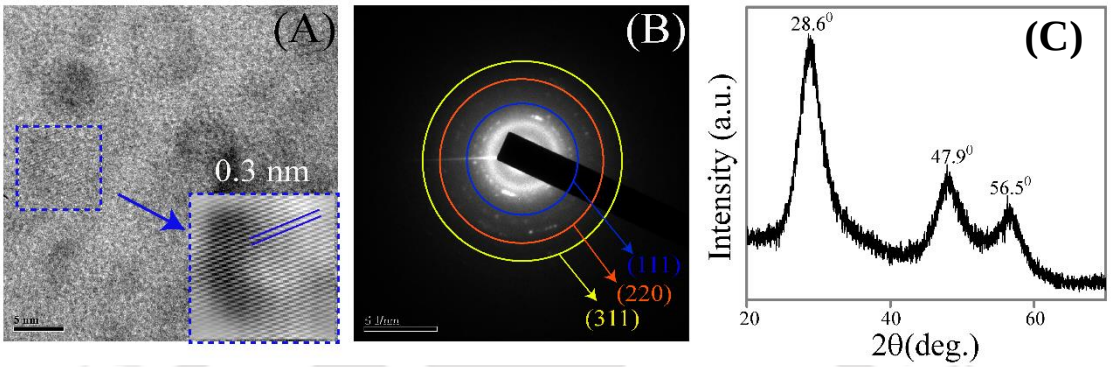

Figure 3.3. (A) High resolution transmission electron microscopic (HRTEM) image (scale bar-5 nm) and corresponding inverse fast Fourier transform (IFFT; inset square box) image; **(B)** selected area electron diffraction (SAED) (scale bar: 5 nm^{-1}) image and **(C)** powder X-ray diffraction (XRD) pattern of Au NC-ZnS Qdot composite following complexation with HQ (NC-QDC composite).

Upon irradiation of 365 nm light (using a spectrofluorimeter), the aquoeus dispersion of BSA stabilized Au NCs exhibited bright red color, which turned reddish violet upon incorporation of ZnS Qdots (Figure. 3.4Ai and Figure. 3.4Aii). Interestingly, the HQ treatment to the BSA stabilized Au NC-ZnS Qdot composite led to generation of bright white color in the presence of 365 nm light (Figure. 3.4Aiii). The aquoeus dispersions of BSA stabilized Au NCs and NC-Qdot (following complexation with HQ too) exhibited dark brown and milky white color, respectively, in presence of day light (Figure A.3.3, Appendix). The BSA stabilized Au NCs (pH~6.8) showed two emission peaks, one at 430 (due to the weak luminescence of the tryptophan residue of the BSA protein) and the other at 650 nm due to the NCs (originating from the Au NCs in BSA due to the Förster resonance energy transfer from the tryptophan residue of the BSA protein to Au NCs), when excited by 365 nm light (Figure. 3.4Bi).[1,2,12,19] The luminescence of Au NCs at 650 nm has been attributed to the intraband or interband

transitions between the 6sp conduction band and filled 5d band of Au or the ligand to metal charge transfer via Au-S bond. [1,2,11,12,18,19]

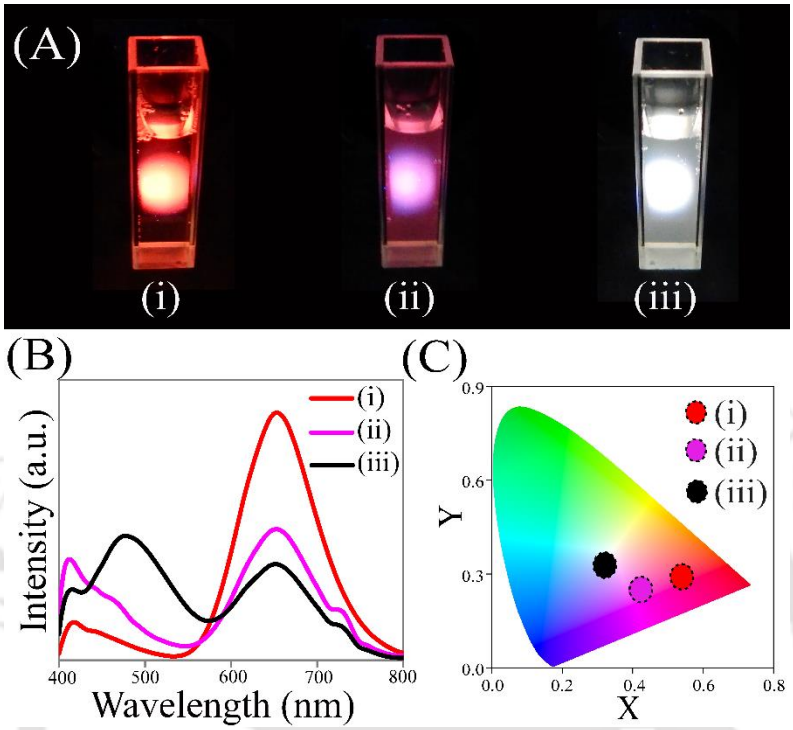

Figure 3.4. (A) Digital photographs (recorded in the presence of 365 nm light from spectrofluorimeter); **(B)** emission spectra (λ_{ex}-365 nm) and **(C)** corresponding CIE chromaticity diagram of the aqueous dispersions of (i) BSA stabilized Au NCs (pH~6.8), (ii) BSA-stabilized Au NC-ZnS Qdot (NC-Qdot) composite (pH~6.8) and (iii) HQ-treated BSA-stabilized Au NC-ZnS Qdot (NC-QDC) composite (pH~6.8).

Further, incorporation of ZnS Qdot in the BSA stabilized Au NCs led to the decrease in emission intensity at 650 nm (pH~6.8). This could either result from conformational change of the BSA protein (as a result of formation of ZnS Qdots in BSA)[1,2,13] or the energy transfer from BSA to the ZnS Qdots as the emission of BSA at λ_{ex}-365 nm (Figure A.3.4, Appendix), overlaps with the absorbance tail of the Au NC-ZnS Qdot composite, or both (Figure A.3.5, Appendix). The peak in the emission range of 400-450 nm was weak (probably due to lack of absorbance of ZnS at 365 nm; Figure 1Bii). But, at an excitation wavelength corresponding to the absorption peak of ZnS Qdot i.e. at 320 nm, the same NC-Qdot composite exhibited significant increase in the emission intensity in the 400-450 nm region, because of the midgap surface trap state emission of ZnS Qdot (Figure A.3.6, Appendix).[22] This indicated the in situ formation of

ZnS Qdots in BSA matrix of Au NCs. It is to be mentioned here that the factors such as pH, solvent and presence of any other chemical substances can affect the local environment of the BSA stabilized Au NCs and that would lead to changes in their emission characteristics. [1,2,13] In the current context, the formation of the ZnS Qdots in the host BSA stabilized Au NCs may be the reason for the observed change in emission spectrum of the NC-Qdot composite compared to only BSA stablized Au NCs. Further, a new and intense peak at 490 nm appeared, following addition of HQ to BSA stabilized Au NC-ZnS Qdot composite (upon excitation at 365 nm; Figure 3.4Biii). No signficant change in the pH of the aqueous dispersion of the NC-Qdot composite was observed following complexation, which clearly discounted the role of the pH on the observed changes in their emission characteristics. On the other hand, there was no emission peak appearing at 490 nm upon addition of HQ to BSA stabilized Au NCs (upon excitation at 365 nm), which ruled out the possibility of the emission at 490 nm due to formation of any species resulting from complexation between HQ and BSA stabilized Au NCs (Figure A.3.7,Appendix). Furthermore, the HQ treated BSA stabilized ZnS Qdots exhibited emission peak at 490 nm (upon excitation at 365 nm), clearly indicating that the source of 490 nm emission (Figure A.3.8, Appendix) is solely due to the HOMO–LUMO transition of the octahedral ZnQ_2 complexes present on the surface of ZnS Qdot following complexation, which is also supported by our earlier observations.[3,5,6,21] Earlier studies revealed that the attachment of the ZnQ_2 complexes to the ZnS Qdot may occur through the dangling sulphide bond following replacement of one of the labile water molecules of the octahedral $ZnQ_2.2H_2O$ complex and this resulted in the observed changes in the optical properties such as emission maximum, life time and quantum yield of the bare complex. [3,5,6,21] Therefore, the white light emission of the NC-QDC composite (at an excitation wavelength of 365 nm) originated from three different luminescent sources – blue emitting tryptophan residue of the BSA protein, green emitting ZnQ_2 complex attached to the ZnS Qdot (QDC) and red emitting Au NCs. Similarly, the observed changes in excitation spectra of BSA stabilized Au NCs following ZnS incorporation and then complexation with HQ clearly supported the formation of the new white light emitting nanocomposite (Figure A.3.9, Appendix).

Table 3.1. Chromaticity color coordinates of (i) BSA stabilized Au NCs (λ_{ex}- 365 nm at pH 6.8), (ii) Au NC-ZnS Qdot composite (λ_{ex}- 365 nm at pH 6.8) and (iii) HQ treated Au NC-ZnS Qdot composite (λ_{ex}- 365 nm at pH 6.8).

Samples	λ_{ex} (nm)	Chromaticity Coordinates (x, y)
(i) BSA stabilized Au NCs	365	(0.54, 0.29)
(ii) Au NC-ZnS Qdot composite	365	(0.42, 0.25)
(iii) HQ treated Au NC-ZnS Qdot composite	365	(0.32, 0.33)

The importance of the emission characteristics of the NC-QDC composite was evident from the chromaticity color coordinates. Figure 3.4C (as well as Table 3.1) shows the chromaticity coordinates in CIE (Commission Internationale del'Eclairage 1931) diagram of the as-synthesized Au NCs (0.54, 0.29), NC-Qdot composite (0.42, 0.25) and NC-QDC composite (0.32, 0.33), calculated based on the emission spectra (refer to Figure 3.4B) in the liquid phase. The coordinates are in support of the observed visual changes under UV light during NC-QDC formation from Au NC (via NC-Qdot; as shown in Figure 1A). Importantly, the chromaticity color coordinates of NC-QDC (0.32, 0.33) appeared near to the perfect white light (0.33, 0.33)[3] – which strongly supported its WLE nature and thus its application potential in light emitting devices. It is to be mentioned here that the white light emission (in terms of chromaticity coordinates based on emission with an excitation wavelength of 365 nm) could be best achieved following reaction between NC-Qdot (having absorbance value 0.198 at 365 nm) and 4.98 μM of HQ (Figure A.3.10 and Table A.3.1, Appendix). Additionally, (0.31, 0.26) and (0.59, 0.41) chromaticity coordinates were observed when the same WLE QDC was probed at excitation wavelengths of 320 (of ZnS Qdot) and 505 nm (of Au NC), respectively (Figure A.3.11, Appendix). The observations supported the presence of the different luminescent species (Au NCs, QDC and BSA) – in the NC-QDC composite, which synchronously generated white light at an excitation wavelength of 365 nm. It may be mentioned here that a mixture of ZnQ_2 synthesized on the surface of ZnS Qdot (stabilized by BSA) and Au nanoclusters stabilized by BSA provided the same results as far as emission spectrum (Figure A.3.12, Appendix) was concerned, thus further substantiating the observations reported. However, the preparation of a composite with all components

together has advantage in device fabrication (and sample handling) in comparison to having individual components mixed physically (Figure A.3.12, Appendix).

Further, the aqueous dispersion of as synthesized WLE NC-QDC composite (at pH~6.8) exhibited photoluminescence quantum yield (PLQY) of 3.2 % (with excitation at 365 nm, Table A.3.2, Appendix). On the other hand, Au NCs (at pH~6.8) and the Au NC-ZnS Qdot composite (at pH~6.8) resulted in 4.6 and 1.7 % QYs, respectively. Additionally, the WLE NC-QDC composite (at pH~6.8) exhibited average life times (τ_{av}) of 0.63 μs (with respect to λ_{em} - 650 nm) and 12.82 ns (with respect to λ_{em} - 500 nm) (Figures A.3.13 and A.3.14 and Tables A.3.3 and A.3.4, Appendix).[12, 23] It is to be mentioned here that the average life time (λ_{ex} - 375 nm and λ_{em} - 650 nm) of the Au NCs (at pH~6.8) decreased from 0.93 μs to 0.75 μs upon formation of NC-Qdot composite and further decreased to 0.63 μs when NC-QDC composite was formed. [12, 23] This may be due to the environmetal changes of the BSA protein of Au NCs during NC-Qdot and thus NC-QDC composite formation. Based on literature reports, it may be mentioned here that the spectral overlap of the emission of BSA (mainly due to tryptophan residue, Figure A.3.4, Appendix) and the absorption of the Au NCs (Figure A.3.5 A, Appendix) with possible spatial the proximity of the Au NCs to the tryptophan residues (present inside BSA) made the energy transfer from tryptophan (donor) to Au NCs (acceptor) facile.[12,16] In the current WLE NC-QDC system, there may be two acceptors: one is Au NCs and another one is ZnQ_2 attached to ZnS Qdot , based on their overlap of absorption wavelength (maxima) with the emission wavelength of tryptophan residue (present in BSA). Hence, there may simultaneous energy transfer from tryptophan residue to Au NCs as well as to ZnQ_2 attached to ZnS Qdot. This may be one of the reasons for the observed decrease in emission intensity and also the life time of Au NCs in the NC-QDC composite (at pH 6.8) compared to as synthesized Au NCs (at pH 6.8). Further, the observed average life time of 12.82 ns (with respect to λ_{em} - 490 nm) in the WLE NC-QDC composite clearly demonstrated the formation of the ZnQ_2 complex on the surface of the ZnS Qdot.[5,6]

In addition, the WLE NC-QDC was found to be six times more photostable (when measured at three different emitting wavelengths) as compared to an organic dye (rhodamine 6G) at excitation wavelength 365 nm (Figure A.3.15 and Table A.3.5, Appendix). For example, WLE NC-QDC showed decrease in PL with a rate of 0.09, 0.10

and 0.10 % per min with respect to emission maxima at 650, 490 and 430 nm, respectively; while 0.61 % per min decrease in PL was observed for rhodamine 6G (emission maximum at 570 nm). Furthermore, the aqueous dispersion of the WLE NC-QDC composite showed zeta potential value of –25.5 ± 0.6 mV, indicating their stability in colloidal form.[3,5,6] In addition, the NC-QDC composite was found to be stable (in terms of luminescence) in water when measured for 3 days (Figure A.3.16 and Table A.3.6, Appendix). The high PLQY, excellent photostability and colloidal stability (in water) of the NC-QDC composite make it an attractive material for future biological sensing and imaging, in addition to their potential application in light emitting devices.

Importantly, the bright WLE nature of NC-QDC was also observed in their solid form – which is essential for practical utilization (Figure 3.6A). Additionally, the solid NC-QDC exhibited emission spectrum consisting two main peaks at 490 and 650 nm – in addition to a weak peak at 430 nm – with a chromaticity coordinate value of (0.30, 0.31) (Figure 3.6B,C). The observed emission spectrum and corresponding chromaticity value of solid NC-QDC also depicted that there was no significant change in their white light nature when they were transformed from liquid dispersion to solid phase. Further, the white light emitting nature of the solid NC-QDC was found to be stable (in terms of luminescence) for more than 3 months' time period (Figure 3.7 and Table A.3.7, Appendix).

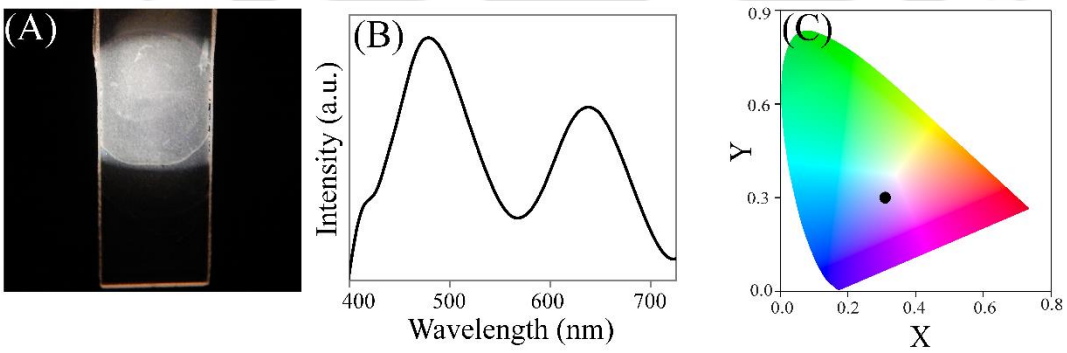

Figure 3.5. (A) Digital photograph; **(B)** emission spectrum (λ_{ex}-365 nm) and **(C)** corresponding CIE diagram of HQ treated BSA stabilized Au NC-ZnS Qdot (NC-QDC) composite in solid state

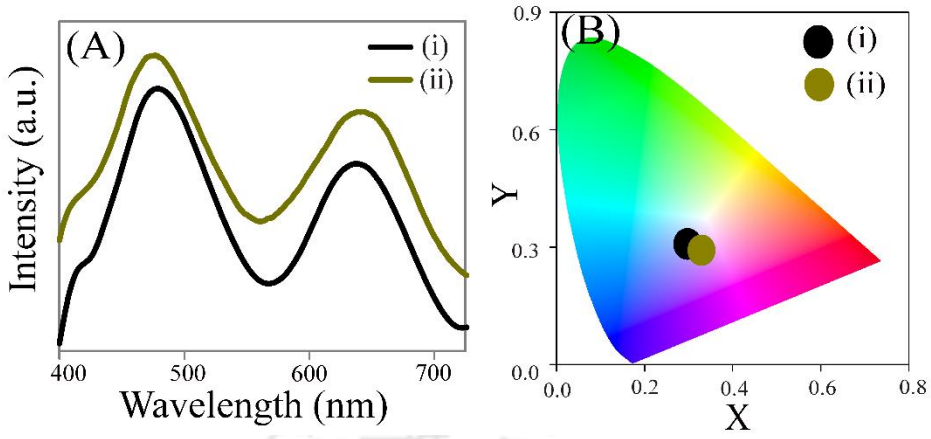

Figure 3.6. (A) Emission spectra (λ_{ex}-365 nm) and corresponding **(B)** CIE chromaticity diagram of HQ treated BSA stabilized Au NC-ZnS composite at solid state at (i) initially and (ii) after 3 months.

The bio-friendly nature of the aqueous dispersion of the WLE NC-QDC nanocomposite was confirmed by incubating the human embryonic kidney HEK 293 cells with different concentrations of the nanocomposite and carrying out 3-(4,5-dimethylthiazol-2-yl)-2,5-diphenyltetrazolium bromide (MTT)-based cell viability assay after 24 h. The results indicated that more than 90 % of the cells were viable when incubated with 15.2 µg/mL or lesser amount of nanocomposite (Figure 3.7.A). Even with concentration as high as 480 µg/mL, the cell viability was around 70 % (Figure 3.7.B). This clearly demonstrated the low cytotoxicity behaviour of the nanocomposites.

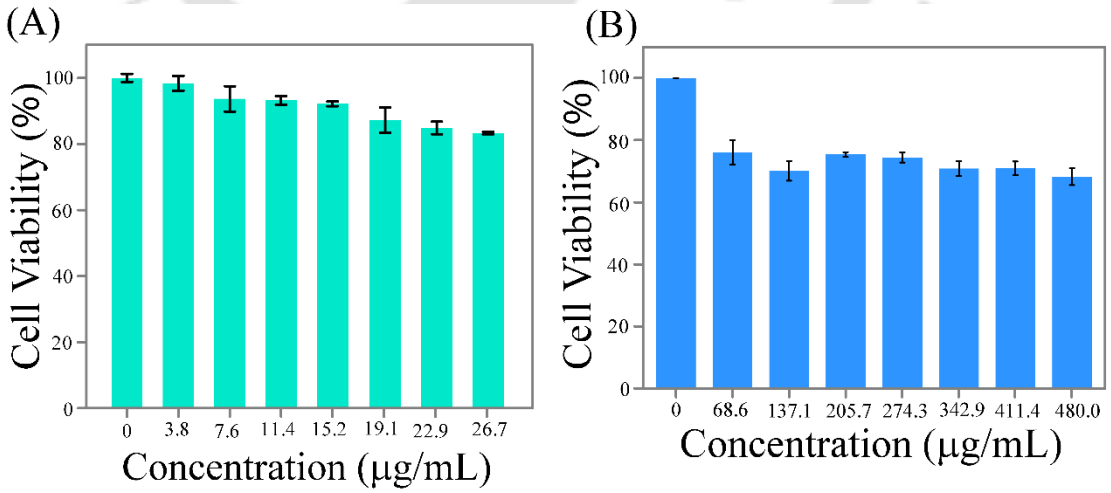

Figure 3.7. MTT based cell viability assay of HEK 293 cells after 24 h incubation using different concentrations of NC-QDC composite, upto maximum concentration of **(A)** 26.7 µg/mL and **(B)** 480 µg/mL.

3.3. Conclusion

In conclusion, a new and bio-friendly WLE nanocomposite has been synthesized using BSA-stabilized Au NCs and QDC (composed of ZnQ_2 complexes on ZnS Qdot). The high PLQY, photostability, colloidal stability, near white light chromaticity coordinates (both in liquid and solid phases) and non-toxic nature of the NC-QDC nanocomposite would make it an advanced material for fabricating bio-friendly light emitting diodes (LED). Apart from the LED application, the WLE NC-QDC may have future application in selective sensing of different chemical or biological species -based on their specific chemical interaction with the individual components (i.e. either Au NCs or QDCs) present in the BSA protein or with BSA protein itself and also in cellular imaging.

References:

(1) Xie, J.; Zheng, Y.; Ying, J. Y. Protein-Directed Synthesis of Highly Fluorescent Gold Nanoclusters. *J. Am. Chem. Soc.* **2009**, *131*, 888−889.

(2) Khandelia, R.; Bhandari, S.; Pan, U. N.; Ghosh, S.S.; Chattopadhyay, A. Gold Nanocluster Embedded Albumin Nanoparticles for Two-Photon Imaging of Cancer Cells Accompanying Drug Delivery. *Small* **2015**, *11*, 4075−4081.

(3) Pramanik, S.; Bhandari, S.; Roy, S.; Chattopadhyay, A. Synchronous Tricolor Emission-Based White Light from Quantum Dot Complex. *J. Phys. Chem. Lett.* **2015**, *6*, 1270−1274.

(4) Tsoi, K. M.; Dai, Q.; Alman, B. A.; Chan, W. C. W. Are Quantum Dots Toxic? Exploring the Discrepancy between Cell Culture and Animal Studies. *Acc. Chem. Res.* **2013**, *46*, 662−671.

(5) Bhandari, S.; Roy, S.; Pramanik, S.; Chattopadhyay, A. Double Channel Emission from a Redox Active Single Component Quantum Dot Complex. *Langmuir* **2015,** *31*, 551−561.

(6) Bhandari, S.; Roy, S.; Chattopadhyay, A. Enhanced Photoluminescence and Thermal Stability of Zinc Quinolate Following Complexation on the Surface of Quantum Dot. *RSC Adv.* **2014**, *4*, 24217−24221.

(7) Begum, R.; Bhandari, S.; Chattopadhyay, A. Surface Ion Engineering of Mn^{2+}-Doped ZnS Quantum Dots Using Ion-Exchange Resins. *Langmuir* **2012**, *28*, 9722−9728.

(8) Kuznetsov, A.S.; Tikhomirov, V.K.; Moshchalkov, V.V. UV-Driven Efficient White Light Generation by Ag Nanoclusters Dispersed in Glass Host. *Mater. Lett.***2013**, *92*, 4−6.

(9) Maiti, D.K.; Roy, S.; Baral, A.; Banerjee, A. A Fluorescent Gold-Cluster Containing a New Three Component System for White Light Emission through a Cascade of Energy Transfer. *J. Mater. Chem. C* **2014**, *2*, 6574−6581.

(10) Zhu, M.; Aikens, C. M.; Hollander, F. J.; Schatz, G. C.; Jin, R. Correlating the Crystal Structure of A Thiol-Protected Au_{25} Cluster and Optical Properties. *J. Am. Chem. Soc.* **2008**, *130*, 5883−5885.

(11) Wen, X.; Yu, P.; Toh, Y.; Hsu, A.; Lee, Y.; Tang, J. Fluorescence Dynamics in BSA-Protected Au_{25} Nanoclusters. *J. Phys. Chem. C* **2012**, *116*, 19032−19038.

(12) Xavier, P.L.; Chaudhari, K.; Verma, P. K.; Pal, S. K.; Pradeep, T. Luminescent Quantum Clusters of Gold in Transferrin Family Protein, Lactoferrin Exhibiting FRET. *Nanoscale* **2010**, *2*, 2769−2776.

(13) Xu, Y. L.; Sherwood, J.; Qin, Y.; Crowley, D.; Bonizzoni, M.; Bao, Y. P. The Role of Protein Characteristics in the Formation and Fluorescence of Au Nanoclusters. *Nanoscale* **2014**, *6*, 1515– 1524.

(14) Stamplecoskie, K. G.; Kamat, P. V. Synergistic Effects in the Coupling of Plasmon Resonance of Metal Nanoparticles with Excited Gold Clusters. *J. Phys. Chem. Lett.* **2015**, *6*, 1870−1875.

(15) Aldeek, F.; Muhammed, M. A. H.; Palui, G.; Zhan, N.; Mattoussi, H.; Growth of Highly Fluorescent Polyethylene Glycol and Zwitterion Functionalized Gold Nanoclusters. *ACS Nano* **2013**,*7*, 2509−2521.

(16) Chaudhari, K.; Xavier, P. L.; Pradeep, T. Understanding the Evolution of Luminescent Gold Quantum Clusters in Protein Templates. *ACS Nano* **2011**, 5, 8816–8827.

(17) Cao, X.L.; Li, H.W.; Yue, Y.; Wua, Y. pH-Induced Conformational Changes of BSA in Fluorescent AuNCs@BSA and its Effects on NCs Emission. *Vib. Spectrosc.* **2013,** *65*, 186– 192.

(18) Wu, Z.; Jin, R. On the Ligand's Role in the Fluorescence of Gold Nanoclusters. *Nano Lett*. **2010**, *10*, 2568-2573.

(19) Yu, K.; Luo, Z.; Chevrier, D.M.; Leong, D.T; Zhang, P.; Jiang, D. Xie, J. Identification of a Highly Luminescent $Au_{22}(SG)_{18}$ Nanocluster. *J. Am. Chem. Soc.* **2014**, *136*, 1246–1249.

(20) He, X.; Gao, Li.; Ma. N. One-Step Instant Synthesis of Protein-Conjugated Quantum Dots at Room Temperature. *Sci. Rep.* **2013**, *3*, 2825–2835.

(21) Bhandari, S.; Khandelia, R.; Pan, U. N.; Chattopadhyay, A. Surface Complexation-Based Biocompatible Magnetofluorescent Nanoprobe for Targeted Cellular Imaging. *ACS Appl. Mater. Interfaces*, **2015**, *7*, 17552–17557.

(22) Mooney, J.; Krause, M.M.; Saari, J.I.; Kambhampati, P. Challenge to the Deep-Trap Model of the Surface in Semiconductor Nanocrystals. *Phys. Rev. B* **2013**, *87*, 081201−5.

(23) Wen, X.; Yu, P.; Toh, Y.R; Tang, J. Structure-Correlated Dual Fluorescent Bands in BSA-Protected Au_{25} Nanoclusters *J. Phys. Chem. C* **201**2, 116, 11830−11836.

Chapter 4

Zinc Quinolate Complex Decorated $CuInS_2$/ZnS Core/Shell Quantum Dots for White Light Emission

Fabrication of a single component white light emitting (WLE) nanocomposite –following the formation of a luminescent zinc quinolate complex (using 8-hydroxyquinoline (HQ) as a complexation agent) on the surface of the ZnS shell of $CuInS_2$/ZnS core/shell quantum dots is described here. The synchronous contribution of greenish blue emission by the zinc quinolate surface complex and red emission by the $CuInS_2$/ZnS core/shell quantum dots led to white light generation from the nanocomposite upon UV excitation. The reported nanocomposite exhibited bright natural cool white light emission with chromaticity color coordinates of (0.32, 0.35) and (0.32, 0.33), color rendering indices (CRI) of 91 and 83 and correlated color temperatures (CCT) of 6087 K and 5930 K in the solution and solid phase, respectively. Importantly, the higher temperature (up to 200 ^{0}C) sustainable white light emitting nature and long term stability of the solid nanocomposite may have importance for solid state light emitting applications.

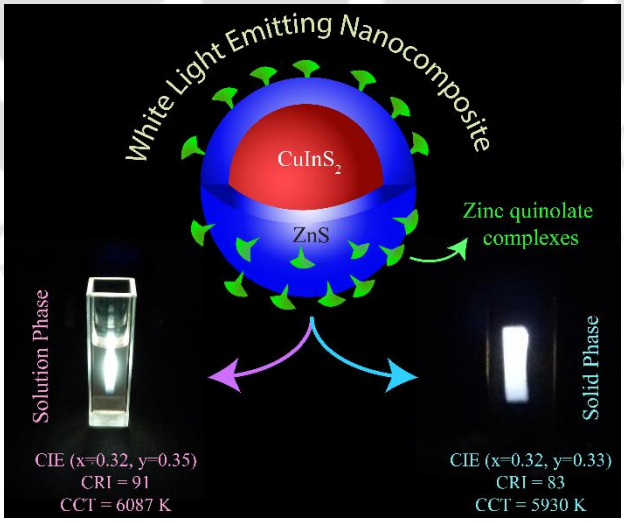

*** Reproduced from [*J. Mater. Chem. C*, 2017, 5, 7291--7296]**

4.1. Experimental Section

4.1.1. Materials. Copper(I) iodide (99.5%, Sigma-Aldrich), 1-dodecanethiol (98%, Sigma-Aldrich), indium(III) chloride (99%, Fluka), zinc acetate dihydrate (99%, Merck, India), 8-hydroxyquinoline (HQ, Merck, India), quinine sulfate (Fluka, USA), sulphuric acid (Merck, India) and ethanol (Tedia) were purchased and used without any further purification.

4.1.2. Synthesis of CuInS2 Qdots. $CuInS_2$ Qdots were synthesized following an earlier reported method with slight modifications.[1] Briefly, 5.0 mM of indium chloride was added to 5.0 mL of dodecanethiol, where dodecanethiol acts as the capping agent, source of sulphur and solvent for this reaction. Under an N_2 atmosphere and constant stirring, the reaction mixture was heated at 100°C to completely dissolve the indium salt. Then, 5.0 mM of copper iodide was added to the reaction mixture and the resulting solution was heated to 230°C under constant flow of N_2 and reflux conditions for 20 min. During the progress of the reaction, the color of the solution changed from colorless to yellow to red and finally to dark brown. This clearly indicated the formation of $CuInS_2$ Qdots. The so obtained $CuInS_2$ Qdots were precipitated by adding excess ethanol and then centrifugation at a speed 25000 rpm for 15 min to remove the unreacted thiol and metal salts. The obtained pellet (from centrifugation) was dispersed in hexane and again precipitated using excess ethanol and centrifuged. This cycle was repeated for 4–5 times to purify the $CuInS_2$ Qdots by completely removing the unreacted precursor materials. Finally, the dark brown pellet was dried at 60°C and the dry brown powder and its hexane dispersion were used for further experiments. The synthesized $CuInS_2$ Qdots were characterized using powder X-ray diffraction (XRD), transmission electron microscopy (TEM), high resolution transmission electron microscopy (HRTEM), UV-vis and photoluminescence (PL) spectroscopy.

4.1.3. Synthesis of $CuInS_2$/ZnS core/shell Qdots. To overcoat the $CuInS_2$ Qdots, a reported method was followed with appropriate modifications.[2] For in-situ ZnS shell formation, the $CuInS_2$ Qdot-growth dispersion was cooled from 230°C to 100°C and then 5.0 mM zinc acetate was added into that. After that, the temperature of the resulting mixture was again increased to 230°C and the mixture was stirred continuously under an N_2 atmosphere for 2 h. The previously mentioned purification procedure was followed in order to obtain the purified $CuInS_2$/ZnS core/shell Qdots. The so obtained purified

Qdots were characterized by PXRD, TEM, HRTEM, UV-vis spectroscopy, PL spectroscopy.

4.1.4. Preparation of Ligand (HQ) Solutions. 5.0 mM of 8-hydroxyquinoline (HQ) solution in ethanol was prepared using sonication.

4.1.5. Synthesis of white light emitting (WLE) nanocomposite (in dispersion and solid phases). The WLE nanocomposite was synthesized following room temperature reaction between the hexane dispersion of the $CuInS_2$/ZnS core/shell Qdots and an ethanolic dispersion of the HQ ligand. At first, the absorbance of the so obtained $CuInS_2$/ZnS core/shell Qdots was fixed to 0.12 (at a wavelength of 365 nm). Then, 5.0 μL of 5.0 mM HQ (in ethanol) was sequentially added to 3.0 mL of the hexane dispersion of $CuInS_2$/ZnS core/shell Qdots. It is to be mentioned here that the chromaticity (with respect to the obtained emission from the HQ-treated $CuInS_2$/ZnS core/shell Qdots) was monitored to calculate the optimum amount of HQ needed for generating near white light chromaticity. It was found that 10.0 μL of 5.0 mM HQ was the optimum amount for generating near white light chromaticity from3.0 mL of a hexane dispersion of the $CuInS_2$/ZnS core/shell Qdots. Then the resulting mixture, with the optimum amount of HQ added to the $CuInS_2$/ZnS core/shell Qdots, was centrifuged at a speed of 25000 rpm for 15 min following addition of excess ethanol. The so obtained pellet was dispersed into the same amount (3.0 mL) of hexane and used for further experiments. The hexane dispersion of the WLE nanocomposite was deposited on a quartz slide followed by the room temperature evaporation of the hexane. The solid form of the WLE nanocomposite on a quartz slide was used for thermal stability, photostability and long-term stability studies. The powder XRD, TEM, HRTEM, UV-vis spectroscopy and PL spectroscopy analysis were carried out to characterize the WLE nanocomposite.

4.2. Results and Discussion

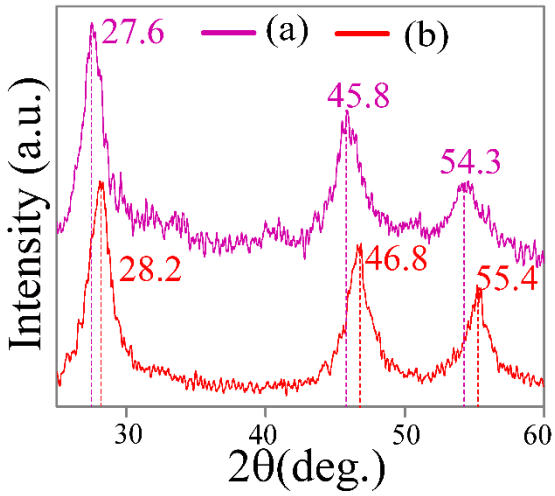

Figure 4.1. Powder X-ray diffraction (XRD) patterns of (a) $CuInS_2$ Qdots and (b) $CuInS_2$/ZnS core/shell Qdots.

The change in structural characteristics (mainly crystal plane's diffraction pattern and size) and optical parameters (such as emission maximum, photoluminescence quantum yield (PLQY) and emission life time), of the as obtained $CuInS_2$ Qdots, following the growth of the ZnS shell on their surface, was used to confirm the formation of $CuInS_2$/ZnS core/shell Qdots.[3-7] The powder XRD pattern of the solid $CuInS_2$ Qdots exhibited characteristic peaks at 27.61°, 45.81° and 54.31° corresponding to the (112), (204)/(220), and (312) planes of chalcopyrite $CuInS_2$ and the observed shift in the 2θ value upon growing ZnS on their surface indicated the formation of the $CuInS_2$/ZnS core/shell Qdots (Figure 4.1).[1,2,8,9] As the ZnS grew on the surface of the $CuInS_2$ Qdots, the size of the particles increased from 4.0 ± 0.3 nm to 4.2 ± 0.2 nm, which is in support of the earlier reported method for the formation of $CuInS_2$/ZnS core/shell Qdots (Figure 4.2).[1,2,7-9] Furthermore, the $CuInS_2$ Qdots showed the main characteristic (112), (204)/(220) and (312) planes of chalcopyrite $CuInS_2$ in selected area electron diffraction (SAED; Figure 4.2C1) analysis, while the (111), (220) and (311) planes – which are the characteristic planes of ZnS – were observed when the ZnS shell was grown on the surface of the $CuInS_2$ Qdots (Figure 4.2C2). In addition, the observed lattice fringe of 0.32 nm in HRTEM images supported the crystalline nature of the particles and formation of the $CuInS_2$/ZnS core/shell Qdots (Figure A.4.1, Appendix).[5,10] The results clearly demonstrated the successful formation of $CuInS_2$ Qdots and then $CuInS_2$/ZnS core/shell Qdots.[1,2,7-9]

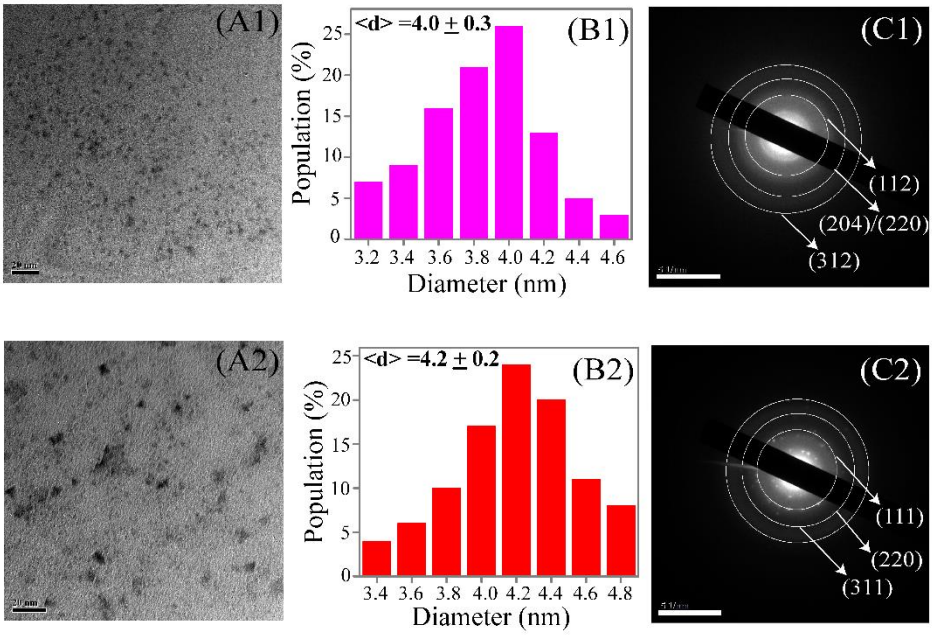

Figure 4.2. (A) transmission electron microscopic (TEM) images (scale bar – 20 nm), **(B)** corresponding particle size distributions and **(C)** selected area electron diffraction (SAED; scale bar – 5 nm^{-1}) patterns of (1) $CuInS_2$ and (2) $CuInS_2$/ZnS core/shell Qdots.

Upon ZnS shell formation on the $CuInS_2$ Qdots, the UV-vis spectrum of the Qdots (in hexane; with an absorption edge at 365 nm) was sharpened – while the weak emission of the Qdots (at 700 nm) was significantly enhanced with a 70 nm blue shift in the emission maximum (shifted to 630 nm), at an excitation wavelength of 365 nm (Figure 4.3A and B). There was no significant change (except sharpening) in the excitation spectrum of $CuInS_2$ following ZnS shell formation (Figure A.4.2, Appendix). Importantly, with the formation of the ZnS shell on the Qdots, the PLQY and the average emission life time of the as-synthesized Qdots increased from 0.8% to 3.3% and from 127.7 ns to 365.1 ns, respectively (Tables A.4.1, A.4.2 and Figure A.4.3, Appendix). It is to be mentioned here that the luminescence properties of the $CuInS_2$ Qdots originate from radiative recombination of a donor–acceptor pair (DAP) – in which interstitial In ions, vacancies at the Cu sites and Cu replacing In sites act as acceptor states and interstitial Cu ions, vacancies at the sulphur sites and In replacing Cu sites act as donors – within the bandgap of the nanocrystals,[11,3-6] whereas the non-radiative transition from the surface defect states account for the lowering in PLQY of only the $CuInS_2$ Qdots. Upon ZnS shell formation on the $CuInS_2$ Qdots, a blue shift and increase in PLQY were observed – which are because of the reduction of the size of the core $CuInS_2$ Qdots during substitution of surface cations (Cu^{1+} and In^{3+}) by Zn^{2+} ions at higher temperature and the

removal of surface defects respectively.[1,2,7-9,12] It is to be mentioned here that the observed relatively low PLQY of the $CuInS_2$/ZnS Qdots may be due to the changes in the ratio of the precursors (Cu: In) and the use of excess 1-dodecanethiol, during the synthesis, in comparison to earlier reported protocols.[1,2,8,12,13] As is clear from our results, the shift in the X-ray diffraction pattern, the observed blue shift in the emission maximum and the enhancement in PLQY and average emission life time of the $CuInS_2$ Qdots – upon ZnS shell formation – clearly demonstrated the successful formation of the $CuInS_2$/ZnS core/shell Qdots.

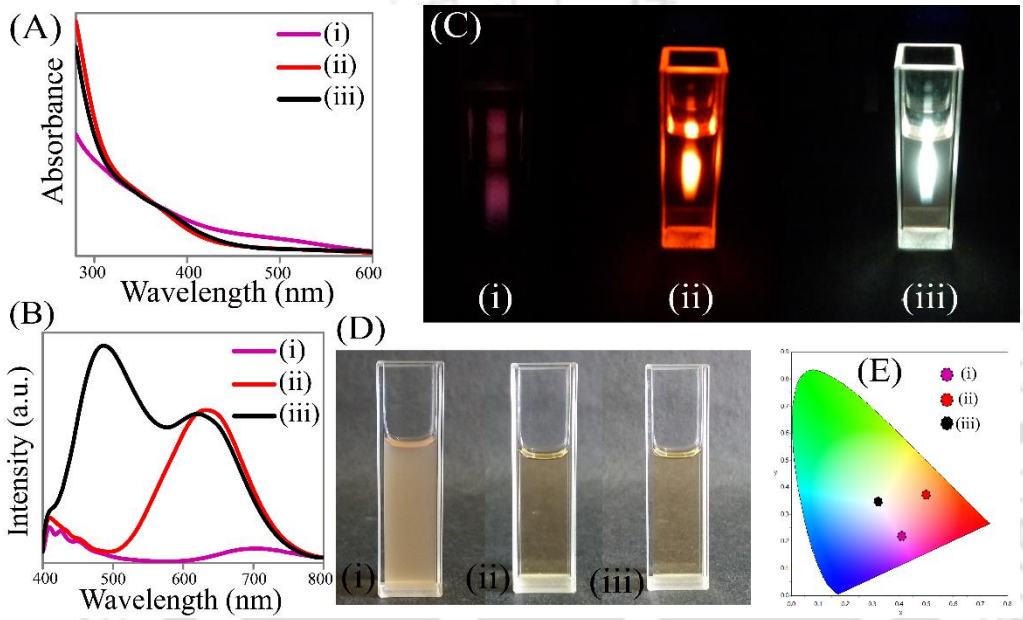

Figure. 4.3. (A) UV-vis spectra; **(B)** emission spectra (λ_{ex} – 365 nm); **(C)** digital photographs (captured in the presence of 365 nm light from a spectrofluorimeter); **(D)** digital photographs (captured in the presence of room light); and **(E)** CIE chromaticity diagram of the hexane dispersions of (i) $CuInS_2$ Qdots, (ii) $CuInS_2$/ZnS core/shell Qdots and (iii) HQ-treated $CuInS_2$/ZnS core/shell Qdots.

Upon a room temperature complexation reaction with HQ, no significant change was noticed in the UV-vis spectrum of the $CuInS_2$/ZnS core/shell Qdots (in hexane) (Figure 4.3 A). On the other hand, at an excitation wavelength of 365 nm, a new emission peak at 485 nm appeared – in addition to the original emission peak (at 630 nm) of the $CuInS_2$/ZnS core/shell Qdots (Figure 4.3B). The appearance of the new peak at 485 nm is attributed to the electronic transition from the highest occupied molecular orbital (HOMO; electron-rich phenoxide ring) to the lowest unoccupied molecular orbital

(LUMO; electron deficient pyridyl ring) of the HQ moiety of the formed ZnQ_2 complex on the surface of the ZnS shell – which is also supported by earlier observations.[14-19]

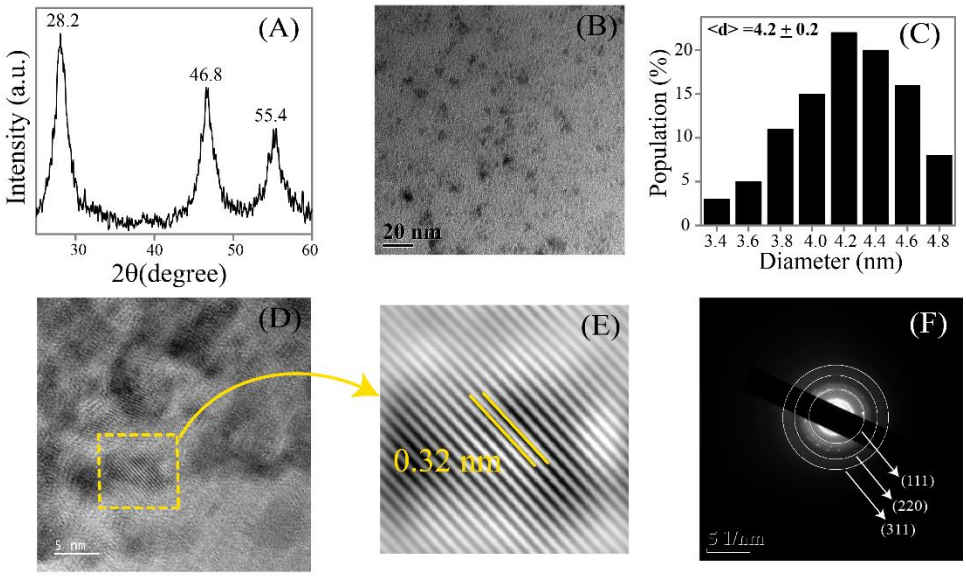

Figure. 4.4. (A) Powder x-ray diffraction (XRD) pattern, **(B)** transmission electron microscopic (TEM) image (scale bar – 20 nm), **(C)** corresponding particle size distribution, **(D)** High resolution transmission electron microscopic (HRTEM) image (scale bar – 5 nm), **(E)** corresponding inverse fast Fourier transform (IFFT) image and **(F)** selected area electron diffraction (SAED; scale bar – 5 nm^{-1}) pattern of HQ treated $CuInS_2$/ZnS core/shell Qdots.

Interestingly, the HQ treated $CuInS_2$/ZnS core/shell Qdots exhibited a sharp peak at 365 nm in the excitation spectrum when the emission maximum was probed at 485 nm; while no significant change was observed in the excitation spectrum when the emission maxima were probed at 630 nm (Figure A.4.2, Appendix). In addition, at an excitation wavelength of 365 nm, the treatment of HQ (with the same concentration – which was used for complexation of the $CuInS_2$/ZnS core/shell Qdots) to only $CuInS_2$ Qdots exhibited very weak emission at 485 nm (compared to HQ treated $CuInS_2$/ZnS core/shell Qdots; Figure A.4.4, Appendix).This may be due to the formation of a weakly luminescent In-quinolate complex on the surface of the $CuInS_2$ Qdots (since the CuQ_2 complex is non-fluorescent in nature).[20] In addition, the experiments were performed in hydrophobic solvent (here hexane), which ruled out the effect of pH on the observed changes in the luminescence. The presence of the characteristic stretching frequencies of the main functional groups due to the ZnQ_2 complexes,[14-19] which were absent in the as-synthesized $CuInS_2$/ZnS core/shell Qdots in the Fourier transformed infrared (FTIR) spectra (Figure A.4.5 and Table A.4.3, Appendix), further confirmed the formation of

the ZnQ_2 complex on the surface of the ZnS shell of the core/shell Qdots. As per our earlier results, [14-19] the attachment of the ZnQ_2 complex on the surface of metal sulphide Qdots (mainly ZnS) – without deteriorating the crystal integrity – is thought to be facilitated via involvement of dangling sulphide ions. Interestingly, the XRD and TEM analyses (measuring the size and lattice fringe) of the HQ treated $CuInS_2$/ZnS core/shell Qdots revealed the morphological preservation of the $CuInS_2$/ZnS core/shell Qdots[5,10,14-19] following the complexation reaction (Figure 4.4). These results clearly indicated the formation of the ZnQ_2 complex on the ZnS shell surface without deterioration of the optical properties of $CuInS_2$/ZnS core/shell Qdots.

Figure 4.3C shows digital photographs of the samples in the solution phase, under the irradiation of 365 nm light using a spectrofluorimeter. The photographs revealed that only $CuInS_2$ (core) exhibited weak dull red color while bright red color was observed for the $CuInS_2$/ZnS (core/shell) Qdots. Interestingly, under the same conditions, a bright white color was observed in the case of the dispersion of the HQ treated $CuInS_2$/ZnS core/shell Qdots. On the other hand, under normal room light, the dispersions (in hexane) of only $CuInS_2$ Qdots, $CuInS_2$/ZnS core/shell Qdots and HQ treated $CuInS_2$/ZnS core/shell Qdots showed dark brown color (Figure 4.3D). The WLE nanocomposite (HQ treated $CuInS_2$/ZnS core/shell Qdots) exhibited a photoluminescence quantum yield (PLQY) of 5.1% (at an excitation wavelength of 365 nm and with respect to quinine sulphate as the standard) and average emission life times of 335.4 ns (with λ_{em} – 630 nm and λ_{ex} – 375 nm) and 12.5 ns (with λ_{em} – 485 nm and λ_{ex} – 375 nm) (Tables A.4.1, A.4.2 and Figure A.4.3, Appendix).[1,8,16] The decrease in average emission life time (with respect to λ_{em} – 630 nm; at λ_{ex} – 375 nm) in the WLE nanocomposite, compared to the $CuInS_2$/ZnS core/shell Qdots, may be either due to the energy transfer from the surface ZnQ_2 complex to the $CuInS_2$/ZnS core/shell Qdots (since the broad absorption spectrum of the $CuInS_2$/ZnS core/shell Qdots overlaps with the emission range of the ZnQ_2 complex) or the division of the energy to the respective emitting species $CuInS_2$/ZnS core/shell Qdots and ZnQ_2 complex, since both of the emitting species in the WLE nanocomposite exhibited the same excitation wavelength maximum of 365 nm. In addition, the observed lifetime, 12.5 ns (with respect to λ_{em} – 485 nm at λ_{ex} – 375 nm), is close to the lifetime value when the ZnQ_2 complex was formed on the surface of ZnS Qdots.[14-19] This further confirmed the formation of the ZnQ_2 complex on the surface of

the ZnS shell of the $CuInS_2$/ZnS core/shell Qdots and thus the formation of the WLE nanocomposite.

The whiteness, brightness and cool/warm nature of the white light emitted by the HQ-treated $CuInS_2$/ZnS core/shell Qdots were determined by using the CIE (Commission Internationale del'Eclairage 1931) chromaticity coordinates, color rendering index (CRI) and correlated color temperature (CCT) values, respectively. The dispersion of the HQ treated $CuInS_2$/ZnS core/shell Qdots (in hexane) exhibited chromaticity coordinates of (0.32, 0.35), a CRI value of 91 and a CCT value of 6087 K (Figure 4.3E and Table 4.1) – which are very close to bright cool white light parameters (chromaticity – 0.33, 0.33; CRI ≥ 80 and CCT > 3500 K for cool light and > 6000 K for day light).[21-24] This clearly indicated that bright and cool white light was emitted from the reported nanocomposite in its liquid phase. On the other hand, the $CuInS_2$/ZnS core/shell Qdots showed chromaticity coordinates of (0.50, 0.37), a CRI value of 81, and a CCT value of 1956 K; while chromaticity coordinates of (0.41, 0.22), a value of 9 and no appropriate CCT were found for the only $CuInS_2$ Qdots (Figure 4.3E and Table 1). Furthermore, it was found that 16.6 μM of HQ was the optimum amount required for the complexation reaction with $CuInS_2$/ZnS core/shell Qdots (having absorbance value 0.12 at 365 nm) in order to achieve chromaticity coordinates close to the perfect white light (Figure A.4.6 and Table A.4.4, Appendix). In addition, the hexane dispersion of the HQ treated $CuInS_2$/ZnS core/shell Qdots (i.e. white light emitting material in the dispersion phase) was found to be stable up to the as measured time of 48 h (Figure A.4.7 and Table A.4.5, Appendix).

Table 4.1. Tabulated form of CIE color coordinates, color rendering indices (CRI) and correlated color temperatures (CCT) of (i) $CuInS_2$ Qdots (in liquid phase: hexane) (ii) $CuInS_2$/ZnS core/shell Qdots (in liquid phase: hexane) and (ii) HQ treated $CuInS_2$/ZnS core/shell Qdots (in liquid phase: hexane and in solid phase). These parameters were calculated with respect to the emission spectra in Figure 4.3B (for liquid phase) and Figure 4.5A (for solid phase).

Samples	Phase	Chromaticity (x,y)	CRI	CCT (K)
(i) $CuInS_2$	Liquid	(0.41, 0.22)	9	-
(ii) $CuInS_2$/ZnS	Liquid	(0.50, 0.37)	81	1956
(iii) HQ treated $CuInS_2$/ZnS	Liquid	(0.32, 0.35)	91	6087
	Solid	(0.32, 0.33)	83	5930

The white light emission in the solid form of the nanocomposite is very important in solid state lighting for its practical use in fabricating LEDs. In the current scenario, the presence of the two main peaks at 630 (due to $CuInS_2$/ZnS core/shell Qdots) and 485 nm (due to the ZnQ_2 complex being on the ZnS shell of the $CuInS_2$/ZnS core/shell Qdots) in the emission spectrum of the solid WLE nanocomposite (at an excitation wavelength of 365 nm; Figure 4.5A) revealed that there was no significant change in their white light nature during transformation from the liquid to solid phase. Importantly, the solid form of the nanocomposite (coated on a quartz substrate) showed bright white light in the presence of 365 nm light (which was digitally captured using a light source from the spectrofluorimeter; Figure 4.5B). The solid form of the WLE nanocomposite showed chromaticity color coordinates of (0.32, 0.33), with CRI and CCT values of 83 and 5930 K, respectively (Figure 4.5C and Table 4.1), which clearly demonstrated that the solid form of the nanocomposite emitted bright cool white light.[21-24] Interestingly, no significant change (in terms of emission and the corresponding color chromaticity) was observed when the same solid nanocomposite (coated on a quartz substrate) was heated at 200^0 C for 15 min (Figure 4.6 and Figure A.4.8, Appendix).

In addition, the WLE nanocomposite was found to be photostable under continuous irradiation of 365 nm light (with power of about one milliwatt) for half an hour (Figure. A.4.9, Appendix). These clearly demonstrated the higher temperature sustainable and photostable white light emitting nature of the presented nanocomposite. In addition, the white light nature of the solid form of the nanocomposite was found to be stable for 30 days (as measured in terms of color chromaticity) and thus demonstrated long term stability for potential usage (Figure. 4.6).

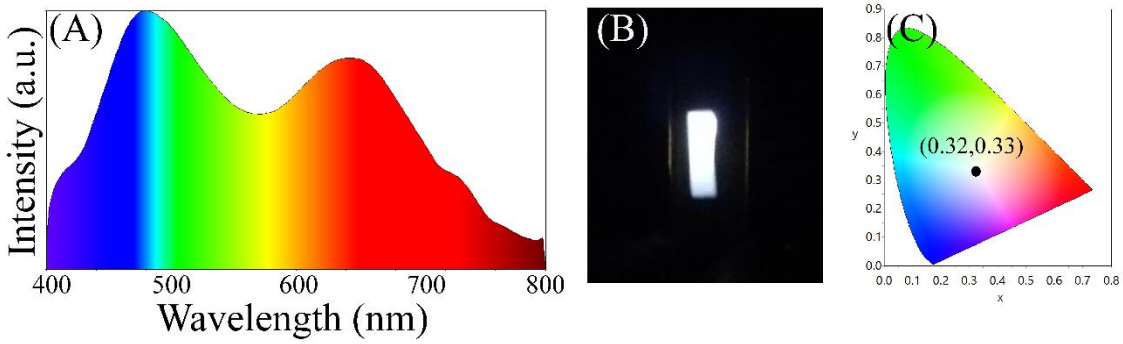

Figure 4.5. (A) Emission spectrum (λ_{ex}-365 nm); **(B)** digital photograph (captured in the presence of 365 nm light from a spectrofluorimeter); and **(C)** corresponding CIE chromaticity diagram of the solid form of HQ treated $CuInS_2$/ZnS core/shell Qdot (coated on a quartz substrate).

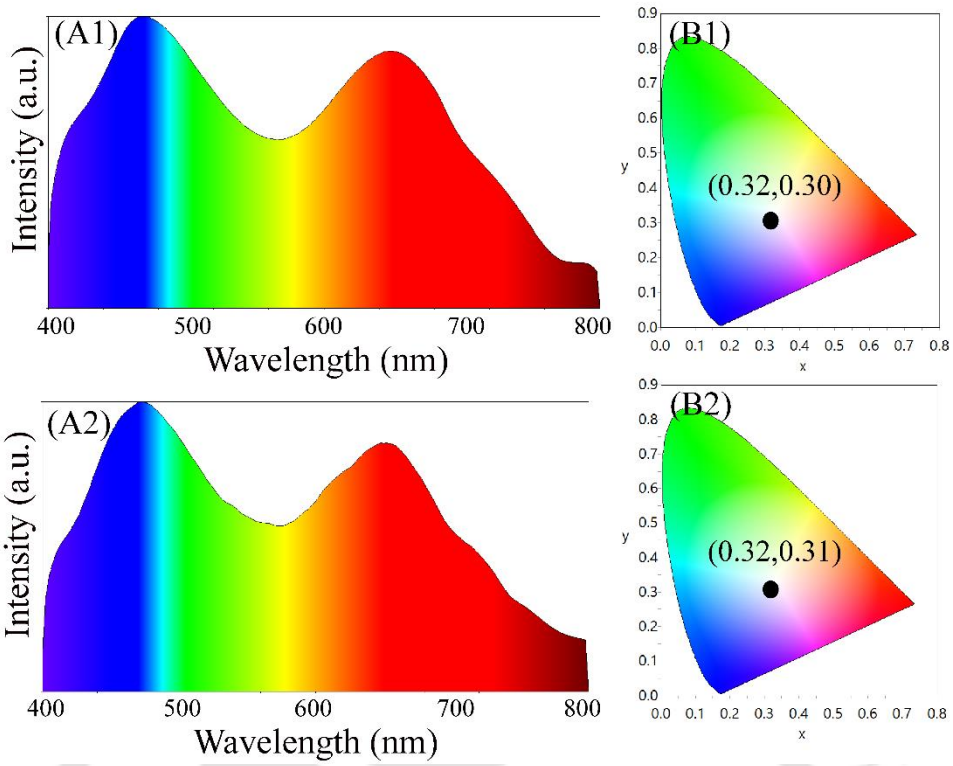

Figure 4.6. (A) Emission spectra (λ_{ex}-365 nm) and corresponding and **(B)** CIE chromaticity diagrams of the solid films of white light emitting nanocomposite, deposited on a quartz slide (1) followed by heating at 200 ^{o}C (emission spectrum of the sample was recorded after cooling down to room temperature) and (2) recorded after 30 days of deposition.

Scheme. 4.1 shows a schematic representation of the room-temperature complexation reaction (with HQ) on the ZnS shell surface of the $CuInS_2$/ZnS core/shell Qdots – following their synthesis. The overall process involves three steps: (1) at first, weakly red emitting CuInS2 Qdots were synthesized; (2) then over coating of the ZnS shell on the $CuInS_2$ Qdot core (the formation of bright red emitting $CuInS_2$/ZnS core/shell Qdots) was carried out and finally (3) the formation of a greenish blue emitting ZnQ_2 complex on the surface of the ZnS shell of the Qdots – following a complexation reaction with HQ – was achieved. This provided the final single component WLE nanocomposite – based on the synchronous contribution of the two independent emitting species: one is the $CuInS_2$/ZnS core/shell Qdots (emitting at 630 nm) and the other is the attached ZnQ2 complex (emitting at 485 nm; being on the surface of the ZnS shell of the Qdots).

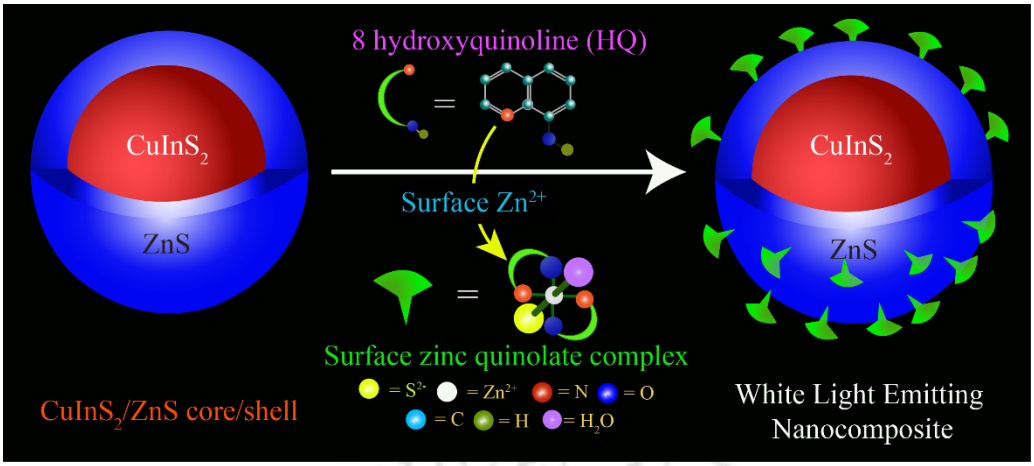

Scheme. 4.1. Schematic representation of the stepwise fabrication of the white light emitting nanocomposite.

4.3. Conclusion

In summary, the complexation reaction between $CuInS_2$/ZnS core/shell Qdots (following their synthesis) and HQ led to the formation of a single component white light emitting nanocomposite – which consisted of $CuInS_2$/ZnS core/shell Qdots and a surface ZnQ_2 complex (formed on the ZnS shell). Importantly, the reported nanocomposite exhibited high temperature sustainable bright cool white light emission, with close to perfect white light chromaticity coordinates, high CRI and near daylight CCT in their liquid and solid phases. The presented material may be an advanced material for fabricating low cost, environment friendly WLE devices in SSL research. Also, as a part of future applications, the reported WLE nanocomposite may have use in fabricating sensing devices depending upon the selective interaction of one of the present emitting species (here either $CuInS_2$/ZnS Qdots or the shell surface ZnQ_2 complex) with the external chemical or biological species of interest.

References:

(1) Li, L.; Pandey, A.; Werder, D. J.; Khanal, B. P.; Pietryga, M.; Klimov, V. I. Efficient Synthesis of Highly Luminescent Copper Indium Sulfide-Based Core/Shell Nanocrystals with Surprisingly Long-Lived Emission. *J. Am. Chem. Soc*. **2011**, *133*, 1176– 1179.

(2) Park, J.; and Kim, S. $CuInS_2$/ZnS core/shell quantum dots by cation exchange and their blue-shifted photoluminescence. *J. Mater. Chem.* **2011**, *21*, 3745–3750.

(3) Li, L.; Daou, T. J.; Texier, I.; Kim Chi, T. T.; Liem, N. Q.; Reiss, P. Highly Luminescent $CuInS_2$/ZnS Core/Shell Nanocrystals: Cadmium-Free Quantum Dots for In Vivo Imaging. *Chem. Mater*. **2009**, *21*, 2422– 2429.

(4) Jara, D. H.; Yoon, S.; Stamplecoskie, K. G.; Kamat, P. V. Size-Dependent Photovoltaic Performance of $CuInS_2$ Quantum Dots Sensitized Solar Cells. *Chem. Mater*. **2014**, *26*, 7221–7228.

(5) Niyamakom, P.; Quintilla, A.; Kohler, K.; Cemernjak, M.; Ahlswede, E.; Roggan, Scalable Synthesis of $CuInS_2$ Nanocrystal Inks for Photovoltaic Applications *J. Mater. Chem. A* **2015**, 3, 4470– 4476.

(6) Pons, T.; Pic, E.; Lequeux, N.; Cassette, E.; Bezdetnaya, L.; Guillemin, F.; Marchal, F.; Dubertret, B. Cadmium-Free $CuInS_2$/ZnS Quantum Dots for Sentinel Lymph Node Imaging with Reduced Toxicity. *ACS Nano* **2010**, *4*, 2531– 2538.

(7) Zhang, J.; Xie, R. and Yang, W. A Simple Route for Highly Luminescent Quaternary Cu-Zn-In-S Nanocrystal Emitters. *Chem. Mater*. **2011**, *23*, 3357–3361.

(8) Berends, A. C.; Rabouw, F. T.; Spoor, F. C. M.; Bladt, E.; Grozema, F. C.; Houtepen, A. J.; Siebbeles, L. D. A.; Donegá, C. M. Radiative and Nonradiative Recombination in $CuInS_2$ Nanocrystals and $CuInS_2$-Based Core/Shell Nanocrystals. *J. Phys. Chem. Lett*. **2016**, *7*, 3503– 3509.

(9) Akdas, T.; Walter, J.; Segets, D.; Distaso, M.; Winter, B.; Birajdar, B.; Spieckerb, E.; Peukert, W. Investigation of the size–property relationship in $CuInS_2$ quantum dots. *Nanoscale* **2015**, *7*, 18105 –18118.

(10) Park, S. H.; Hong, A.; Kim, J.-H.; Yang, H.; Lee, K.; Jang, H. S. Highly Bright Yellow-Green-Emitting $CuInS_2$ Colloidal Quantum Dots with Core/Shell/Shell Architecture for White Light-Emitting Diodes. *ACS Appl. Mater. Interfaces* **2015**, *7*, 6764– 6771.

(11) Fanizza, E.; Urso, C.; Pinto, V.; Cardone, A.; Ragni, R.; Depalo, N.; Curri, M. L.; Agostiano, A.; Farinola, G. M.; Striccoli, M. Single White Light Emitting Hybrid Nanoarchitectures Based on Functionalized Quantum Dots. *J. Mater. Chem. C* **2014**, *2*, 5286– 5291.

(12) Aldakov, D.; Lefrançois, A.; Reiss, P. Ternary and Quaternary Metal Chalcogenide Nanocrystals: Synthesis, Properties and Applications. *J. Mater. Chem. C* **2013**, *1*, 3756-3776.

(13) Zhong, H.; Bai, Z.; and Zou, B. Tuning the Luminescence Properties of Colloidal I−III−VI Semiconductor Nanocrystals for Optoelectronics and Biotechnology Applications *J. Phys. Chem. Lett.* **2012**, *3*, 3167−3175.

(14) Pramanik, S.; Bhandari, S.; Roy, S.; Chattopadhyay, A. Synchronous Tricolor Emission-Based White Light from Quantum Dot Complex. *J. Phys. Chem. Lett*. **2015**, *6*, 1270– 1274.

(15) Bhandari, S.; Pramanik, S.; Khandelia, R.; Chattopadhyay, A. Gold Nanocluster and Quantum Dot Complex in Protein for Biofriendly White-Light-Emitting Material. *ACS Appl. Mater. Interfaces* **2016**, *8*, 1600−1605

(16) Bhandari, S.; Roy, S.; Chattopadhyay, A. Enhanced Photoluminescence and Thermal Stability of Zinc Quinolate Following Complexation on the Surface of Quantum Dot. *RSC Adv*. **2014**, *4*, 24217– 24221.

(17) Bhandari, S.; Roy, S.; Pramanik, S.; Chattopadhyay, A. Double Channel Emission from a Redox Active Single Component Quantum Dot Complex. *Langmuir* **2015**, *31*, 551– 561.

(18) Bhandari, S.; Khandelia, R.; Pan, U. N.; Chattopadhyay, A. Surface Complexation-Based Biocompatible Magnetofluorescent Nanoprobe for Targeted Cellular Imaging. *ACS Appl. Mater. Interfaces* **2015**, *7*, 17552– 17557.

(19) Bhandari, S.; Roy, S.; Pramanik, S.; Chattopadhyay, A. Surface Complexation Reaction for Phase Transfer of Hydrophobic Quantum Dot from Nonpolar to Polar Medium. *Langmuir* **2014**, *30*, 10760– 10765.

(20) Thangarajua, K.; Kumaranb, R.; Ramamoorthy, P., Narayanan, V.; Kumara, J. Study on photoluminescence from tris-(8-hydroxyquinoline)indium thin films and influence of light. *Optik* **2012** 123, 1393– 1396.

(21) Chen, B.; Zhong, H.;Wang, M.; Liua, R.; Zoua, B. Integration of $CuInS_2$-based Nanocrystals for High Efficiency and High Colour Rendering White Light-Emitting Diodes. *Nanoscale* **2013**, *5*, 3514-3519.

(22) Ilaiyaraja, P.; Mocherla, P.S.V.; Srinivasan, T. K. and Sudakar, C. Synthesis of Cu-Deficient and Zn-Graded Cu−In−Zn−S Quantum Dots and Hybrid Inorganic−Organic Nanophosphor Composite for White Light Emission *ACS Appl. Mater. Interfaces* **2016**, *8*, 12456−12465.

(23) Chuang, P.; Lin, C.C. and Liu, R. Emission-Tunable $CuInS_2$/ZnS Quantum Dots: Structure, Optical Properties, and Application in White Light-Emitting Diodes with High Color Rendering Index. *ACS Appl. Mater. Interfaces* **2014**, *6*, 15379−15387.

(24) Yuan, X.; Ma, R.; Zhang, W.; Hua, J.; Meng, X.; Zhong, X.; Zhang, J.; Zhao, J.; Li, H. Dual Emissive Manganese and Copper Co-Doped Zn−In−S Quantum Dots as a Single Color-Converter for High Color Rendering White-Light-Emitting Diodes. *ACS Appl. Mater. Interfaces* **2015**, *7*, 8659−8666.

Chapter 5

A White Light Emitting Quantum Dot Complex for Single Particle Level Interaction with Dopamine Leading to Changes in Color and Blinking Profile

Interaction of the neurotransmitter dopamine with a single particle white light emitting (WLE) quantum dot complex (QDC) is shown here. The QDC composed of yellow emitting ZnO quantum dots (Qdots) and blue emitting $Zn(MSA)_2$ complex (MSA = N-methylsalicylaldimine) being synthesized on their surfaces. The sensing was achieved by the combined changes in the visual luminescence color from white to blue, chromaticity color coordinates from (0.31, 0.33) to (0.24, 0.23) and the ratio of the exponents (α_{on}/α_{off}) of on/off probability distribution (from 0.24 to 3.21) in the blinking statistics of WLE QDC. The selectivity of dopamine towards ZnO Qdots, present in WLE QDC, helped detect approximately 13 number of dopamine molecules per Qdot. Additionally, the WLE QDC exhibited high sensitivity, with a limit of detection of 3.3 nM (in the linear range of 1 – 100 nM) and high selectivity in presence of interfering biological species. Moreover, the single particle on-off bilking statistics based detection strategy may provide an innovative way for ultrasensitive detection of analytes.

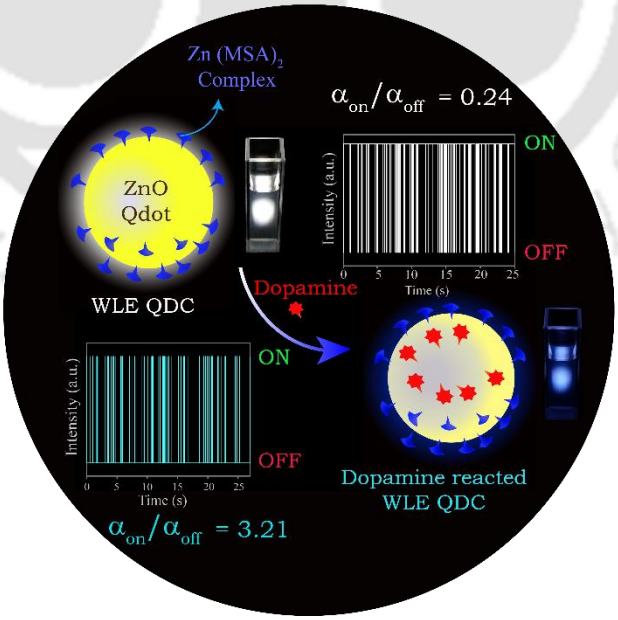

***[*Small* 2018, 14, 1800323]-Reproduced by permission from John Wiley and Sons.**

5.1. Experimental Section

5.1.1. Materials. Zinc acetate dihydrate (Merck), potassium hydroxide (KOH, Merck), salicylaldehyde (Sigma Aldrich), 1 M methyl amine in methanol (Sigma Aldrich), dopamine hydrochloride (Sigma Aldrich), quinine sulfate (Fluka, USA), sulphuric acid (Merck, India), benzoquione (Sigma Aldrich), cysteine (Sigma Aldrich), tryptophan (Sigma Aldrich), arginine (Sigma Aldrich), phenyl alanine (Sigma Aldrich), glutamic acid (Sigma Aldrich), aspartic acid (Sigma Aldrich), tyrosine (Sigma Aldrich) and uric acid (Sigma Aldrich) and ethanol (Tedia) were procured and used directly without any purification.

5.1.2. Synthesis of ZnO Qdots. ZnO Qdots were synthesized – following a reported process[1,2] – with the use of ethanol as solvent. Briefly, under vigorous stirring at 25^{o}C, 2.0 mL 0.5 M KOH (dissolved in ethanol) was added dropwise to a 50.0 mL ethanolic solution of zinc acetate having concentration of 5.0 mM and the resulting mixture, of milky white color, was kept for half an hour. Then, the resulting reaction mixture was centrifuged with a speed of 25000 rpm for 15 min and the so obtained pellet was washed with ethanol (in order to remove excess unreacted salts). The same cycle was repeated and the final pellet was dispersed in 50.0 mL of ethanol for further experiments. As synthesized ZnO Qdots were characterized using powder X-ray diffraction (XRD), transmission electron microscopy (TEM), high resolution transmission electron microscopy (HRTEM), UV-vis and photoluminescence (PL) spectroscopy.

5.1.3. Synthesis of *N-methylsalicylaldimine (MSA) ligand.* A reported condensation reaction between salicyaldehyde and methylamine was followed to synthesize N-methylsalicylaldimine (MSA).[1-3] In brief, 2 milli mole of methyl amine was added dropwise to the solution of 2.0 millimole of salicylaldehyde in 20.0 mL methanol and the resulting mixture, of yellow color, was allowed to stir for 4 h at 25 ^{o}C. The column chromatographic technique was used to purify the product (MSA).

5.1.4. Preparation of Ligand Solutions. 1.0 mM of MSA solution in ethanol was prepared using sonication.

5.1.5. Synthesis of white light emitting (WLE) quantum dot complex (QDC). The luminescence (under spectrofluorimeter) and chromaticity (in CIE-1931 diagram) were monitored to get optimum amount of MSA (in ethanol) needed to generate white

light from 3.0 mL of ZnO Qdots (in ethanol: with absorbance of 0.10 at an excitation wavelength of 350 nm). The 1.0 mM MSA was sequentially added to the ethanolic dispersion of ZnO Qdots (having absorbance of 0.10 at 350 nm) at 25 ^{o}C. The optimum amount of MSA was found to be of 9.9 μM. The resulting mixture, obtained from the treatment of 9.9 μM MSA to 3.0 mL ZnO Qdots, was centrifuged, with a speed of 25000 rpm for 15 min. Then, the so obtained pellet was repeatedly washed with ethanol and finally was redispersed in same amount of ethanol. The dispersion and corresponding solid form (obtained from centrifugation and drying at room temperature) of the QDC were used for further experiments. The powder XRD, TEM, HRTEM, UV-vis spectroscopy and PL spectroscopy analyses were carried out to characterize the WLE nanocomposite.

5.1.6. ***Confocal Microscopic Measurements and Blinking Analysis.*** Confocal imaging and single particle experiment of WLE QDC and dopamine added WLE QDC were performed by depositing the as-prepared dispersion (which was obtained from the treatment of 9.9 μM MSA to 3.0 mL ZnO Qdots with absorbance of 0.10 at 350 nm at 25 ^{o}C) of the materials on a glass cover slip. Imaging and blinking analysis of the samples were carried out using Zeiss LSM-880 confocal laser scanning microscope, equipped with a 355 nm diode-pumped solid-state UV laser (63 mW) for excitation and Plan-Apochromat, 63x /1.40, oil- immersion objective for imaging. The resulting fluorescence data of different channel images and single particle experiments were collected through the GaAsP detector and Airyscan detector, respectively. The blinking profile and video were recorded in acquisition mode under super resolution with 64 x 64 μm^2 frame size and by using binning time of 27 ms, with excitation power of 63 mW for a time duration of 27 s. The so obtained images and data were analyzed by ZEN black software.

5.1.7. Calculation of On-Off probability density distributions of Qdot. The on and off state probability densities of single Qdots were calculated by using the reported method[4-11] and using the following equation - $P_{(i)}(t) = \frac{N_i(t)}{N_{i,total}} \times \frac{1}{\Delta t_{i,av}}$; (i= on or off). Here P_i is the probability density of on or off events at time t, N_i is the number of on or off events, $N_{i,total}$ is the total number of events and $\Delta t_{i,av}$ is average of the time intervals of the events. These P_{on} or P_{off} distributions can be fitted to the truncated power law: $P_i(t) = At^{-\alpha}e^{-t\tau}$; where (i=on or off), A= amplitude, α= power law exponent, τ = saturation rate.

5.2. Results and Discussion

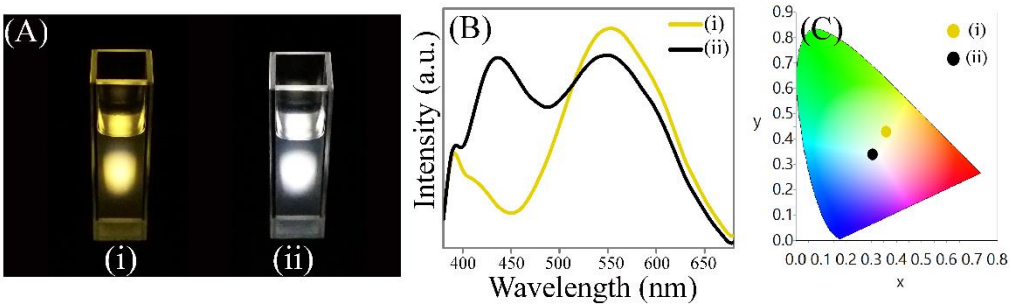

Figure 5.1. (A) Photographs (digitally captured under 350 nm light from a spectrofluorimeter), **(B)** emission spectra (λ_{ex} – 350 nm), and (C) corresponding chromaticity color coordinates in CIE diagram of the ethanolic dispersion of (i) ligand-free ZnO Qdots and (ii) WLE QDC.

Digital photographs (captured under a 350 nm light from a spectrofluorimeter) showed that the treatment of MSA ligand to presynthesized ZnO Qdots led to the change in their luminescence color from yellow to white due to the formation of QDC **(**Figure 5.1A**)**. The QDC (at λ_{ex}-350 nm) exhibited a new blue emission peak at 440 nm (due to the electronic transition from the highest occupied molecular orbital (HOMO) to the lowest unoccupied molecular orbital (LUMO) of surface $Zn(MSA)_2$ complex)[1] – in addition to the pristine broad yellow emission (centered at 550 nm) of ZnO Qdot (originating from surface trap states of the Qdots)[1] (Figure 5.1B). Similarly, a new peak at 318 nm appeared (indicative of the formation of $Zn(MSA)_2$ complex), along with the band edge of ZnO Qdots at 350 nm, for QDC in the absorption spectrum (Figure A.5.1, Appendix). No significant change was observed in the excitation spectrum (at λ_{em}-550 nm) of the ZnO Qdots, following addition of MSA (Figure A.5.2, Appendix). Furthermore, QDC exhibited the chromaticity coordinates of (0.31, 0.33) – which is for near to perfect white light emitter while (0.36, 0.43) chromaticity coordinates were observed for only ZnO Qdots (Figure 5.1C). The results clearly indicated the WLE nature of QDC. It is to be mentioned here that the concentration of MSA ligand was chosen based on the chromaticity coordinates near to perfect white light (0.33, 0.33)[1] and it was found that the optimum amount of MSA needed to generate white light from ZnO Qdots (with absorbance of 0.11 at 350 nm) was 9.9 μM (Figure A.5.3 and Table A.5.1, Appendix).

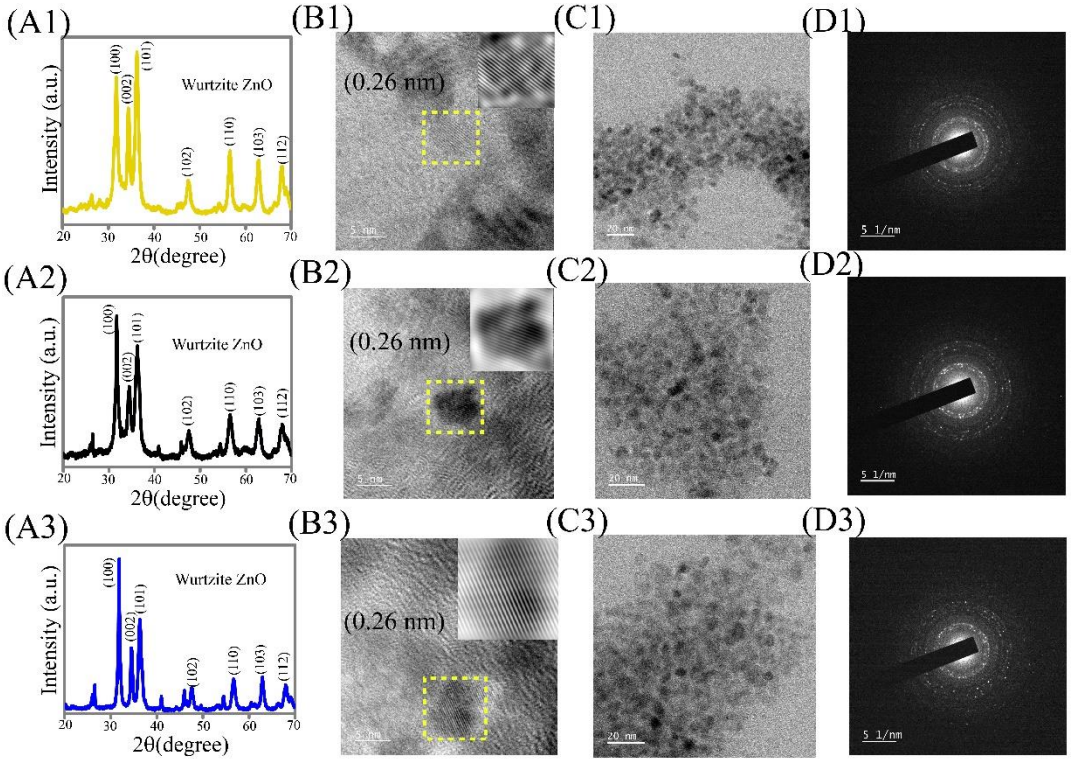

Figure 5.2. (A) Powder x-ray diffraction (XRD) patterns; **(B)** high resolution TEM images (scale bar-5 nm) and corresponding inverse fast Fourier transform (IFFT; inset square box) image; **(C)** transmission electron microscopic (TEM) images (scale bar – 20 nm); and **(D)** selected area electron diffraction (SAED) patterns (scale bar – 5 nm^{-1}) of (1) ligand free ZnO Qdots, (2) WLE QDC, and (3) dopamine added WLE QDC.

The photoluminescence quantum yield (PLQY; measured with respect to quinine sulphate) of the WLE QDC was found to be 2.4% while as such ZnO Qdots showed 1.2 % of PLQY (Table A.5.2, Appendix). Additionally, QDC exhibited average emission life times of 4.1 ns (for emission at 440 nm) and 38.0 ns (for emission at 550 nm) and no significant change was observed with respect to the average life time of the ZnO Qdots (λ_{em}-550 nm, τ_{av} = 38.8 ns), following MSA addition (Figure A.5.4 and Table A.5.3, Appendix). The observed diffraction peaks of the main characteristics planes of wurtzite ZnO in the x-ray diffraction (XRD) and the lattice fringe due to the 002 plane of wurtzite ZnO (0.26 nm) in the high resolution TEM image confirmed the formation of ZnO Qdots and also the preservation of their crystalline integrity following formation of WLE QDC (Figure 5.2)[1]

Furthermore, the stability of the luminescence (at λ_{ex}-350 nm; probed up to 48 h) and the cell viability of (after 24 h) assay of the different concentrations of colloidal WLE QDC indicated their colloidal stability and no apparent toxicity and thus to their application potential, especially in making biosensors (Figure A.5.5, Appendix).

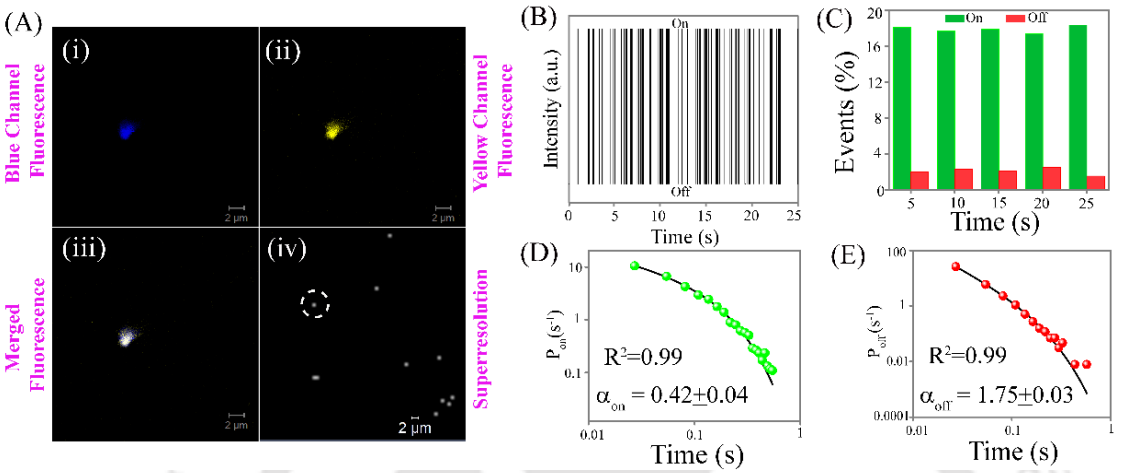

Figure 5.3. (A) Confocal laser scanning microscopic images (scale bar – 2.0 μm) of WLE QDC recorded in (i) blue, (ii) yellow emission channels and (iii) their merged version. (iv) Superresolution confocal laser scanning microscopic image of WLE QDC (scale bar – 2.0 μm; with respect to the area as obtained in the merged portion of panel (A)(iii)). **(B)** Representative time-dependent blinking profile of WLE QDC (related to the encircled particle shown in the panel (A)(iv)). **(C)** Histogram of proportion of on and off states of a Qdot (present in WLE QDC with respect to the blinking profile mentioned in panel (B). **(D,E)** Corresponding probability densities of on-states ($P_{on}(t)$) and off-states ($P_{off}(t)$) for single Qdots (present in WLE QDC).The data were obtained by using frame size of 64 × 64 μm^2, binning time of 27 ms, excitation power of 63 mW, and for a time duration of 27 s. The 355 nm laser was used to excite the samples

When viewed under a confocal laser scanning microscope (using 355 nm laser), QDC exhibited intense color owing to blue and yellow emissions (due to the presence of two emitting species $Zn(MSA)_2$ complex and ZnO Qdots) and the merged image clearly supports the bright white light nature to the QDC (Figure 5.3A). Single particle nature of WLE QDC (deposited on a glass cover slip) was demonstrated based on the blinking activity i.e., time dependent alteration between on state (emitting state) and off state (dark state) using confocal laser scanning microscopy (CLSM) under super-resolution. This is a primary signature, of possibly single luminescent nanocrystals, which distinguishes them from multiple nanocrystals.[4-13] Figure 5.3.A (iv) shows the super resolution representative image of the white colored particles as obtained from Figure 5.3.A (iii).

Corresponding blinking activity of a single WLE QDC was recorded for the marked particle. It clearly demonstrates the blinking activity of the WLE QDC, which confirmed the possibility of single particle nature. Importantly, WLE QDC exhibited square wave shaped on-off blinking[4,5], in time varying fluorescence intensity profile (Figure 5.3B) This is also in support of the possibly single particle nature of the WLE QDC and ruled out the probability of observation of multiple particles (which generally exhibit flickering in-between on and dim states, as shown in Figure A.5.6, Appendix).[4-13] Histogram (based on the blinking data obtained from Figure 5.3B) showed the occurrence of more number of on states, compared to off states, in the blinking profile of the WLE QDC and the on/off occurrence ratio was found to be 8.44 (Figure 5.3.C).

Table 5.1. Fitting parameters for probability density of on-states ($P_{on}(t)$) and off-states ($P_{off}(t)$) for 40 single WLE QDC particles – before and after dopamine addition.

Samples	α_{on}	α_{off}	α_{on}/α_{off}	On/off occurrence ratio	No. of events
WLE QDC	0.42 ± 0.04	1.75 ± 0.03	0.24	8.44	9389
Dopamine added WLE QDC	1.09 ± 0.06	0.34 ± 0.05	3.21	0.07	8837

In our case, the probability distributions of the events (on and off) could be fitted well by a truncated power law[6-11] through a log-log plot extracted from the obtained data points for 40 single particles (Figures 5.3.D and 5.3.E). It is to be mentioned here that the exponent of the power-law distribution (known as α_{on} and α_{off}) of the on and off events, is an important parameter with regard to the luminescence behavior of a blinking single nanocrystal.[4-13] Hence, any chemical reaction or physical interaction that alters the emission characteristics of a single nanocrystal, may lead to change in the exponents (α_{on} and α_{off}) and their ratio (α_{on}/α_{off}) in the blinking statistics.[4.12,13] In other words, the exponents (α_{on} and α_{off}) and their ratio (α_{on}/α_{off}) of a blinking single nanocrystal can be considered useful in describing the presence of any chemically reactive analyte on the surface and thus have important consequences in sensing application.[4.12,13] Importantly, the value of the exponent (α_{on}) of the on-duration probability distribution (P_{on}) was found to be lesser compared to the exponent (α_{off}) of the off-duration probability distribution (P_{off}) for possibly single WLE QDC ($\alpha_{on} = 0.42 \pm 0.04 < \alpha_{off} = 1.75 \pm 0.03$; Figures 5.3.D and 5.3E, Table 5.1). This was calculated using a fixed frame size of 64 x 64 μm^2 and

binning time of 27 ms[6-11] with excitation power of 63 mW for a time duration of 27 s for each single particle. This result clearly supported the presence of more number of on states in comparison to off states in the blinking behavior of possibly single WLE QDC, with a (α_{on}/α_{off}) ratio of 0.24.

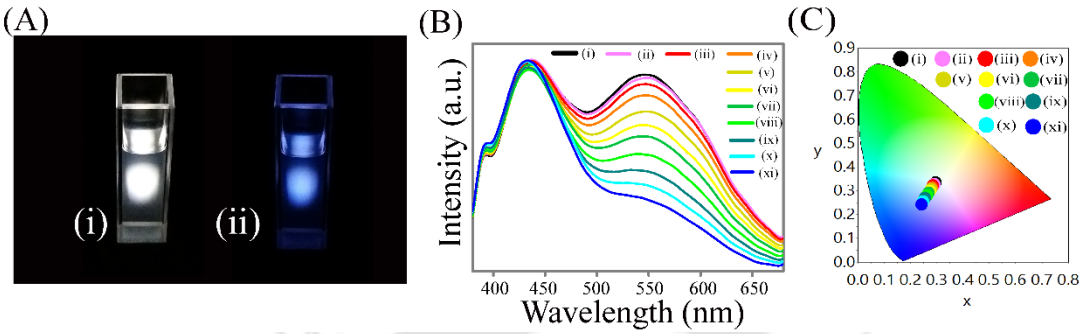

Figure 5.4. (A) Photographs (digitally captured under 350 nm light from a spectrofluorimeter) of (i) WLE QDC nanocomposite and (ii) dopamine added to WLE QDC nanocomposite dispersions. **(B)** Emission spectra (λ_{ex} – 350 nm) and **(C)** changes in chromaticity color coordinates in CIE diagram of (i) 0.0, (ii) 6.6, (iii) 13.3, (iv)26.6, (v) 46.4, (vi) 72.8, (vii) 99.0, (viii) 196.0, (ix) 322.0, (x) 625.0, and (xi) 1176.5 nM dopamine added to WLE QDC nanocomposite.

Importantly, the digital photographs (captured with an excitation of 350 nm light from a spectrofluorimeter) of WLE QDC upon dopamine addition clearly showed the visual color changes from white to blue (Figure 5.4.A). The sequential addition of dopamine (in the range of 6.6 nM-1.2 μM) to the WLE QDC nanocomposite (in ethanol; having absorbance of 0.11 at 350 nm) led to the gradual quenching in the emission intensity at 550 nm while no significant change was observed with respect to the other emission intensity at 440 nm of the WLE QDC (Figure 5.4.B). Further, the change in the chromaticity color coordinates from (0.31, 0.33) to (0.24, 0.23) of WLE QDC nanocomposite, upon dopamine addition, clearly supported the visual color change from white to blue (Figure 5.4.C and Table A.5.4, Appendix). The quenching effect of dopamine on the emission intensity, at 550 nm, of WLE QDC was demonstrated by Stern-Volmer equation[14-20] (Figure 5.5.A). Figure 5.5.A depicts an excellent linear relationship between I_o/I and the concentration of dopamine in the range of 1-100 nM, with K_{sv} value of 3.4 $\times 10^6$ M^{-1} and correlation coefficient of 0.98. The limit of detection of dopamine was found to be 3.3 nM. Similarly, the decrease in the average lifetime (with respect to the emission at 550 nm) of WLE QDC, following dopamine addition, clearly

demonstrated the dynamic quenching behavior in the linear range of 1-100 nM (Figure A.5.7 and Table A.5.5, Appendix).

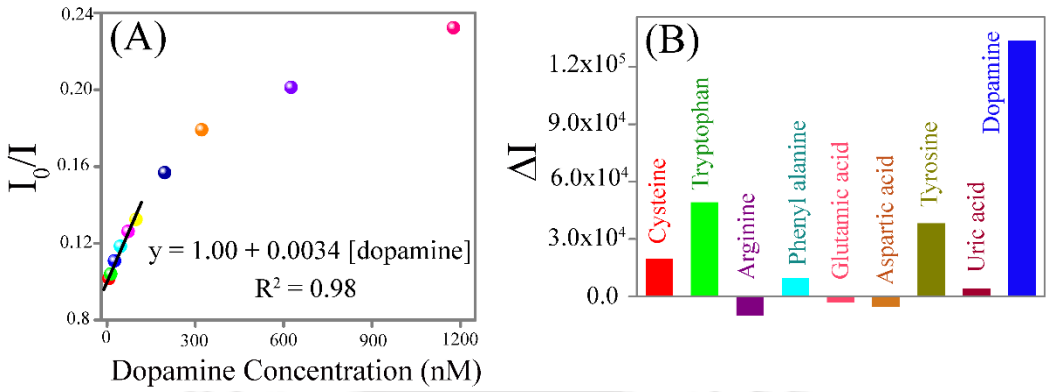

Figure 5.5. **(A)** Stern-Volmer plot (I_o/I vs dopamine conc.) against the data points obtained from Figure 5.4.B. $I_o/I = 1 + K_{sv}$ [dopamine]. Where I_o, I, are the emission intensities at 550 nm in the absence and presence of dopamine and K_{sv} is the quenching constant. **(B)** Selectivity of the WLE QDC, for dopamine, in comparison to the mentioned interfering molecules. The concentration of each of the other molecules was 2.0 µM while 1.2 µM of dopamine was used for selectivity test. The Y-axis represents the change in photoluminescence intensity of the WLE QDC nanocomposite upon addition of the analyte.

Further, the selectivity of the luminescence of WLE QDC nanocomposite towards dopamine was confirmed by incubating them with interfering biomolecules, such as cysteine, tryptophan , arginine, phenylalanine, glutamic acid, aspartic acid, tyrosine and uric acid and at higher amounts (2.0 µM) compared to dopamine (1.2 µM) (Figure 5.5.B). The results showed no noticeable effects on the yellow emission of the WLE QDC nanocomposite and thus clearly indicated the high selectivity of WLE QDC towards dopamine in the presence of mentioned interfering molecules.

Additionally, no significant change was observed in the absorption spectrum of the WLE QDC nanocomposite, following dopamine addition (Figure A.5.8, Appendix). The WLE QDC showed quenching in the excitation intensity at 350 nm, when emission maxima was probed at 550 nm. However, there was no significant change in the excitation spectrum of WLE QDC, at λ_{em}-440, nm (Figure A.5.2, Appendix). The selectivity of reaction of dopamine with ZnO Qdots over $Zn(MSA)_2$ complex was further confirmed by observing similar quenching in the luminescence intensity of only ZnO Qdots (at 550 nm) (Figure A.5.9, Appendix). No noticeable change in the luminescence

intensity of only $Zn(MSA)_2$ complex (at 440 nm) upon dopamine addition was observed (Figure A.5.9, Appendix). The results indicated that the yellow emission of the WLE QDC nanocomposite was sensitive to dopamine, compared to the blue emission, in the liquid medium. Furthermore, the preservation of the crystalline integrity (in terms of size and lattice fringe) of wurtzite ZnO Qdots[1] in WLE QDC nanocomposite – following interaction with dopamine – was confirmed by TEM and XRD analyses (Figure 5.2).

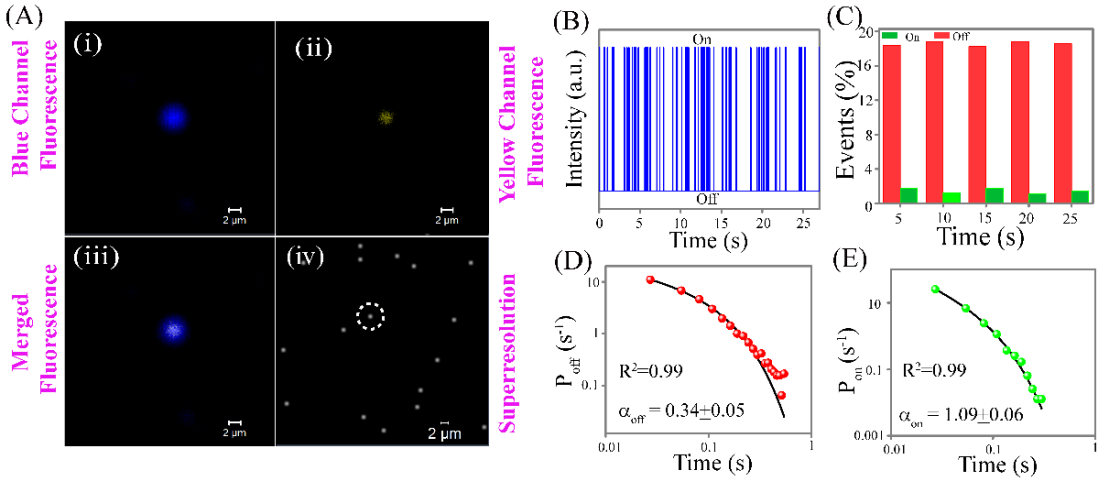

Figure 5.6. (**A**) Confocal laser scanning microscopic images of dopamine treated WLE QDC (scale bar – 2.0 μM) recorded using (i) blue and (ii) yellow emission channels and (iii) their merged version. (iv) Super resolution confocal laser scanning microscopic image of dopamine added WLE QDC. (scale bar – 2.0 μM; with respect to the area as obtained in the merged portion of Figure A(iii)) **(B)** Representative time dependent blinking profile of dopamine added WLE QDC (which is related to the encircled particle shown in panel A(iv)). **(C)** Histogram of proportion of on and off states of a Qdot with respect to the blinking profile mentioned in panel (B) **(D, E)** Corresponding probability density of off-states ($P_{off}(t)$) and on-states ($P_{on}(t)$) for single Qdots. The data were obtained by using frame size of 64 × 64 μm^2, binning time of 27 ms, excitation power of 63 mW, and for a time duration of 27 s. The 355 nm laser was used to excite the samples

Notably, when dopamine reacted with WLE QDC, the representative CLSM image showed that the intensity of the particle in the yellow channel became weak while no significant change was observed in the blue channel (Figure 5.6.A). Thus the merged image of dopamine added WLE QDC exhibited blue color upon reacting with dopamine (Figure 5.6.A (iii)). However, a negligible white shade was noticed in the centre of the merged CLSM image (Figure 5.6.A (iii)). This may be due to the presence of partial yellow luminescence of ZnO Qdot – which was not completely quenched when a fixed number of dopamine molecules reacted with WLE QDC. The result, however,

demonstrated the color change from white to blue of a WLE QDC following interaction with dopamine. Figure 5.6.A (iv) shows the superresolution representative image of the blue color particles as obtained from Figure Figure 5.6.A(iii). Corresponding blinking of a single WLE QDC, following dopamine addition, was recorded for the marked particle. It clearly demonstrates the blinking activity of the dopamine added WLE QDC. Significantly, as dopamine reacted with WLE QDC, the ratio of the on/off states, in the time varying blinking intensity profile changed from 8.44 to 0.07 (Figure 5.6.C). Importantly, upon dopamine addition to WLE QDC, the value of α_{on} increased from 0.42 $\pm$ 0.04 to 1.09 $\pm$ 0.06 while the value of α_{off} decreased from 1.75 $\pm$ 0.03 to 0.34 $\pm$ 0.05 (Figures 5.6.D and 5.6E, Table 5.1). The results were obtained by fitting the data points to truncated power law[6-11] using a log-log plot while considering the blinking profile of 40 single particles under same experimental condition. That is the conditions were similar to those used for WLE QDC (frame size – 64 x 64 μm^2, binning time – 27 ms[10-11], excitation power – 63 mW, time duration of 27 s). The results indicated the presence of higher numbers of off states compared to on states in the blinking profile of dopamine added WLE QDC and supported the preservation of possibly single particle nature of WLE QDC, even after reaction with dopamine. Interestingly, the changes in the value of (α_{on}/α_{off}) ratio from 0.24 to 3.21 helped to detect approximately 13 number of dopamine molecules by Qdot (present in WLE QDC) possibly at single particle level (Table 5.1). The details of the calculation performed by combining the obtained results from atomic absorption and size analysis are described in appendix section (A.5.1 and Figure A.5.10, Appendix). On the other hand, the value of (α_{on}/α_{off}) ratio changed from 0.55 to 3.52 when dopamine (with same concentration, which was used for WLE QDC) was added to only ZnO Qdots (Figure A.5.11 and Table A.5.6, Appendix). This is in further support of the observation of selective reactivity of dopamine with ZnO Qdots compared to $Zn(MSA)_2$ complexes, present in WLE QDC. Hence, the reported strategy based on the changes in the on-off blinking statistics, visual luminescence color (from white to blue) and chromaticity of a single particle WLE QDC is a new, simple and cost-effective method, for the detection of dopamine. This is different in comparison to other reported strategies, wherein no changes in the visual luminescence color and chromaticity were observed since only quenching of emission of Qdots was studied,[14-20] the details of which are summarized in the Table 5.2.

Scheme 5.1 illustrates a schematic representation of the formation of WLE QDC following complexation on the surface of ZnO Qdots (using MSA as the complexing agent). The scheme also represents the use of single particle WLE QDC for the ultrasensitive detection of dopamine, based on the selective chemical interaction with ZnO Qdots, compared to $Zn(MSA)_2$ complex.

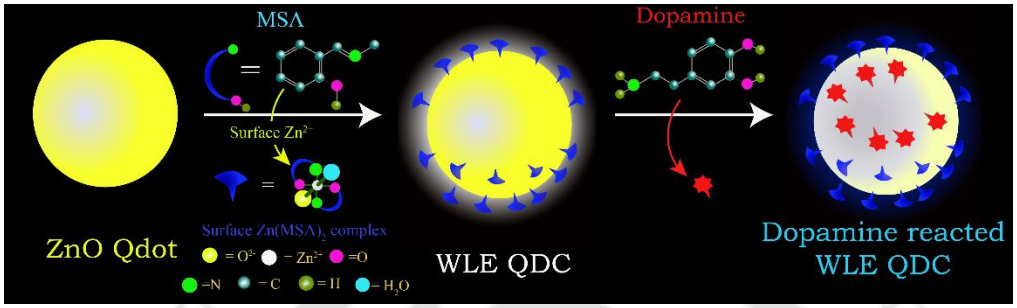

Scheme 5.1. Schematic representation of the formation of WLE QDC from yellow emitting ZnO Qdot, following complexation with MSA and thus the use of single particle WLE QDC for the ultrasensitive detection of dopamine based on the selective quenching of the yellow emission compared to blue emission.

The electron transfer from photo excited ZnO Qdots to their surface adsorbed oxidized dopamine (i.e., the *in situ* formation of quinone, which usually acts as an electron quencher, in the alkaline solution as is case here) present in WLE QDC through noncovalent hydrogen bonding interactions with surface hydroxyl ligands of ZnO Qdots,[14-24] may be one of the reasons for selective quenching of yellow emission of WLE QDC following dopamine addition. This was further supported by the results obtained when the quenching of yellow emission of WLE QDC following the addition of benzoquinone (which is a well-known electron quencher) was observed (Figure A.5.12, Appendix). Additionally, the formation of non-fluorescent Zn-dopamine complex, which also acts as quencher of the emission of ZnO Qdots, via the chelating ability of the catechol part of dopamine towards surface free Zn^{2+} ions of WLE QDC may be the other reason for the observed selective quenching of yellow emission of ZnO Qdots, present in WLE QDC.[21] It may be mentioned here that complexation reaction that was performed to get white light from ZnO Qdots following reaction with MSA might not have resulted in the complete coverage of the surface of the Qdots. This further helped reaction of the free Zn^{2+} ions with dopamine.

Table 5.2. Tabulated form of the comparison of different fluorescent nanoprobes, especially based on quantum dots, for the detection of dopamine.

Ref. No.	***Journals***	**Used Techniques**	**Monitored Properties**	**Used Nanoprobe**	**Change in luminescence color and chromaticity**	**Sensitivity /Range**
Our Work	*Small* **2018** (just accepted)	***Confocal Laser Scanning Microscopy (CLSM; with fluorescence)***	***Change in on-off blinking statistics and luminescence color and chromaticity***	***White Light Emitting Quantum Dot Complex***	***Yes (from white to blue)***	***3.3 nM***
14	*ACS Appl. Mater. Interfaces* **2015**, *7*, 11741−11747.	Fluorometric	Quenching in single emission	Polyindole/ Graphene Qdots	No	0.1 nM/ 0.5−1200 nM
15	*Biosens. Bioelectron.* **2017**, *87*, 693–700.	Fluorometric	Quenching in single emission	Mn doped ZnS Qdots	No	7.80 nM/ 0.15–3.00 μM
16	*Biosens. Bioelectron.* **2015**, *64*, 404–410.	Fluorometric	Quenching in single emission	Polypyrrole/ Graphene Qdots core/shell hybrids	No	0.01 nM/ 0.005–8 μM
17	*Biosens. Bioelectron.* **2013**, *47*, 379–384.	Fluorometric	Quenching in single emission	$CuInS_2$ Qdots	No	200 nM/ 0.5–40 μM
18	*Talanta* **2013**, *107*, 133–139	Fluorometric	Quenching in single emission	ZnO Qdots	No	12.0 nM/ 0.05 – 10 μM
19	Analyst **2014** *139*, 93–98.	Fluorometric	Quenching in single emission	CdSe/ZnS Qdots	No	29.3 nM / 100 nM – 20 μM
20	*Analyst* **2012** *137*, 5553–5559.	Fluorometric	Quenching in single emission	CdTe QDs	No	0.16 μM/ 0.3–100 μM

5.3. Conclusion

In conclusion, a highly sensitive and selective strategy for the visual detection of dopamine, following the change in luminescence color of WLE QDC from white to blue with corresponding chromaticity change from (0.31, 0.33) to (0.24, 0.23), has been developed. Sensing possibly at the level of single Qdot particle (present in WLE QDC) was demonstrated using the time dependent changes in the on/off states of the blinking statistics of possibly single particle of WLE QDC. Importantly, the changes in the value of (α_{on}/α_{off}) ratio from 0.24 to 3.21 and the on/off occurrence ratio 8.44 to 0.07 of possibly single particle of WLE QDC helped to detect approximately 13 number of

dopamine molecules. Additionally, the limit of detection of dopamine was found to be 3.3 nM (using spectrofluorimeter). The results presented herein might propel new research in biomolecular sensing at the level of single particle using blinking as an important tool.

References:

(1) Roy, S.; Pramanik, S.; Bhandari, S.; Chattopadhyay, A. Surface Complexed ZnO Quantum Dot for White Light Emission with Controllable Chromaticity and Color Temperature. *Langmuir* **2017**, *33*, 14627–14633.

(2) Nikitina, P. A.; Peregudov, A. S.; Koldaeva, T. Y.; Kuz'mina, L. G.; Adiulin, E. I.; Tkach, I. I.; Perevalov, V. P. Synthesis and Study of Prototropic Tautomerism of 2-(2-hydroxyphenyl)-1-hydroxyimidazoles. *Tetrahedron* **2015**, *71*, 5217– 5228.

(3) Komiya, N.; Okada, M.; Fukumoto, K.; Jomori, D.; Naota, T. Highly Phosphorescent Crystals of Vaulted trans-Bis(salicylaldiminato)platinum(II) Complexes *J. Am. Chem. Soc.* **2011**, *133*, 6493– 6496.

(4) Scholl, B.; Liu, H. Y.; Long, B. R.; McCarty, O. J. T.; O'Hare, T.; Druker, B. J.; Vu, T. Q. Single Particle Quantum Dot Imaging Achieves Ultrasensitive Detection Capabilities for Western Immunoblot Analysis. *ACS Nano* **2009**, *3*, 1318–1328.

(5) Fichter, K. M.; Flajolet, M.; Greengard, P.; Vu, T. Q. Kinetics of G-Protein–coupled Receptor Endosomal Trafficking Pathways Revealed by Single Quantum Dots. *Proc. Natl. Acad. Sci. U.S.A.* **2010**, *107*, 18658– 18663.

(6) Suppressing the Fluorescence Blinking of Single Quantum Dots Encased in N-type Semiconductor Nanoparticles. Li, B.; Zhang, G. F.; Wang, Z.; Li, Z. J.; Chen, R. Y.; Qin, C. B.; Gao, Y.; Xiao, L. T.; Jia, S. T. *Sci. Rep.* **2016**, *6*, 32662.

(7) Bae, Y. J.; Gibson, N. A.; Ding, T. X.; Alivisatos, A. P.; Leone, S. R. Understanding the Bias Introduced in Quantum Dot Blinking Using Change Point Analysis. *J. Phys. Chem. C* **2016**, *120*, 29484– 29490.

(8) Crouch, C. H.; Sauter, O.; Wu, X.; Purcell, R.; Querner, C.; Drndic, M.; Pelton, M. Facts and Artifacts in the Blinking Statistics of Semiconductor Nanocrystals. *Nano Lett.* **2010**, *10*, 1692– 1698.

(9) Xu, W.; Liu, W.; Schmidt, J. F.; Zhao, W.; Lu, X.; Raab, T.; Diederichs, C.; Gao, W.; Seletskiy, D. V.; Xiong, Q. Correlated Fluorescence Blinking in Two-Dimensional Semiconductor Heterostructures. *Nature* **2016**, *541*, 62– 67.

(10) Zhou, J.; Zhu, M.; Meng, R.; Qin, H.; Peng, X.; Ideal CdSe/CdS Core/Shell Nanocrystals Enabled by Entropic Ligands and Their Core Size-, Shell Thickness-, and Ligand-Dependent Photoluminescence Properties. *J. Am. Chem. Soc.* **2017**, *139*, 16556−16567.

(11) Zhang, A.; Dong, C.; Liu, H.; Ren, J. Blinking Behavior of CdSe/CdS Quantum Dots Controlled by Alkylthiols as Surface Trap Modifiers. *J. Phys. Chem. C* **2013**, *117*, 24592−24600.

(12) De, C. K.; Routh,T.; Roy, D.; Saptarshi Mandal, S,; Mandal, P. K. Highly Photoluminescent InP Based Core Alloy Shell QDs from Air-Stable Precursors: Excitation Wavelength Dependent Photoluminescence Quantum Yield, Photoluminescence Decay Dynamics, and Single Particle Blinking Dynamics. *J. Phys. Chem. C*, **2018**, *122*, 964–973.

(13) Gomez, D. E.; van Embden, J.; Jasieniak, J.; Smith, T. A.; Mulvaney, P. Blinking and Surface Chemistry of Single CdSe Nanocrystals. *Small* **2006**, 2, 204– 208.

(14) Zhou, X.; Wang, A.; Yu, C.; Wu, S.; Shen, J. Facile Synthesis of Molecularly Imprinted Graphene Quantum Dots for the Determination of Dopamine with Affinity-Adjustable. *ACS Appl. Mater. Interfaces* **2015**, *7*, 11741– 11747.

(15) Diaz-Diestra, D.; Thapa, B.; Beltran-Huarac, J.; Weiner, B. R.; Morell, G. L-Cysteine Capped ZnS:Mn Quantum Dots for Room-Temperature Detection of Dopamine with High Sensitivity and Selectivity. *Biosens. Bioelectron*. **2017**, *87*, 693– 700.

(16) Zhou, X.; Ma, P.; Wang, A.; Yu, C.; Qian, T.; Wu, S.; Shen, J. Dopamine Fluorescent Sensors based on Polypyrrole/Graphene Quantum Dots Core/Shell Hybrids. *Biosens. Bioelectron*. **2015**, *64*, 404–410.

(17) Liu, S.; Shi, F.; Zhao, X.; Chen, L.; Su, X. 3-Aminophenyl Boronic Acid-Functionalized $CuInS_2$ Quantum Dots as a Near Infrared Fluorescence Probe for the Determination of Dopamine. *Biosens. Bioelectron*. **2013**, *47*, 379– 384.

(18) Zhao, D.; Song, H.J.; Hao, L. Y.; Liu, X.; Zhang, L. C.; Lv, Y. Luminescent ZnO Quantum Dots for Sensitive and Selective Detection of Dopamine. *Talanta* **2013**, *107*, 133–139.

(19) Shamsipur, M.; Shanehasz, M.; Khajeh, K.; Mollania, N.; Kazemi, S. H. A Novel Quantum Dot-Laccase Hybrid Nanobiosensor for Low Level Determination of Dopamine. *Analyst* **2012**, *137*, 5553–5559.

(20) Mu, Q.; Xu, H.; Li, Y.; Ma, S. J.; Zhong, X. H. Adenosine Capped QDs Based Fluorescent Sensor for Detection of Dopamine with High Selectivity and Sensitivity. *Analyst* **2014**, *139*, 93–98.

(21) Khatchadourian, R.; Bachir, A.; Clarke, S. J.; Heyes, C. D.; Wiseman, P. W.; Nadeau, J. L. Fluorescence Intensity and Intermittency as Tools for Following Dopamine Bioconjugate Processing in Living Cells. *J. Biomed. Biotechnol*. **2007**, *2007*, 70145.

(22) Van Dersarl, J. J.; Mercanzini, A.; Renaud, P. Integration of 2d and 3d Thin Film Glassy Carbon Electrode Arrays for Electrochemical Dopamine Sensing in Flexible Neuroelectronic Implants *Adv. Funct. Mater*. **2015**, *25*, 78– 84.

(23) Valdez, C. N.; Schimpf, A. M.; Gamelin, D. R.; Mayer, J. M. Low Capping Group Surface Density on Zinc Oxide Nanocrystals *ACS Nano* **2014**, *8*, 9463– 9470.

(24) Lin, W.; Walter, J.; Burger, A.; Maid, H.; Hirsch, A.; Peukert, W.; Segets, D. A General Approach To Study the Thermodynamics of Ligand Adsorption to Colloidal Surfaces Demonstrated by Means of Catechols Binding to Zinc Oxide Quantum Dots. *Chem. Mater*. **2015**, *27*, 358−369.

Chapter 6

Summary and Future Prospects

6.1 Summary

Through the present thesis I have been able to demonstrate the formation of single white light emitting nanocomposites, based on (i) the formation of two different inorganic complexes (having blue and green emissive properties) on the surface of a presynthesized orange emitting quantum dot (Qdot), (ii) conjugating a green emitting complex attached Qdot with red emitting gold nanocluster in a blue emitting protein matrix, (iii) the formation of greenish blue emitting inorganic complex on the shell surface of a red emitting core/shell Qdot and (iv) the formation of blue emitting complex on the surface of a yellow emitting Qdot . These are simple, unique, greener and cost-effective strategies to fabricate single component photostable biocompatible white light emitting (WLE) materials, with properties close to day bright light in terms of their chromaticity, color rendering index (CRI) and correlated color temperature (CCT). Additionally, the tunability in chromaticity, CRI, CCT – which is an important factor for solid state lighting – based on the degree of complexation, has been achieved herein. The complexed quantum dot is called herein as quantum dot complex (QDC). Importantly, one of the main aims of this thesis is to detect disease responsive molecules (here neurotransmitter dopamine is used) at possible single particle level, by monitoring the changes in the visual color, chromaticity and on/off blinking characteristics of a single WLE QDC, which has been demonstrated here. This was achieved through selective chemical interaction of dopamine with the one of the emitting species present in a single WLE QDC. This is important in terms of the sensitivity of the detection of dopamine, with change in visual color – which is a better strategy compared to detection based on the quenching of a single wavelength nanoscale emitters. In a nutshell, the current thesis described the formation of a biofriendly single component WLE materials, with an aim to detect disease responsive molecule at possible single particle level.

6.2 Future Prospects

The current thesis's outcome WLE QDC and the presented strategy may pave new roads in the solid state research, especially in fabricating low cost biofriendly white light emitting diodes (WLEDs), with desirable chromaticity, CRI and CCT. Apart from that, the presented single WLE QDC will add a new dimension towards sensing of important molecules, which are responsible for human diseases and/or environmental pollutants. Thus, WLE QDC may have their future applications in fabricating ultrasensitive biodiagnostics devices, in addition to their conventional use in WLEDs. Furthermore, the understanding of the chemistry of the formation of complexes on the surface of Qdot may unravel the hidden surface chemistry of Qdots and provide a new kind of chemistry involving inorganic complex and Qdot towards the versatile use of their composites ranging from optoelectronics to biodiagnostics to catalysis.

Appendix

A2: Chapter 2

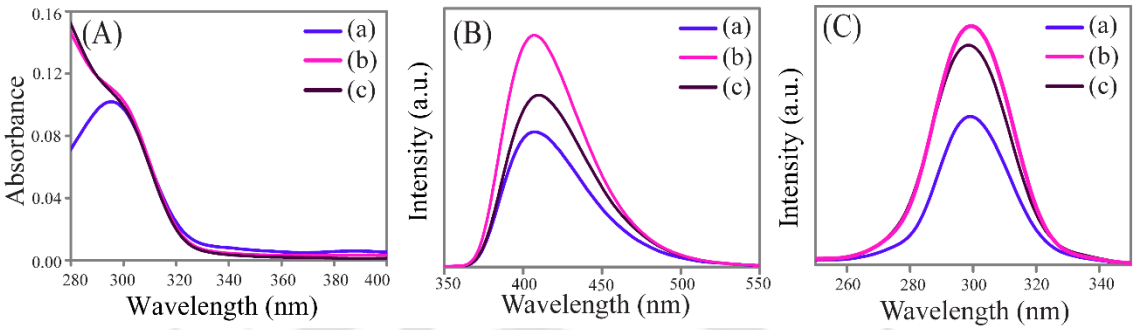

Figure A.2.1. (A) UV-vis absorption, **(B)** emission spectra (λ_{ex} =295 nm) and **(C)** excitation spectra (λ_{em} =410 nm) of (a) ASA, (b) $Mn(ASA)_2$, and (c) $Zn(ASA)_2$ in water-methanol mixture.

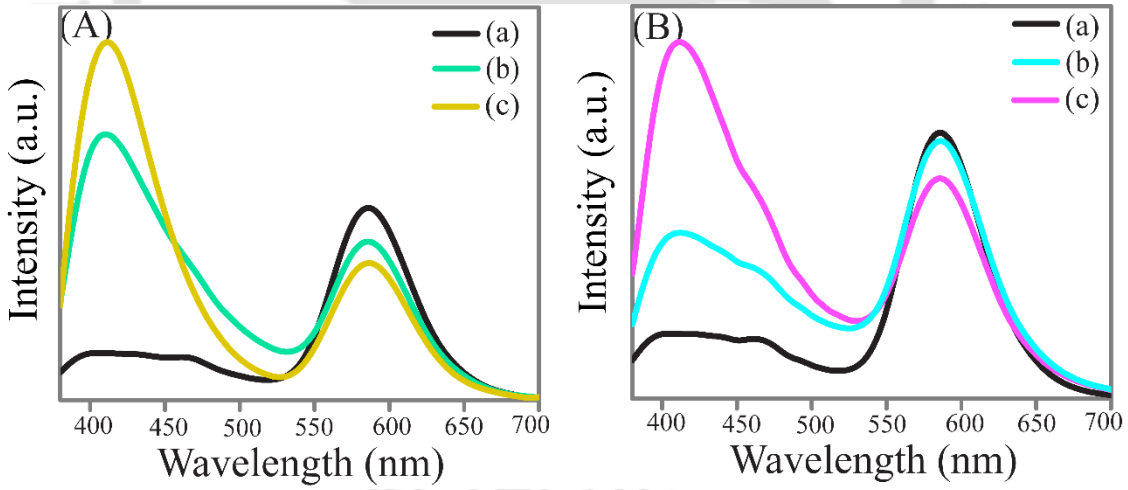

Figure A.2.2. (A) Emission spectra of (a) Qdots (λ_{ex} = 320 nm) and $Mn(ASA)_2$ added Qdots at (b) λ_{ex} = 320 nm and (c) λ_{ex} = 295 nm. **(B)** Emission spectra of (a) Qdots (λ_{ex} = 320 nm) and $Zn(ASA)_2$ added Qdots at (b) λ_{ex} = 320 nm and (c) λ_{ex} = 295 nm.

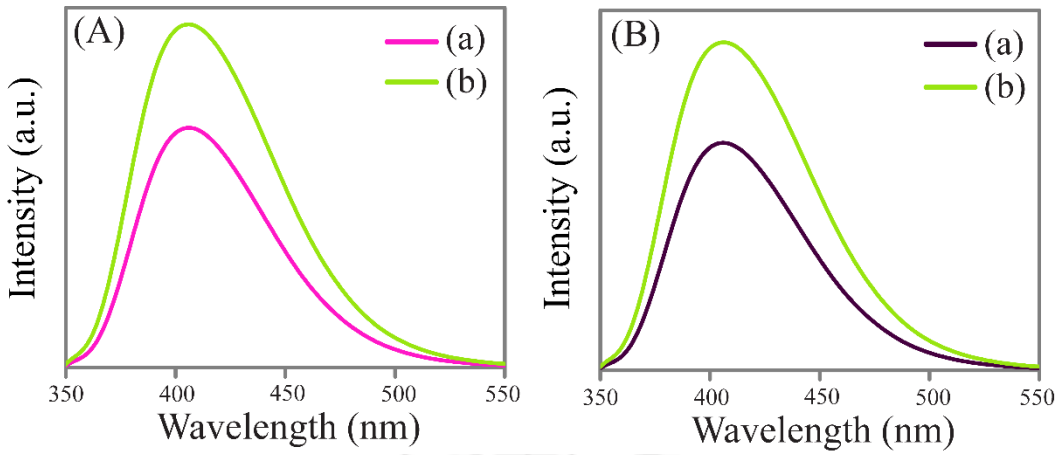

Figure A.2.3. (A) Emission (λ_{ex} = 295 nm) spectra of (a) 0.5 mM of $Mn(ASA)_2$ complex and (b) that after addition of solid Na_2S. **(B)** Emission (λ_{ex} = 295 nm) spectra of (a) 0.5 mM of $Zn(ASA)_2$ complex and (b) that after addition of solid Na_2S.

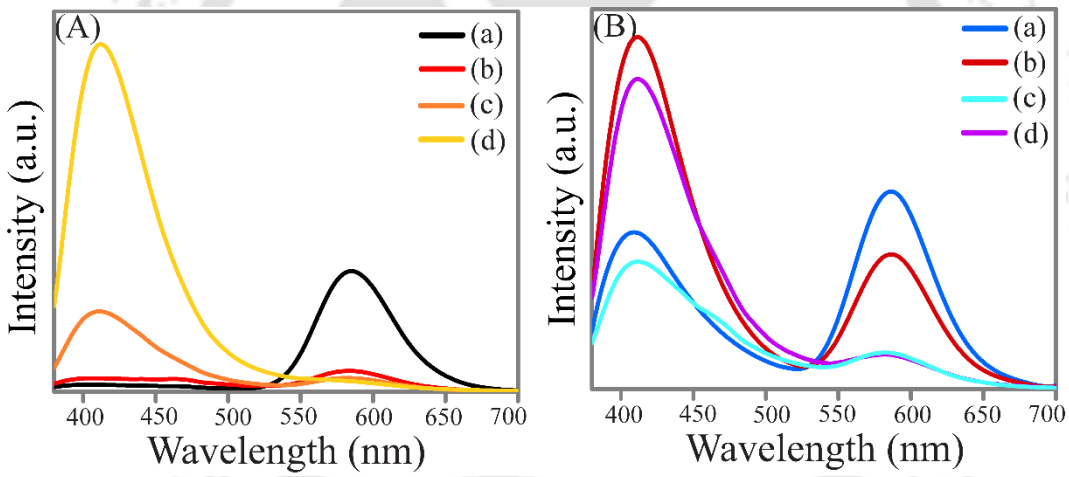

Figure A.2.4. (A) Emission spectra of (a) Qdots (λ_{ex} = 320 nm), (b) Cu^{2+}- treated Qdots (λ_{ex} = 320 nm) as recorded following centrifugation of the mixture and (c, d) Cu^{2+}- treated Qdots to which ASA was added, with excitation at the wavelengths of 320 and 295 nm, respectively (as recorded following centrifugation of the mixture). **(B)** Emission spectra of (a, b) ASA treated Qdots at λ_{ex} = 320 and 295 nm, respectively and (c, d) ASA treated Qdots to which Cu^{2+} was added, with the excitation at the wavelengths of 320 and 295 nm, respectively (as recorded following centrifugation of the mixture).

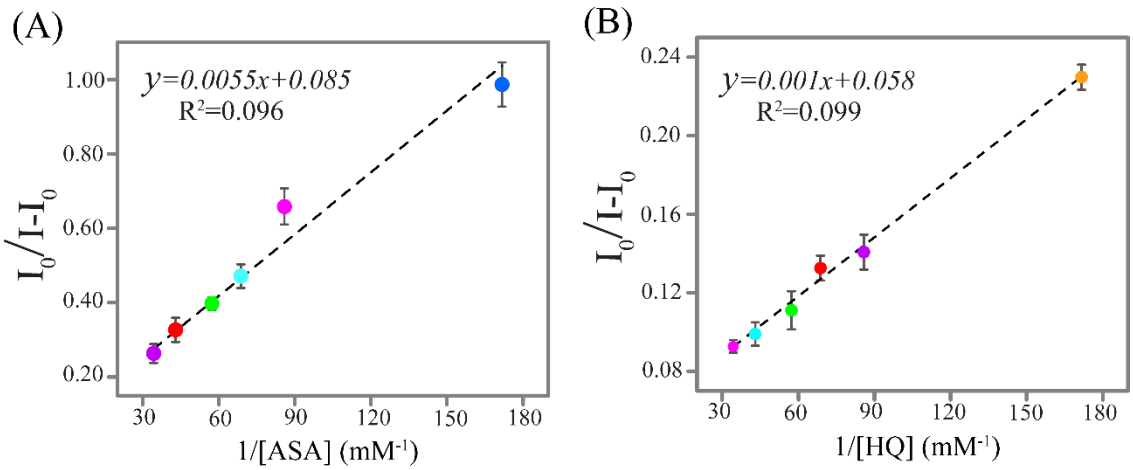

Figure A.2.5. Double reciprocal plot representing the enhancement of the emission **(A)** at 410 nm, following addition of different concentrations of ASA to Qdots and **(B)** at 500 nm, following addition of different concentrations of HQ to Qdots. The enhancement in emission at 410 and 500 nm (due to ratiometric addition of ASA and HQ) was obtained from Figure 2.1 D.

Calculation of complexation constants

The complexation constants (K_{com}) for both the ligands were calculated separately by monitoring the enhancement in emission intensities at 410 and 500 nm, respectively, at different concentrations of ASA and HQ (as shown in Figure 2.1 D). The K_{com} can be estimated from the slope and intercept of the double reciprocal plot using following equation

$$\frac{I_0}{I-I_0} = \frac{I_0}{I_\infty - I_0} + \frac{I_0}{K_{com}(I_\infty - I_0)[Ligand]}$$

Here I_0= emission intensity in absence of ligand; I= emission intensity in presence of ligand at particular concentration and I_∞ = emission intensity when all of the ligands are in the complex.

From the slope and intercept of the linear plot of $I_0/(I-I_0)$ vs 1/[Ligand], K_{com} can be obtained as, K_{com} = Intercept/Slope.

The calculated K_{com} values of ASA and HQ for the Qdots are as follows;

K_{com} (ASA) = (1.50 $\pm$ 0.38) $\times 10^4$ M^{-1} and K_{com} (HQ) = (5.80 $\pm$ 0.18) $\times 10^4$ M^{-1}.

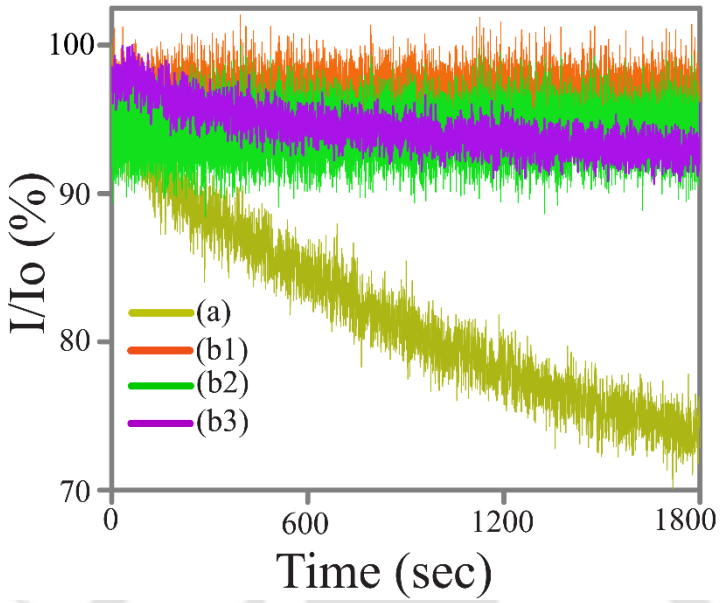

Figure A.2.6. Effect of photo irradiation with time (for half an hour) at the excitation wavelength of 320 nm of (a) rhodamine- 6G (λ_{em}-570 nm) and (b) QDC monitored with emission maxima at (1) 588 nm, (2) 500 nm and (3) 410 nm.

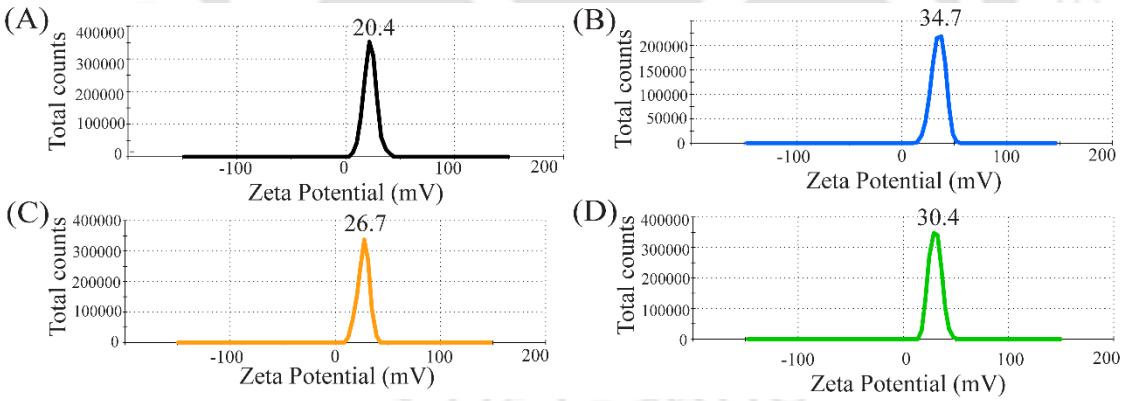

Figure A.2.7. Zeta potential measurement graphs of **(A)** Qdots, **(B)** ASA treated Qdots, **(C)** HQ treated Qdots and **(D)** QDC

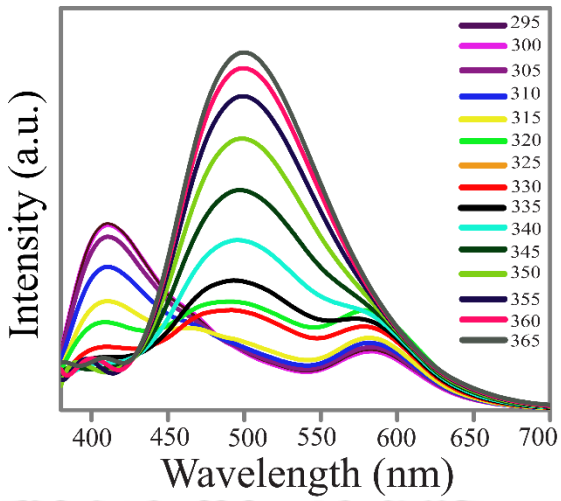

Figure A.2.8. Emission spectra of QDC at different excitation wavelengths (as indicated in the legends).

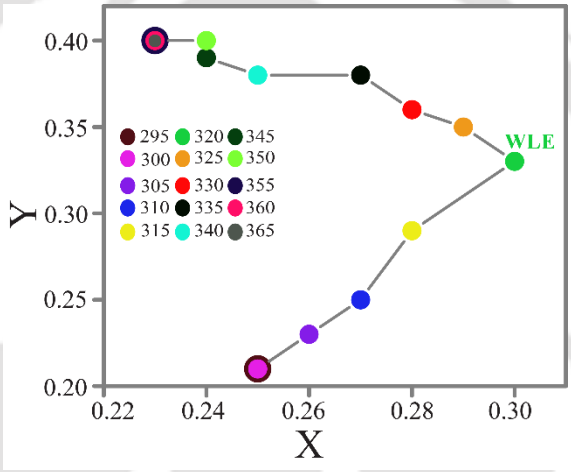

Figure A.2.9. Variation in chromaticity coordinates of QDC at different excitation wavelengths.

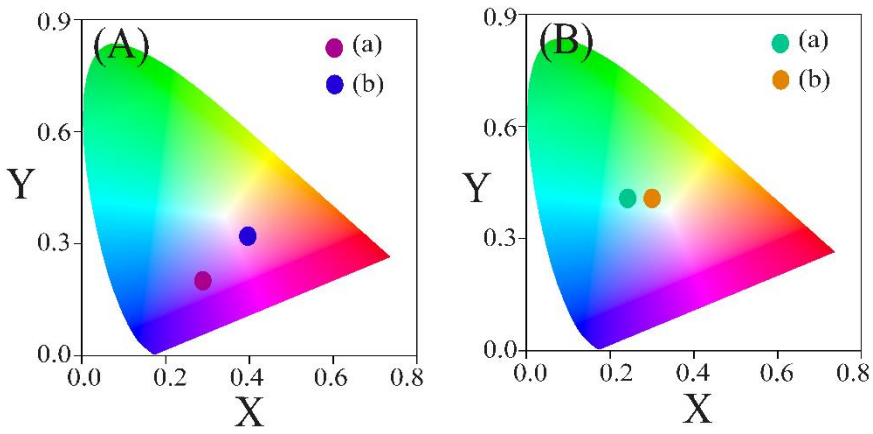

Figure A.2.10. CIE chromaticity diagram of **(A)** only ASA treated Qdots at λ_{ex} - (a) 295 and (b) 320 nm; and **(B)** only HQ treated Qdots at λ_{ex} (a) -365 and (b) 320 nm.

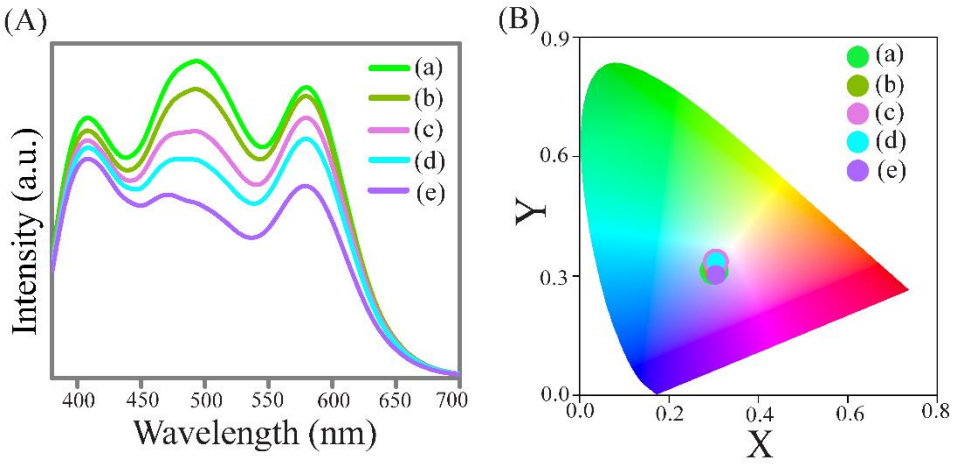

Figure A.2.11. (A) Emission spectra (λ_{ex}-320 nm) and (B) their corresponding CIE diagram of WLE QDC (in water) at different temperatures: (a) 25, (b) 40, (c) 55, (d) 70 and (e) 85 ^{0}C.

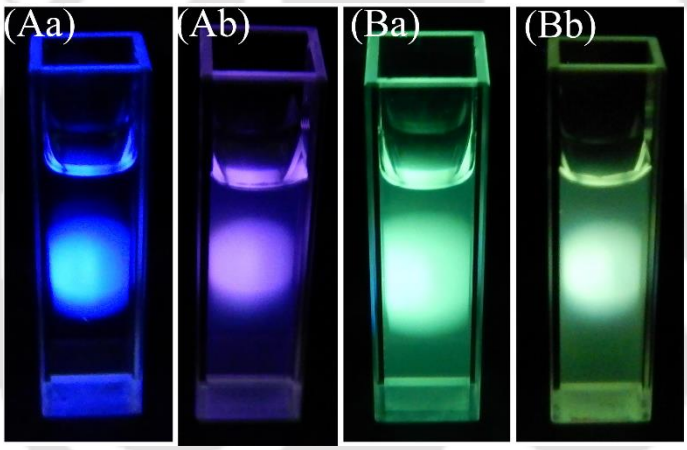

Figure A.2.12. Digital photographs of **(A)** only ASA treated Qdots at λ_{ex}- (a) 295 and (b) 320 nm; and **(B)** only HQ treated Qdots (a) at λ_{ex}-365 and (b) 320 nm.

Table A.2.1. Quantum yield (λ_{ex}-320 nm; using quinine sulphate as a standard) of **(A)** Qdots, **(B)** ASA treated Qdots, **(C)** HQ treated Qdots and **(D)** QDC.

Sample	λ_{ex} (nm)	QY (%)
(A) Qdots	320 nm	0.6
(B) Only ASA treated Qdots		0.7
(C) Only HQ treated Qdots		0.8
(D) QDC		2.2

Table A.2.2. Photoluminescence decrease rate (% per sec) of (a) rhodamine 6G (λ_{ex}-320 nm and λ_{em}-570 nm) and (b) QDC (λ_{ex}-320 nm and λ_{em}-588/500/410nm) monitored for half an hour with 0.1 sec data interval.

Sample	λ_{ex} (nm)	λ_{em} (nm)	Photoluminescence decrease rate (%.sec^{-1})
(a) Rhodamine 6G	320	570	0.015
(b) QDC	320	588	0.003
		500	0.003
		410	0.004

Table A.2.3. Measurement of zeta Potential of **(A)** Qdots, **(B)** ASA treated Qdots, **(C)** HQ treated Qdots and **(D)** QDC in tabulated form.

Sample	Zeta Potential (mV)
(A) Qdots	20.4 $\pm$ 0.8
(B) Only ASA treated Qdots	34.7$\pm$ 1.2
(C) Only HQ treated Qdots	26.7$\pm$ 0.9
(D) QDC	30.4$\pm$ 1.0

Table A.2.4. Tabulated bands (or functional groups) against vibrational frequencies obtained from FTIR spectral data of QDC.

Vibrational Frequency (Cm^{-1})	Band Assignment	Vibrational Frequency (Cm^{-1})	Band Assignment
1623	C=O stretching (ASA)	**1007**	C-H in plane deformation (ASA)
1605	C-C/C-N stretching (ASA & HQ)	**912**	C-H out plane deformation (ASA)
1580	-COO asymmetric stretching (ASA)	**860**	C-H out plane deformation (ASA)
	C-C/C-N stretching (ASA & HQ)	**823**	C-H out plane deformation (HQ)
1500	Pyridyl group (HQ)	**804**	C-H out plane deformation (HQ)
1468	Phenyl group (ASA & HQ)	**784**	C-H out plane deformation (ASA)
1422	-COO asymmetric stretching (ASA)	**742**	C-H in and out plane deformation(HQ)
1386	-COO asymmetric stretching (ASA)	**664**	-C-H bending vibration (ASA)
1320	C-O stretching (ASA)	**642**	C-H in plane deformation (HQ)
1243	-C-H in plane deformation (ASA)	**605**	C-H in plane deformation (HQ)
1110	-C-O-M (ASA & HQ)		

Table A.2.5. Concentration of metal ions (Mn^{2+} and Zn^{2+}) and their ratio (Mn^{2+}: Zn^{2+}) in Qdots and QDC in tabulated form.

Sample	Conc. of Mn^{2+} (ppm)	Mn (%)	Conc. of Zn^{2+} (ppm)	Zn(%)	Mn^{2+}:Zn^{2+}
Qdots	2.07	2.84	70.8	97.16	0.029
QDC	1.97	2.75	69.6	97.75	0.028

Table A.2.6. CIE chromaticity coordinates value (at λ_{ex} -320 nm) of (a) Qdots and (b) QDCs.

Sample	CIE Coordinates	
	X	Y
(a) Qdots	0.48	0.41
(b) QDC	0.30	0.33

Table A.2.7. Tabulated form of chromaticity coordinates of QDC at different excitation wavelengths.

QDC at λ_{ex} (nm)	CIE Coordinates	
	X	Y
295	0.25	0.21
300	0.25	0.21
305	0.26	0.23
310	0.27	0.25
315	0.28	0.29
320	0.30	0.33
325	0.29	0.35
330	0.28	0.36
335	0.27	0.38
340	0.25	0.38
345	0.24	0.39
350	0.24	0.40
355	0.23	0.40
360	0.23	0.40
365	0.23	0.40

Table A.2.8. CIE chromaticity coordinates value of (a) only ASA added Qdots and (b) only HQ added Qdots at different excitation wavelengths.

Sample	λ_{ex} (nm)	CIE Coordinates	
		X	Y
(a) Only ASA treated Qdots	320	0.40	0.32
	295	0.29	0.20
(b) Only HQ treated Qdots	320	0.30	0.41
	365	0.24	0.41

Table A.2.9. Variation in chromaticity coordinates of QDC (at 320 nm) depending upon temperature.

Temperature (°C)	CIE Coordinates	
25	0.30	0.33
40	0.30	0.33
55	0.30	0.34
70	0.30	0.34
85	0.29	0.32

Table A.2.10. Variation in quantum yield of QDC (at 320 nm) depending upon temperature.

Temperature (°C)	λ_{ex} (nm)	QY (%)
25	320	2.3
40	320	2.2
55	320	2.0
70	320	1.9
85	320	1.6

A3: Chapter 3

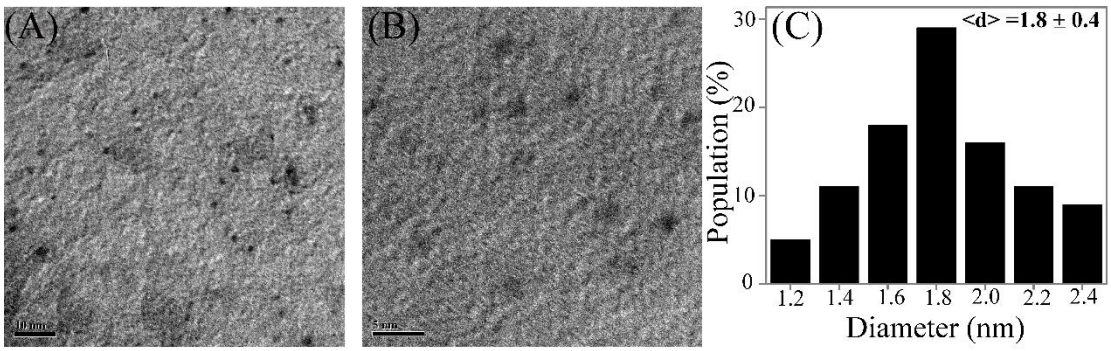

Figure A.3.1. (A, B) Transmission electron microscopic (TEM; scale bar-10 and 5 nm) images and **(C)** corresponding particle size distribution of BSA-stabilized Au NCs in water.

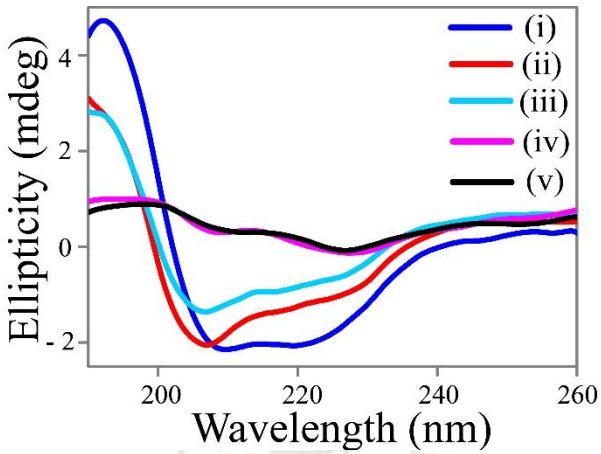

Figure A.3.2. Circular dichroism (CD) spectra of (i) native BSA in water (pH~ 6.9), (ii) BSA stabilized Au NC (pH~12), (iii) BSA stabilized Au NC (pH ~6.8), (iv) BSA stabilized Au NC-ZnS composite (NC-Qdot) (pH~6.8), (v) HQ treated BSA stabilized Au NC-ZnS composite (NC-QDC) (pH~6.8).

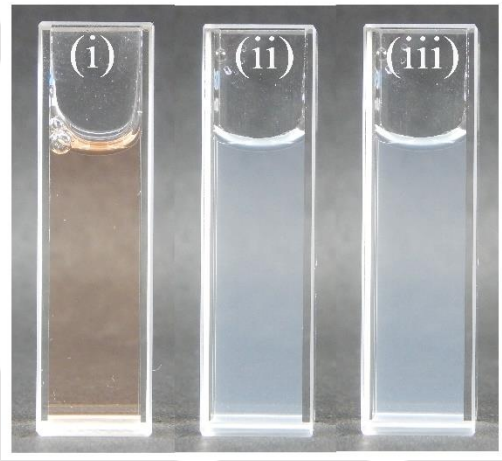

Figure A.3.3. Digital photographs (under day light) of the aqueous dispersion of (i) BSA stabilized Au NCs, (ii) Au NC-ZnS Qdot composite (NC-Qdot) and (iii) HQ treated Au NC-ZnS Qdot composite (NC-QDC).

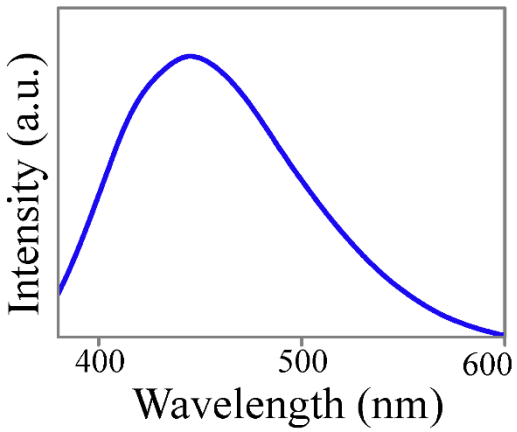

Figure A.3.4. Emission spectrum (λ_{ex}-365 nm) of BSA in water.

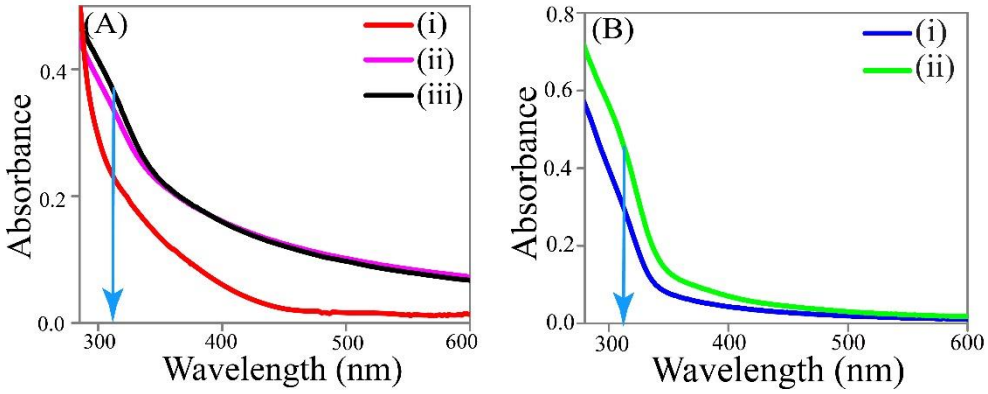

Figure A.3.5. UV-vis spectra of the aqueous dispersion of **(A)** (i) BSA stabilized Au NCs, (ii) Au NC-ZnS Qdot composite and (iii) HQ treated Au NC-ZnS Qdot composite and **(B)** (i) BSA stabilized ZnS Qdots and (ii) HQ treated BSA stabilized ZnS Qdots. The arrow in cyan color indicates the absorption peak of ZnS Qdot (at 320 nm).

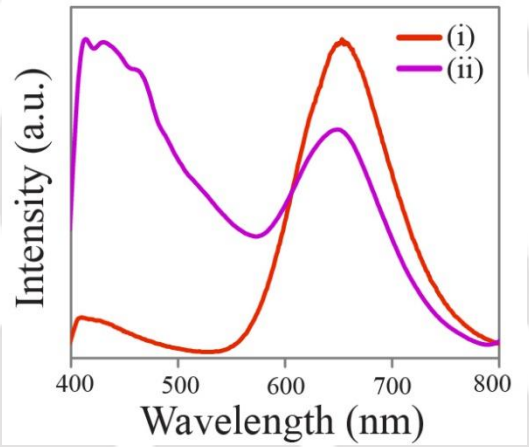

Figure A.3.6. Emission spectra of (λ_{ex} - 320 nm) of (i) BSA stabilized Au NCs and (ii) BSA stabilized Au NC-ZnS Qdot composite

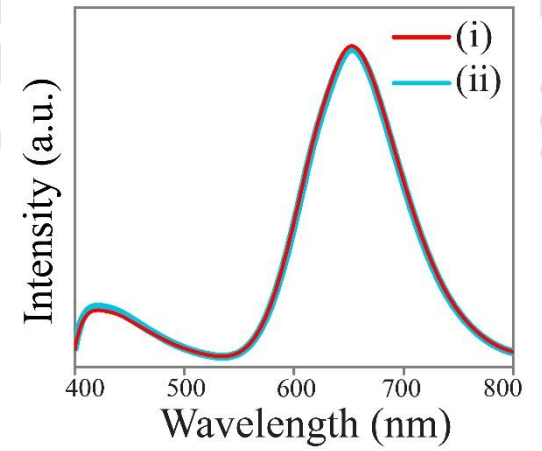

Figure A.3.7. Emission spectra (λ_{ex}- 365 nm) of (i) 3.0 mL water dispersion of BSA stabilized Au NCs and (ii) 15.0 µL of 1.0 mM HQ added to 3.0 mL water dispersion of BSA stabilized Au NCs.

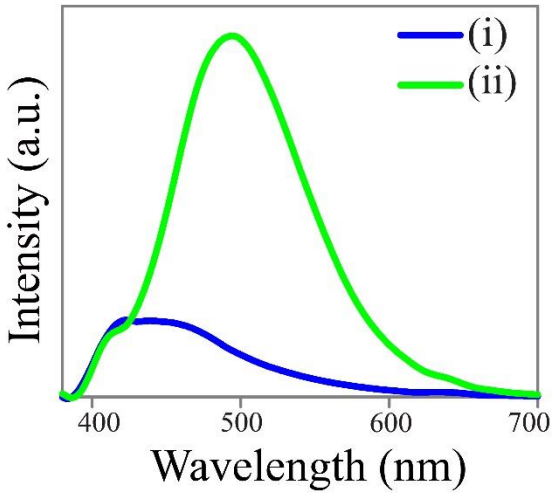

Figure A.3.8 Emission spectra of (i) 3.0 mL water dispersion of BSA stabilized ZnS Qdots (λ_{ex}- 320 nm) and (ii) 15.0 µl of 1.0 mM HQ added 3.0 mL water dispersion of BSA stabilized ZnS Qdots (λ_{ex}- 365 nm).

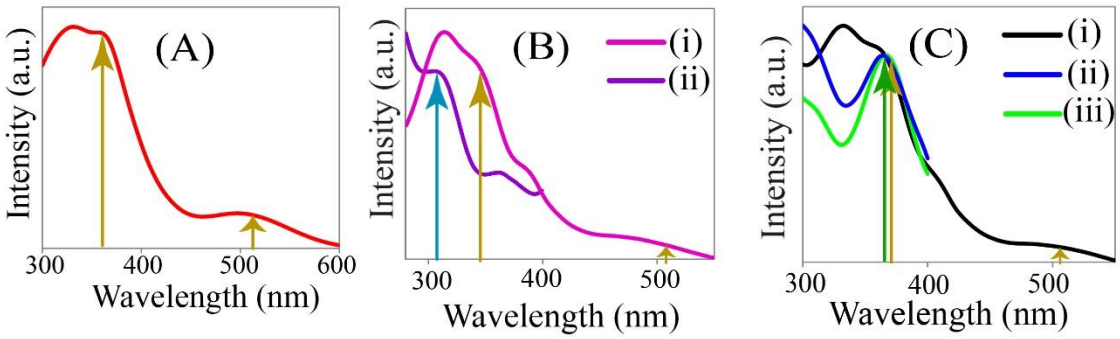

Figure A.3.9. Excitation spectra of the aqueous dispersion of **(A)** BSA stabilized Au NCs at λ_{em}- 650 nm; **(B)** BSA stabilized Au NC-ZnS Qdot composite at (i) λ_{em}- 650 and (ii) 430 nm and **(C)** HQ treated BSA stabilized Au NC-ZnS Qdot composite at (i) λ_{em} - 650 nm, (ii) 490 nm and (iii) 430 nm.The presence of characteristics excitation peaks of Au NCs indicated by dark yellow line while the formation of ZnS Qdot and ZnQ2 complexes via excitation peaks are indicated by cyan line and green line, respectively.

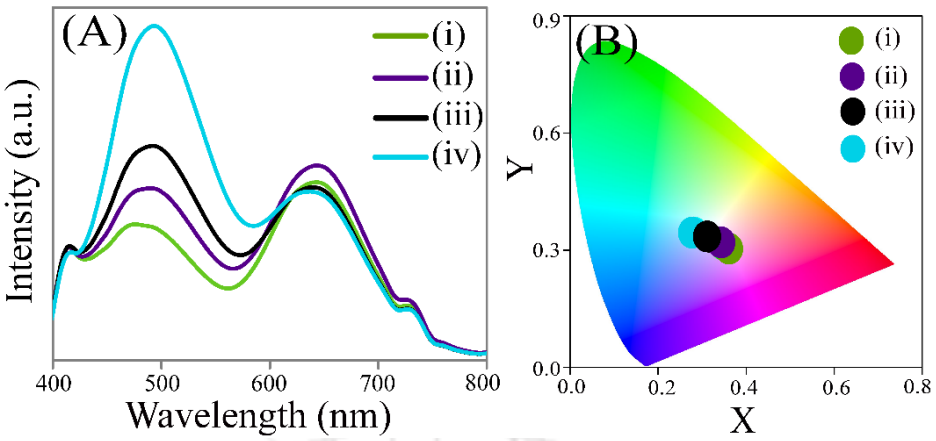

Figure A.3.10. (A) Emission spectra (λ_{ex} -365 nm) and **(B)** corresponding CIE chromaticity diagram of the different amounts i.e. (i) 5.0 µL, (ii) 10.0 µL, (iii) 15.0 µL and (iv) 20.0 µL of 1.0 mM HQ added BSA stabilized Au NC-ZnS Qdot composite (with absorbance of 0.198 at 365 nm and pH 6.8).

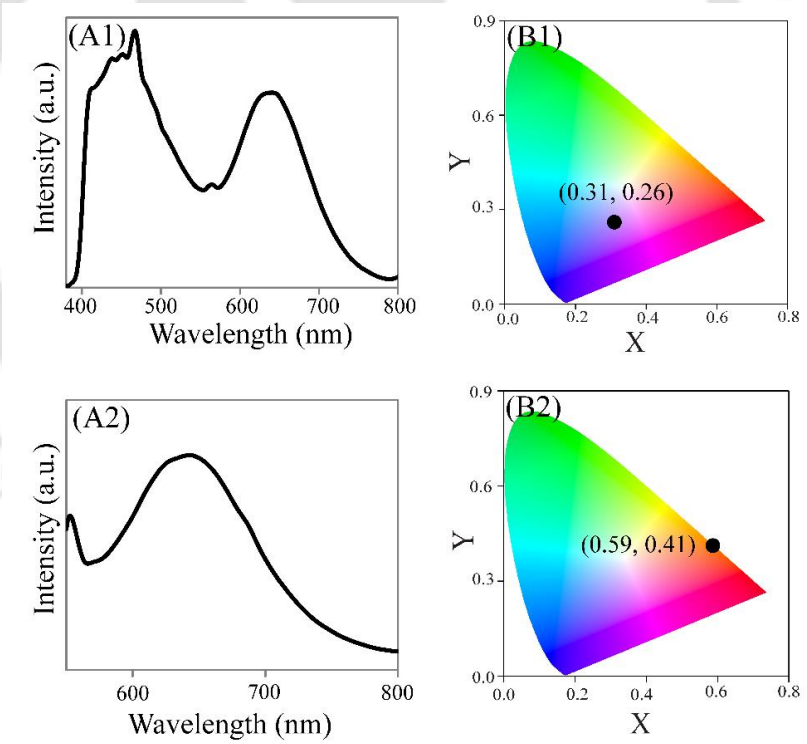

Figure A.3.11. (A) Emission spectra and **(B)** corresponding CIE chromaticity diagram of HQ treated BSA stabilized Au NC-ZnS Qdot composite (NC-QDC) at (1) λ_{ex} -320 nm and (2) λ_{ex} - 505 nm.

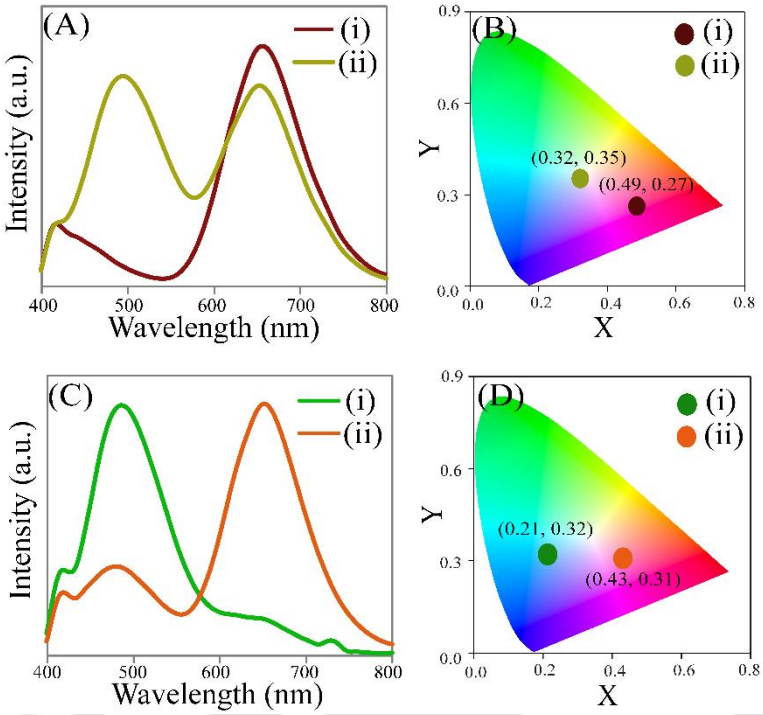

Figure A.3.12. (A) Emission spectra (λ_{ex} -365 nm) and **(B)** corresponding CIE chromaticity diagram of (i) mixture of BSA stabilized ZnS Qdot and BSA stabilized Au NCs and (ii) mixture of BSA stabilized ZnS Qdot and BSA stabilized Au NCs following HQ treatment. **(C)** Emission spectra (λ_{ex} -365 nm) and **(D)** corresponding CIE chromaticity diagram of the (i) pellet and (ii) supernatant obtained from the mixture of HQ treated BSA stabilized ZnS Qdot and BSA stabilized Au NCs following centrifugation.

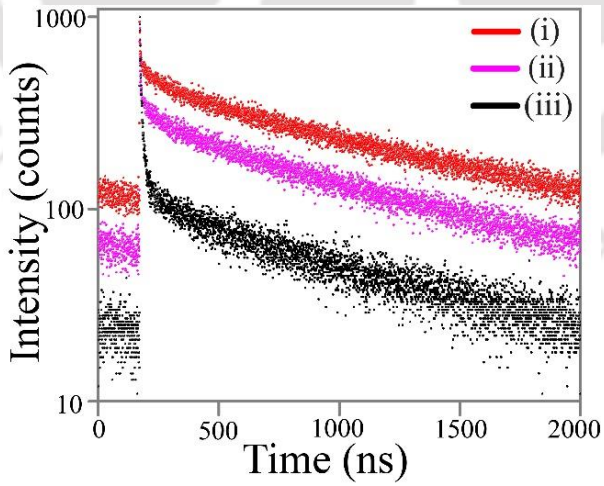

Figure A.3.13. Time resolved photoluminescence spectra (λ_{ex} -375 nm and monitored at λ_{em} - 650 nm) of (i) BSA stabilized Au NCs (pH 6.8), (ii) BSA stabilized Au NC- ZnS nanocomposite (NC-Qdot) (pH 6.8) and (iii) HQ treated BSA stabilized Au NC-ZnS composite (NC-QDC) (pH 6.8).

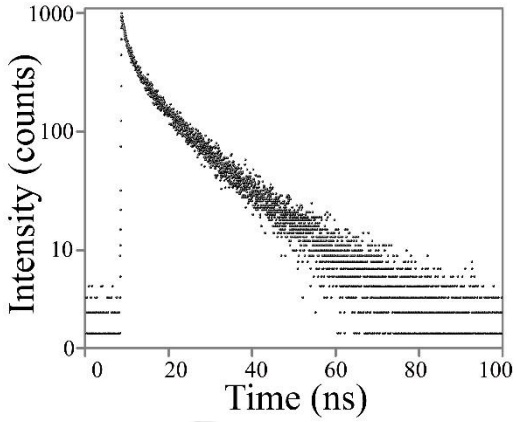

Figure A.3.14. Time resolved photoluminescence spectra (λ_{ex} -375 nm and monitored at λ_{em} - 500 nm) of HQ treated BSA stabilized Au NC-ZnS composite (NC-QDC).

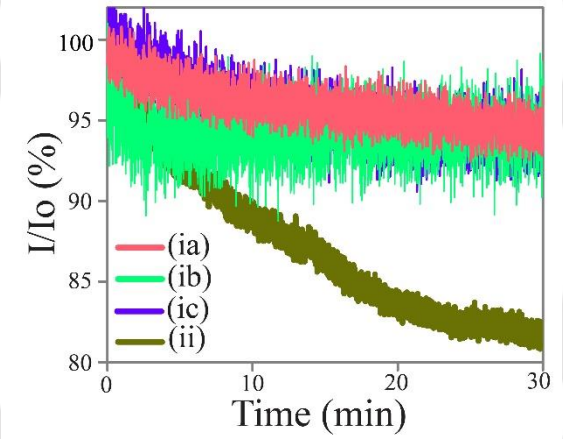

Figure A.3.15. Photostability (λ_{ex} -365 nm) - under continuous irradiation of light for half-an-hour of (i) HQ treated BSA stabilized Au NC-ZnS Qdot (NC-QDC) composite (in water) at λ_{em} – (a) 650, (b) 490 and (c) 430 nm and (ii) rhodamine 6G (in ethanol; λ_{em} -570 nm).

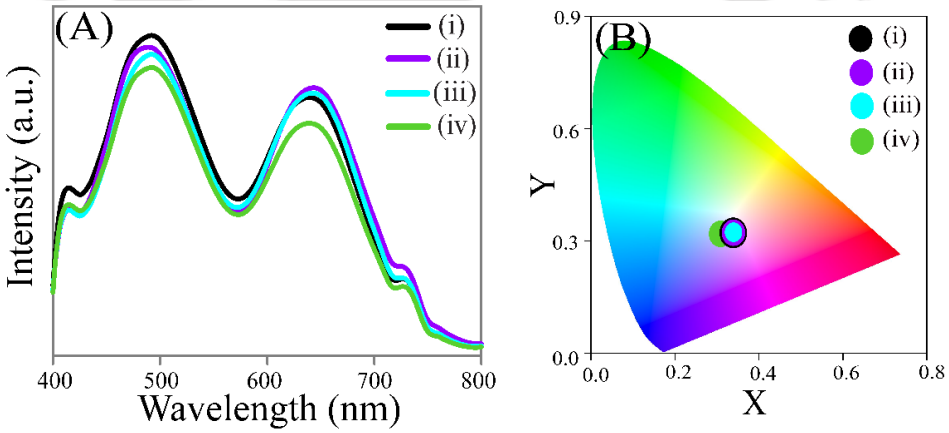

Figure A.3.16. (A) Emission spectra (λ_{ex} -365 nm) and **(B)** corresponding CIE chromaticity diagram of the water dispersion of HQ treated Au NC-ZnS Qdot composite (NC-QDC) at (i) 0, (ii) 1, (iii) 2 and (iii) 3 days.

Table A.3.1. Chromaticity color coordinates of different amounts i.e. (i) 5.0 μL, (ii) 10.0 μL, (iii) 15.0 μL and (iv) 20.0 μL of 1.0 mM HQ added to 3.0 mL of water dispersion of BSA stabilized Au NC-ZnS Qdot composite (with absorbance of 0.198 at 365 nm).

Amount of HQ added (in μl)	Final Conc. of HQ (μM)	Chromaticity Coordinates (x, y)
(i) 5.0	1.67	(0.35, 0.31)
(ii) 10.0	3.32	(0.34, 0.32)
(iii) 15.0	4.98	(0.32, 0.33)
(iv) 20.0	6.62	(0.28, 0.35)

Table A.3.2. Quantum yield (λ_{ex}- 365 nm at pH 6.8) of (i) BSA stabilized Au NCs, (ii) Au NC-ZnS Qdot composite (NC-Qdot) and (iii) HQ treated Au NC-ZnS Qdot composite (NC-QDC).

Samples	Quantum Yield (%)
(i) BSA stabilized Au NCs	4.6*
(ii) Au NC-ZnS Qdot composite	1.7
(iii) HQ treated Au NC-ZnS Qdot composite	3.2

*The decrease in QY of the Au NCs (at pH-6.8) is attributed to the change in pH of the aqueous dispersion of as synthesized Au NCs (pH- 12.0 and Q.Y- 5.8%).

Table A.3.3. Fluorescence life time decay parameters (using 375 nm laser source and monitored at λ_{em}- 650 nm) obtained following tri-exponential fitting of the time resolved photoluminescence spectra of (i) BSA stabilized Au NCs (pH 6.8), (ii) Au NC-ZnS Qdot composite (NC-Qdot) (pH 6.8) and (iii) HQ treated Au NC-ZnS Qdot composite (NC-QDC) (pH 6.8).

Samples	α_i (%)	τ_i (ns)	τ_{av} (μs)	χ^2
(i) BSA stabilized Au NCs (pH – 6.8)	0.74	2.29	0.93	1.02
	2.36	75.47		
	96.91	933.45		
(ii) Au NC-ZnS Qdot composite (pH – 6.8)	1.03	1.84	0.75	0.99
	2.38	49.59		
	96.59	749.43		
(iii) HQ treated Au NC-ZnS Qdot composite (pH – 6.8)	3.53	3.12	0.63	1.02
	7.55	15.67		
	88.92	626.34		

Table A.3.4. Fluorescence life time decay parameters (using 375 nm laser source and monitored at λ_{em} - 500 nm) obtained following tri-exponential fitting of the time resolved photoluminescence spectra of HQ treated Au NC-ZnS Qdot composite (NC-QDC) (pH 6.8).

Samples	α_i (%)	τ_i (ns)	τ_{av} (ns)	χ^2
HQ treated Au NC-ZnS Qdot composite (pH-6.8)	8.54	0.786	12.82	1.07
	21.2	3.731		
	70.26	13.649		

Table A.3.5. Photoluminescence decrease rate (% per min) of (i) HQ treated Au NC-ZnS Qdot composite (NC-QDC) at λ_{em} – 650, 490 and 430 nm and (ii) rhodamine 6G λ_{em} – 570 nm; monitored for 30 mins with 0.1 sec data interval and the excitation wavelength was 365 nm.

Samples	λ_{ex} (nm)	λ_{em} (nm)	PL decrease rate (% per min)
(i) HQ treated Au NC-ZnS Qdot composite	365	650	0.09
	365	490	0.10
	365	430	0.10
(ii) Rhodamine 6G	365	570	0.61

Table A.3.6. CIE chromaticity coordinates value of HQ treated BSA stabilized Au NC-ZnS composite (NC-QDC) at different time intervals.

Time (days)	Chromaticity Coordinates (x, y)
(i) 0	(0.32, 0.33)
(ii) 1	(0.32, 0.33)
(iii) 2	(0.32, 0.33)
(iv) 3	(0.31, 0.33)

Table A.3.7. CIE chromaticity coordinates value of HQ treated BSA stabilized Au NC-ZnS composite (NC-QDC) in the solid state.

Solid Samples	Chromaticity Coordinates (x, y)
(i) Initial	(0.30, 0.31)
(ii)After 3 months	(0.32, 0.30)

A4: Chapter 4

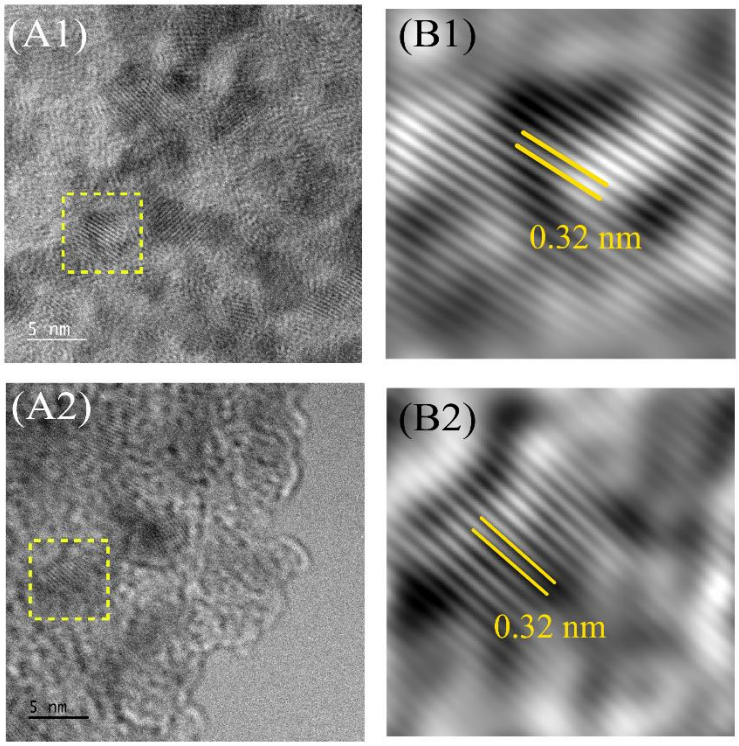

Figure A.4.1. (A) High resolution transmission electron microscopic (HRTEM) images (scale bar - 5 nm) and **(B)** corresponding inverse fast Fourier transform (IFFT) images of (1) $CuInS_2$ and (2) $CuInS_2$/ZnS Qdots, respectively.

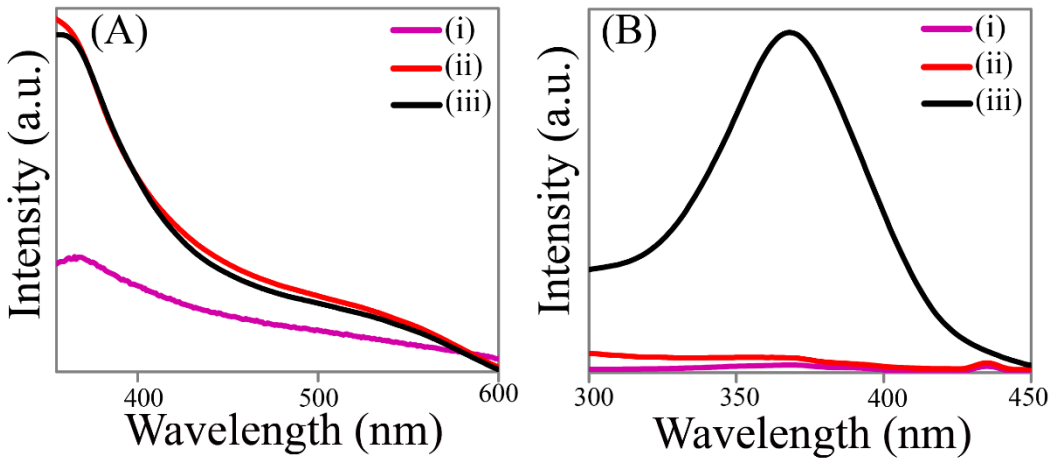

Figure A.4.2. Excitation spectra monitored with respect to the emission of **(A)** the Qdot (at λ_1 nm) and **(B)** the surface ZnQ_2 complexes (at λ_2 nm) of (i) only $CuInS_2$ Qdots (λ_1-700 nm and λ_2-485 nm; in hexane) (ii) $CuInS_2$/ZnS core/shell Qdots (λ_1-630 nm and λ_2-485 nm; in hexane) and (iii) HQ treated $CuInS_2$/ZnS core/shell Qdots (λ_1-630 nm and λ_2-485 nm; in hexane).

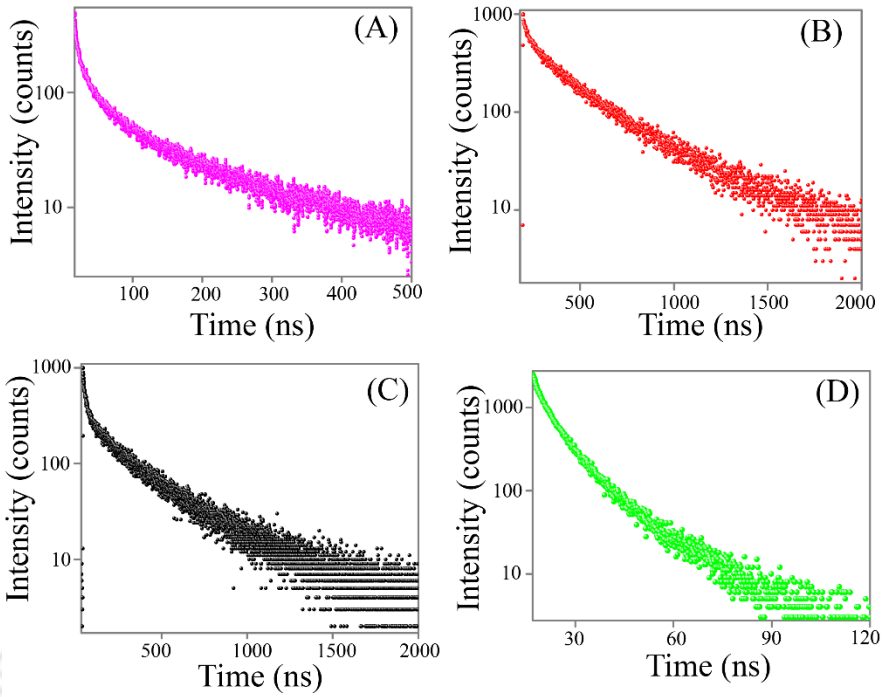

Figure A.4.3. Time resolved photoluminescence spectra (λ_{ex}-375 nm) of **(A)** only $CuInS_2$ Qdot (with λ_{em}- 700 nm; in hexane), **(B)** $CuInS_2$/ZnS core/shell Qdot (with λ_{em}- 630 nm; in hexane), **(C)** HQ treated $CuInS_2$/ZnS core/shell Qdot (with λ_{em}- 630 nm; in hexane) and **(D)** HQ treated $CuInS_2$/ZnS core/shell Qdot (with λ_{em}- 485 nm; in hexane).

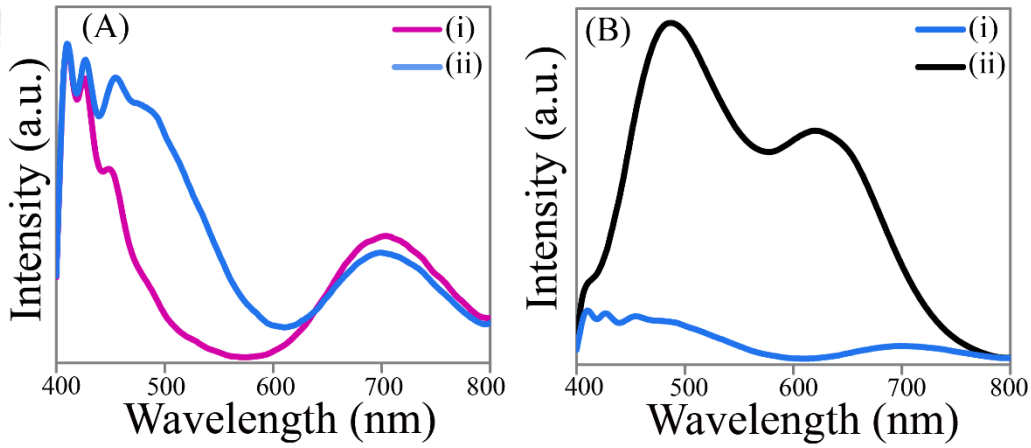

Figure A.4.4. (A) Emission spectra (λ_{ex}-365 nm) of (i) only 3.0 mL hexane dispersion of $CuInS_2$ Qdot and (ii) 10.0 µL of 5.0 mM HQ added to 3.0 mL hexane dispersion of $CuInS_2$ Qdot. **(B)** Comparison of emission spectra (λ_{ex}-365 nm) of 10.0 µL of 5.0 mM HQ added to (i) 3.0 mL hexane dispersion of $CuInS_2$ Qdot and (ii) 3.0 mL hexane dispersion of $CuInS_2$/ZnS core/shell Qdot.

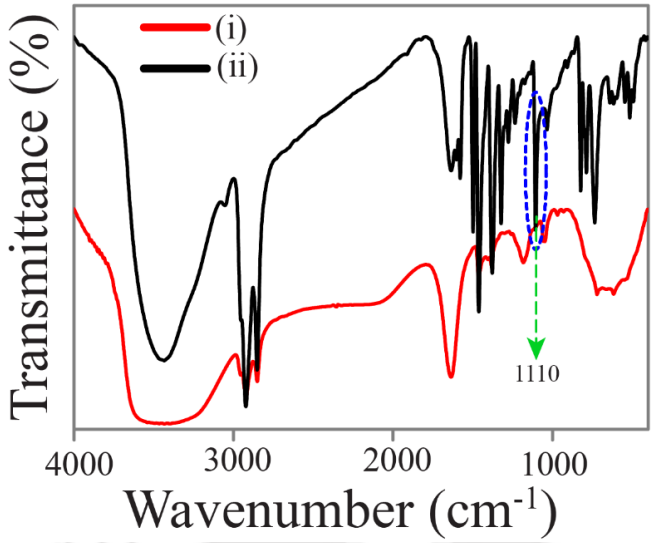

Figure A.4.5. Fourier transformed infrared (FTIR) spectra of the solid form of (i) $CuInS_2$/ZnS core/shell Qdot and (ii) HQ treated $CuInS_2$/ZnS core/shell Qdot.

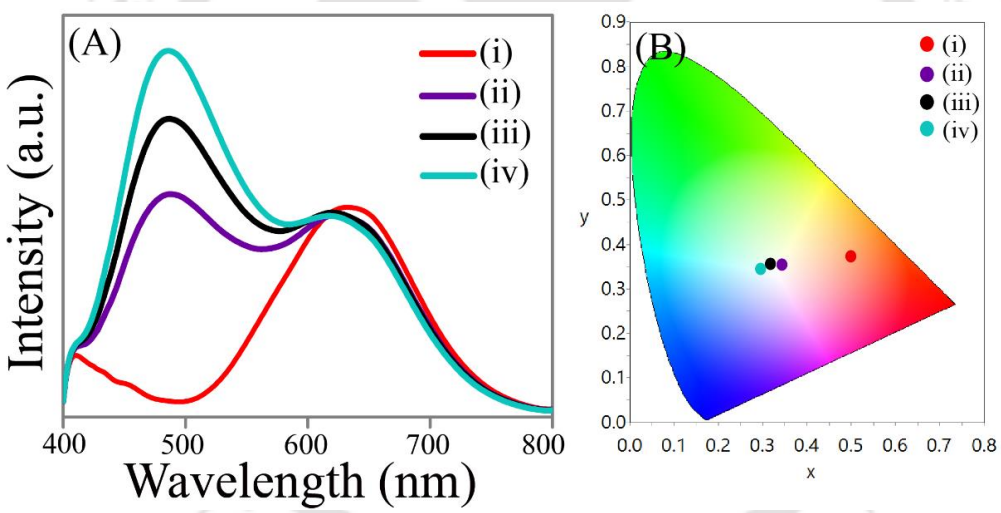

Figure A.4.6. (A) Emission spectra (λ_{ex}-365 nm) and **(B)** corresponding CIE chromaticity diagram of the different amounts i.e. (i) 0.0 µL, (ii) 5.0 µL, (iii) 10.0 µL and (iv) 15.0 µL of 5.0 mM HQ added to 3.0 mL hexane dispersion of $CuInS_2$/ZnS core/shell Qdot (with absorbance of 0.12 at 365 nm).

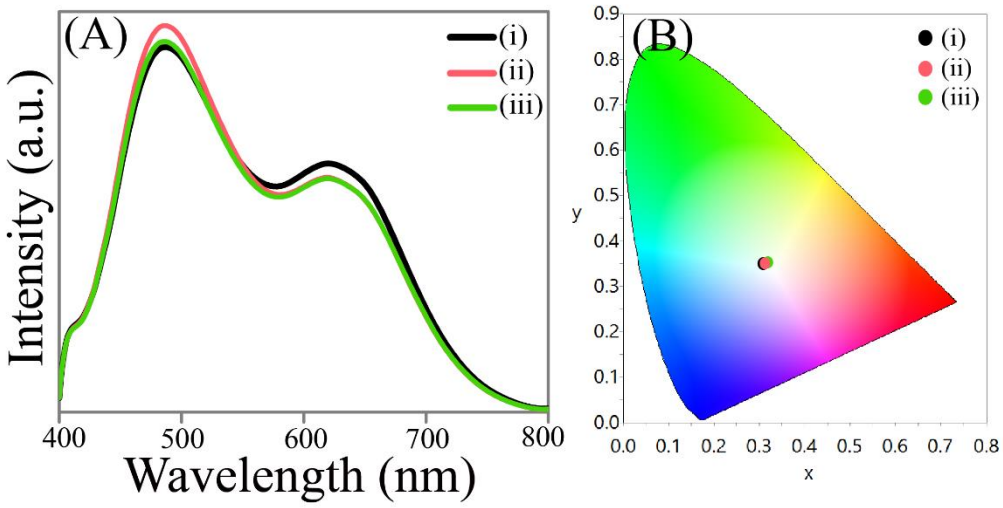

Figure A.4.7. (A) Emission spectra (λ_{ex}-365 nm) and corresponding **(B)** CIE chromaticity diagram of white light emitting nanocomposite at different time intervals: (i) 0 h, (ii) 24 h and (iii) 48 h after HQ addition.

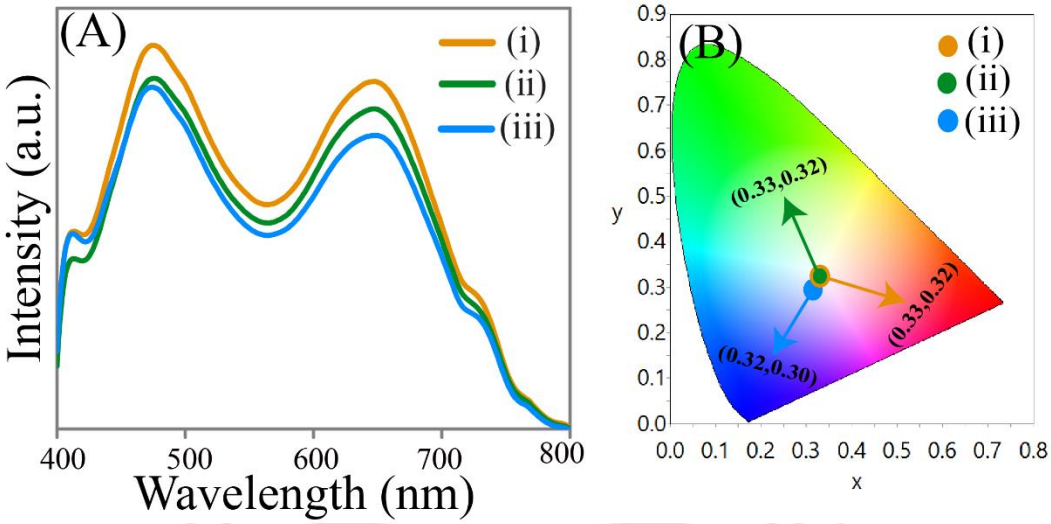

Figure A.4.8. (A) Emission spectra (λ_{ex}-365 nm) and **(B)** corresponding CIE coordinates in CIE chromaticity diagram of solid (coated on a quartz slide) white light emitting nanocomposite recorded after heating at 200 ^{o}C for (i) 5 min, (ii) 10 min and (iii) 15 min, respectively .The emission spectra of the solid WLE nanocomposite were recorded after cooling down to room temperature.

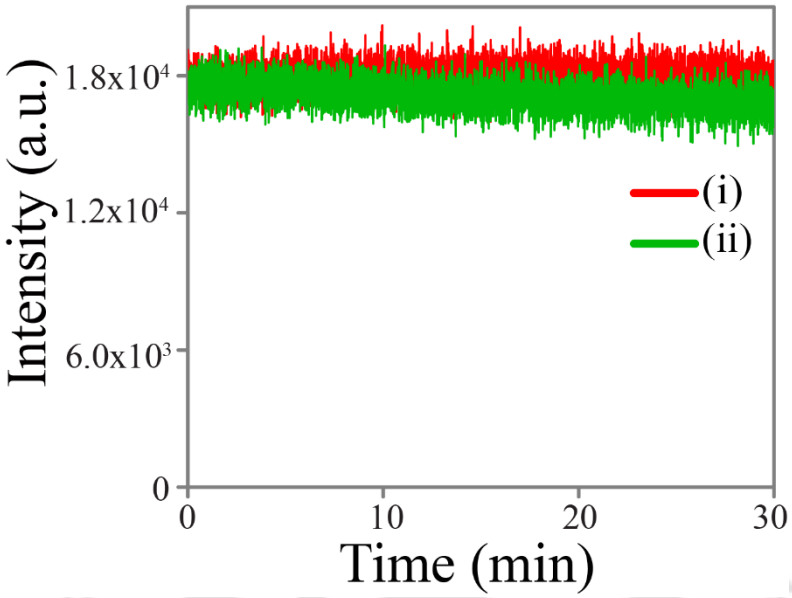

Figure A.4.9. Effect of photo irradiation (using 365 nm light from a spectrofluorimeter) with time on the emission intensity at (i) 650 and (ii) 485 nm, respectively, of the white light emitting nanocomposite. Horiba Fluoromax-4 spectrofluorimeter, fitted with light source of 150-watt ozone-free xenon arc-lamp, was used for photo irradiation. The power of excitation light was about one milliwatt[5] and the emission intensity at respective emission maximum was recorded with 0.1 s interval of time for half-an-hour.

Table A.4.1. Quantum yield (λ_{ex}-365 nm; with respect to quinine sulphate (QY-54% in 0.1 M H_2SO_4) of (i) only $CuInS_2$ Qdot (λ_{em}-700 nm; in hexane), (ii) $CuInS_2$/ZnS core/shell Qdot (λ_{em}-630 nm; in hexane) and (iii) HQ treated $CuInS_2$/ZnS core/shell Qdot (λ_{em}-630 nm and λ_{em}-485 nm; in hexane).

Sample	λ_{ex} (nm)	λ_{em} (nm)	Quantum Yield (%)
(i) $CuInS_2$	365	700	0.8
(ii) $CuInS_2$/ZnS	365	630	3.31
(iii) HQ treated $CuInS_2$/ZnS	365	630, 485	5.07

Table A.4.2. Photoluminescence life time decay parameters obtained by analyzing the Photoluminescence decay curves of (i) only $CuInS_2$ Qdot (λ_{em}-700 nm; in hexane), (ii) $CuInS_2$/ZnS core/shell Qdot (λ_{em}-630 nm; in hexane) and (iii) HQ treated $CuInS_2$/ZnS core/shell Qdot (λ_{em}-630 nm and λ_{em}-485 nm; in hexane). 375 nm LASER source was used for excitation.

Sample	λ_{em} (nm)	α_i (%)	τ_i (ns)	τ_{av} (ns)	χ^2
(i) $CuInS_2$	700	5.58	2.67	127.65	1.03
		23.11	21.23		
		71.31	133.34		
(ii) $CuInS_2$/ZnS	630	20.13	77.58	365.18	1.06
		79.87	379.98		
(iii) HQ treated $CuInS_2$/ZnS	630	7.20	10.84	335.44	1.08
		16.56	89.25		
		76.24	350.03		
	485	5.96	0.66	12.50	1.01
		55.95	5.37		
		38.09	16.08		

Table A.4.3. Tabulated bands (or functional groups) against the stretching frequencies obtained from Figure A.4.5. FTIR spectral data of HQ treated $CuInS_2$/ZnS core/shell Qdot.

Vibrational Frequency (cm^{-1})	Band Assignment	Vibrational Frequency (cm^{-1})	Band Assignment
1605	C-C/C-N stretching of HQ	823	C-H out plane deformation (HQ)
1578	C-C/C-N stretching of HQ	802	C-H out plane deformation (HQ)
1500	Pyridyl group of HQ	737	C-H in and out plane deformation(HQ)
1462	Phenyl group HQ)	642	C-H in plane deformation (HQ)
1322	C-H bending	600	C-H in plane deformation (HQ)
1110	-C-O-Zn stretching		

Table A.4.4. Chromaticity color coordinates of different amounts i.e. (i) 0.0 µL, (ii) 5.0 µL, (iii) 10.0 µL and (iv) 15.0 µL of 5.0 mM HQ added to 3.0 mL hexane dispersion of $CuInS_2$/ZnS core/shell Qdot (with absorbance of 0.12 at 365 nm).

Amount of 5.0 mM HQ added (in µl)	Final Conc. of HQ (µM)	Chromaticity Coordinates (x, y)
(i) 0.0	0.00	(0.50, 0.37)
(ii) 5.0	8.32	(0.34, 0.36)
(iii) 10.0	16.61	(0.32, 0.35)
(iii) 15.0	24.88	(0.30,0.35)

Table A.4.5. Chromaticity color coordinates of white light emitting nanocomposite at different time intervals: (i) 0 h, (ii) 24 h and (iii) 48 h after HQ addition.

Time interval (hours)	Chromaticity Coordinates (x, y)
(i) 0	(0.32, 0.35)
(ii) 24	(0.31, 0.35)
(iii) 48	(0.31, 0.35)

A5: Chapter 5

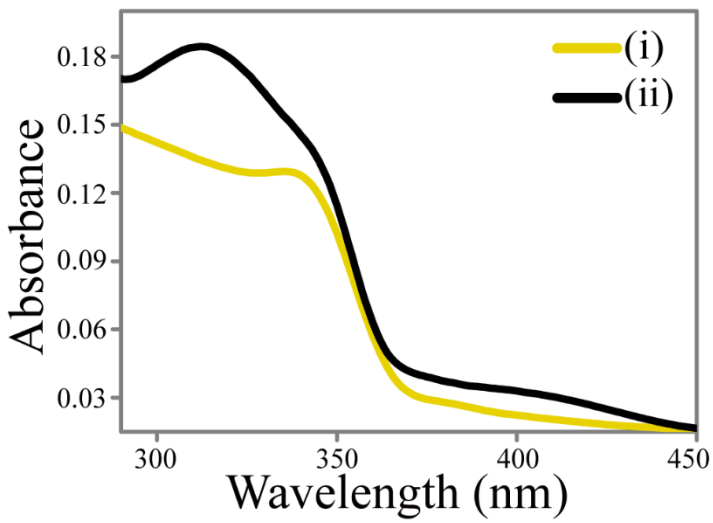

Figure A.5.1. UV-vis spectra of the ethanolic dispersions of (i) ZnO Qdots and (ii) WLE QDC.

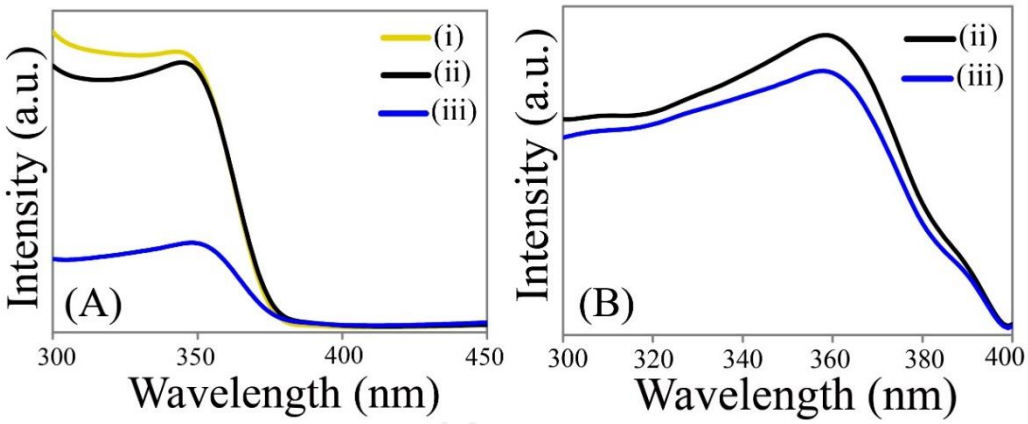

Figure A.5.2. Excitation spectra recorded with respect to emission maxima at (**A**) 550 nm and (**B**) 440 nm of (i) ZnO Qdots, (ii) WLE QDC and (iii) dopamine added WLE QDC.

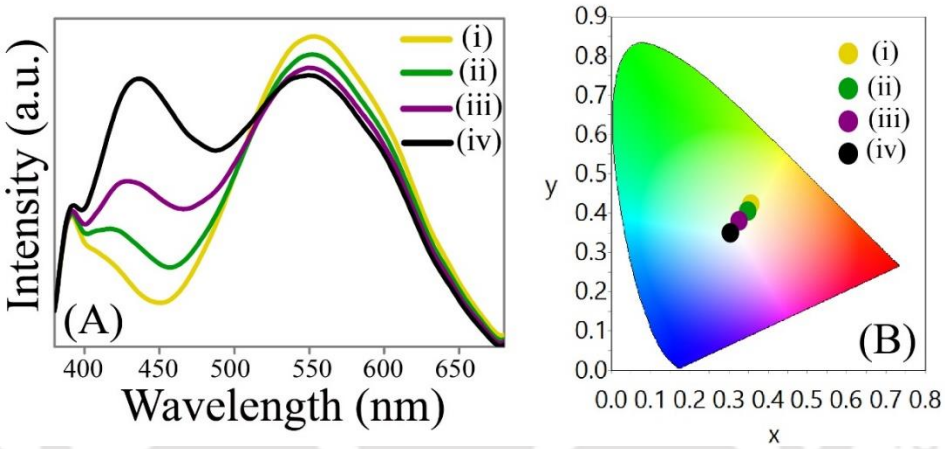

Figure A.5.3. (A) Emission spectra (λ_{ex}-350 nm) and **(B)** corresponding CIE chromaticity diagram of samples with different amounts i.e., (i) 0.0 µL, (ii) 10.0 µL, (iii) 20.0 µL and (iv) 30.0 µL of 1.0 mM MSA added to 3.0 mL ethanolic dispersion of ZnO Qdots (with absorbance of 0.10 at 350 nm).

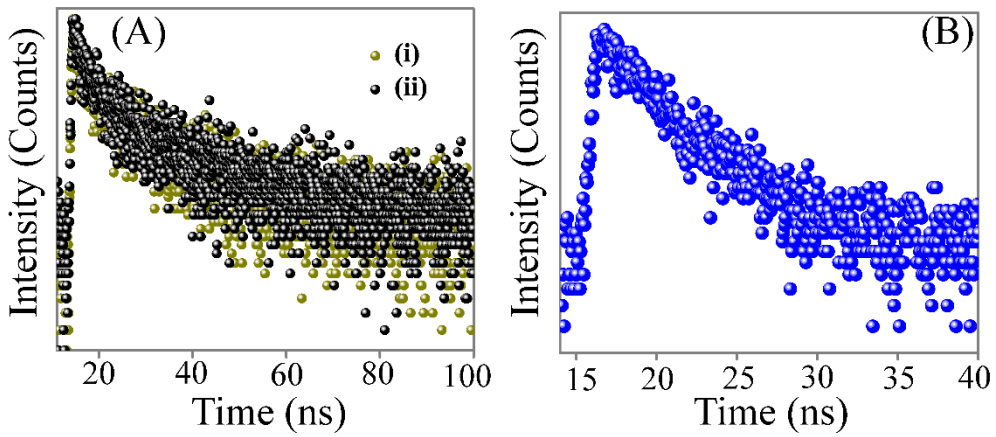

Figure A.5.4. Time resolved PL spectra (recorded using 336 nm LED excitation source) monitored with respect to emission maxima at **(A)** 550 nm of (i) ZnO Qdots (in ethanol), (ii) WLE QDC (in ethanol) and **(B)** 440 nm of WLE QDC (in ethanol).

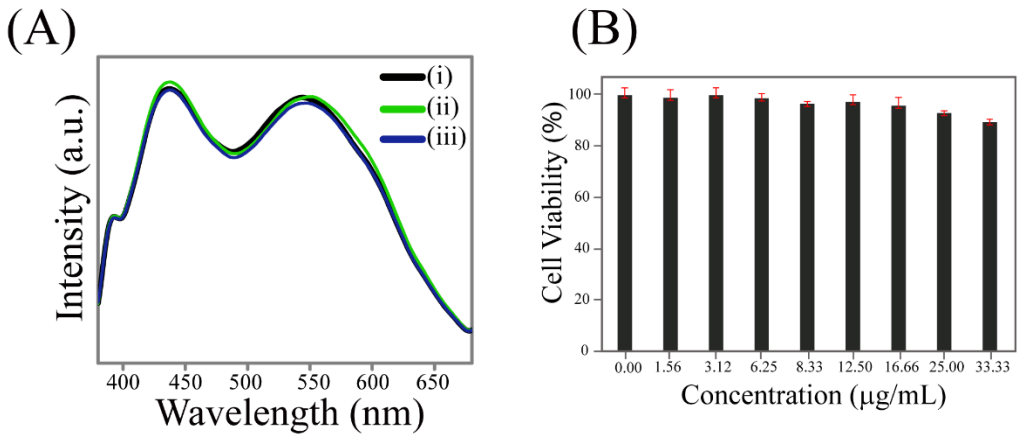

Figure A.5.5. (**A**) Luminesce stability (up to 48 h) in colloidal form, and (**B**) MTT-based cell viability assay of HEK 293 cells (after 24 h) upon incubation with different concentrations of WLE QDC nanocomposite. 3-(4,5-dimethylthiazol-2-yl)-2,5-diphenyltetrazolium bromide (MTT) - based cell viability (after 24 h) showed that nearly 89% of the cells were viable when incubated with 33.3 μg/mL or lesser quantity of WLE nanocomposite.

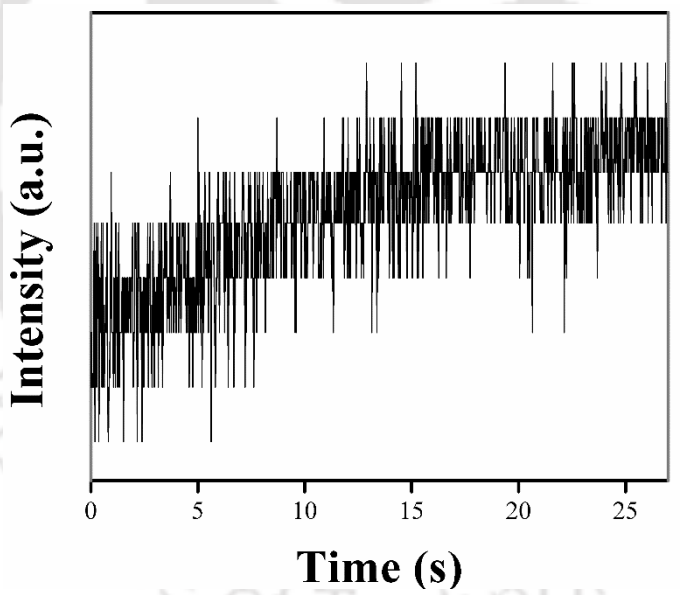

Figure A.5.6. Time dependent blinking profile (recorded using frame size of 64 x 64 μm^2 and binning time of 27 ms with excitation power of 63 mW for a time duration of 27 s) of multiple particles of WLE QDC. The 355 nm laser was used to excite the samples.

It is to be mentioned here that the absence of clear on-off blinking help to distinguish multiple particles from single ones. Usually, multiple particles exhibited intermittent intensity values i.e., their intensity fluctuated in between on and dim (or grey states) and did not return to off states (which has zero intensity).

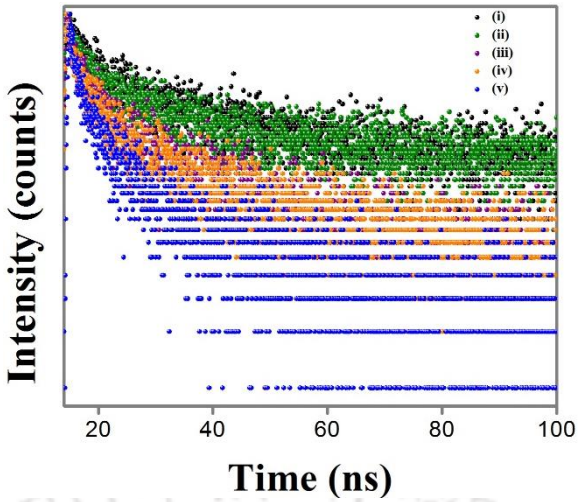

Figure A.5.7. Time resolved PL spectra (recorded using 336 nm LED excitation source) monitored with respect to emission peak of ZnO Qdots (at 550 nm) of (i) 0.0, (ii) 6.6, (iii) 46.4, (iv) 99.0, (v) 1176.5 nM dopamine added to WLE QDC (in ethanol).

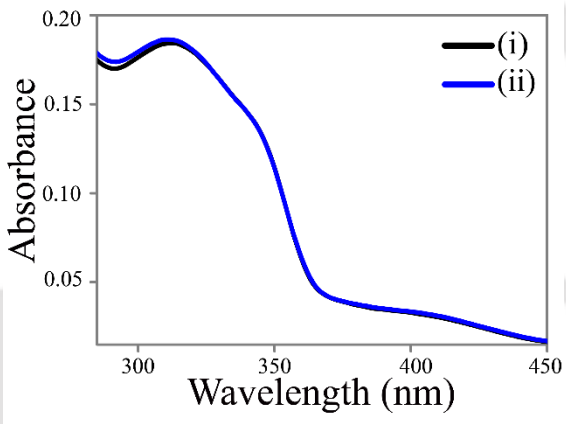

Figure A.5.8. UV-vis spectra of (i) WLE QDC nanocomposite and (ii) dopamine added WLE QDC nanocomposite.

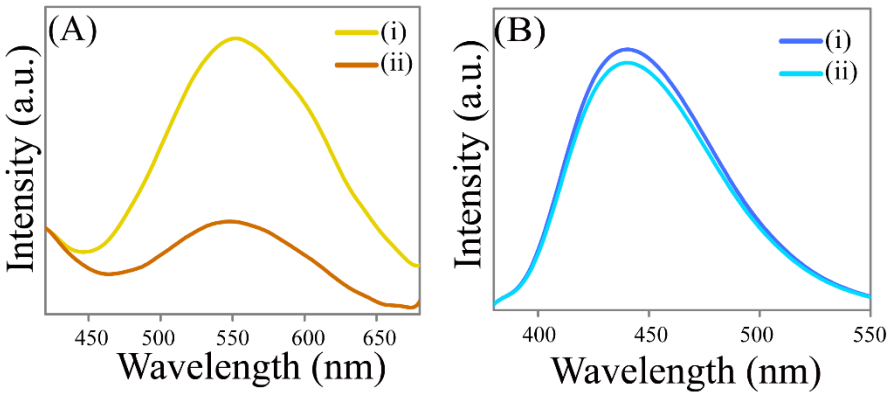

Figure A.5.9. (A) Emission spectra (λ_{ex}-350 nm) of (i) as synthesized ZnO Qdots and (ii) 1176.5 nM dopamine added ZnO Qdots. **(B)** Emission spectra (λ_{ex}-350 nm) of (i) as synthesized $Zn(MSA)_2$ complex and (ii) 1176.5 nM dopamine added $Zn(MSA)_2$ complex.

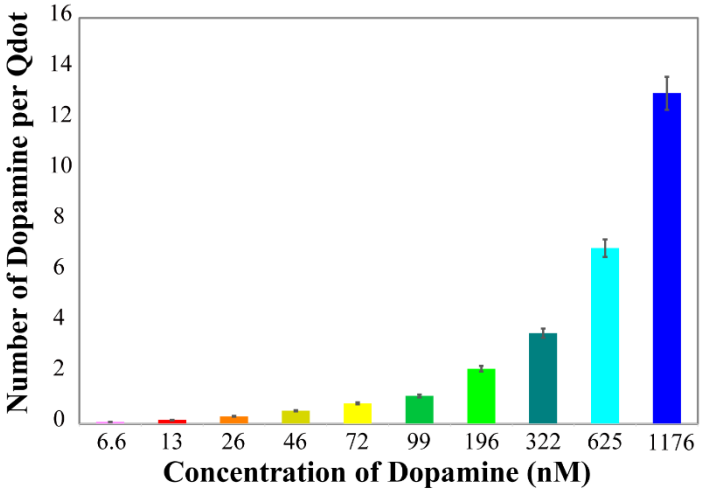

Figure A.5.10. Histogram of number of dopamine molecules per Qdot present in WLE QDC.

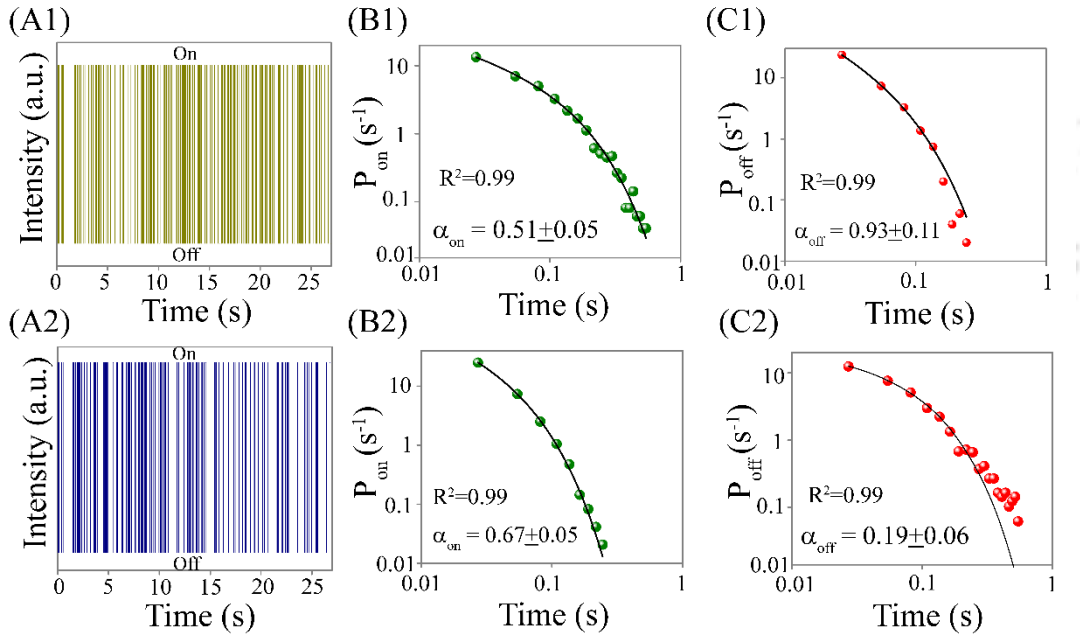

Figure A.5.11. **(A)** Representative time dependent blinking profile and corresponding probability density of **(B)** on-states ($P_{on}(t)$) and **(C)** off-states ($P_{off}(t)$) of (1) ZnO Qdot and (2) dopamine added ZnO Qdot (the same amount of dopamine, which was used for WLE QDC i.e., 1176.5 nM). The data were obtained for 10 particles using frame size of 64 x 64 μm^2 and binning time of 27 ms with excitation power of 63mW and for a time duration of 27 s. The 355 nm laser was used to excite the samples.

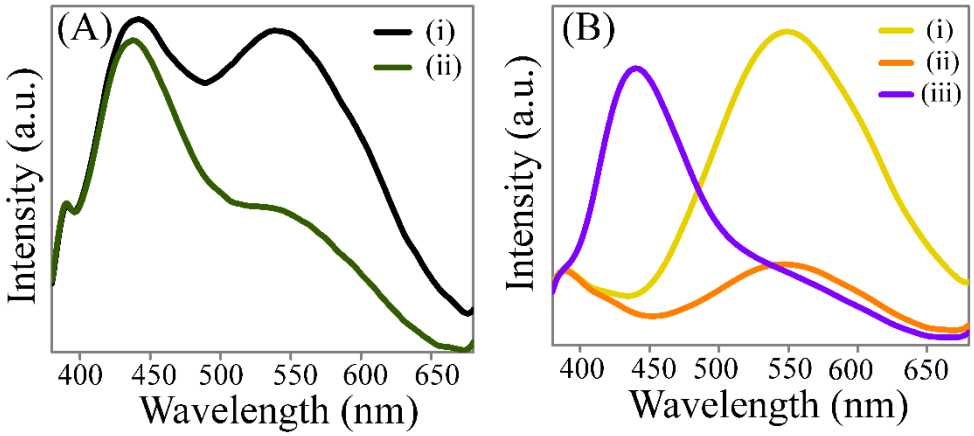

Figure A.5.12. (**A**) Emission spectra (λ_{ex} = 350 nm) of (i) WLE QDC and (ii) *p*-benzoquinone (BQ) – which is a well-known electron quencher – added WLE QDC (recorded following centrifugation and then redispersion). (**B**) Emission spectra (λ_{ex} = 350 nm) of (i) ZnO Qdots and (ii) *p*-benzoquinone (BQ) treated ZnO Qdots recorded following centrifugation plus redispersion and then (iii) into that same solution (i.e., BQ-treated Qdots) MSA was added.

Table A.5.1. Chromaticity color coordinates of samples with of different amounts i.e., (i) 0.0 µL, (ii) 10.0 µL, (iii) 20.0 µL and (iv) 30.0 µL of 1.0 mM MSA added to 3.0 mL ethanolic dispersion of ZnO Qdots (with absorbance of 0.10 at 350 nm).

Amount of 1.0 mM MSA added (in µl)	Final Conc. of MSA (µM)	Chromaticity Coordinates (x, y)
(i) 0.0	0.00	(0.36, 0.43)
(ii) 10.0	3.32	(0.35, 0.41)
(iii) 20.0	6.62	(0.33, 0.38)
(iii) 30.0	9.90	(0.31, 0.33)

Table A.5.2. Quantum yield (λ_{ex}-350 nm; using quinine sulphate (QY-54% in 0.1 M H_2SO_4) as standard) of (i) ZnO Qdots and (ii) WLE QDC nanocomposite.

Sample	λ_{ex} (nm)	λ_{em} (nm)	Quantum Yield (%)
(i) ZnO Qdots	350	550	1.2
(ii) WLE QDC	350	440, 550	2.4

Table A.5.3. Photoluminescence life time decay parameters obtained by analyzing the photoluminescence decay curves of ethanolic dispersion of (i) ZnO Qdots (λ_{em}-550 nm) and (ii) WLE QDC (λ_{em}-550 and 440 nm).

Samples	λ_{em} (nm)	α_i (%)	τ_i (ns)	τ_{av} (ns)	χ^2
(i) ZnO Qdots	550	18.9	5.1	38.8	1.1
		81.1	39.7		
(ii) WLE QDC	550	24.7	5.4	38.0	1.0
		75.3	39.5		
	440	100	4.43	4.43	1.0

Table A.5.4. Chromaticity color coordinates in CIE diagram of (i) 0.0, (ii) 6.6, (iii) 13.3, (iv) 26.6, (v) 46.4, (vi) 72.8, (vii) 99.0, (viii) 196.0, (ix) 322.0, (x) 625.0 and (xi) 1176.5 nM dopamine added to WLE QDC nanocomposite (with absorbance of 0.11 fixed at 350 nm).

Amount of dopamine added (nM)	Chromaticity Coordinates (x, y)
(i) 0.0	(0.31,0.33)
(ii) 6.6	(0.30,0.33)
(iii) 13.3	(0.29,0.33)
(iv) 26.6	(0.29,0.32)
(v) 46.0	(0.29,0.31)
(vi) 72.0	(0.28,0.30)
(vii) 99.0	(0.28,0.29)
(viii) 196.0	(0.27,0.28)
(ix) 322.0	(0.26,0.27)
(x) 622.0	(0.25,0.25)
(xi) 1176.5	(0.24,0.23)

Table A.5.5. Tabulated form of photoluminescence lifetime decay parameters, obtained by analyzing the photoluminescence decay curves, from Figure A.5.7.

Amount of dopamine added (nM)	λ_{em} (nm)	α_i (%)	τ_i (ns)	τ_{av} (ns)	χ^2
(i) 0.0	550	24.7	5.4	38.0	1.0
		75.3	39.5		
(ii) 6.6		18.7	3.6	33.0	1.1
		81.2	33.8		
(iii) 46.4		35.6	3.8	26.5	1.3
		64.3	28.2		
(iv) 99.0		22.5	2.7	25.7	1.3
		77.4	26.4		
(v) 1176.5		31.1	2.1	17.2	1.0
		68.8	18.0		

Table A.5.6. Fitting parameters for probability density of on-states ($P_{on}(t)$) and off-states ($P_{off}(t)$) for single ZnO Qdot before and after dopamine addition, data points are obtained from Figure A.5.11. A.

Samples	α_{on}	α_{off}	α_{on}/α_{off}	No. of events
ZnO Qdot	0.51 $\pm$ 0.05	0.93 $\pm$ 0.11	0.55	3638
Dopamine added ZnO Qdot	0.67 $\pm$ 0.05	0.19 $\pm$ 0.06	3.52	3572

A.5.1. *Calculation of Number of Dopamine Molecules per Qdot, Present in QDC.*

Assumption:

1. Hexagonally closed pack wurtzite structure of nanocrystal (supported by powder XRD).
2. Lattice defects are not considered.

Quantum dots have spherical shape with wurtzite lattice structure where Zn^{2+} and O^{2-} are in hexagonally closed pack.

From TEM analysis, we have got that average particle diameter is 4.5 nm. We assume that shape of all quantum dots is identical for ease of calculation.

Diameter of Qdot = 4.5 nm, so, r = radius of Qdot = 2.25 nm

So, Volume of a Qdot (V_{Qdot}) = $\frac{4}{3}\pi r^3$ = 47712.94 Å^3 and surface area of a Qdot (A_{Qdot}) = $4\pi r^2$=6361.73 Å^2.

Volume of a ZnO wurtzite unit cell (V_{cell}) = 47.66 Å^3 and a wurtzite unit cell of ZnO is shared by 2 Zn^{2+} ions (r_+= 0.74 Å) and 2 O^{2-} ions (r_-= 1.40 Å).

So, one Qdot consists of (V_{Qdot} / V_{cell}) = 1001 unit cell of wurtzite ZnO

From atomic absorption spectroscopic (AAS) analysis, we found that the concentration of Zn^{2+} ion in the 3 mL (taken for photoluminescence experiment, absorbance = 0.11) Qdot dispersion was 0.226 mM

So, the number of Zn^{2+} ions in 3 mL Qdot dispersion = 4.08×10^{17}

Number of quantum dots in the same quantum dots dispersion = $(4.08 \times 10^{17}) / (1001 \times 2) = 2.03 \times 10^{14}$

(A) Limit of Detection of dopamine (obtained from fluorescence measurement) = 6.66 nM = $(6.66\times10^{-9}) \times (6.023\times10^{23}) = 40.11\times10^{14}$ number of molecules /L

Number of molecules in 3 mL = $(40.11 \times 10^{14}) \times 3/1000 = 1.2 \times 10^{13}$

Sensing of Dopamine molecules per QD = $1.2 \times10^{13}/2.03 \times10^{14}$ = 0.06

Following measurements in triplicate, the obtained number of dopamine molecules per Qdot = 0.07 ± 0.01

(B) Concentration of dopamine required for white to proper blue color change (obtained from fluorescence measurement) = 1176.5 nM = $(1176.5\times10^{-9}) \times (6.023\times10^{23}) = 70.83 \times10^{16}$ number of molecules /L

Number of molecules in 3 mL = $(70.83 \times 10^{16}) \times 3/1000 = 2.12 \times 10^{15}$

Sensing of dopamine molecules per QD = $2.12 \times10^{15}/2.03 \times10^{14}$ = 10.5

Following measurements in triplicate, the obtained number of dopamine molecules per Qdot = 13.03 ± 2.22

Hence, approximately 13 dopamine molecules can be detected through observing the change in color from white to blue of WLE QDC following reaction with dopamine.

Instruments and Softwares:

Chapter 2. Perkin Elmer Lambda spectrophotometer and Horiba Fluoromax-4 spectrofluorimeter were used to record the UV-vis and photoluminescence of the samples, respectively. Fourier transform infrared spectra were recorded in a Perkin-Elmer (Model: Spectrum Two) spectrophotometer. Zeta potentials of the colloidal samples were recorded by using a Malvern Zetasizer Nano ZS instrument. Electron paramagnetic resonance (EPR) spectrometer (JEOL, Model: JES-FA200) and atomic absorption spectrometer (Varian AA240FS model) were used to record the EPR and elemental composition of the samples. The XRD pattern of the powder samples were obtained by using Brucker D2 Phaser X-ray diffractometer with Cu Kα radiation at 1.5418Å. TEM images were recorded on a JEOL JEM-2100 transmission electron microscope at an accelerating voltage 200 kV. TEM analysis and inverse fast Fourier transform (IFFT) were done by using Gatan Digital Micrograph software The "go cie" software was used to calculate the chromaticity point in the CIE (1931) diagram.

Chapter 3. All the samples were characterized using Perkin Elmer LAMBDA 750 UV/Vis/NIR spectrophotometer, HORIBA Jobin Yvon FluoroMax-4 spectrofluorimeter, transmission electron microscope (TEM, JEOL JEM 2100, maximum accelerating voltage 200 kV) and Rigaku TTRAX III X-ray diffractometer. JASCO J-1500 circular dichroism (CD) spectrometer was used to record the CD spectra of the samples. The quantum yield and the photostability of the NC-QDC nanocomposite were measured using quinine sulfate (in 0.1 M H_2SO_4) and rhodamine 6G (in ethanol) as the standards, respectively. The NC-QDC nanocomposite zeta potential was measured using Malvern Zetasizer Nano ZS90 (Model No. ZEN3690). Time resolved photoluminescence (TRPL) measurements of the samples were carried out by using Life-Spec-II spectrofluorimeter (Edinburgh Instrument, using Pico Quant 375 nm laser source) and the time-resolved spectra of the samples were analyzed by FAST software. The CIE chromaticity coordinates were calculated using the GoCIE software.

Chapter 4. UV-vis and photoluminescence measurements of the samples were carried out by using the Perkin Elmer LAMBDA 750 UV/Vis/NIR spectrophotometer and HORIBA Jobin Yvon FluoroMax-4 spectrofluorimeter, respectively. Morphological analyses of the samples were performed using the JEOL JEM-2100 transmission electron

microscope (maximum accelerating voltage 200 kV) and Rigaku TTRAX III X-ray diffractometer (where Cu-Kα radiation, λ = 1.54056 Å used as x-ray source at an acceleration voltage 50kV). Perkin-Elmer (Model: Spectrum Two) spectrophotometer was used for Fourier transform infrared spectroscopy measurements. The photoluminescence decay of the samples was recorded by using Life-Spec-II spectrofluorimeter (Edinburgh Instrument, using Pico Quant 375 nm LASER source) and the decay curves were analyzed by FAST software. The CIE chromaticity analyses were done by using the CIE-1931 color space of the OSRAM color calculator. Quinine sulfate solution in 0.1 M H_2SO_4 was used as a standard dye for the quantum yield calculation of the samples.

Chapter 5. Rigaku TTRAX III X-ray diffractometer and transmission electron microscope (TEM, JEOL JEM 2100F, maximum accelerating voltage 200 kV) were used to analyze the morphology and size of the samples. TEM and inverse fast Fourier transform (IFFT) analyses were done by using Gatan Digital Micrograph software. HORIBA Jobin Yvon FluoroMax-4 spectrofluorimeter and Perkin Elmer LAMBDA 750 UV/Vis/NIR spectrophotometer were used to record the luminescence and absorbance of the samples, respectively. Life-Spec-II spectrofluorimeter (Edinburgh Instrument, using 336 nM LED source and Pico Quant 375 nm laser source) was used to record the time resolved photoluminescence (TRPL) measurements and FAST software was used to analyze the time-resolved spectra. CIE-1931 color space of the OSRAM color calculator was used to calculate the chromaticity of the samples. Atomic absorption spectrophotometer (AAS; Varian AA240FS model) was used to find the concentration of metal ions. LSM 880 Confocal laser scanning microscope (Zeiss) was used to record the single particle behavior of the solid samples (deposited on a glass cover slip) using 355 nm laser excitation.

Cell Viability Assay:

Chapter 2. Human embryonic kidney HEK 293 cells were procured from National Center for Cell Sciences (NCCS), Pune, India and cultured in Dulbecco's modified Eagle's medium, supplemented with 10 % (v/v) fetal bovine serum, penicillin (50 units/mL) and streptomycin (50 mg/mL). Cells were maintained in 5 % CO_2 humidified incubator at 37 °C. For cell viability assay, 10^4 HEK 293 cells/well were seeded in a 96 well microplate and allowed to grow overnight. Then, the medium was removed and

fresh media containing varying concentrations of NC-QDC nanocomposite (3.8 μg/mL – 26.7 μg/mL) were added to the cells and incubated for 24 h. After this, the 3-(4,5-dimethylthiazol-2-yl)-2,5-diphenyltetrazolium bromide (MTT) based cell viability assay was carried out and the absorbance (at wavelength 550 nm) was recorded using the Bio-Rad 680 microplate reader.

Chapter 5. For cell viability assay, 10^4 human embryonic kidney (HEK 293) cells (which were procured from National Center for Cell Sciences (NCCS), Pune, India and cultured in Dulbecco's modified Eagle's medium, supplemented with 10 % (v/v) fetal bovine serum, penicillin (50 units/mL) and streptomycin (50 mg/mL) and maintained in 5 % CO_2 humidified incubator at 37 °C) per well were seeded in a 96 well microplate and left for overnight for proper growing. Then, the fresh media containing varying concentrations of WLE QDC (1.6 μg/mL – 33.3 μg/mL), following removal of the old medium, were added to the cells and incubated for 24 h. Finally, the 3-(4,5-dimethylthiazol-2-yl)-2,5-diphenyltetrazolium bromide (MTT) based cell viability assay was performed and the Bio-Rad 680 microplate reader was used to monitored the absorbance at wavelength 550 nm.

Quantum Yield Calculation:

The photoluminescence quantum yields (PLQYs) of the samples were calculated using quinine sulphate (in 0.1 M H_2SO_4) as standard and following equation:

$$Q_s = Q_R \times \frac{I_s}{I_R} \times \frac{A_R}{A_S} \times \frac{\eta_S^2}{\eta_R^2}$$

Where, Q_S = sample's PLQY; Q_R = standard's PLQY (0.54 in 0.1 M H_2SO_4); I_S = area under the emission curve of sample; I_R = area under the emission curve of standard; A_R = standard's absorbance; A_S = sample's absorbance; η_S = refractive index of solvent, which was used for dispersion of sample; η_R = refractive index of solvent, which was used for dispersion of standard. The concentration of all samples and the standard were fixed by adjusting their absorbance to 0.1 ± 0.01 at the corresponding excitation wavelength.

Photoluminescence Life time Calculation:

The decay profile was fitted to a multi-exponential model using following equation

$$I(t) = \sum_i \alpha_i \exp\left(-t/\tau_i\right)$$

Where, single, bi and tri exponential functions were used to fit respective emission with obtaining χ^2 close to 1.0. The averaged life times (τ_{av}) was calculated from the results of exponential model using the following equation

$$\tau_{av} = \frac{\sum_i \alpha_i \tau_i^2}{\sum_i \alpha_i \tau_i}$$

Where, α_i and τ_i are the pre-exponential factors and excited-state luminescence decay time associated with the *i*-th component, respectively.

List of Abbreviations

AAS	Atomic absorption spectroscopy
ASA	Acetylsalicylic acid
AuNCs	Gold nanoclusters
BSA	Bovine serum albumin
CD	Circular dichroism
CCT	Correlated color temperature
CIE	Commission internationale de l'éclairage (International Commission on Illumination)
CRI	Color rendering index
EPR	Electron paramagnetic resonance
FTIR	Fourier-transform infrared
HQ	8-Hydroxyquinoline
HRTEM	High resolution transmission electron microscopy
IFFT	Inverse fast Fourier transform
MSA	N-methylsalicylaldimine
NCQdot	Nanoclusters Qdot composite
NCQDC	Nanoclusters quantum dot complex composite
PL	Photoluminescence
Qdot	Quantum dot
QDC	Quantum dot complex
QY	Quantum yield
SAED	Selected area electron diffraction
TRPL	Time resolved photoluminescence
WLE	White light emitting
XRD	X-ray diffraction
ZnQ_2	Zinc quinolato complex

List of Publications

1. **Pramanik, S.**; Bhandari, S.; Pan, U.N.; Roy, S.; Chattopadhyay, A. A White Light Emitting Quantum Dot Complex for Single Particle Level Interaction with Dopamine Leading to Changes in Color and Blinking Profile. *Small* **2018**, 14, 1800323

2. **Pramanik, S.**; Bhandari, S.; Chattopadhyay, A. Zinc quinolate complex decorated $CuInS_2$/ZnS core/shell quantum dots for white light emission *J. Mater. Chem. C*, **2017**, 5, 7291−7296.

3. Roy, S.; **Pramanik, S.**; Bhandari, S.; Chattopadhyay, A. Surface Complexed ZnO Quantum Dot for White Light Emission with Controllable Chromaticity and Color Temperature. *Langmuir* **2017**, 33, 14627−14633.

4. Bhandari, S.; **Pramanik, S.**; Khandelia, R.; Chattopadhyay, A. Gold Nanocluster and Quantum Dot Complex in Protein for Biofriendly White-Light-Emitting Material. *ACS Appl. Mater. Interfaces* **2016**, 8, 1600−1605. ***(S.B., S.P. and R.K have equal contribution)***

5. **Pramanik, S.**; Bhandari, S.; Roy, S.; Chattopadhyay, A. Synchronous Tricolor Emission-Based White Light from Quantum Dot Complex *J. Phys. Chem. Lett.* **2015**, *6*, 1270–1274. (*This article has been has been featured in* ***C&E News*** *and* ***ACS Live Slides*** *presentation*).

6. Bhandari, S.; Roy, S.; **Pramanik, S.**; Chattopadhyay, A. Double Channel Emission from a Redox Active Single Component Quantum Dot Complex *Langmuir* **2015**, *31*, 551–561.

7. Bhandari, S.; Roy, S.; **Pramanik, S.**; Chattopadhyay, A. Surface Complexation Reaction for Phase Transfer of Hydrophobic Quantum Dot from Nonpolar to Polar Medium *Langmuir* **2014**, *30*, 10760–10765.

Conferences Attended

1) Presented an oral talk in **MRSI YSC-2017** held at Indian Institute of Engineering Science and Technology, Shibpur, India.

2) Presented a poster in **ChemConvene-2017** held at Indian Institute of Technology Guwahati, India.

3) Presented a poster in DAE-BRNS 6th Interdisciplinary Symposium on Materials Chemistry, **ISMC-2016** held at Bhabha Atomic Research Centre, (BARC) Mumbai, India.

4) Presented a poster in International Conference on Nano Science and Technology, International Conference on Nanoscience and Technology**,** **ICONSAT-2016** held at Indian Institutes of Science Education and Research (IISER) Pune, India.

5) Presented a poster in International Conference on Advanced Nanomaterials and Nanotechnology, **ICANN- 2015** held at Indian Institute of Technology Guwahati, India.

6) Presented a poster in **Nano Sci-2014** held at Institute of Advanced Study in Science and Technology, Guwahati, India.

Permissions

JOHN WILEY AND SONS LICENSE TERMS AND CONDITIONS

Jul 20, 2018

This Agreement between Mr. SABYASACHI PRAMANIK ("You") and John Wiley and Sons ("John Wiley and Sons") consists of your license details and the terms and conditions provided by John Wiley and Sons and Copyright Clearance Center.

License Number	4393130316289
License date	Jul 20, 2018
Licensed Content Publisher	John Wiley and Sons
Licensed Content Publication	Advanced Functional Materials
Licensed Content Title	Organization of Matter on Different Size Scales: Monodisperse Nanocrystals and Their Superstructures
Licensed Content Author	A.L. Rogach, D.V. Talapin, E.V. Shevchenko, et al
Licensed Content Date	Oct 21, 2002
Licensed Content Volume	12
Licensed Content Issue	10
Licensed Content Pages	12
Type of Use	Dissertation/Thesis
Requestor type	University/Academic
Format	Print and electronic
Portion	Figure/table
Number of figures/tables	1
Original Wiley figure/table number(s)	Figure 1
Will you be translating?	No
Title of your thesis / dissertation	Surface Complexation Reaction for White Light Emission from Quantum Dots
Expected completion date	Aug 2018
Expected size (number of pages)	150
Requestor Location	Mr. SABYASACHI PRAMANIK DEPARTMENT OF CHEMISTRY IIT GUWAHATI GUWAHATI, 781039 India Attn: Mr. SABYASACHI PRAMANIK
Publisher Tax ID	EU826007151
Total	**0.00 USD**
Terms and Conditions	

TERMS AND CONDITIONS

This copyrighted material is owned by or exclusively licensed to John Wiley & Sons, Inc. or one of its group companies (each a"Wiley Company") or handled on behalf of a society with which a Wiley Company has exclusive publishing rights in relation to a particular work (collectively "WILEY"). By clicking "accept" in connection with completing this licensing transaction, you agree that the following terms and conditions apply to this transaction (along with the billing and payment terms and conditions established by the Copyright Clearance Center Inc., ("CCC's Billing and Payment terms and conditions"), at the time that you opened your RightsLink account (these are available at any time at http://myaccount.copyright.com).

Terms and Conditions

- The materials you have requested permission to reproduce or reuse (the "Wiley Materials") are protected by copyright.

- You are hereby granted a personal, non-exclusive, non-sub licensable (on a stand-alone basis), non-transferable, worldwide, limited license to reproduce the Wiley Materials for the purpose specified in the licensing process. This license, **and any CONTENT (PDF or image file) purchased as part of your order,** is for a one-time use only and limited to any maximum distribution number specified in the license. The first instance of republication or reuse granted by this license must be completed within two years of the date of the grant of this license (although copies prepared before the end date may be distributed thereafter). The Wiley Materials shall not be used in any other manner or for any other purpose, beyond what is granted in the license. Permission is granted subject to an appropriate acknowledgement given to the author, title of the material/book/journal and the publisher. You shall also duplicate the copyright notice that appears in the Wiley publication in your use of the Wiley Material. Permission is also granted on the understanding that nowhere in the text is a previously published source acknowledged for all or part of this Wiley Material. Any third party content is expressly excluded from this permission.

- With respect to the Wiley Materials, all rights are reserved. Except as expressly granted by the terms of the license, no part of the Wiley Materials may be copied, modified, adapted (except for minor reformatting required by the new Publication), translated, reproduced, transferred or distributed, in any form or by any means, and no derivative works may be made based on the Wiley Materials without the prior permission of the respective copyright owner.**For STM Signatory Publishers clearing permission under the terms of the STM Permissions Guidelines only, the terms of the license are extended to include subsequent editions and for editions in other languages, provided such editions are for the work as a whole in situ and does not involve the separate exploitation of the permitted figures or extracts,** You may not alter, remove or suppress in any manner any copyright, trademark or other notices displayed by the Wiley Materials. You may not license, rent, sell, loan, lease, pledge, offer as security, transfer or assign the Wiley Materials on a stand-alone basis, or any of the rights granted to you hereunder to any other person.

- The Wiley Materials and all of the intellectual property rights therein shall at all times remain the exclusive property of John Wiley & Sons Inc, the Wiley Companies, or their respective licensors, and your interest therein is only that of having possession of and the right to reproduce the Wiley Materials pursuant to Section 2 herein during the continuance of this Agreement. You agree that you own no right, title or interest in or to the Wiley Materials or any of the intellectual property rights therein. You shall have no rights hereunder other than the license as provided for above in Section 2. No right, license or interest to any trademark, trade name, service mark or other branding ("Marks") of WILEY or its licensors is granted hereunder, and you agree that you shall not assert any such right, license or interest with respect thereto

- NEITHER WILEY NOR ITS LICENSORS MAKES ANY WARRANTY OR REPRESENTATION OF ANY KIND TO YOU OR ANY THIRD PARTY, EXPRESS, IMPLIED OR STATUTORY, WITH RESPECT TO THE MATERIALS OR THE ACCURACY OF ANY INFORMATION CONTAINED IN THE MATERIALS, INCLUDING, WITHOUT LIMITATION, ANY IMPLIED WARRANTY OF MERCHANTABILITY, ACCURACY, SATISFACTORY QUALITY, FITNESS FOR A PARTICULAR PURPOSE, USABILITY, INTEGRATION OR NON-INFRINGEMENT AND ALL SUCH WARRANTIES ARE HEREBY EXCLUDED BY WILEY AND ITS LICENSORS AND WAIVED BY YOU.

- WILEY shall have the right to terminate this Agreement immediately upon breach of this Agreement by you.

- You shall indemnify, defend and hold harmless WILEY, its Licensors and their respective directors, officers, agents and employees, from and against any actual or threatened claims, demands, causes of action or proceedings arising from any breach of this Agreement by you.

- IN NO EVENT SHALL WILEY OR ITS LICENSORS BE LIABLE TO YOU OR ANY OTHER PARTY OR ANY OTHER PERSON OR ENTITY FOR ANY SPECIAL, CONSEQUENTIAL, INCIDENTAL, INDIRECT, EXEMPLARY OR PUNITIVE DAMAGES, HOWEVER CAUSED, ARISING OUT OF OR IN CONNECTION WITH THE DOWNLOADING, PROVISIONING, VIEWING OR USE OF THE MATERIALS REGARDLESS OF THE FORM OF ACTION, WHETHER FOR BREACH OF CONTRACT, BREACH OF WARRANTY, TORT, NEGLIGENCE, INFRINGEMENT OR OTHERWISE (INCLUDING, WITHOUT LIMITATION, DAMAGES BASED ON LOSS OF PROFITS, DATA, FILES, USE, BUSINESS OPPORTUNITY OR CLAIMS OF THIRD PARTIES), AND WHETHER OR NOT THE PARTY HAS BEEN ADVISED OF THE POSSIBILITY OF SUCH DAMAGES. THIS LIMITATION SHALL APPLY NOTWITHSTANDING ANY FAILURE OF ESSENTIAL PURPOSE OF ANY LIMITED REMEDY PROVIDED HEREIN.

- Should any provision of this Agreement be held by a court of competent jurisdiction to be illegal, invalid, or unenforceable, that provision shall be deemed amended to achieve as nearly as possible the same economic effect as the original provision, and the legality, validity and enforceability of the remaining provisions of this Agreement shall not be affected or impaired thereby.

- The failure of either party to enforce any term or condition of this Agreement shall not constitute a waiver of either party's right to enforce each and every term and condition of this Agreement. No breach under this agreement shall be deemed waived or excused by either party unless such waiver or consent is in writing signed by the party granting such waiver or consent. The waiver by or consent of a party to a breach of any provision of this Agreement shall not operate or be construed as a waiver of or consent to any other or subsequent breach by such other party.

TH-1887_136122001

- This Agreement may not be assigned (including by operation of law or otherwise) by you without WILEY's prior written consent.
- Any fee required for this permission shall be non-refundable after thirty (30) days from receipt by the CCC.
- These terms and conditions together with CCC's Billing and Payment terms and conditions (which are incorporated herein) form the entire agreement between you and WILEY concerning this licensing transaction and (in the absence of fraud) supersedes all prior agreements and representations of the parties, oral or written. This Agreement may not be amended except in writing signed by both parties. This Agreement shall be binding upon and inure to the benefit of the parties' successors, legal representatives, and authorized assigns.
- In the event of any conflict between your obligations established by these terms and conditions and those established by CCC's Billing and Payment terms and conditions, these terms and conditions shall prevail.
- WILEY expressly reserves all rights not specifically granted in the combination of (i) the license details provided by you and accepted in the course of this licensing transaction, (ii) these terms and conditions and (iii) CCC's Billing and Payment terms and conditions.
- This Agreement will be void if the Type of Use, Format, Circulation, or Requestor Type was misrepresented during the licensing process.
- This Agreement shall be governed by and construed in accordance with the laws of the State of New York, USA, without regards to such state's conflict of law rules. Any legal action, suit or proceeding arising out of or relating to these Terms and Conditions or the breach thereof shall be instituted in a court of competent jurisdiction in New York County in the State of New York in the United States of America and each party hereby consents and submits to the personal jurisdiction of such court, waives any objection to venue in such court and consents to service of process by registered or certified mail, return receipt requested, at the last known address of such party.

WILEY OPEN ACCESS TERMS AND CONDITIONS

Wiley Publishes Open Access Articles in fully Open Access Journals and in Subscription journals offering Online Open. Although most of the fully Open Access journals publish open access articles under the terms of the Creative Commons Attribution (CC BY) License only, the subscription journals and a few of the Open Access Journals offer a choice of Creative Commons Licenses. The license type is clearly identified on the article.

The Creative Commons Attribution License

The Creative Commons Attribution License (CC-BY) allows users to copy, distribute and transmit an article, adapt the article and make commercial use of the article. The CC-BY license permits commercial and non-

Creative Commons Attribution Non-Commercial License

The Creative Commons Attribution Non-Commercial (CC-BY-NC)License permits use, distribution and reproduction in any medium, provided the original work is properly cited and is not used for commercial purposes.(see below)

Creative Commons Attribution-Non-Commercial-NoDerivs License

The Creative Commons Attribution Non-Commercial-NoDerivs License (CC-BY-NC-ND) permits use, distribution and reproduction in any medium, provided the original work is properly cited, is not used for commercial purposes and no modifications or adaptations are made. (see below)

Use by commercial "for-profit" organizations

Use of Wiley Open Access articles for commercial, promotional, or marketing purposes requires further explicit permission from Wiley and will be subject to a fee.

Further details can be found on Wiley Online Library http://olabout.wiley.com/WileyCDA/Section/id-410895.html

Other Terms and Conditions:

v1.10 Last updated September 2015

Questions? customercare@copyright.com or +1-855-239-3415 (toll free in the US) or +1-978-646-2777.

TH-1887_136122001

Title: Rainbow Emission from an Atomic Transition in Doped Quantum Dots

Author: Abhijit Hazarika, Anshu Pandey, D. D. Sarma

Publication: Journal of Physical Chemistry Letters

Publisher: American Chemical Society

Date: Jul 1, 2014

PERMISSION/LICENSE IS GRANTED FOR YOUR ORDER AT NO CHARGE

This type of permission/license, instead of the standard Terms & Conditions, is sent to you because no fee is being charged for your order. Please note the following:

- Permission is granted for your request in both print and electronic formats, and translations.
- If figures and/or tables were requested, they may be adapted or used in part.
- Please print this page for your records and send a copy of it to your publisher/graduate school.
- Appropriate credit for the requested material should be given as follows: "Reprinted (adapted) with permission from (COMPLETE REFERENCE CITATION). Copyright (YEAR) American Chemical Society." Insert appropriate information in place of the capitalized words.
- One-time permission is granted only for the use specified in your request. No additional uses are granted (such as derivative works or other editions). For any other uses, please submit a new request.

If credit is given to another source for the material you requested, permission must be obtained from that source.

TH-1887_136122001

Title:	Advances in Light-Emitting Doped Semiconductor Nanocrystals
Author:	Narayan Pradhan, D. D. Sarma
Publication:	Journal of Physical Chemistry Letters
Publisher:	American Chemical Society
Date:	Nov 1, 2011

PERMISSION/LICENSE IS GRANTED FOR YOUR ORDER AT NO CHARGE

This type of permission/license, instead of the standard Terms & Conditions, is sent to you because no fee is being charged for your order. Please note the following:

- Permission is granted for your request in both print and electronic formats, and translations.
- If figures and/or tables were requested, they may be adapted or used in part.
- Please print this page for your records and send a copy of it to your publisher/graduate school.
- Appropriate credit for the requested material should be given as follows: "Reprinted (adapted) with permission from (COMPLETE REFERENCE CITATION). Copyright (YEAR) American Chemical Society." Insert appropriate information in place of the capitalized words.
- One-time permission is granted only for the use specified in your request. No additional uses are granted (such as derivative works or other editions). For any other uses, please submit a new request.

If credit is given to another source for the material you requested, permission must be obtained from that source.

TH-1887_136122001

Title: Tuning the Emission of CdSe Quantum Dots by Controlled Trap Enhancement

Author: David R. Baker, Prashant V. Kamat

Publication: Langmuir

Publisher: American Chemical Society

Date: Jul 1, 2010

PERMISSION/LICENSE IS GRANTED FOR YOUR ORDER AT NO CHARGE

This type of permission/license, instead of the standard Terms & Conditions, is sent to you because no fee is being charged for your order. Please note the following:

- Permission is granted for your request in both print and electronic formats, and translations.
- If figures and/or tables were requested, they may be adapted or used in part.
- Please print this page for your records and send a copy of it to your publisher/graduate school.
- Appropriate credit for the requested material should be given as follows: "Reprinted (adapted) with permission from (COMPLETE REFERENCE CITATION). Copyright (YEAR) American Chemical Society." Insert appropriate information in place of the capitalized words.
- One-time permission is granted only for the use specified in your request. No additional uses are granted (such as derivative works or other editions). For any other uses, please submit a new request.

If credit is given to another source for the material you requested, permission must be obtained from that source.

TH-1887_136122001

Title: Small GSH-Capped CuInS2 Quantum Dots: MPA-Assisted Aqueous Phase Transfer and Bioimaging Applications

Author: Chuanzhen Zhao, Zelong Bai, Xiangyou Liu, et al

Publication: Applied Materials

Publisher: American Chemical Society

Date: Aug 1, 2015

PERMISSION/LICENSE IS GRANTED FOR YOUR ORDER AT NO CHARGE

This type of permission/license, instead of the standard Terms & Conditions, is sent to you because no fee is being charged for your order. Please note the following:

- Permission is granted for your request in both print and electronic formats, and translations.
- If figures and/or tables were requested, they may be adapted or used in part.
- Please print this page for your records and send a copy of it to your publisher/graduate school.
- Appropriate credit for the requested material should be given as follows: "Reprinted (adapted) with permission from (COMPLETE REFERENCE CITATION). Copyright (YEAR) American Chemical Society." Insert appropriate information in place of the capitalized words.
- One-time permission is granted only for the use specified in your request. No additional uses are granted (such as derivative works or other editions). For any other uses, please submit a new request.

If credit is given to another source for the material you requested, permission must be obtained from that source.

TH-1887_136122001

ROYAL SOCIETY OF CHEMISTRY LICENSE TERMS AND CONDITIONS

Jul 20, 2018

This Agreement between Mr. SABYASACHI PRAMANIK ("You") and Royal Society of Chemistry ("Royal Society of Chemistry") consists of your license details and the terms and conditions provided by Royal Society of Chemistry and Copyright Clearance Center.

License Number	4393130838515
License date	Jul 20, 2018
Licensed Content Publisher	Royal Society of Chemistry
Licensed Content Publication	RSC Advances
Licensed Content Title	Enhanced photoluminescence and thermal stability of zinc quinolate following complexation on the surface of quantum dots
Licensed Content Author	Satyapriya Bhandari,Shilaj Roy,Arun Chattopadhyay
Licensed Content Date	May 23, 2014
Licensed Content Volume	4
Licensed Content Issue	46
Type of Use	Thesis/Dissertation
Requestor type	academic/educational
Portion	figures/tables/images
Number of figures/tables/images	2
Format	print and electronic
Distribution quantity	10
Will you be translating?	no
Order reference number	
Title of the thesis/dissertation	Surface Complexation Reaction for White Light Emission from Quantum Dots
Expected completion date	Aug 2018
Estimated size	150
Requestor Location	Mr. SABYASACHI PRAMANIK DEPARTMENT OF CHEMISTRY IIT GUWAHATI GUWAHATI, 781039 India Attn: Mr. SABYASACHI PRAMANIK
Billing Type	Invoice
Billing Address	Mr. SABYASACHI PRAMANIK DEPARTMENT OF CHEMISTRY IIT GUWAHATI GUWAHATI, India 781039 Attn: Mr. SABYASACHI PRAMANIK
Total	**0.00 USD**

Terms and Conditions

This License Agreement is between {Requestor Name} (“You”) and The Royal Society of Chemistry (“RSC”) provided by the Copyright Clearance Center (“CCC”). The license consists of your order details, the terms and conditions provided by the Royal Society of Chemistry, and the payment terms and conditions.

RSC / TERMS AND CONDITIONS

TH-1887_136122001

INTRODUCTION

The publisher for this copyrighted material is The Royal Society of Chemistry. By clicking “accept” in connection with completing this licensing transaction, you agree that the following terms and conditions apply to this transaction (along with the Billing and Payment terms and conditions established by CCC, at the time that you opened your RightsLink account and that are available at any time at .

LICENSE GRANTED

The RSC hereby grants you a non-exclusive license to use the aforementioned material anywhere in the world subject to the terms and conditions indicated herein. Reproduction of the material is confined to the purpose and/or media for which permission is hereby given.

RESERVATION OF RIGHTS

The RSC reserves all rights not specifically granted in the combination of (i) the license details provided by your and accepted in the course of this licensing transaction; (ii) these terms and conditions; and (iii) CCC’s Billing and Payment terms and conditions.

REVOCATION

The RSC reserves the right to revoke this license for any reason, including, but not limited to, advertising and promotional uses of RSC content, third party usage, and incorrect source figure attribution.

THIRD-PARTY MATERIAL DISCLAIMER

If part of the material to be used (for example, a figure) has appeared in the RSC publication with credit to another source, permission must also be sought from that source. If the other source is another RSC publication these details should be included in your RightsLink request. If the other source is a third party, permission must be obtained from the third party. The RSC disclaims any responsibility for the reproduction you make of items owned by a third party.

PAYMENT OF FEE

If the permission fee for the requested material is waived in this instance, please be advised that any future requests for the reproduction of RSC materials may attract a fee.

ACKNOWLEDGEMENT

The reproduction of the licensed material must be accompanied by the following acknowledgement:
Reproduced (“Adapted” or “in part”) from {Reference Citation} (or Ref XX) with permission of The Royal Society of Chemistry.
If the licensed material is being reproduced from New Journal of Chemistry (NJC), Photochemical & Photobiological Sciences (PPS) or Physical Chemistry Chemical Physics (PCCP) you must include one of the following acknowledgements:
For figures originally published in NJC:
Reproduced (“Adapted” or “in part”) from {Reference Citation} (or Ref XX) with permission of The Royal Society of Chemistry (RSC) on behalf of the European Society for Photobiology, the European Photochemistry Association and the RSC.
For figures originally published in PPS:
Reproduced (“Adapted” or “in part”) from {Reference Citation} (or Ref XX) with permission of The Royal Society of Chemistry (RSC) on behalf of the Centre National de la Recherche Scientifique (CNRS) and the RSC.
For figures originally published in PCCP:
Reproduced (“Adapted” or “in part”) from {Reference Citation} (or Ref XX) with permission of the PCCP Owner Societies.

HYPERTEXT LINKS

With any material which is being reproduced in electronic form, you must include a hypertext link to the original RSC article on the RSC’s website. The recommended form for the hyperlink is http://dx.doi.org/10.1039/DOI suffix, for example in the link http://dx.doi.org/10.1039/b110420a the DOI suffix is ‘b110420a’. To find the relevant DOI suffix for the RSC article in question, go to the Journals section of the website and locate the article in the list of papers for the volume and issue of your specific journal. You will find the DOI suffix quoted there.

LICENSE CONTINGENT ON PAYMENT

While you may exercise the rights licensed immediately upon issuance of the license at the end of the licensing process for the transaction, provided that you have disclosed complete and accurate details of your proposed use, no license is finally effective unless and until full payment is received from you (by CCC) as provided in CCC's Billing and Payment terms and conditions. If full payment is not received on a timely basis, then any license preliminarily granted shall be deemed automatically revoked and shall be void as if never granted. Further, in the event that you breach any of these terms and conditions or any of CCC's Billing and Payment terms and conditions, the license is automatically revoked and shall be void as if never granted. Use of materials as described in a revoked license, as well as any use of the materials beyond the scope of an unrevoked license, may constitute copyright infringement and the RSC reserves the right to take any and all action to protect its copyright in the materials.

WARRANTIES

The RSC makes no representations or warranties with respect to the licensed material.

INDEMNITY

You hereby indemnify and agree to hold harmless the RSC and the CCC, and their respective officers, directors, trustees, employees and agents, from and against any and all claims arising out of your use of the licensed material other than as specifically authorized pursuant to this licence.

NO TRANSFER OF LICENSE

This license is personal to you or your publisher and may not be sublicensed, assigned, or transferred by you to any other person without the RSC's written permission.

NO AMENDMENT EXCEPT IN WRITING

This license may not be amended except in a writing signed by both parties (or, in the case of “Other Conditions, v1.2”, by CCC on the RSC's behalf).

OBJECTION TO CONTRARY TERMS

You hereby acknowledge and agree that these terms and conditions, together with CCC's Billing and Payment terms and

conditions (which are incorporated herein), comprise the entire agreement between you and the RSC (and CCC) concerning this licensing transaction, to the exclusion of all other terms and conditions, written or verbal, express or implied (including any terms contained in any purchase order, acknowledgment, check endorsement or other writing prepared by you). In the event of any conflict between your obligations established by these terms and conditions and those established by CCC's Billing and Payment terms and conditions, these terms and conditions shall control.

JURISDICTION

This license transaction shall be governed by and construed in accordance with the laws of the District of Columbia. You hereby agree to submit to the jurisdiction of the courts located in the District of Columbia for purposes of resolving any disputes that may arise in connection with this licensing transaction.

LIMITED LICENSE

The following terms and conditions apply to specific license types:

Translation

This permission is granted for non-exclusive world English rights only unless your license was granted for translation rights. If you licensed translation rights you may only translate this content into the languages you requested. A professional translator must perform all translations and reproduce the content word for word preserving the integrity of the article.

Intranet

If the licensed material is being posted on an Intranet, the Intranet is to be password-protected and made available only to bona fide students or employees only. All content posted to the Intranet must maintain the copyright information line on the bottom of each image. You must also fully reference the material and include a hypertext link as specified above.

Copies of Whole Articles

All copies of whole articles must maintain, if available, the copyright information line on the bottom of each page.

Other Conditions

v1.2

Gratis licenses (referencing $0 in the Total field) are free. Please retain this printable license for your reference. No payment is required.

If you would like to pay for this license now, please remit this license along with yourpayment made payable to "COPYRIGHT CLEARANCE CENTER" otherwise you will be invoiced within 48 hours of the license date. Payment should be in the form of a check or money order referencing your account number and this invoice number {Invoice Number}.

Once you receive your invoice for this order, you may pay your invoice by credit card.

Please follow instructions provided at that time.

Make Payment To:

Copyright Clearance Center

29118 Network Place

Chicago, IL 60673-1291

For suggestions or comments regarding this order, contact Rightslink Customer Support: customercare@copyright.com or +1-855-239-3415 (toll free in the US) or +1-978-646-2777.

Questions? customercare@copyright.com or +1-855-239-3415 (toll free in the US) or +1-978-646-2777.

TH-1887_136122001

Title: Surface Complexation Reaction for Phase Transfer of Hydrophobic Quantum Dot from Nonpolar to Polar Medium

Author: Satyapriya Bhandari, Shilaj Roy, Sabyasachi Pramanik, et al

Publication: Langmuir

Publisher: American Chemical Society

Date: Sep 1, 2014

PERMISSION/LICENSE IS GRANTED FOR YOUR ORDER AT NO CHARGE

This type of permission/license, instead of the standard Terms & Conditions, is sent to you because no fee is being charged for your order. Please note the following:

- Permission is granted for your request in both print and electronic formats, and translations.
- If figures and/or tables were requested, they may be adapted or used in part.
- Please print this page for your records and send a copy of it to your publisher/graduate school.
- Appropriate credit for the requested material should be given as follows: "Reprinted (adapted) with permission from (COMPLETE REFERENCE CITATION). Copyright (YEAR) American Chemical Society." Insert appropriate information in place of the capitalized words.
- One-time permission is granted only for the use specified in your request. No additional uses are granted (such as derivative works or other editions). For any other uses, please submit a new request.

If credit is given to another source for the material you requested, permission must be obtained from that source.

TH-1887_136122001

Title: Double Channel Emission from a Redox Active Single Component Quantum Dot Complex

Author: Satyapriya Bhandari, Shilaj Roy, Sabyasachi Pramanik, et al

Publication: Langmuir

Publisher: American Chemical Society

Date: Jan 1, 2015

PERMISSION/LICENSE IS GRANTED FOR YOUR ORDER AT NO CHARGE

This type of permission/license, instead of the standard Terms & Conditions, is sent to you because no fee is being charged for your order. Please note the following:

- Permission is granted for your request in both print and electronic formats, and translations.
- If figures and/or tables were requested, they may be adapted or used in part.
- Please print this page for your records and send a copy of it to your publisher/graduate school.
- Appropriate credit for the requested material should be given as follows: "Reprinted (adapted) with permission from (COMPLETE REFERENCE CITATION). Copyright (YEAR) American Chemical Society." Insert appropriate information in place of the capitalized words.
- One-time permission is granted only for the use specified in your request. No additional uses are granted (such as derivative works or other editions). For any other uses, please submit a new request.

If credit is given to another source for the material you requested, permission must be obtained from that source.

TH-1887_136122001

AIP PUBLISHING LICENSE TERMS AND CONDITIONS

Jul 21, 2018

This Agreement between Mr. SABYASACHI PRAMANIK ("You") and AIP Publishing ("AIP Publishing") consists of your license details and the terms and conditions provided by AIP Publishing and Copyright Clearance Center.

License Number	4393460864760
License date	Jul 21, 2018
Licensed Content Publisher	AIP Publishing
Licensed Content Publication	Applied Physics Letters
Licensed Content Title	High color rendering index white light emitting diodes fabricated from a combination of carbon dots and zinc copper indium sulfide quantum dots
Licensed Content Author	Chun Sun, Yu Zhang, Yu Wang, et al
Licensed Content Date	Jun 30, 2014
Licensed Content Volume	104
Licensed Content Issue	26
Type of Use	Thesis/Dissertation
Requestor type	Student
Format	Print and electronic
Portion	Figure/Table
Number of figures/tables	1
Title of your thesis / dissertation	Surface Complexation Reaction for White Light Emission from Quantum Dots
Expected completion date	Aug 2018
Estimated size (number of pages)	150
Requestor Location	Mr. SABYASACHI PRAMANIK DEPARTMENT OF CHEMISTRY IIT GUWAHATI GUWAHATI, 781039 India Attn: Mr. SABYASACHI PRAMANIK
Billing Type	Invoice
Billing Address	Mr. SABYASACHI PRAMANIK DEPARTMENT OF CHEMISTRY IIT GUWAHATI GUWAHATI, India 781039 Attn: Mr. SABYASACHI PRAMANIK
Total	0.00 USD

Terms and Conditions

AIP Publishing -- Terms and Conditions: Permissions Uses

AIP Publishing hereby grants to you the non-exclusive right and license to use and/or distribute the Material according to the use specified in your order, on a one-time basis, for the specified term, with a maximum distribution equal to the number that you have ordered. Any links or other content accompanying the Material are not the subject of this license.

TH-1887_136122001

1. You agree to include the following copyright and permission notice with the reproduction of the Material:"Reprinted from [FULL CITATION], with the permission of AIP Publishing." For an article, the credit line and permission notice must be printed on the first page of the article or book chapter. For photographs, covers, or tables, the notice may appear with the Material, in a footnote, or in the reference list.
2. If you have licensed reuse of a figure, photograph, cover, or table, it is your responsibility to ensure that the material is original to AIP Publishing and does not contain the copyright of another entity, and that the copyright notice of the figure, photograph, cover, or table does not indicate that it was reprinted by AIP Publishing, with permission, from another source. Under no circumstances does AIP Publishing purport or intend to grant permission to reuse material to which it does not hold appropriate rights.
   You may not alter or modify the Material in any manner. You may translate the Material into another language only if you have licensed translation rights. You may not use the Material for promotional purposes.
3. The foregoing license shall not take effect unless and until AIP Publishing or its agent, Copyright Clearance Center, receives the Payment in accordance with Copyright Clearance Center Billing and Payment Terms and Conditions, which are incorporated herein by reference.
4. AIP Publishing or Copyright Clearance Center may, within two business days of granting this license, revoke the license for any reason whatsoever, with a full refund payable to you. Should you violate the terms of this license at any time, AIP Publishing, or Copyright Clearance Center may revoke the license with no refund to you. Notice of such revocation will be made using the contact information provided by you. Failure to receive such notice will not nullify the revocation.
5. AIP Publishing makes no representations or warranties with respect to the Material. You agree to indemnify and hold harmless AIP Publishing, and their officers, directors, employees or agents from and against any and all claims arising out of your use of the Material other than as specifically authorized herein.
6. The permission granted herein is personal to you and is not transferable or assignable without the prior written permission of AIP Publishing. This license may not be amended except in a writing signed by the party to be charged.
7. If purchase orders, acknowledgments or check endorsements are issued on any forms containing terms and conditions which are inconsistent with these provisions, such inconsistent terms and conditions shall be of no force and effect. This document, including the CCC Billing and Payment Terms and Conditions, shall be the entire agreement between the parties relating to the subject matter hereof.

This Agreement shall be governed by and construed in accordance with the laws of the State of New York. Both parties hereby submit to the jurisdiction of the courts of New York County for purposes of resolving any disputes that may arise hereunder.

V1.2

Questions? customercare@copyright.com or +1-855-239-3415 (toll free in the US) or +1-978-646-2777.

TH-1887_136122001

JOHN WILEY AND SONS LICENSE TERMS AND CONDITIONS

Jul 21, 2018

This Agreement between Mr. SABYASACHI PRAMANIK ("You") and John Wiley and Sons ("John Wiley and Sons") consists of your license details and the terms and conditions provided by John Wiley and Sons and Copyright Clearance Center.

License Number	4393461185299
License date	Jul 21, 2018
Licensed Content Publisher	John Wiley and Sons
Licensed Content Publication	Angewandte Chemie
Licensed Content Title	Bright White-Light Emitting Manganese and Copper Co-Doped ZnSe Quantum Dots
Licensed Content Author	Subhendu K. Panda, Stephen G. Hickey, Hilmi Volkan Demir, et al
Licensed Content Date	Apr 7, 2011
Licensed Content Volume	123
Licensed Content Issue	19
Licensed Content Pages	5
Type of Use	Dissertation/Thesis
Requestor type	University/Academic
Format	Print and electronic
Portion	Figure/table
Number of figures/tables	1
Original Wiley figure/table number(s)	Figure 3
Will you be translating?	No
Title of your thesis / dissertation	Surface Complexation Reaction for White Light Emission from Quantum Dots
Expected completion date	Aug 2018
Expected size (number of pages)	150
Requestor Location	Mr. SABYASACHI PRAMANIK DEPARTMENT OF CHEMISTRY IIT GUWAHATI GUWAHATI, 781039 India Attn: Mr. SABYASACHI PRAMANIK
Publisher Tax ID	EU826007151
Total	**0.00 USD**
Terms and Conditions	

TERMS AND CONDITIONS

This copyrighted material is owned by or exclusively licensed to John Wiley & Sons, Inc. or one of its group companies (each a"Wiley Company") or handled on behalf of a society with which a Wiley Company has exclusive publishing rights in relation to a particular work (collectively "WILEY"). By clicking "accept" in connection with completing this licensing transaction, you agree that the following terms and conditions apply to this transaction (along with the billing and payment terms and conditions established by the Copyright Clearance Center Inc., ("CCC's Billing and Payment terms and conditions"), at the time that you opened your RightsLink account (these are available at any time at http://myaccount.copyright.com).

Terms and Conditions

- The materials you have requested permission to reproduce or reuse (the "Wiley Materials") are protected by copyright.

TH-1887_136122001

- You are hereby granted a personal, non-exclusive, non-sub licensable (on a stand-alone basis), non-transferable, worldwide, limited license to reproduce the Wiley Materials for the purpose specified in the licensing process. This license, **and any CONTENT (PDF or image file) purchased as part of your order,** is for a one-time use only and limited to any maximum distribution number specified in the license. The first instance of republication or reuse granted by this license must be completed within two years of the date of the grant of this license (although copies prepared before the end date may be distributed thereafter). The Wiley Materials shall not be used in any other manner or for any other purpose, beyond what is granted in the license. Permission is granted subject to an appropriate acknowledgement given to the author, title of the material/book/journal and the publisher. You shall also duplicate the copyright notice that appears in the Wiley publication in your use of the Wiley Material. Permission is also granted on the understanding that nowhere in the text is a previously published source acknowledged for all or part of this Wiley Material. Any third party content is expressly excluded from this permission.

- With respect to the Wiley Materials, all rights are reserved. Except as expressly granted by the terms of the license, no part of the Wiley Materials may be copied, modified, adapted (except for minor reformatting required by the new Publication), translated, reproduced, transferred or distributed, in any form or by any means, and no derivative works may be made based on the Wiley Materials without the prior permission of the respective copyright owner.**For STM Signatory Publishers clearing permission under the terms of the STM Permissions Guidelines only, the terms of the license are extended to include subsequent editions and for editions in other languages, provided such editions are for the work as a whole in situ and does not involve the separate exploitation of the permitted figures or extracts,** You may not alter, remove or suppress in any manner any copyright, trademark or other notices displayed by the Wiley Materials. You may not license, rent, sell, loan, lease, pledge, offer as security, transfer or assign the Wiley Materials on a stand-alone basis, or any of the rights granted to you hereunder to any other person.

- The Wiley Materials and all of the intellectual property rights therein shall at all times remain the exclusive property of John Wiley & Sons Inc, the Wiley Companies, or their respective licensors, and your interest therein is only that of having possession of and the right to reproduce the Wiley Materials pursuant to Section 2 herein during the continuance of this Agreement. You agree that you own no right, title or interest in or to the Wiley Materials or any of the intellectual property rights therein. You shall have no rights hereunder other than the license as provided for above in Section 2. No right, license or interest to any trademark, trade name, service mark or other branding ("Marks") of WILEY or its licensors is granted hereunder, and you agree that you shall not assert any such right, license or interest with respect thereto

- NEITHER WILEY NOR ITS LICENSORS MAKES ANY WARRANTY OR REPRESENTATION OF ANY KIND TO YOU OR ANY THIRD PARTY, EXPRESS, IMPLIED OR STATUTORY, WITH RESPECT TO THE MATERIALS OR THE ACCURACY OF ANY INFORMATION CONTAINED IN THE MATERIALS, INCLUDING, WITHOUT LIMITATION, ANY IMPLIED WARRANTY OF MERCHANTABILITY, ACCURACY, SATISFACTORY QUALITY, FITNESS FOR A PARTICULAR PURPOSE, USABILITY, INTEGRATION OR NON-INFRINGEMENT AND ALL SUCH WARRANTIES ARE HEREBY EXCLUDED BY WILEY AND ITS LICENSORS AND WAIVED BY YOU.

- WILEY shall have the right to terminate this Agreement immediately upon breach of this Agreement by you.

- You shall indemnify, defend and hold harmless WILEY, its Licensors and their respective directors, officers, agents and employees, from and against any actual or threatened claims, demands, causes of action or proceedings arising from any breach of this Agreement by you.

- IN NO EVENT SHALL WILEY OR ITS LICENSORS BE LIABLE TO YOU OR ANY OTHER PARTY OR ANY OTHER PERSON OR ENTITY FOR ANY SPECIAL, CONSEQUENTIAL, INCIDENTAL, INDIRECT, EXEMPLARY OR PUNITIVE DAMAGES, HOWEVER CAUSED, ARISING OUT OF OR IN CONNECTION WITH THE DOWNLOADING, PROVISIONING, VIEWING OR USE OF THE MATERIALS REGARDLESS OF THE FORM OF ACTION, WHETHER FOR BREACH OF CONTRACT, BREACH OF WARRANTY, TORT, NEGLIGENCE, INFRINGEMENT OR OTHERWISE (INCLUDING, WITHOUT LIMITATION, DAMAGES BASED ON LOSS OF PROFITS, DATA, FILES, USE, BUSINESS OPPORTUNITY OR CLAIMS OF THIRD PARTIES), AND WHETHER OR NOT THE PARTY HAS BEEN ADVISED OF THE POSSIBILITY OF SUCH DAMAGES. THIS LIMITATION SHALL APPLY NOTWITHSTANDING ANY FAILURE OF ESSENTIAL PURPOSE OF ANY LIMITED REMEDY PROVIDED HEREIN.

- Should any provision of this Agreement be held by a court of competent jurisdiction to be illegal, invalid, or unenforceable, that provision shall be deemed amended to achieve as nearly as possible the same economic effect as the original provision, and the legality, validity and enforceability of the remaining provisions of this Agreement shall not be affected or impaired thereby.

- The failure of either party to enforce any term or condition of this Agreement shall not constitute a waiver of either party's right to enforce each and every term and condition of this Agreement. No breach under this agreement shall be deemed waived or excused by either party unless such waiver or consent is in writing signed by the party granting such waiver or consent. The waiver by or consent of a party to a breach of any provision of this Agreement shall not operate or be construed as a waiver of or consent to any other or subsequent breach by such other party.

TH-1887_136122001

- This Agreement may not be assigned (including by operation of law or otherwise) by you without WILEY's prior written consent.
- Any fee required for this permission shall be non-refundable after thirty (30) days from receipt by the CCC.
- These terms and conditions together with CCC's Billing and Payment terms and conditions (which are incorporated herein) form the entire agreement between you and WILEY concerning this licensing transaction and (in the absence of fraud) supersedes all prior agreements and representations of the parties, oral or written. This Agreement may not be amended except in writing signed by both parties. This Agreement shall be binding upon and inure to the benefit of the parties' successors, legal representatives, and authorized assigns.
- In the event of any conflict between your obligations established by these terms and conditions and those established by CCC's Billing and Payment terms and conditions, these terms and conditions shall prevail.
- WILEY expressly reserves all rights not specifically granted in the combination of (i) the license details provided by you and accepted in the course of this licensing transaction, (ii) these terms and conditions and (iii) CCC's Billing and Payment terms and conditions.
- This Agreement will be void if the Type of Use, Format, Circulation, or Requestor Type was misrepresented during the licensing process.
- This Agreement shall be governed by and construed in accordance with the laws of the State of New York, USA, without regards to such state's conflict of law rules. Any legal action, suit or proceeding arising out of or relating to these Terms and Conditions or the breach thereof shall be instituted in a court of competent jurisdiction in New York County in the State of New York in the United States of America and each party hereby consents and submits to the personal jurisdiction of such court, waives any objection to venue in such court and consents to service of process by registered or certified mail, return receipt requested, at the last known address of such party.

WILEY OPEN ACCESS TERMS AND CONDITIONS

Wiley Publishes Open Access Articles in fully Open Access Journals and in Subscription journals offering Online Open. Although most of the fully Open Access journals publish open access articles under the terms of the Creative Commons Attribution (CC BY) License only, the subscription journals and a few of the Open Access Journals offer a choice of Creative Commons Licenses. The license type is clearly identified on the article.

The Creative Commons Attribution License

The Creative Commons Attribution License (CC-BY) allows users to copy, distribute and transmit an article, adapt the article and make commercial use of the article. The CC-BY license permits commercial and non-

Creative Commons Attribution Non-Commercial License

The Creative Commons Attribution Non-Commercial (CC-BY-NC)License permits use, distribution and reproduction in any medium, provided the original work is properly cited and is not used for commercial purposes.(see below)

Creative Commons Attribution-Non-Commercial-NoDerivs License

The Creative Commons Attribution Non-Commercial-NoDerivs License (CC-BY-NC-ND) permits use, distribution and reproduction in any medium, provided the original work is properly cited, is not used for commercial purposes and no modifications or adaptations are made. (see below)

Use by commercial "for-profit" organizations

Use of Wiley Open Access articles for commercial, promotional, or marketing purposes requires further explicit permission from Wiley and will be subject to a fee.

Further details can be found on Wiley Online Library http://olabout.wiley.com/WileyCDA/Section/id-410895.html

Other Terms and Conditions:

v1.10 Last updated September 2015

Questions? customercare@copyright.com or +1-855-239-3415 (toll free in the US) or +1-978-646-2777.

TH-1887_136122001

ROYAL SOCIETY OF CHEMISTRY LICENSE TERMS AND CONDITIONS

Jul 21, 2018

This Agreement between Mr. SABYASACHI PRAMANIK ("You") and Royal Society of Chemistry ("Royal Society of Chemistry") consists of your license details and the terms and conditions provided by Royal Society of Chemistry and Copyright Clearance Center.

License Number	4393470834304
License date	Jul 21, 2018
Licensed Content Publisher	Royal Society of Chemistry
Licensed Content Publication	Journal of Materials Chemistry C
Licensed Content Title	Single white light emitting hybrid nanoarchitectures based on functionalized quantum dots
Licensed Content Author	Elisabetta Fanizza,Carmine Urso,Vita Pinto,Antonio Cardone,Roberta Ragni,Nicoletta Depalo,M. Lucia Curri,Angela Agostiano,Gianluca M. Farinola,Marinella Striccoli
Licensed Content Date	Apr 25, 2014
Licensed Content Volume	2
Licensed Content Issue	27
Type of Use	Thesis/Dissertation
Requestor type	academic/educational
Portion	figures/tables/images
Number of figures/tables/images	1
Format	print and electronic
Distribution quantity	10
Will you be translating?	no
Order reference number	
Title of the thesis/dissertation	Surface Complexation Reaction for White Light Emission from Quantum Dots
Expected completion date	Aug 2018
Estimated size	150
Requestor Location	Mr. SABYASACHI PRAMANIK DEPARTMENT OF CHEMISTRY IIT GUWAHATI GUWAHATI, 781039 India Attn: Mr. SABYASACHI PRAMANIK
Billing Type	Invoice
Billing Address	Mr. SABYASACHI PRAMANIK DEPARTMENT OF CHEMISTRY IIT GUWAHATI GUWAHATI, India 781039 Attn: Mr. SABYASACHI PRAMANIK
Total	**0.00 USD**

Terms and Conditions

This License Agreement is between {Requestor Name} (“You”) and The Royal Society of Chemistry (“RSC”) provided by the Copyright Clearance Center (“CCC”). The license consists of your order details, the terms and conditions provided by the Royal Society of Chemistry, and the payment terms and conditions.

RSC / TERMS AND CONDITIONS

TH-1887_136122001

INTRODUCTION

The publisher for this copyrighted material is The Royal Society of Chemistry. By clicking “accept” in connection with completing this licensing transaction, you agree that the following terms and conditions apply to this transaction (along with the Billing and Payment terms and conditions established by CCC, at the time that you opened your RightsLink account and that are available at any time at .

LICENSE GRANTED

The RSC hereby grants you a non-exclusive license to use the aforementioned material anywhere in the world subject to the terms and conditions indicated herein. Reproduction of the material is confined to the purpose and/or media for which permission is hereby given.

RESERVATION OF RIGHTS

The RSC reserves all rights not specifically granted in the combination of (i) the license details provided by your and accepted in the course of this licensing transaction; (ii) these terms and conditions; and (iii) CCC’s Billing and Payment terms and conditions.

REVOCATION

The RSC reserves the right to revoke this license for any reason, including, but not limited to, advertising and promotional uses of RSC content, third party usage, and incorrect source figure attribution.

THIRD-PARTY MATERIAL DISCLAIMER

If part of the material to be used (for example, a figure) has appeared in the RSC publication with credit to another source, permission must also be sought from that source. If the other source is another RSC publication these details should be included in your RightsLink request. If the other source is a third party, permission must be obtained from the third party. The RSC disclaims any responsibility for the reproduction you make of items owned by a third party.

PAYMENT OF FEE

If the permission fee for the requested material is waived in this instance, please be advised that any future requests for the reproduction of RSC materials may attract a fee.

ACKNOWLEDGEMENT

The reproduction of the licensed material must be accompanied by the following acknowledgement:
Reproduced (“Adapted” or “in part”) from {Reference Citation} (or Ref XX) with permission of The Royal Society of Chemistry.
If the licensed material is being reproduced from New Journal of Chemistry (NJC), Photochemical & Photobiological Sciences (PPS) or Physical Chemistry Chemical Physics (PCCP) you must include one of the following acknowledgements:
For figures originally published in NJC:
Reproduced (“Adapted” or “in part”) from {Reference Citation} (or Ref XX) with permission of The Royal Society of Chemistry (RSC) on behalf of the European Society for Photobiology, the European Photochemistry Association and the RSC.
For figures originally published in PPS:
Reproduced (“Adapted” or “in part”) from {Reference Citation} (or Ref XX) with permission of The Royal Society of Chemistry (RSC) on behalf of the Centre National de la Recherche Scientifique (CNRS) and the RSC.
For figures originally published in PCCP:
Reproduced (“Adapted” or “in part”) from {Reference Citation} (or Ref XX) with permission of the PCCP Owner Societies.

HYPERTEXT LINKS

With any material which is being reproduced in electronic form, you must include a hypertext link to the original RSC article on the RSC’s website. The recommended form for the hyperlink is http://dx.doi.org/10.1039/DOI suffix, for example in the link http://dx.doi.org/10.1039/b110420a the DOI suffix is ‘b110420a’. To find the relevant DOI suffix for the RSC article in question, go to the Journals section of the website and locate the article in the list of papers for the volume and issue of your specific journal. You will find the DOI suffix quoted there.

LICENSE CONTINGENT ON PAYMENT

While you may exercise the rights licensed immediately upon issuance of the license at the end of the licensing process for the transaction, provided that you have disclosed complete and accurate details of your proposed use, no license is finally effective unless and until full payment is received from you (by CCC) as provided in CCC's Billing and Payment terms and conditions. If full payment is not received on a timely basis, then any license preliminarily granted shall be deemed automatically revoked and shall be void as if never granted. Further, in the event that you breach any of these terms and conditions or any of CCC's Billing and Payment terms and conditions, the license is automatically revoked and shall be void as if never granted. Use of materials as described in a revoked license, as well as any use of the materials beyond the scope of an unrevoked license, may constitute copyright infringement and the RSC reserves the right to take any and all action to protect its copyright in the materials.

WARRANTIES

The RSC makes no representations or warranties with respect to the licensed material.

INDEMNITY

You hereby indemnify and agree to hold harmless the RSC and the CCC, and their respective officers, directors, trustees, employees and agents, from and against any and all claims arising out of your use of the licensed material other than as specifically authorized pursuant to this licence.

NO TRANSFER OF LICENSE

This license is personal to you or your publisher and may not be sublicensed, assigned, or transferred by you to any other person without the RSC's written permission.

NO AMENDMENT EXCEPT IN WRITING

This license may not be amended except in a writing signed by both parties (or, in the case of “Other Conditions, v1.2”, by CCC on the RSC's behalf).

OBJECTION TO CONTRARY TERMS

You hereby acknowledge and agree that these terms and conditions, together with CCC's Billing and Payment terms and

conditions (which are incorporated herein), comprise the entire agreement between you and the RSC (and CCC) concerning this licensing transaction, to the exclusion of all other terms and conditions, written or verbal, express or implied (including any terms contained in any purchase order, acknowledgment, check endorsement or other writing prepared by you). In the event of any conflict between your obligations established by these terms and conditions and those established by CCC's Billing and Payment terms and conditions, these terms and conditions shall control.

JURISDICTION

This license transaction shall be governed by and construed in accordance with the laws of the District of Columbia. You hereby agree to submit to the jurisdiction of the courts located in the District of Columbia for purposes of resolving any disputes that may arise in connection with this licensing transaction.

LIMITED LICENSE

The following terms and conditions apply to specific license types:

Translation

This permission is granted for non-exclusive world English rights only unless your license was granted for translation rights. If you licensed translation rights you may only translate this content into the languages you requested. A professional translator must perform all translations and reproduce the content word for word preserving the integrity of the article.

Intranet

If the licensed material is being posted on an Intranet, the Intranet is to be password-protected and made available only to bona fide students or employees only. All content posted to the Intranet must maintain the copyright information line on the bottom of each image. You must also fully reference the material and include a hypertext link as specified above.

Copies of Whole Articles

All copies of whole articles must maintain, if available, the copyright information line on the bottom of each page.

Other Conditions

v1.2

Gratis licenses (referencing $0 in the Total field) are free. Please retain this printable license for your reference. No payment is required.

If you would like to pay for this license now, please remit this license along with yourpayment made payable to "COPYRIGHT CLEARANCE CENTER" otherwise you will be invoiced within 48 hours of the license date. Payment should be in the form of a check or money order referencing your account number and this invoice number {Invoice Number}.

Once you receive your invoice for this order, you may pay your invoice by credit card.

Please follow instructions provided at that time.

Make Payment To:

Copyright Clearance Center

29118 Network Place

Chicago, IL 60673-1291

For suggestions or comments regarding this order, contact Rightslink Customer Support: customercare@copyright.com or +1-855-239-3415 (toll free in the US) or +1-978-646-2777.

Questions? customercare@copyright.com or +1-855-239-3415 (toll free in the US) or +1-978-646-2777.

TH-1887_136122001

Title: White-Light Emission from Magic-Sized Cadmium Selenide Nanocrystals

Author: Michael J. Bowers, James R. McBride, Sandra J. Rosenthal

Publication: Journal of the American Chemical Society

Publisher: American Chemical Society

Date: Nov 1, 2005

PERMISSION/LICENSE IS GRANTED FOR YOUR ORDER AT NO CHARGE

This type of permission/license, instead of the standard Terms & Conditions, is sent to you because no fee is being charged for your order. Please note the following:

- Permission is granted for your request in both print and electronic formats, and translations.
- If figures and/or tables were requested, they may be adapted or used in part.
- Please print this page for your records and send a copy of it to your publisher/graduate school.
- Appropriate credit for the requested material should be given as follows: "Reprinted (adapted) with permission from (COMPLETE REFERENCE CITATION). Copyright (YEAR) American Chemical Society." Insert appropriate information in place of the capitalized words.
- One-time permission is granted only for the use specified in your request. No additional uses are granted (such as derivative works or other editions). For any other uses, please submit a new request.

If credit is given to another source for the material you requested, permission must be obtained from that source.

BACK CLOSE WINDOW

TH-1887_136122001

ROYAL SOCIETY OF CHEMISTRY LICENSE TERMS AND CONDITIONS

Jul 21, 2018

This Agreement between Mr. SABYASACHI PRAMANIK ("You") and Royal Society of Chemistry ("Royal Society of Chemistry") consists of your license details and the terms and conditions provided by Royal Society of Chemistry and Copyright Clearance Center.

License Number	4393471052852
License date	Jul 21, 2018
Licensed Content Publisher	Royal Society of Chemistry
Licensed Content Publication	Nanoscale
Licensed Content Title	Composition-dependent trap distributions in CdSe and InP quantum dots probed using photoluminescence blinking dynamics
Licensed Content Author	Heejae Chung,Kyung-Sang Cho,Weon-Kyu Koh,Dongho Kim,Jiwon Kim
Licensed Content Date	May 23, 2016
Licensed Content Volume	8
Licensed Content Issue	29
Type of Use	Thesis/Dissertation
Requestor type	academic/educational
Portion	figures/tables/images
Number of figures/tables/images	1
Format	print and electronic
Distribution quantity	10
Will you be translating?	no
Order reference number	
Title of the thesis/dissertation	Surface Complexation Reaction for White Light Emission from Quantum Dots
Expected completion date	Aug 2018
Estimated size	150
Requestor Location	Mr. SABYASACHI PRAMANIK DEPARTMENT OF CHEMISTRY IIT GUWAHATI GUWAHATI, 781039 India Attn: Mr. SABYASACHI PRAMANIK
Billing Type	Invoice
Billing Address	Mr. SABYASACHI PRAMANIK DEPARTMENT OF CHEMISTRY IIT GUWAHATI GUWAHATI, India 781039 Attn: Mr. SABYASACHI PRAMANIK
Total	**0.00 USD**

Terms and Conditions

This License Agreement is between {Requestor Name} (“You”) and The Royal Society of Chemistry (“RSC”) provided by the Copyright Clearance Center (“CCC”). The license consists of your order details, the terms and conditions provided by the Royal Society of Chemistry, and the payment terms and conditions.

RSC / TERMS AND CONDITIONS

TH-1887_136122001

INTRODUCTION

The publisher for this copyrighted material is The Royal Society of Chemistry. By clicking “accept” in connection with completing this licensing transaction, you agree that the following terms and conditions apply to this transaction (along with the Billing and Payment terms and conditions established by CCC, at the time that you opened your RightsLink account and that are available at any time at .

LICENSE GRANTED

The RSC hereby grants you a non-exclusive license to use the aforementioned material anywhere in the world subject to the terms and conditions indicated herein. Reproduction of the material is confined to the purpose and/or media for which permission is hereby given.

RESERVATION OF RIGHTS

The RSC reserves all rights not specifically granted in the combination of (i) the license details provided by your and accepted in the course of this licensing transaction; (ii) these terms and conditions; and (iii) CCC’s Billing and Payment terms and conditions.

REVOCATION

The RSC reserves the right to revoke this license for any reason, including, but not limited to, advertising and promotional uses of RSC content, third party usage, and incorrect source figure attribution.

THIRD-PARTY MATERIAL DISCLAIMER

If part of the material to be used (for example, a figure) has appeared in the RSC publication with credit to another source, permission must also be sought from that source. If the other source is another RSC publication these details should be included in your RightsLink request. If the other source is a third party, permission must be obtained from the third party. The RSC disclaims any responsibility for the reproduction you make of items owned by a third party.

PAYMENT OF FEE

If the permission fee for the requested material is waived in this instance, please be advised that any future requests for the reproduction of RSC materials may attract a fee.

ACKNOWLEDGEMENT

The reproduction of the licensed material must be accompanied by the following acknowledgement:
Reproduced (“Adapted” or “in part”) from {Reference Citation} (or Ref XX) with permission of The Royal Society of Chemistry.
If the licensed material is being reproduced from New Journal of Chemistry (NJC), Photochemical & Photobiological Sciences (PPS) or Physical Chemistry Chemical Physics (PCCP) you must include one of the following acknowledgements:
For figures originally published in NJC:
Reproduced (“Adapted” or “in part”) from {Reference Citation} (or Ref XX) with permission of The Royal Society of Chemistry (RSC) on behalf of the European Society for Photobiology, the European Photochemistry Association and the RSC.
For figures originally published in PPS:
Reproduced (“Adapted” or “in part”) from {Reference Citation} (or Ref XX) with permission of The Royal Society of Chemistry (RSC) on behalf of the Centre National de la Recherche Scientifique (CNRS) and the RSC.
For figures originally published in PCCP:
Reproduced (“Adapted” or “in part”) from {Reference Citation} (or Ref XX) with permission of the PCCP Owner Societies.

HYPERTEXT LINKS

With any material which is being reproduced in electronic form, you must include a hypertext link to the original RSC article on the RSC’s website. The recommended form for the hyperlink is http://dx.doi.org/10.1039/DOI suffix, for example in the link http://dx.doi.org/10.1039/b110420a the DOI suffix is ‘b110420a’. To find the relevant DOI suffix for the RSC article in question, go to the Journals section of the website and locate the article in the list of papers for the volume and issue of your specific journal. You will find the DOI suffix quoted there.

LICENSE CONTINGENT ON PAYMENT

While you may exercise the rights licensed immediately upon issuance of the license at the end of the licensing process for the transaction, provided that you have disclosed complete and accurate details of your proposed use, no license is finally effective unless and until full payment is received from you (by CCC) as provided in CCC's Billing and Payment terms and conditions. If full payment is not received on a timely basis, then any license preliminarily granted shall be deemed automatically revoked and shall be void as if never granted. Further, in the event that you breach any of these terms and conditions or any of CCC's Billing and Payment terms and conditions, the license is automatically revoked and shall be void as if never granted. Use of materials as described in a revoked license, as well as any use of the materials beyond the scope of an unrevoked license, may constitute copyright infringement and the RSC reserves the right to take any and all action to protect its copyright in the materials.

WARRANTIES

The RSC makes no representations or warranties with respect to the licensed material.

INDEMNITY

You hereby indemnify and agree to hold harmless the RSC and the CCC, and their respective officers, directors, trustees, employees and agents, from and against any and all claims arising out of your use of the licensed material other than as specifically authorized pursuant to this licence.

NO TRANSFER OF LICENSE

This license is personal to you or your publisher and may not be sublicensed, assigned, or transferred by you to any other person without the RSC's written permission.

NO AMENDMENT EXCEPT IN WRITING

This license may not be amended except in a writing signed by both parties (or, in the case of “Other Conditions, v1.2”, by CCC on the RSC's behalf).

OBJECTION TO CONTRARY TERMS

You hereby acknowledge and agree that these terms and conditions, together with CCC's Billing and Payment terms and

conditions (which are incorporated herein), comprise the entire agreement between you and the RSC (and CCC) concerning this licensing transaction, to the exclusion of all other terms and conditions, written or verbal, express or implied (including any terms contained in any purchase order, acknowledgment, check endorsement or other writing prepared by you). In the event of any conflict between your obligations established by these terms and conditions and those established by CCC's Billing and Payment terms and conditions, these terms and conditions shall control.

JURISDICTION

This license transaction shall be governed by and construed in accordance with the laws of the District of Columbia. You hereby agree to submit to the jurisdiction of the courts located in the District of Columbia for purposes of resolving any disputes that may arise in connection with this licensing transaction.

LIMITED LICENSE

The following terms and conditions apply to specific license types:

Translation

This permission is granted for non-exclusive world English rights only unless your license was granted for translation rights. If you licensed translation rights you may only translate this content into the languages you requested. A professional translator must perform all translations and reproduce the content word for word preserving the integrity of the article.

Intranet

If the licensed material is being posted on an Intranet, the Intranet is to be password-protected and made available only to bona fide students or employees only. All content posted to the Intranet must maintain the copyright information line on the bottom of each image. You must also fully reference the material and include a hypertext link as specified above.

Copies of Whole Articles

All copies of whole articles must maintain, if available, the copyright information line on the bottom of each page.

Other Conditions

v1.2

Gratis licenses (referencing $0 in the Total field) are free. Please retain this printable license for your reference. No payment is required.

If you would like to pay for this license now, please remit this license along with yourpayment made payable to "COPYRIGHT CLEARANCE CENTER" otherwise you will be invoiced within 48 hours of the license date. Payment should be in the form of a check or money order referencing your account number and this invoice number {Invoice Number}.

Once you receive your invoice for this order, you may pay your invoice by credit card.

Please follow instructions provided at that time.

Make Payment To:

Copyright Clearance Center

29118 Network Place

Chicago, IL 60673-1291

For suggestions or comments regarding this order, contact Rightslink Customer Support: customercare@copyright.com or +1-855-239-3415 (toll free in the US) or +1-978-646-2777.

Questions? customercare@copyright.com or +1-855-239-3415 (toll free in the US) or +1-978-646-2777.

TH-1887_136122001

Title:	Synchronous Tricolor Emission-Based White Light from Quantum Dot Complex
Author:	Sabyasachi Pramanik, Satyapriya Bhandari, Shilaj Roy, et al
Publication:	Journal of Physical Chemistry Letters
Publisher:	American Chemical Society
Date:	Apr 1, 2015

PERMISSION/LICENSE IS GRANTED FOR YOUR ORDER AT NO CHARGE

This type of permission/license, instead of the standard Terms & Conditions, is sent to you because no fee is being charged for your order. Please note the following:

- Permission is granted for your request in both print and electronic formats, and translations.
- If figures and/or tables were requested, they may be adapted or used in part.
- Please print this page for your records and send a copy of it to your publisher/graduate school.
- Appropriate credit for the requested material should be given as follows: "Reprinted (adapted) with permission from (COMPLETE REFERENCE CITATION). Copyright (YEAR) American Chemical Society." Insert appropriate information in place of the capitalized words.
- One-time permission is granted only for the use specified in your request. No additional uses are granted (such as derivative works or other editions). For any other uses, please submit a new request.

TH-1887_136122001

Title: Gold Nanocluster and Quantum Dot Complex in Protein for Biofriendly White-Light-Emitting Material

Author: Satyapriya Bhandari, Sabyasachi Pramanik, Rumi Khandelia, et al

Publication: Applied Materials

Publisher: American Chemical Society

Date: Jan 1, 2016

PERMISSION/LICENSE IS GRANTED FOR YOUR ORDER AT NO CHARGE

This type of permission/license, instead of the standard Terms & Conditions, is sent to you because no fee is being charged for your order. Please note the following:

- Permission is granted for your request in both print and electronic formats, and translations.
- If figures and/or tables were requested, they may be adapted or used in part.
- Please print this page for your records and send a copy of it to your publisher/graduate school.
- Appropriate credit for the requested material should be given as follows: "Reprinted (adapted) with permission from (COMPLETE REFERENCE CITATION). Copyright (YEAR) American Chemical Society." Insert appropriate information in place of the capitalized words.
- One-time permission is granted only for the use specified in your request. No additional uses are granted (such as derivative works or other editions). For any other uses, please submit a new request.

TH-1887_136122001

JOHN WILEY AND SONS LICENSE TERMS AND CONDITIONS

Jun 13, 2018

This Agreement between Mr. SABYASACHI PRAMANIK ("You") and John Wiley and Sons ("John Wiley and Sons") consists of your license details and the terms and conditions provided by John Wiley and Sons and Copyright Clearance Center.

License Number	4367211058808
License date	Jun 13, 2018
Licensed Content Publisher	John Wiley and Sons
Licensed Content Publication	Small
Licensed Content Title	A White Light-Emitting Quantum Dot Complex for Single Particle Level Interaction with Dopamine Leading to Changes in Color and Blinking Profile
Licensed Content Author	Sabyasachi Pramanik, Satyapriya Bhandari, Uday Narayan Pan, et al
Licensed Content Date	Apr 17, 2018
Licensed Content Volume	14
Licensed Content Issue	20
Licensed Content Pages	7
Type of use	Dissertation/Thesis
Requestor type	Author of this Wiley article
Format	Print and electronic
Portion	Full article
Will you be translating?	No
Title of your thesis / dissertation	Surface Complexation Reaction for White Light Emission from Quantum Dots
Expected completion date	Aug 2018
Expected size (number of pages)	150
Requestor Location	Mr. SABYASACHI PRAMANIK DEPARTMENT OF CHEMISTRY IIT GUWAHATI GUWAHATI, 781039 India Attn: Mr. SABYASACHI PRAMANIK
Publisher Tax ID	EU826007151
Total	0.00 USD
Terms and Conditions	

TERMS AND CONDITIONS

This copyrighted material is owned by or exclusively licensed to John Wiley & Sons, Inc. or one of its group companies (each a"Wiley Company") or handled on behalf of a society with which a Wiley Company has exclusive publishing rights in relation to a particular work (collectively "WILEY"). By clicking "accept" in connection with completing this licensing transaction, you agree that the following terms and conditions apply to this transaction (along with the billing and payment terms and conditions established by the Copyright Clearance Center Inc., ("CCC's Billing and Payment terms and conditions"), at the time that you opened your RightsLink account (these are available at any time at http://myaccount.copyright.com).

Terms and Conditions

- The materials you have requested permission to reproduce or reuse (the "Wiley Materials") are protected by copyright.

- You are hereby granted a personal, non-exclusive, non-sub licensable (on a stand-alone basis), non-transferable, worldwide, limited license to reproduce the Wiley Materials for the purpose specified in the licensing process. This license, **and any CONTENT (PDF or image file) purchased as part of your order,** is for a one-time use only and limited to any maximum distribution number specified in the license. The first instance of republication or reuse granted by this license must be completed within two years of the date of the grant of this license (although copies prepared before the end date may be distributed thereafter). The Wiley Materials shall not be used in any other manner or for any other purpose, beyond what is granted in the license. Permission is granted subject to an appropriate acknowledgement given to the author, title of the material/book/journal and the publisher. You shall also duplicate the copyright notice that appears in the Wiley publication in your use of the Wiley Material. Permission is also granted on the understanding that nowhere in the text is a previously published source acknowledged for all or part of this Wiley Material. Any third party content is expressly excluded from this permission.

- With respect to the Wiley Materials, all rights are reserved. Except as expressly granted by the terms of the license, no part of the Wiley Materials may be copied, modified, adapted (except for minor reformatting required by the new Publication), translated, reproduced, transferred or distributed, in any form or by any means, and no derivative works may be made based on the Wiley Materials without the prior permission of the respective copyright owner.**For STM Signatory Publishers clearing permission under the terms of the STM Permissions Guidelines only, the terms of the license are extended to include subsequent editions and for editions in other languages, provided such editions are for the work as a whole in situ and does not involve the separate exploitation of the permitted figures or extracts,** You may not alter, remove or suppress in any manner any copyright, trademark or other notices displayed by the Wiley Materials. You may not license, rent, sell, loan, lease, pledge, offer as security, transfer or assign the Wiley Materials on a stand-alone basis, or any of the rights granted to you hereunder to any other person.

- The Wiley Materials and all of the intellectual property rights therein shall at all times remain the exclusive property of John Wiley & Sons Inc, the Wiley Companies, or their respective licensors, and your interest therein is only that of having possession of and the right to reproduce the Wiley Materials pursuant to Section 2 herein during the continuance of this Agreement. You agree that you own no right, title or interest in or to the Wiley Materials or any of the intellectual property rights therein. You shall have no rights hereunder other than the license as provided for above in Section 2. No right, license or interest to any trademark, trade name, service mark or other branding ("Marks") of WILEY or its licensors is granted hereunder, and you agree that you shall not assert any such right, license or interest with respect thereto

- NEITHER WILEY NOR ITS LICENSORS MAKES ANY WARRANTY OR REPRESENTATION OF ANY KIND TO YOU OR ANY THIRD PARTY, EXPRESS, IMPLIED OR STATUTORY, WITH RESPECT TO THE MATERIALS OR THE ACCURACY OF ANY INFORMATION CONTAINED IN THE MATERIALS, INCLUDING, WITHOUT LIMITATION, ANY IMPLIED WARRANTY OF MERCHANTABILITY, ACCURACY, SATISFACTORY QUALITY, FITNESS FOR A PARTICULAR PURPOSE, USABILITY, INTEGRATION OR NON-INFRINGEMENT AND ALL SUCH WARRANTIES ARE HEREBY EXCLUDED BY WILEY AND ITS LICENSORS AND WAIVED

BY YOU.

- WILEY shall have the right to terminate this Agreement immediately upon breach of this Agreement by you.

- You shall indemnify, defend and hold harmless WILEY, its Licensors and their respective directors, officers, agents and employees, from and against any actual or threatened claims, demands, causes of action or proceedings arising from any breach of this Agreement by you.

- IN NO EVENT SHALL WILEY OR ITS LICENSORS BE LIABLE TO YOU OR ANY OTHER PARTY OR ANY OTHER PERSON OR ENTITY FOR ANY SPECIAL, CONSEQUENTIAL, INCIDENTAL, INDIRECT, EXEMPLARY OR PUNITIVE DAMAGES, HOWEVER CAUSED, ARISING OUT OF OR IN CONNECTION WITH THE DOWNLOADING, PROVISIONING, VIEWING OR USE OF THE MATERIALS REGARDLESS OF THE FORM OF ACTION, WHETHER FOR BREACH OF CONTRACT, BREACH OF WARRANTY, TORT, NEGLIGENCE, INFRINGEMENT OR OTHERWISE (INCLUDING, WITHOUT LIMITATION, DAMAGES BASED ON LOSS OF PROFITS, DATA, FILES, USE, BUSINESS OPPORTUNITY OR CLAIMS OF THIRD PARTIES), AND WHETHER OR NOT THE PARTY HAS BEEN ADVISED OF THE POSSIBILITY OF SUCH DAMAGES. THIS LIMITATION SHALL APPLY NOTWITHSTANDING ANY FAILURE OF ESSENTIAL PURPOSE OF ANY LIMITED REMEDY PROVIDED HEREIN.

- Should any provision of this Agreement be held by a court of competent jurisdiction to be illegal, invalid, or unenforceable, that provision shall be deemed amended to achieve as nearly as possible the same economic effect as the original provision, and the legality, validity and enforceability of the remaining provisions of this Agreement shall not be affected or impaired thereby.

- The failure of either party to enforce any term or condition of this Agreement shall not constitute a waiver of either party's right to enforce each and every term and condition of this Agreement. No breach under this agreement shall be deemed waived or excused by either party unless such waiver or consent is in writing signed by the party granting such waiver or consent. The waiver by or consent of a party to a breach of any provision of this Agreement shall not operate or be construed as a waiver of or consent to any other or subsequent breach by such other party.

- This Agreement may not be assigned (including by operation of law or otherwise) by you without WILEY's prior written consent.

- Any fee required for this permission shall be non-refundable after thirty (30) days from receipt by the CCC.

- These terms and conditions together with CCC's Billing and Payment terms and conditions (which are incorporated herein) form the entire agreement between you and WILEY concerning this licensing transaction and (in the absence of fraud) supersedes all prior agreements and representations of the parties, oral or written. This Agreement may not be amended except in writing signed by both parties. This Agreement shall be binding upon and inure to the benefit of the parties' successors, legal representatives, and authorized assigns.

- In the event of any conflict between your obligations established by these terms and conditions and those established by CCC's Billing and Payment terms and conditions, these terms and conditions shall prevail.

TH-1887_136122001

- WILEY expressly reserves all rights not specifically granted in the combination of (i) the license details provided by you and accepted in the course of this licensing transaction, (ii) these terms and conditions and (iii) CCC's Billing and Payment terms and conditions.

- This Agreement will be void if the Type of Use, Format, Circulation, or Requestor Type was misrepresented during the licensing process.

- This Agreement shall be governed by and construed in accordance with the laws of the State of New York, USA, without regards to such state's conflict of law rules. Any legal action, suit or proceeding arising out of or relating to these Terms and Conditions or the breach thereof shall be instituted in a court of competent jurisdiction in New York County in the State of New York in the United States of America and each party hereby consents and submits to the personal jurisdiction of such court, waives any objection to venue in such court and consents to service of process by registered or certified mail, return receipt requested, at the last known address of such party.

WILEY OPEN ACCESS TERMS AND CONDITIONS

Wiley Publishes Open Access Articles in fully Open Access Journals and in Subscription journals offering Online Open. Although most of the fully Open Access journals publish open access articles under the terms of the Creative Commons Attribution (CC BY) License only, the subscription journals and a few of the Open Access Journals offer a choice of Creative Commons Licenses. The license type is clearly identified on the article.

The Creative Commons Attribution License

The Creative Commons Attribution License (CC-BY) allows users to copy, distribute and transmit an article, adapt the article and make commercial use of the article. The CC-BY license permits commercial and non-

Creative Commons Attribution Non-Commercial License

The Creative Commons Attribution Non-Commercial (CC-BY-NC)License permits use, distribution and reproduction in any medium, provided the original work is properly cited and is not used for commercial purposes.(see below)

Creative Commons Attribution-Non-Commercial-NoDerivs License

The Creative Commons Attribution Non-Commercial-NoDerivs License (CC-BY-NC-ND) permits use, distribution and reproduction in any medium, provided the original work is properly cited, is not used for commercial purposes and no modifications or adaptations are made. (see below)

Use by commercial "for-profit" organizations

Use of Wiley Open Access articles for commercial, promotional, or marketing purposes requires further explicit permission from Wiley and will be subject to a fee.

Further details can be found on Wiley Online Library

http://olabout.wiley.com/WileyCDA/Section/id-410895.html

Other Terms and Conditions:

v1.10 Last updated September 2015

Questions? customercare@copyright.com or +1-855-239-3415 (toll free in the US) or +1-978-646-2777.

TH-1887_136122001